Università Politecnica delle Marche

Facoltà di Ingegneria

Corso di Dottorato in Ingegneria dell'Informazione

Curriculum Ingegneria Biomedica, Elettronica e delle Telecomunicazioni

XXIX ciclo (XV ciclo n.s.)

Balance and Motor Control in Dynamic Tasks

PhD Candidate:

Alessandro Mengarelli

Tutor:

Prof. Sandro Fioretti

When you have excluded the impossible
whatever remains, however improbable
must be the truth

Once you realize what a joke everything is
being the Comedian is the only thing that makes sense

Fedeli alla Linea anche quando non c'è

n^1 grazie al Prof. Sandro Fioretti per avermi dato la possibilità di lavorare facendo ciò che più mi piace: un privilegio concesso a pochi.

n! grazie a Francesco: senza di lui probabilmente niente sarebbe iniziato.

e^n grazie a tutte le persone che ho incontrato e con cui ho lavorato in questi anni: ognuno di loro nel bene (molti) e nel male (pochi) ha lasciato qualcosa e spero di aver fatto lo stesso.

n^n grazie a Stefano, Giacomo, Giulia e Michela: ognuno di loro sa il perché, con la speranza che non finisca qui.

n^∞ grazie a Federica: non a tutti è concesso di conoscere persone veramente speciali. Sono stato fortunato.

Table of Contents

Part 1

Motor Control in Perturbed Balance

Chapter 1
Introduction

Balance is defined as the ability to keep the body center of mass within the base of support limiting the sway. The study of human upright posture represents a well-known and rooted research field (Maki, 1986; Prieto *et al.*, 1996) and in particular the instrumental assessment of balance is nowadays considered fundamental in order to characterize the principles governing the optimization and deterioration of postural control. However, in some cases a subject can maintain the upright stance without showing abnormal oscillation of both center of pressure and center of mass and at the same time exhibit abnormal responses when his balance encounters perturbations, of environmental as well as proprioceptive origins (Nardone *et al.*, 2006). Starting with the seminal work of Nashner (1976, 1977), the analysis of human ability to maintain balance and recover upright stance after a perturbation has received growing interest throughout the years (Horak and Nashner, 1986; Horak *et al.*, 1989), with the attempts to identify the existence of a single or a set of repeatable response patterns to various type of upright stance perturbations (Horak and Nashner, 1986; Alexander *et al.*, 1992; Hughes *et al.*, 1995; Runge *et al.*, 1999). In recent years, the analysis of balance responses to various type of external stimuli, such as translation, tilt, rotation or backward and forward shift of the base of support, has been applied with subjects suffering from diseases which lead to balance impairment, such as Parkinson's disease, multiple sclerosis, peripheral vestibular deficits or stroke (Dimitrova *et al.*, 2004; Cameron *et al.*, 2008; Geurts *et al.*, 2005,). In these cases, perturbed posturography resulted useful in order to evaluate the sensory-motor integration necessary for balance control, to estimate the risk of fall, to assess the effects of treatments and the impairment due to disease progress (Visser *et al.*, 2008). Moreover, several manipulations can be introduced to make the balance task more challenging, such as reduction of the base of support or sensory deprivation. Indeed, postural control relies mainly on visual, vestibular and proprioceptive

afferent systems and the decreasing or deprivation of one or more of them may provide further insights in understanding physiological and neurological mechanisms which underlie the ability to maintain balance. The possibility to design such a high number of different experimental protocols is due to the high number of perturbation parameters that can be controlled by the examiner; these parameters include principally the type of perturbation, the velocity and the acceleration of the base of support and the direction of perturbation (Maki, 1986). Furthermore, also external perturbations have been used, aimed mainly at upper body segments, such as trunk and shoulders (Santos *et al.*, 2010). An eventual advantage in the use of motor driven devices for the stimulus administration, is that those instruments, are able to provide the same perturbation to each examined subject, irrespective of weight and/or body mass distribution. This aspect represents an improvement on many clinical balance tests and provides an inter-subject independent assessment of balance; unfortunately, this aspect seems to remain, at the moment, the only standardizing element in the instrumental evaluation of balance through external perturbation of the base of support. Indeed, the earlier reported high number of parameters involved in this type of experiments, entails a high number of variables which can be modified separately, obtaining many different experimental conditions. This characteristic leads to a lack of standardization in perturbed balance tests (Visser *et al.*, 2008), hampering direct comparison of results obtained in different studies.

Despite the number of studies focused on understanding mechanisms joined to the upright stance maintenance after various type of perturbations in healthy adults (Horak and Nashner, 1986; Alexander *et al.*, 1992; Hughes *et al.*, 1995; Kavounoudias *et al.*, 1999; Runge *et al.*, 1999), a widespread interest for the assessment of fixed and repeatable balance recovery patterns as well as of the influence of perturbation characteristics, is still present in many research contexts (Creath *et al.*, 2005; Campbell *et al.*, 2009; Oude Nijhuis *et al.*, 2009; Nonnekes *et al.*, 2013; Schmid and Sozzi, 2016). The interest for the integration of postural and muscular adjustments in withstanding destabilizing stimuli is also reflected by the high number of studies in which a model for the human posture control is proposed (Alexandrov *et al.*, 2005; Welch *et al.*, 2008; Davidson *et al.*, 2011; Li *et al.*, 2012).

However, many aspects regarding balance recovery strategies remain still controversial, such as muscular features of the response (Welch *et al.*, 2008; Horlings *et al.*, 2009; Perucca *et al.*, 2013), the role of further joints, respect to the ankle and hip, in controlling upright stance (Alexander *et al.*, 1992; Runge *et al.*, 1999; Creath *et al.*, 2005; Corbeil *et al.*, 2013; Cheng, 2016) and neural pathways involved in perturbation withstand (Kavounoudias *et al.*, 1999; Nardone *et al.*, 2012; Nonnekes *et al.*, 2013). Thus, reference values of postural response to perturbations appeared valuable in order to obtain a more clear frame and some attempts have been yet made (Hughes *et al.*, 1995; Perucca *et al.*, 2013). Nevertheless, due to the high number of possible experimental configurations reported earlier, a characterization performed through a specific perturbative stimulus may be not reliable whether another experimental setup is considered (Visser *et al.*, 2008). Thus, this study represents a first attempt to describe upright stance recovery in different perturbative conditions, related to both stimulus characteristics and sensory afferences, in order to give a frame of the different balance responses between different experimental conditions.

1.1 Utility of Dynamic Posturography

Upright posture analysis plays an important role in the instrumental evaluation of balance, which can help to understand the etiology of the considered balance disorder, evaluating at the same time its temporal evolution (Nardone *et al.*, 2010). Symptoms of the disorder are often not evident through the analysis of the standing posture, while in perturbed conditions, e.g. base of support movement, the risk of falling heavily increases. Such kind of tests can support the clinical evaluation and clinical decision process, regarding whether a rehabilitation treatment is necessary, what kind of rehabilitation treatment is needed and the evaluation of the treatment results, thus covering the entire rehabilitative process (Hirsch *et al.*, 2003).

The most used device to analyze upright stance is the force platform, which allows the evaluation of the center of pressure (CoP) displacement. CoP also in unperturbed configuration,

shows a certain degree of displacement, supported by the activity of postural muscles and the presence of intermittent mechanisms for the balance control (Burdet and Rougier, 2007; Mezzarane *et al.*, 2007). Conversely, the employment of moveable platforms with several degrees of freedom underlines the need for an evaluation of the ability to withstand balance perturbations similar to those the subject could face in the everyday life (Nardone *et al.*, 2006). In this type of test, not only the muscular system is considered, but also the visual, vestibular and proprioceptive systems are analyzed. One of the most used instrument for this kind of evaluations is the EquiTest® (NeuroCom International Inc., Clackamas, OR, USA), which includes a platform able to tilt and translate within a movable visual environment (Susan *et al.*, 2006; Geurts *et al.*, 2005; Wrisley *et al.*, 2007; Perucca *et al.*, 2013; Visser *et al.*, 2008). These features allow to perform the Sensory Organization Test (Wrisley *et al.*, 2007; Yeh *et al.*, 2014), a widely used protocol where the visual reference and the base of support can move according to the spontaneous body sway of the subject, in order to evaluate his ability to maintain upright posture through the remaining sensory information. The Sensory Organization Test (SOT) is composed by 6 different trials: 1) eyes open, fixed base of support, fixed visual reference 2) eyes closed, fixed base of support 3) eyes open, fixed base of support, movable visual reference 4) eyes open, movable base of support, fixed visual reference 5) eyes closed, movable base of support 6) eyes open, movable base of support, movable visual reference.

Others motor tests commonly used in perturbed posture analysis are the Motor Control Test (MCT), the Motor Adaptation Test (ADT) and the Postural Evoked Response Test (PERT), where the myoelectric evoked potentials are considered (Nardone *et al.*, 2010; Perucca *et al.*, 2013; Lee *et al.*, 2012; Vervoort *et al.*, 2013). MCT evaluates myoelectric potentials evoked by platform translations backward and forward, while in the ADT the platform tilts upward and downward and in PERT both type of potentials are evaluated. The most analyzed muscles in all the tests are gastrocnemius and tibialis anterior. The typical test configuration includes harness to secure the tested subject, who is instrumented through electromyography probes and reflective markers, placed in correspondence of joints of interest, in order to acquire body movements in response to the perturbation. Platform

movement is generally not higher than 10 cm and the frequency of the translation, commonly sinusoidal, not overtakes 1 Hz, where 0.2 and 0.6 Hz are used as references for a slow and fast movement. However, in some studies trials have been performed starting from 0.1 Hz up to 1 Hz, throughout progressive increases of 0.1 Hz. Generally, base of support inclination is around 10 degrees (Nardone *et al.*, 2010; Nardone *et al.*, 2006; Nardone *et al.*, 2000; Schieppati *et al.*, 1995; Nardone *et al.*, 2005; Corna *et al.*, 1999; Corna *et al.*, 2003; Schieppati *et al.*, 2002). Tilting velocity has high variability depending to the specific test performed and data are generally analyzed starting from at least 10 s after the beginning of the test, avoiding the initial period in which the subject adapts the postural response to the base of support movement. Translation perturbations are largely used in dynamic posturography (Diener *et al.*, 1988; Dimitrova *et al.*, 2004; Horak and Nashner, 1986; Horak *et al.*, 1989; Hughes *et al.*, 1995; Nonnekes *et al.*, 2013; Chen *et al.*, 2014), with a large variability in both velocity and displacement of the base of support (Maki 1986; Visser *et al.*, 2008). CoP and CoM displacements are seldom considered (Oude Nijhuis *et al.*, 2009), whereas the myoelectric activity has been commonly evaluated on the basis of the latency time, i.e. the temporal interval between the movement start and the arise of the first muscular burst, commonly classified as short latency response and medium latency response (Nardone *et al.*, 2006; Schieppati *et al.*, 1995; Nardone *et al.*, 2005; Schieppati and Nardone, 1997; Nardone *et al.*, 2008; Nardone *et al.*, 2001; Nardone and Schieppati, 2004; Nardone *et al.*, 2000; Chastan *et al.*, 2008; Nardone and Schieppati, 1998).

Markers position allow to analyze relative joints movement and joint movements respect to the displacement of the base of support (Nardone *et al.*, 2010; Nardone *et al.*, 2006; Nardone *et al.*, 2000; Schieppati *et al.*, 1995; Corna *et al.*, 1999; Schieppati *et al.*, 2002; Chastan *et al.*, 2008; Schieppati *et al.*, 2003; Runge *et al.*, 1999; Horak and Nashner, 1986; Nanhoe-Mahabier *et al.*, 2012; Visser *et al.*, 2010; Henry *et al.*, 2001). A kinematic based parameter easy to represent is the standard deviation (SD) of the marker trace: SD of the marker placed in correspondence of the external auditory meatus is considered a simple but effective way to represent the head displacement and an index of the subject

stabilizing ability among different test configurations (Corna *et al.*, 1999; Schieppati *et al.*, 2002). Cross-correlation between pairs of marker displacement traces give an indication of the degree of coupling of the body segments (Corna *et al.*, 1999; Schieppati *et al.*, 2002).

Posturographic trials are often performed in eyes open (EO) and eyes closed (EC) conditions, highlighting different behaviors: in EO condition the subject acts as a classical pendulum keeping trunk and head stable and the movement is focused on the ankle joint. In EC condition, the subject acts as an inverted pendulum, controlling sway through the ankle joint, following the platform oscillation and withstanding the fall only when the platform movement inverts (Schieppati *et al.*, 2002). In EO condition head movement resulted smaller than the hip, which presented a smaller movement respect to the lateral malleolus; on the contrary, in the EC condition the head presented the larger oscillation (Schieppati *et al.*, 2002). In translational perturbations two strategies for maintaining balance have been suggested, the hip and ankle strategy, which arise with larger and smaller perturbation condition respectively (Horak and Nashner, 1986; Runge *et al.*, 1999). More recently, evidences about a non-negligible role of the knee have been reported, suggesting the possibility to model upright posture in perturbed conditions with a multi-link pendulum rather than the classical double inverted pendulum (Hughes *et al.*, 1995; Alexandrov *et al.*, 2005; Cheng, 2016). Also, a characteristic muscular activation sequence is observed for ankle and hip strategy, with a distal-to-proximal activation pattern for the ankle strategy, where the first muscles to activate are the ankle plantar-flexors, and a proximal-to-distal sequence, where trunk and hip muscles presents the shorter latencies (Horak and Nashner, 1986; Diener *et al.*, 1988; Schieppati *et al.*, 1995; Perucca *et al.*, 2013).

Perturbed posturography is commonly used in clinical research. For example, a reduced ability to weigh different sensory inputs depending on changes in the environment has been identified in populations with different balance deficits: Parkinson's disease (Colnat-Coulbois *et al.*, 2005), peripheral vestibular deficits (Peterka, 2002), peripheral neuropathy (Reid *et al.*, 2002) or stroke (Marigold *et al.*, 2004). In PD patients posturographic tests in EO condition seem not able to

distinguish between fallers and non-fallers subjects, while in EC condition fallers PD subjects have shown a larger head oscillation with slower responses when the condition changes from EC to EO condition (Rossi-Izquierdo *et al.*, 2014). Subjects with peripheral neuropathy showed better control indexes in dynamic conditions respect to the static ones; this aspect could refer to a feedforward control in dynamic conditions for this kind of patients (Nardone *et al.*, 2000; Nardone and Schieppati., 2004; Nardone *et al.*, 2005). Subjects with peripheral vestibular deficits maintain balance in static conditions, while the instability arises when sensory input are modified (Corna *et al.*, 2003).

Risk of falling is one of the major problems connected to neurological diseases, thus an index capable to quantify or even predict this feature would have an overwhelming importance (Gu *et al.*, 1996; Henry *et al.*, 2006; Visser *et al.*, 2008; Nardone *et al.*, 2010; Ganesan *et al.*, 2010; Kasser *et al.*, 2011; Sosnoff *et al.*, 2011; Johnson *et al.*, 2013; Prosperini *et al.*, 2011; Prosperini *et al.*, 2013; Rossi-Izquierdo *et al.*, 2014,). The use of moveable platform seems to be useful in evaluating those aspects related to the risk of falling, as the undesired stiffness effects and muscular activations, which resulted overrated in perturbation withstanding and thus increasing the risk of falling. Static upright stance sway seems to not represent a reliable indicator of the risk of falling, since no correlations have been recognized between sway and falling in PD patients. However, through moveable platform, the limits of stability and its critical points can be stressed and analyzed.

Dynamic posturography can be useful also in evaluating rehabilitation treatments: the SOT seems able to give a measure of the after treatment functional recovery in both PD and stroke patients (Geurts *et al.*, 2005). However, in peripheral vestibular deficits, the measurement of the functional recovery appeared more difficult, with similar results in evaluation test between subjects with peripheral vestibular deficits and those with neuropathy (Nardone *et al.*, 2005; Nardone *et al.*, 2008). Static and dynamic posturography are seldom employed as diagnosis support (Visser *et al.*, 2008; Nardone *et al.*, 2010), because there are several pathologies which can lead to balance impairments and moreover the same postural deficit could be related to different pathologies in different subjects and on the contrary subjects suffering from the same pathologies can present

different balance impairments; the use of dynamic posturography is not always able to provide a clear and univocal indication about the nature of the pathology and thus has no large employment as a support for the diagnosis, considering also the requirement for a complex measurement setup. The use of dynamic posturography seems more oriented to the balance disorder analysis and quantification, with the opportunity to push the subject to his limits of stability and to manipulate the sensorial information used in balance control and perturbations withstanding.

In PD patients, as reported earlier, dynamic posturography appears particularly useful, due to their reduced ability in maintaining balance, also in unperturbed conditions and to their high risk of falling. Thus, a number of studies focused their analysis on the assessment of the risk of falling and on deriving index for a reliable distinction between fallers and non-fallers subjects. Perturbed posturography for this kind of patients appeared particularly useful due to the possibility to give destabilizing stimuli similar to those a subject can experiment during his everyday life, allowing an evaluation of the patient ability in withstanding this kind of threat. The most employed perturbation for this kind of subjects appeared to be the tilt of the base of support rather than its translation. This aspect reflects the frequent use of the SOT, where the platform tilt follows the spontaneous body sway and it is not imposed by the examiner (Ganesan *et al.*, 2010; Lee *et al.*, 2012). A moveable and sway referenced base of support can be used also without the SOT (Ebersbach and Gunkel, 2011), extracting in this case the path length of the cylinder which allows the platform movement rather than CoP displacement, as in the unperturbed posturography. When the platform tilt is imposed in a single direction (Nanhoe-Mahabier *et al.*, 2012) or in multiple directions (Carpenter *et al.*, 2004; Visser *et al.*, 2010), the tilting angle is bounded between 8.25° and 4.25°, for anterior and posterior tilt respectively, in order to avoid falls (Lee *et al.*, 2012). Base of support translation are often used in antero-posterior and medio-lateral directions in the MCT (Nardone *et al.*, 2010) but often also others directions have been tested, up to 12 translation directions (Henry *et al.*, 1998; Henry *et al.*, 2001). Platform displacement in this case presents a narrow range of variation, between 6 and 9 cm, while acceleration and velocity are often tuned to the pathological condition of the subject, in order to

avoid falls during the test (Dimitrova *et al.*, 2004). CoP and CoM are always measured in static tests but in dynamic tests they are often considered only with tilt perturbations (Ganesan *et al.*, 2010).

Muscular activity is commonly acquired through the surface electromyography (sEMG) and the muscles of interest are usually ankle plantar-flexors, thigh and trunk muscles and also arms muscles (Henry *et al.*, 1998; Henry *et al.*, 2001; Carpenter *et al.*, 2004; Dimitrova *et al.*, 2004; Visser *et al.*, 2010). Reflective markes are usually placed on ankle, knee and hip joints but often the interest is also in the movement of pelvis, arms, trunk and head, which play a significant role also in ankle and hip balance strategies (Henry *et al.*, 2001; Chastan *et al.*, 2008; Nanhoe-Mahabier *et al.*, 2012), whereas trunk displacement resulted involved in balance maintenance (Henry *et al.*, 2001; Visser *et al.*, 2010; Nanhoe-Mahabier *et al.*, 2012), together with arms and head (Henry *et al.*, 2001; Chastan *et al.*, 2008; Visser *et al.*, 2010). The width between feet represents another perturbation parameter, where the distance between the heels defines a wide (≈30 cm) and a narrow (≈10 cm) stance; this distance can be changed asking the subject to modify feet position, in order to test two different conditions (Henry *et al.*, 2001; Dimitrova *et al.*, 2004; Dimitrova *et al.*, 2004a). In translational trials, the measure of CoP and CoM displacement in static and perturbed period quantifies the spontaneous and induced body sway, which can be estimated also through the trunk (Carpenter *et al.*, 2004; Nanhoe-Mahabier *et al.*, 2012) and pelvis and head angular displacement (Chastan *et al.*, 2008). The use of force platforms allows the evaluation of the GRF components, linked to the perturbation directions and provide a measure of the imbalance magnitude, also respect to the stance width (Henry *et al.*, 2001; Dimitrova *et al.*, 2004a). Ankle and hip angles represent the main measures of the body displacement, based on the classical modeling that involves ankle and hip strategies as the two most employed strategies to recover balance (Horak and Nashner, 1986). However, also the upper limbs have been recognized to play a significant role in withstanding perturbations of the base of support and recovering upright stance (Morris, 2000; Carpenter *et al.*, 2004). In accordance with these observations, also muscles of the upper body have been considered in several studies (Henry *et al.*, 1998; Henry *et al.*, 2001; Dimitrova *et al.*, 2004). Muscular activity is described not only by the

temporal delay between perturbation onset and muscular burst but also through the signal amplitude and its integration, which provides a characterization of the PD subjects muscular characteristics respect to healthy subjects (Henry *et al.*, 1998; Henry *et al.*, 2001; Carpenter *et al.*, 2004; Dimitrova *et al.*, 2004; Lee *et al.*, 2012). Some authors (Henry *et al.*, 1998; Henry *et al.*, 2001; Dimitrova *et al.*, 2004) use the muscle tuning curve, obtained from the integrated sEMG signal, in order to evaluate muscular activity in each direction of perturbed body sway. This feature gives an indication of which muscles activates in response to each perturbation direction, evaluating also their role in co-contraction activity; this kind of analysis provides information also about the direction where the risk of falling increases and also about the subject ability to tune his postural response when environmental conditions change. The analysis of muscular response allows also an evaluation of which neurological pathways are involved in parkinson's disease and in which measure (Chastan *et al.*, 2008; Dimitrova *et al.*, 2004a).

Results obtained by the analyses performed through dynamic posturography are often compared with the outcomes provided by clinical test or balance scale, which assess the pathology development and the subject residual ability to maintain balance. The most used tests are the tandem stance and gait test, single leg standing test, timed up-and-go test and the sit-to-walk test (Ganesan *et al.*, 2010; Ebersbach *et al.*, 2011; Johnson *et al.*, 2013). The most used balance scales are the Berg balance scale, Activities-specific balance confidence, balance evaluation system test, functional gait assessment and the unified Parkinson disease rating scale (Ganesan *et al.*, 2010; Ebersbach *et al.*, 2011; Nanhoe-Mahabier *et al.*, 2012; Johnson *et al.*, 2013). Parameters extracted from dynamic posturography test could support the evaluations made on the basis of the classical clinical tests and balance scales; in particular, it has been observed that a series of indexes obtained through the use of perturbed posturography correlate with the classical clinical evaluations, providing also a reliable instrument to distinguish fallers and non-fallers PD patients (Johnson *et al.*, 2013). Another index of the balance ability is the evaluation of the limits of stability (LOS), which point out the maximum reachable body displacement without moving feet or make a step. LOS can be analyzed using visual

targets the subject has to follows up to the loss of balance (Ganesan *et al.*, 2010; Vervoort *et al.*, 2013), evaluating the sway in the bending direction, the velocity and the accuracy in maintaining CoM within a tolerance zone (Johnson *et al.*, 2013).

Freezing of gait represents another feature of parkinson's disease which has been analyzed through perturbed posturography (Vervoort *et al.*, 2013; Jacobs *et al.*, 2008). Surprisingly, freezers subjects have shown a better ability in integrating sensorial information and a better balance control respect to the non-freezers, but a lower accuracy in reaching the target (Vervoort *et al.*, 2013). Difficulties in voluntarily moving CoM in the antero-posterior direction could indicate a relationship between freezing of gait and risk of falling, since the subject would not be able to counteract movement inertia caused by the sudden freezing of gait (Vervoort *et al.*, 2013; Bloem *et al.*, 2004). A central issue in Parkinson's disease tests regards the pharmacological therapy: tests can be performed after 1 or 2 hours after the drug assumption (Visser *et al.*, 2010; Ganeasn *et al.*, 2010; Vervoort *et al.*, 2013) or after 12 hours, when subject is in the OFF state of therapy (Nanhoe-Mahabier *et al.*, 2012; Dimitrova *et al.*, 2004). Moreover, subjects are asked to perform two tests at a distance of few hours, in order to evaluate the effects of pharmacological therapy on balance (Jacobs *et al.*, 2008; Nallegowda *et al.*, 2004) or conversely subjects which are following a pharmacological therapy that can affect balance or gait can be discarded before the beginning of the tests (Lee *et al.*, 2012; Nardone *et al.*, 2012).

Regarding the number and the sequence of trials, for PD patients the first trial resulted the most analyzed, in part to avoid the habituation rate due to the ensuing trials and in part because the first trial reflects better the everyday conditions that could lead to the risk of falling (Visser *et al.*, 2008; Visser *et al.*, 2010). The first trial responses can also be compared to those of the ensuing trials, in order to evaluate the subject ability in elaborating and maintaining the postural balance strategy (Nanhoe-Mahabier *et al.*, 2012).

Perturbed posturography shows a large employment also for balance evaluation in subjects affected by multiple sclerosis (MS), which leads, as in parkinson's disease, to postural and balance

deficits (Sosnoff *et al.*, 2011; Prosperini *et al.*, 2011; Boes *et al.*, 2012; Huisinga *et al.*, 2012; Prosperini *et al.*, 2013; Prosperini *et al.*, 2013a). Trials can be performed in EO and EC conditions and also in dual task condition: This paradigm allows an evaluation of cognitive processing required to maintain standing balance, simply by applying a concurrent cognitive task (Boes *et al.*, 2012; Prosperini *et al.*, 2013a). The deterioration of the balance control appeared independent of pathology development or aging (Boes *et al.*, 2012) and thus the hypothesis that balance and cognitive tasks may share neurological pathways, leading to the impossibility to perform both task at the same time.

In MS analysis, the effect of fatigue has been investigated also through the perturbed posturography (van Emmerik *et al.*, 2010) and Hebert and Corboy *(*2012) assessed the relationship between fatigue and reduce ability to maintain balance through the use of the SOT. Their findings suggested that the fatigue could be influenced by the reduced ability to maintain balance, showing high correlations between fatigue and the most challenging configurations of the SOT Also translational perturbations have been used with MS patients (Cameron *et al.*, 2008), measuring however only muscular responses, in terms of latencies and amplitude, to backward perturbations which lead to an anterior body sway. The low muscular strength seems not to affect balance, with an increased response in terms of signal amplitude respect to control subjects; this aspect could reflect the need to compensate a retarded muscular response observed in this kind of patients (Horak and Diener, 1994).

In conclusion, the use of dynamic posturography showed a wide employment with both healthy and pathological subjects. However, the several number of variables connected to this type of test (perturbation velocity, acceleration, displacement, direction, impulsive or continuous movement) leads to a lack of standardization which could bias outcomes comparison between different studies and hamper the diffusion of this technique in clinical practice. Moreover, the relative complexity of the instrumentation, the needed to synchronize several different acquisition systems and the weight of data processing can contribute to limit the diffusion of the dynamic posturography in clinical routine analysis. However, following what has been reported previously, dynamic posturography

appears to be valuable in both clinical and research contexts, to gain further insight in neurological and neuromuscular mechanisms which control upright stance and balance maintenance, to distinguish disease stages and in particular to understand neural and sensory pathways involved in each part of the global body response that follows a change in stance conditions.

Chapter References

Alexander N.B., Shepard N., Gu M.J., Schultz A., "Postural Control in Young and Elderly Adults When Stance Is Perturbed: Kinematics", *Journal of Gerontology*, 1992.

Alexandrov A.V., Frolov A.A., Horak F.B., Carlson-Kuhta P., Park S., "Feedback equilibrium control during human standing", *Biological Cybernetics*, 2005.

Bloem B.L., Hausdorff J.M., Visser J.E., Giladi N., "Falls and freezing of gait in Parkinson's disease: a review of two interconnected, episodic phenomena", *Movement Disorder*, 2004.

Boes M.K., Sosnoff J.J., Socie M.J., Sandroff B.M., Pula J.H., Motl R.W., "Postural control in multiple sclerosis: Effects of disability status and dual task", *Journal of the Neurological Sciences*, 2012.

Burdet C., Rougier P.," Analysis of center-of-pressure data during unipedal and bipedal standing using fractional Brownian motion modeling", *Journal of Applied Biomechanics*, 2007.

Cameron M.H., Horak F.B., Herndon R.R., Bourdette D., "Imbalance in Multiple Sclerosis: A Result of Slowed Spinal Somatosensory Conduction", *Somatosensory and Motor Research*, 2008.

Campbell A.D., Dakin C.J., Carpenter M.G., "Postural responses explored through classical conditioning", *Neuroscience*, 2009.

Carpenter M.G., Allum J.H., Honegger F., Adkin A.L., Bloem B.R., "Postural abnormalities to multidirectional stance perturbations in Parkinson's disease", *Journal of Neurology, Neurosurgery and Psychiatry*, 2004.

Chastan N., Debono B., Maltête D., Weber J., "Discordance Between Measured Postural Instability and Absence of Clinical Symptoms in Parkinson's Disease Patients in the Early Stages of the Disease", *Movement Disorders*, 2008.

Chen C.L., Lou S.Z., Wu H.W., Wu S.K., Yeung K.T., Su F.C., "Effects of the type and direction of support surface perturbation on postural responses", *Journal of Neuroengineering and Rehabilitation*, 2014.

Cheng K.B., "Does knee motion contribute to feet-in-place balance recovery?", *Journal of Biomechanics*, 2016.

Colnat-Coulbois S., Gauchard G.C., Maillard L., Barroche G., Vespignani H., Auque J., Perrin P.P., "Bilateral subthalamic nucleus stimulation improves balance control in Parkinson's disease *Journal of Neurology, Neurosurgery and Psychiatry*, 2005.

Corbeil P., Bloem B.R., van Meel M., Maki B.E., "Arm reactions evoked by the initial exposure to a small balance perturbation: A pilot study", *Gait and Posture*, 2013.

Corna S., Tarantola J., Nardone A., Giordano A., Schieppati M., "Standing on a continuously moving platform: is body inertia counteracted or exploited?", *Experimental Brain Research*, 1999.

Corna S., Nardone A., Prestinari A., Galante M., Grasso M., Schieppati M., "Comparison of Cawthorne-Cooksey Exercises and Sinusoidal Support Surface Translations to Improve Balance in Patients With Unilateral Vestibular Deficit", *Archives of Physical Medicine and Rehabilitation*, 2003.

Creath R., Kiemel T., Horak F., Peterka R., Jeka J., "A unified view of quiet and perturbed stance: simultaneous co-existing excitable modes", *Neuroscience Letters*, 2005.

Davidson B.S., Madigan M.L., Southward S.C., Nussbaum M.A., "Neural Control of Posture During Small Magnitude Perturbations: Effects of Aging and Localized Muscle Fatigue", *IEEE Transactions on Biomedical Engineering*, 2011.

Diener H.C., Horak F.B., Nashner L.M., "Influence of Stimulus Parameters on Human Postural Responses", *Journal of Neurophysiology*, 1988.

Dimitrova D., Horak F.B., Nutt JG., "Postural Muscle Responses to Multidirectional Translations in Patients with Parkinson's Disease", *Journal of Neurophysiology*, 2004.

Dimitrova D., Nutt J., Horak F.B., "Abnormal force patterns for multidirectional postural responses in patients with Parkinson's disease", *Experimental Brain Research*, 2004a.

Ebersbach G., Gunkel M., "Posturography Reflects Clinical Imbalance in Parkinson's Disease", *Movement Disorders*, 2011.

Ganesan M. Pal P.K., Gupta A., Sathyaprabha T.N., "Dynamic posturography in evaluation of balance in patients of Parkinson's disease with normal pull test: Concept of a diagonal pull test", *Parkinsonism and Related Disorders*, 2010.

Geurts A.C., de Haart M., van Nes I.J., Duysens J., "A review of standing balance recovery from stroke", *Gait and Posture*, 2005.

Gu M.J., Schultz A.B., Shepard N.T., Alexander N.B., "Postural control in young and elderly adults when stance is perturbed: dynamics", *Journal of Biomechanics*, 1996.

Hebert J.R., Corboy J.R., "The association between multiple sclerosis-related fatigue and balance as a function of central sensory integration", *Gait and Posture*, 2012.

Henry S.M., Fung J., Horak F.B., "EMG Responses to Maintain Stance During Multidirectional Surface Translations", *Journal of Neurophysiology*, 1998.

Henry S.M., Fung J., Horak F.B., "Effect of Stance Width on Multidirectional Postural Responses", *Journal of Neurophysiology*, 2001.

Hirsch M.A., Toole T., Maitland C.G., Rider R.A., "The effects of balance training and high-intensity resistance training on persons with idiopathic Parkinson's disease", *Archives of Physical Medicine and Rehabilitation*, 2003.

Horak F.B., Diener H.C., Nashner L.M., "Influence of Central Set on Human Postural Responses", *Journal of Neurophysiology*, 1989.

Horak F.B., Nashner L.M., "Central programming of postural movements: adaptation to altered support-surface configurations", *Journal of Neurophysiology*, 1986.

Horak F.B., Diener H.C., "Cerebellar control of postural scaling and central set in stance", *Journal of Neurophysiology*, 1994.

Horlings C.G., Küng U.M., van Engelen B.G., Voermans N.C., Hengstman G.J., van der Kooi A.J., Bloem B.R., Allum J.H., "Balance control in patients with distal versus proximal muscle weakness", *Neuroscience*, 2009.

Hughes M.A., Schenkman M.L., Chandler J.M., Studenski S.A., "Postural responses to platform perturbation: kinematics and electromyography", *Clinical Biomechanics*, 1995.

Huisinga J.M., Yentes J.M., Filipi M.L., Stergiou N., "Postural control strategy during standing is altered in patients with multiple sclerosis", *Neuroscience Letters*, 2012.

Jacobs J.V., Nutt J.G., Carlson-Kuhta P., Stephens M., Horak F.B., "Knee trembling during freezing of gait represents multiple anticipatory postural adjustments", *Experimental Neurology*, 2008.

Johnson L., James I., Rodrigues J., Stell R., Thickbroom G., Mastaglia F., "Clinical and Posturographic Correlates of Falling in Parkinson's Disease", *Movements Disorders*, 2013.

Kasser L.S., Jacobs J.V., Foley J.T., Cardinal B.J., Maddalozzo G.F., "A Prospective Evaluation of Balance, Gait, and Strength to Predict Falling in Women With Multiple Sclerosis", *Archives of Physical Medicine and Rehabilitation*, 2011.

Kavounoudias A., Gilhodes J.C., Roll R., Roll J.P., "From balance regulation to body orientation: two goals for muscle proprioceptive information processing?", *Experimental Brain Research*, 2009.

Lee J.M., Koh S.B., Chae S.W., Seo W.K., Kwon D.Y., Kim J.H., Oh K., Baik J.S., Park K.W., "Postural Instability and Cognitive Dysfunction in Early Parkinson's Disease", *Canadian Journal of Neurological Sciences*, 2012.

Li Y., Levine W.S., Loeb G.E., "A Two-Joint Human Posture Control Model With Realistic Neural Delays", *IEEE Transactions on Neural Systems and Rehabilitation Engineering*, 2012.

Maki B.E., "Selection of perturbation parameters for identification of the posture-control system", *Medical and Biological Engineering and Computing*, 1986.

Marigold D.S., Eng J.J., Tokuno C.D., Donnelly C.A., "Contribution of muscle strength and integration of afferent input to postural instability in persons with stroke". *Neurorehabilitation and Neural Repair*, 2004.

Mezzarane R.A., Kohn A.F., "Control of upright stance over inclined surfaces", *Experimental Brain Research*, 2007.

Morris M.E., "Movement Disorders in People With Parkinson Disease: A Model for Physical Therapy", *Physical Therapy*, 2000.

Nallegowda M., Singh U., Handa G., Khanna M., Wadhwa S., Yadav S.L., Kumar G., Behari M., "Role of Sensory Input and Muscle Strength in Maintenance of Balance, Gait, and Posture in Parkinson's Disease", *American Journal of Physical Medicine and Rehabilitation*, 2004.

Nanhoe-Mahabier W., Allum J.H.J., Overeem S., Borm G.F., Oude Nijhuis L.B., Bloem B.R., "First Trial Reactions and Habituation Rates over Successive Balance Perturbations in Parkinson's Disease", *Neuroscience*, 2012.

Nardone A. Grasso M., Tarantola J., Corna S., Schieppati M., "Postural Coordination in Elderly Subjects Standing on a Periodically Moving Platform", *Archives of Physical Medicine and Rehabilitation*, 2000.

Nardone A., Tarantola J., Miscio G., Pisano F., Schenone A., Schieppati M., "Loss of large-diameter spindle afferent fibres is not detrimental to the control of body sway during upright stance: evidence from neuropathy, *Experimental Brain Research*, 2000.

Nardone A., Galante M., Lucas B., Schieppati M., "Stance control is not affected by paresis and reflex hyperexcitability: the case of spastic patients", *Journal of Neurology, Neurosurgery and Psychiatry*, 2001.

Nardone A., Schieppati M., "Medium-latency response to muscle stretch in human lower limb: estimation of conduction velocity of group II fibresand central delay", *Neuroscience Letters*, 1998.

Nardone A., Schieppati M., "Group II spindle fibres and afferent control of stance. Clues from diabetic neuropathy", *Clinical Neurophysiology*, 2004.

Nardone A., Schieppati M.," The role of instrumental assessment of balance in clinical decision making", *European Journal of Physical and Rehabilitation Medicine*, 2010.

Nardone A., Galante M., Pareyson D., Schieppati M., "Balance control in Sensory Neuron Disease", *Clinical Neurophysiology*, 2006.

Nardone A, Grasso M., Schieppati M., "Balance control in peripheral neuropathy: Are patients equally unstable under static and dynamic conditions?", *Gait and Posture*, 2005.

Nardone A., Galante M., Grasso M., Schieppati M., "Stance ataxia and delayed leg muscle responses to postural perturbations in cervical spondylotic myelopathy", *Journal of Rehabilitation Medicine*, 2008.

Nardone A., Pasetti C., Schieppati M., "Spinal and supraspinal stretch responses of postural muscles in early Parkinsonian patients", *Experimental Neurology*, 2012.

Nashner L.M., "Adapting reflexes controlling the human posture", *Experimental Brain Research*, 1976.

Nashner L.M., "Fixed patterns of rapid postural responses among leg muscles during stance", *Experimental Brain Research*, 1977.

Nonnekes J., Scotti A., Oude Nijhuis L.B., Smulders K., Queralt A., Geurts A.C.H., Bloem B.R., Weerdesteyn V., "Are postural responses to backward and forward perturbations processed by different neural circuits?", *Neuroscience*, 2013.

Oude Nijhuis L.B, Allum J.H.J., Borm G.F., Honegger F., Overeem S., Bloem B.R., "Directional Sensitivity of "First Trial" Reactions in Human Balance Control", *Journal of Neurophysiology*, 2009.

Peterka R.J., "Sensorimotor integration in human postural control", *Journal of Neurophysiology*, 2002.

Perucca L., Caronni A., Vidmar G., Tesio L., "Electromyographic latency of postural evoked responses from the leg muscles during EquiTest Computerised Dynamic Posturography: Reference data on healthy subjects", *Journal of Electromyography and Kinesiology*, 2014.

Prieto T.E., Myklebust J.B., Hoffman R.G., Lovett E.G., Myklebust B.M., "Measures of Postural Steadiness: Differences Between Healthy Young and Elderly Adults", *IEEE Transaction on Biomedical Engineering*, 1996.

Prosperini L., Kouleridou A., Petsas N., Leonardi L., Tona F., Pantano P., Pozzilli C., "The relationship between infratentorial lesions, balance deficit and accidental falls in multiple sclerosis", *Journal of the Neurological Sciences*, 2011.

Prosperini L., Fortuna D., Giannì C., Leonardi L., Pozzilli C., "The Diagnostic Accuracy of Static Posturography in Predicting Accidental Falls in People With Multiple Sclerosis", *Neurorehabilitation and Neural Repair*, 2013.

Prosperini L., Pozzilli C., "The Clinical Relevance of Force Platform Measures in Multiple Sclerosis: A Review", *Multiple Sclerosis International*, 2013a.

Reid V.A., Adbulhadi H., Black K.R., Kerrigan C., Cros D., "Using posturography to detect unsteadiness in 13 patients with peripheral neuropathy: a pilot study". *Neurology and Clinical Neurophysiology*, 2002.

Rossi-Izquierdo M. Basta D., Rubio-Rodríguez J.P., Santos-Pérez S., Ernst A., Sesar-Ignacio Á., Alberte-Woodward M., Guijarro-Del Amo M., Estany-Gestal A., San Román-Rodríguez E., Faraldo-García A., Zubizarreta-Gutiérrez A., Soto-Varela A., "Is posturography able to identify fallers in patients with Parkinson's disease?", *Gait and Posture*, 2014.

Runge C.F., Shupert C.L., Horak F.B., Zajac F.E., "Ankle hip postural strategies defined by joint torques", *Gait and Posture*, 1999.

Santos M.J., Kanekar N., Aruin A.S., "The role of anticipatory postural adjustments in compensatory control of posture: 1. Electromyographic analysis", *Journal of Electromyography and Kinesiology*, 2010.

Schieppati M., Nardone A., "Medium-latency stretch reflexes of foot and leg muscles analysed by cooling the lower limb in standing humans", *Journal of Physiology*, 1997.

Schieppati M, Nardone A., Siliotto R., Grasso M., "Early and late stretch responses of human foot muscles induced by perturbation of stance", *Experimental Brain Research*, 1995.

Schieppati M., Giordano A., Nardone A., "Variability in a dynamic postural task attests ample flexibility in balance control mechanisms", *Experimental Brain Research*, 2002.

Schieppati M. Nardone A., Schmid M., "Neck Muscle Fatigue Affects Postural Control in Man", *Neuroscience*, 2003.

Schmid M., Sozzi S., "Temporal features of postural adaptation strategy to prolonged and repeatable balance perturbation", *Neuroscience Letters*, 2016.

Sosnoff J.J., Socie M.J., Boes M.K., Sandroff B.M., Pula J.H., Suh Y., Weikert M., Balantrapu S., Morrison S., Motl R.W., "Mobility, Balance and Falls in Persons with Multiple Sclerosis", *PLOSONE*, 2011.

Susan L.W., Marchetti G.F., Schade A.I., "The Relationship Between Falls History and Computerized Dynamic Posturography in Persons With Balance and Vestibular Disorders", *Archives of Physical Medicine and Rehabilitation*, 2006.

Van Emmerik R.E., Remelius J.G., Johnson M.B., Chung L.H., Kent-Braun J.A., "Postural control in women with multiple sclerosis: effects of task, vision and symptomatic fatigue", *Gait and Posture*, 2010.

Vervoort G., Nackaerts E., Mohammadi F., Heremans E., Verschueren S., Nieuwboer A., Vercruysse S., "Which Aspects of Postural Control Differentiate between Patients with Parkinson's Disease with and without Freezing of Gait?", *Parkinson's Disease*, 2013.

Visser J.E., Carpenter M.G., van der Kooij H., Bloem B.R., "The clinical utility of posturography", *Clinical Neurophysiology*, 2008.

Visser J.E., Oude Nijhuis L.B., Janssen L., Bastiaanse C.M., Form G.F., Duysens J., Bloem B.R., "Dynamic Posturography in Parkinson's Disease: Diagnostic Utility and the "First Trial Effect"", *Neuroscience*, 2010.

Welch T.D.J., Ting L.H., "A Feedback Model Reproduces Muscle Activity During Human Postural Responses to Support-Surface Translations", *Journal of Neurophysiology*, 2007.

Wrisley D.N., Stephens M.J., Mosley S., Wojnowski A., Duffy J., Burkard R., "Learning Effects of Repetitive Administrations of the Sensory Organization Test in Healthy Young Adults", *Archives of Physical Medicine and Rehabilitation*, 2007.

Yeh J.R., Hsu L.C., Lin C., Chang F.L., Lo M.T., "Nonlinear Analysis of Sensory Organization Test for Subjects with Unilateral Vestibular Dysfunction", *PLOSONE*, 2014.

Chapter 2
Methods

Ten healthy and young adults volunteered for this study (nine females and one male). Mean values of age, height and weight were 23.6±1.2 years, 168±8 cm and 55.6±5.5 kg. None of them suffered from neurological or motor disorder that could affect balance in either static or dynamic condition. Before the experiment, purposes and procedures of the study have been explained and informed consent was obtained from each participant.

2.1 Experimental protocol and setup

A movable platform was used as perturbation device, actuated by electro-mechanical servos and able to translate horizontally in forward and backward direction, with variable velocity and displacement. Subjects stood on the platform, looking forward with arms hanging comfortably on their sides. Subjects self-selected their stance width and were asked to maintain balance in response to the perturbation, without any guidance about how to remain in the upright posture. Perturbation trials in which the subjects had to step in order to maintain balance were not included in the analysis and the trials were repeated. No practice trials were given to the subjects before the beginning of the test.

Each subject was exposed to three different perturbation blocks: the first type of perturbation block consisted of 5 consecutive backward perturbation trials with fixed velocity (15 cm/s) followed by five consecutive forward perturbation trial with fixed velocity (15 cm/s). This kind of experimental condition aimed to allow the evaluation of the first trial effect and the habituation rate. The second type of perturbation block consisted of 5 consecutive perturbation trials in backward direction, with increasing velocity sequence (15 cm/s, 20 cm/s, 25 cm/s, 30 cm/s, 35 cm/s), followed by 5 consecutive

perturbation trials in forward direction with the same platform velocity sequence. The purpose of this kind of trial block was the evaluation of the perturbation speed on the balance response. Platform displacement in the former case (fixed velocity trial block) was set at 5 cm, while in the latter trial block (increasing velocity) was fixed at 15 cm. The eventual type of perturbation consisted of two consecutive backward perturbation at 20 cm/s and with a displacement of 5 cm: during the first perturbation, the subject maintained eyes open and in the second perturbation subject was asked to maintain eyes closed. The same configuration was repeated with forward platform displacement. This kind of experimental test aimed at the evaluation of the sensorial deprivation weight on the balance maintenance. In all the trial blocks, platform acceleration was set at 3 m/s^2 and a resting period of 2 minutes was included after each perturbation block, whereas consecutive trials were at most 10 seconds apart. The perturbation amplitudes and velocities were large enough to provoke body sway that is known to exceed natural sway (Winter *et al.*, 2001) and were chosen according with the seminal study of Diener *et al.* (1988), where the influence of different amplitudes and velocities on postural responses were tested.

Dynamics, kinematics and electromyographic responses were recorded for each subject and all trials were analyzed 1 s before the platform movement onset and 3 s after the platform movement offset. All data were averaged across all trials of the same perturbation amplitude for each subject.

2.2 Dynamic data acquisition and processing

Ground reaction force (GRF) and center of pressure (CoP) displacements are seldom acquired and analyzed in dynamic posturography tests, however, they contributed in obtaining a broader characterization of balance response. Classical force plates (FP) are able to acquire 3 GRF components, i.e. the antero-posterior (AP), medio-lateral (ML) and vertical one, and the AP, ML and vertical momentum; then the CoP displacement in both AP and ML direction can be computed. The characteristics of the moveable platform, a pure mechanical actuator without any embedded

measurement system, the need to remain in a measurement volume defined by the stereophogrammetric system and a series of environmental limits, did not allow the use of a classical FP for dynamic data acquisition. Thus, after a reliability evaluation (see the next chapter), the employment of a commercial and low cost device (Nintendo Wii Balance Board, WBB) has been decided. This instrument allows the acquisition of the vertical GRF component and thus both the CoP displacement components can be extracted. The WBB was placed upon the moveable platform and connected to the latter in order to avoid undesired WBB shifting respect to the support base. Four reflective markers were placed in correspondence of the middle of each WBB side, in order to obtain the WBB position, the platform movement profile and to be able to refer kinematic-based data to the WBB own reference frame if needed. Due to the perturbation characteristics (backward and forward horizontal translation), only the AP CoP component has been considered and analyzed. The vertical component of the GRF was firstly low-pass filtered at 10 Hz (Quant *et al.*, 2005, Nonnekes *et al.*, 2013) through a zero-lag, second order Butterworth filter and then CoP displacement was computed according with the method reported by Leach *et al.* (2014) and explained in the next chapter.

Due to its characteristic double peak shape (Fig. 1), a series of temporal and spatial parameters have been extracted from the CoP AP displacement for both backward and forward trial type:

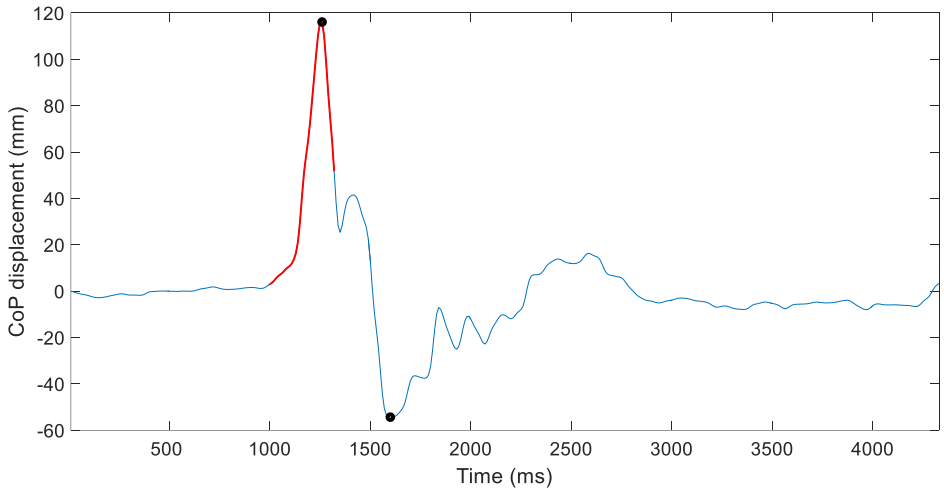

Figure 1. Representative CoP displacement during a backward trial. Increasing values indicate anterior displacement while negative values stand for posterior displacement. First and second peaks are indicated by black dots. CoP displacement during platform movement is highlighted by red color line.

First peak time (FPT): defines the temporal delay between the perturbation onset and the first peak achievement.

Inter peaks time (IPT): represents the temporal delay between the first peak and the second peak.

First peak amplitude (FPA): amplitude value of the first peak respect to a mean value computed on 1 s before the perturbation onset. The FPA was normalized to the distance between the heel and the first metatarsal head, considered as the foot length.

Second peak amplitude (SPA): amplitude value of the second peak respect to the value of the FPA. The SPA was normalized to the foot length.

First peak space (FPS): CoP path length computed from the perturbation onset to the first peak reaching. FPS was normalized to the foot length.

Second peak space (SPS): CoP path length computed from the perturbation onset to the second peak reaching. SPS was normalized to the foot length.

Movement displacement (MD): CoP path length computed from the perturbation onset to the perturbation offset. MD was normalized to the foot length.

Inter-peaks space (IPS): CoP path length computed between the first and the second peak. IPS was normalized to the foot length.

Steady state time (SST): temporal interval between the perturbation offset and the reaching of a steady state. Steady state value was computed as the time instant when CoP enters in an interval defined as its mean value computed in the last 1 s of data acquisition plus two standard deviations (Fig. 2).

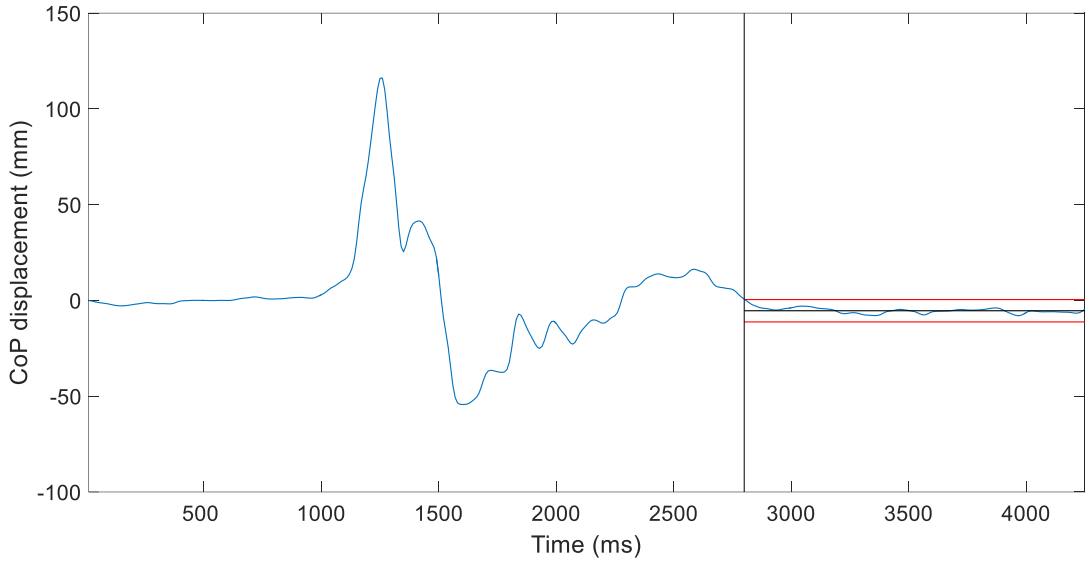

Figure 2. Steady state time calculation of CoP AP displacement (blue line) in a representative case. Horizontal black line indicates mean CoP displacement value computed in the last 1 s, while horizontal red lines define confidence interval as mean value±2*standard deviation. Vertical black line indicates time instant of the steady state reaching.

2.3 Kinematic data acquisition and processing

Kinematic data were acquired through a six camera, 3D motion analysis system (BTS, Italy) with a sample rate of 100 Hz and a total of 26 reflective markers have been placed on subject anatomical landmarks, on bilateral sides (Fig. 3).

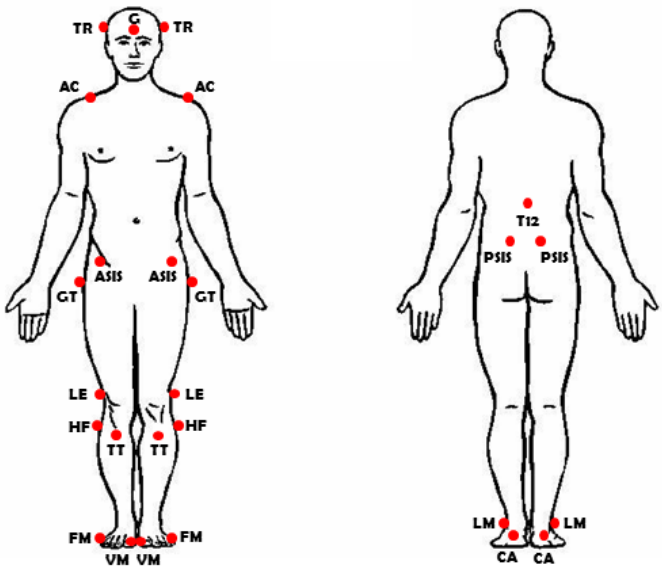

Figure 3. Marker set illustration.

A total of four markers were placed on foot, in correspondence of the first (FM) and the fifth (VM) metatarsal heads, lateral malleolus (LM) and calcaneus (CA). Four markers have been placed on tibialis tuberosity (TT), head of the fibula (HF), lateral epicondyle (LE) and great trochanter (GT). Four markers were applied on anterior superior iliac crest (ASIS) and posterior superior iliac spinae (PSIS). This marker-set follows what has been reported by Leardini *et al.* (2007) and thus calibration through a pointer with two markers in known position respect to the tip was performed in order to track the position of second metatarsal head, medial malleolus and medial epicondyle (Leardini *et al.*, 2007) Eventually six markers were placed on 12th thoracic vertebra (T12), acromion (AC), temporal bone (TR) and glabella (G).

Markers positions were acquired, low-pass filtered at 5 Hz and then used for angular joints displacement calculation. Anatomical reference frames for foot, shank, thigh and pelvis have been defined according with Cappozzo *et al.* (1995). For trunk and head, anatomical reference frames have been defined as follows: for the trunk, the origin is at the midpoint between right and left AC, z axis is oriented as the line passing through the ACs and with its positive direction from left to right, x axis is orthogonal to the quasi-frontal plane defined by the z axis and the T12, with its positive direction forward and the y axis is orthogonal to the zx plane with its positive direction distal (Fig. 4). For the head the origin is at the midpoint between left and right TR, z axis is oriented as the line passing through the TRs with its positive direction from left to right, y axis is orthogonal to the quasi-transverse plane defined by z axis and T12, with its positive direction distal and the x axis is orthogonal to the zy plane, with its positive direction forward (Fig. 4). Standard coordinate systems were adopted according with Grood and Suntay (1983), defining flexion/extension, internal/external rotation and abduction/adduction for all the considered joints. Trunk joint kinematics was considered as the relative movement between trunk (proximal) and pelvis (distal), whereas head joint kinematics was considered as the relative movement between head (proximal) and trunk (distal).

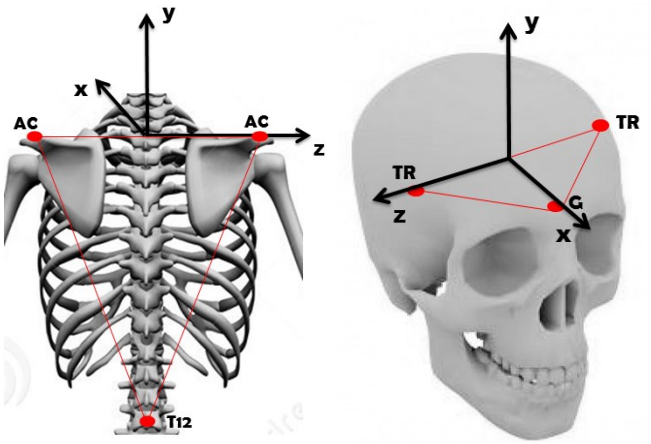

Figure 4. Graphical representation of trunk and head reference frames.

Trajectories of markers and joint kinematic were processed and analyzed from 1 s before the perturbation onset to 2.5 s after perturbation offset (Diener *et al.*, 1988). For each joint, from the absolute angle variation, the offset value has been subtracted by the corresponding static posture angle, computed 500 ms prior the perturbation onset, when the subject maintains the upright posture on the moveable platform. Thus, the kinematic measurements were all referenced to the moving platform and to the standing position during the quiet period. As indicate in the previous section for dynamic data, translational backward or forward balance perturbations induce sagittal plane variations and thus flexion/extension angles for each joint and AP and vertical markers trajectories were considered mainly. In order to give a measure of which joints play the most important role in maintaining balance in different configurations, angular range of variation has been computed bilaterally for each joint as the difference between the maximum and the minimum value detected from perturbation onset until 2.5 s after perturbation offset. Moreover, to evaluate the inter-joint coordination and thus postural movement strategies adopted to maintain or restore balance, an ellipse embracing 95% of the values of the angle-angle plot for each couple of joints was fitted (de Lima Pardini *et al.*, 2012, Fig. 5). Ratios of the short axis versus the long axis, ellipse area were then calculated and furthermore also the ellipse slope has been assessed through a regression analysis (Fig. 5). Albeit the ankle and hip strategies were identified as the two principal strategies for balance recovery (Horak and Nashner, 1986), evidences of an even more complex motor recovery

strategy have been reported (Alexandrov *et al.*, 2005; Runge *et al.*, 1999; Cheng, 2016), which involved the knee joint. Therefore, in order to assess which strategy has been employed under the different trail conditions and in what extent respect to the others, the slope of the ellipse embracing the 95% of the angle-angle plot values computed for ankle, knee and hip joints was considered.

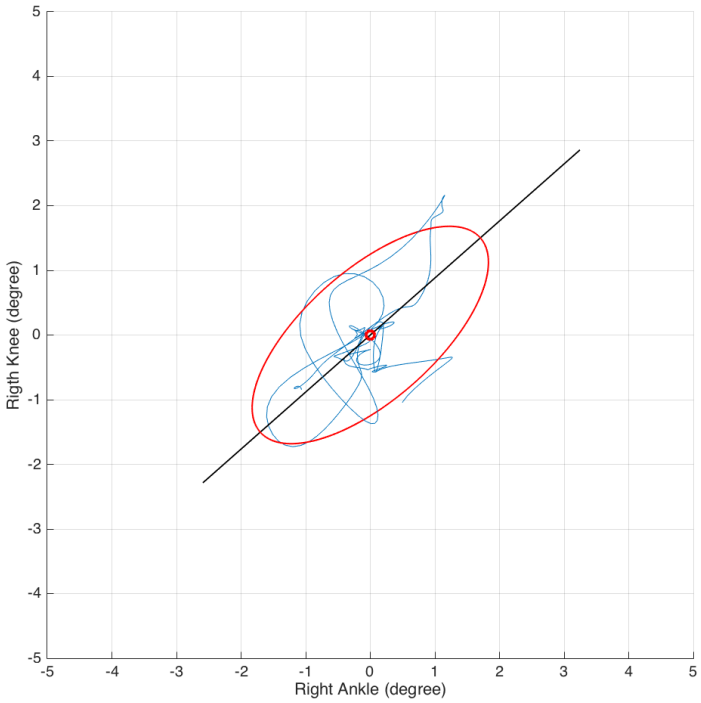

Figure 5. Representative plot of ankle and knee joint angles. The two angle distributions were demeaned and thus the 0 value represents the center of the final distribution. Increasing variations indicate joint flexion whereas decreasing variations stand for joint extension. The ellipse fitting the 95% of the distribution values is represented by the red line whereas the ellipse slope is represented by the black line.

For each couple of joints, a slope equal to 1 indicated an equal extent of both the considered joints and thus an undefined prevalent strategy; instead, a slope value equal or lower than 0.8 indicated a prevalence of the balance strategy identified by the joint plotted on the abscissa axis. Eventually, a slope value equal or higher than 1.2 indicated a prevalence of the balance strategy identified by the joint plotted on the ordinate axis. The slope value was computed bilaterally for each three joints and after the identification of a dominant strategy in each trial and for each subject, the recurrence of the dominant strategy among all the subjects has been assessed in percentage of the total subjects.

Center of mass (CoM) displacement in AP and vertical directions has been estimated through kinematic measurements of body segments, following what has been reported by Winter *et al.* (1998), using foot, shank, thigh and HAT (head, arms, trunk) body segments. CoM ML displacement was assumed to be coincident with the center of pelvis ML movement, computed as the centroid defined by right and left ASISs and PSISs. As for the CoP, due to the characteristics of the perturbation, only the AP component of CoM displacement was considered (Fig. 6). CoM showed a smoother wave form (Fig. 7) respect to the CoP, as expected (Winter *et al.*, 1998); however, AP CoM followed the double peaks path observed for the CoP (Fig. 1 and 7) and then all the aforementioned spatial and temporal parameters calculated for the CoP have been computed for the CoM as well. Also for the CoM the spatial parameters values were normalized to the foot length. Furthermore, the 3D CoM spatial evolution was computed (Fig. 8) in order to assess the distance between the initial (perturbation onset) and final (steady state reaching time) position of the CoM. (de Lima *et al.*, 2012). CoM coordinates have been referred to the WBB reference frame by subtracting the platform movement to the markers positions, allowing a direct comparison with the CoP displacement.

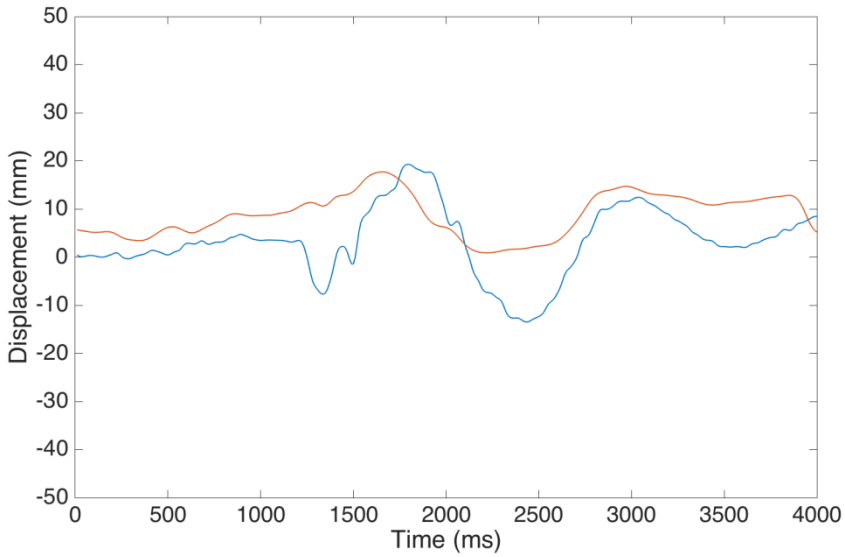

Figure 6. Representative case of CoP (blue line) and CoM (red line) displacement in ML direction. For both CoP and CoM the maximum variation do not exceed 20 mm.

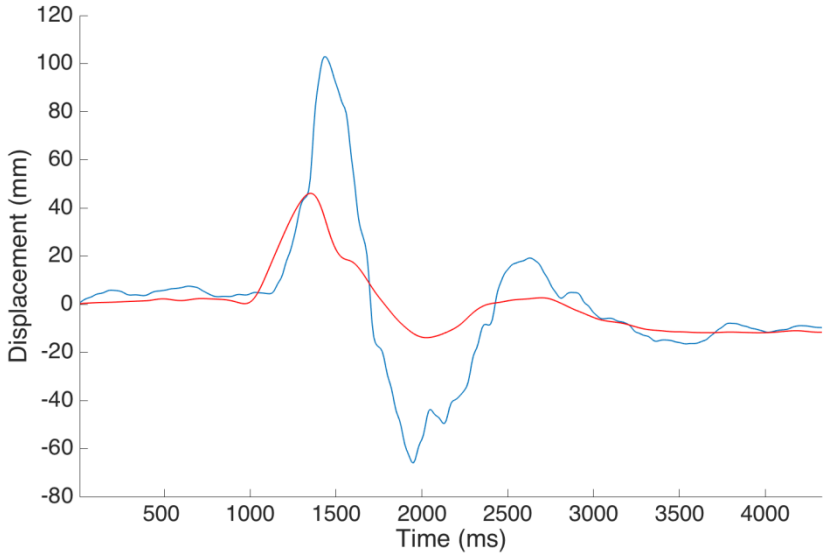

Figure 7. Representative CoP (blue line) and CoM (red line) AP displacement. CoM shows a smoother but clear double peak wave form that follows that of the CoP.

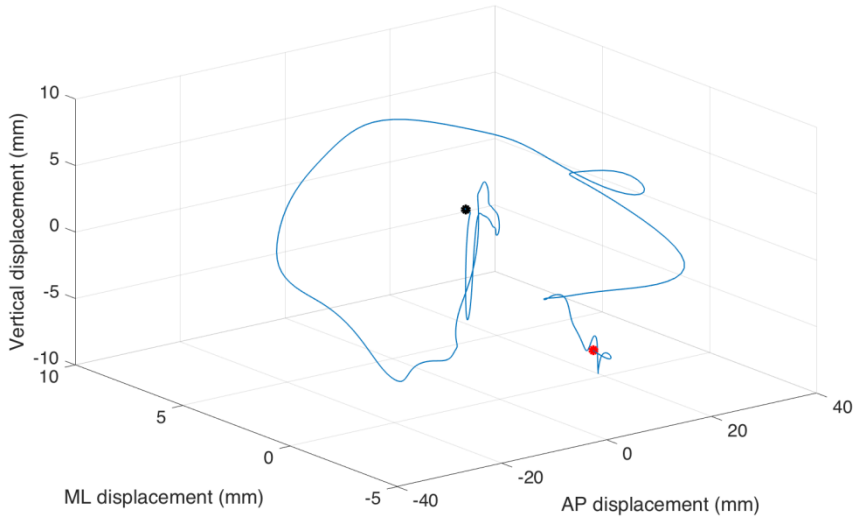

Figure 8. Representative CoM 3D movement. Increasing displacement indicates forward lean of CoM. Red and black dots highlight initial and final position respectively.

CoP and CoM AP displacements have been also related computing the IPA as the amplitude difference between the first peak of CoP and CoM and the IPT as the temporal gap between the first peaks of CoP and CoM (Fig. 9). Moreover, from the curve obtained subtracting CoM AP displacement to the CoP AP displacement (Winter *et al.*, 1998, de Lima Pardini *et al.*, 2012), the area under the curve has been computed from the perturbation onset until perturbation offset (Fig. 10),

with its positive and negative parts. Positive area values indicate that CoP moves ahead the CoM, while negative values stand for CoP behind CoM; this measure can be interpreted as a postural stability indicator, where the more the area value is high, the more the postural stability is substantial (Winter *et al.*, 1998; de Lima Pardini *et al.*, 2012).

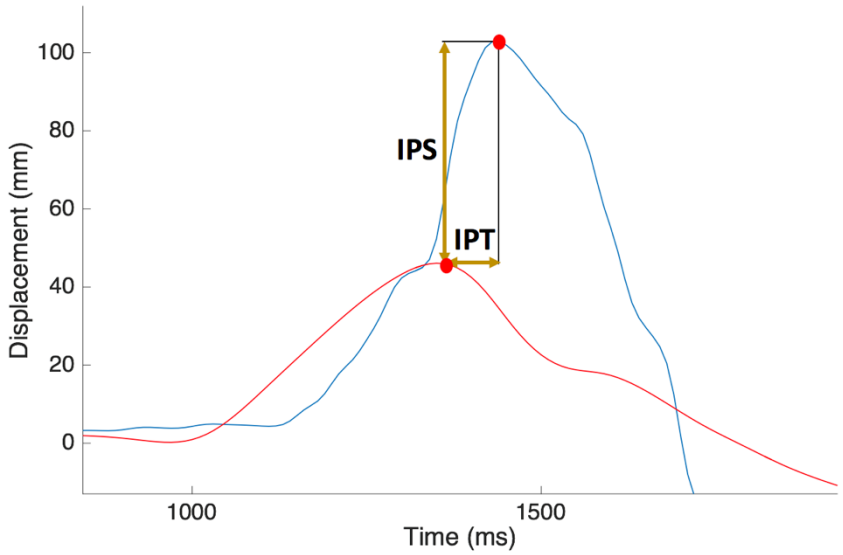

Figure 9. Inter-peaks space and inter-peaks time calculation from CoP (blue line) and CoM (red line) displacement. Red dots indicate maximum peaks for both curves.

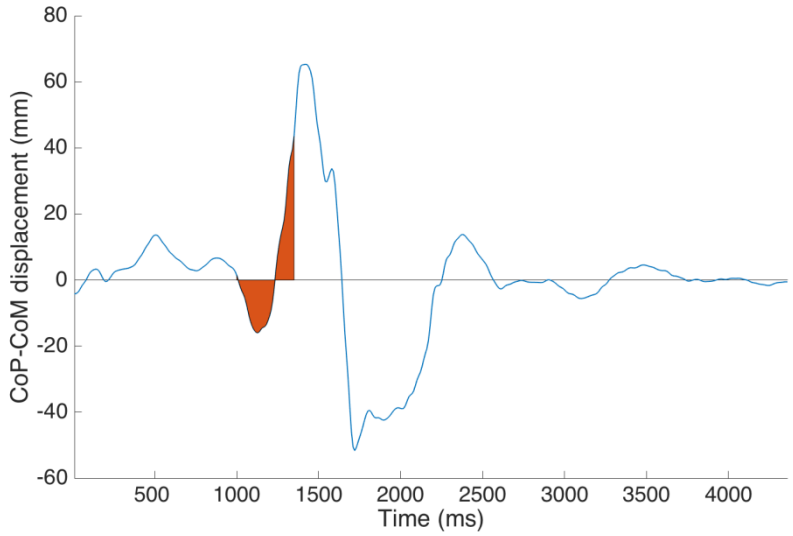

Figure 10. Area under the CoP-CoM curve computed during the platform movement. Positive values indicate CoP ahead of CoM, whereas negative values stand for a CoP behind the CoM. Area is highlighted by red color.

Due to the role played by the area under the curve and in particular its positive section, a further parameter connecting CoP and CoM AP displacement appeared to be the time at which the CoP overtakes CoM respect to the perturbation onset (overtake time, OTT), whether at this time CoP lies behind the CoM (Fig. 11).

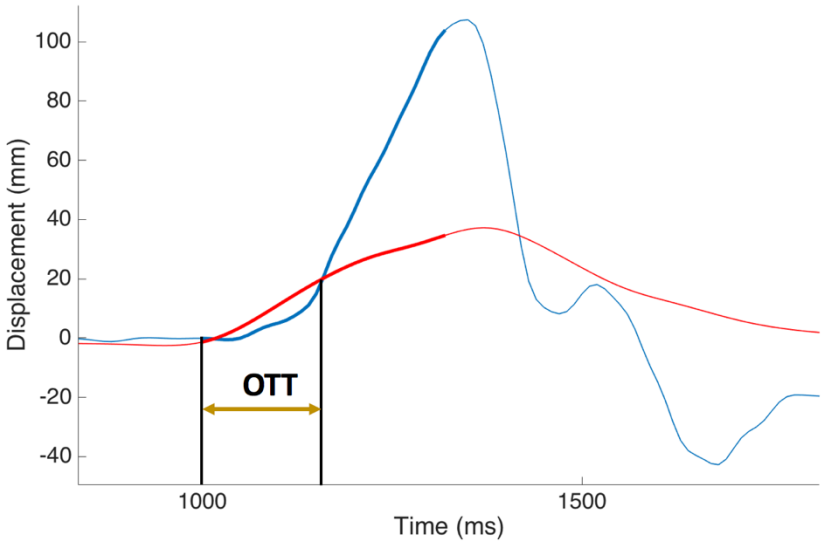

Figure 11. Overtake time between CoP and CoM calculation. Blue trace indicates CoP displacement while CoM displacement is reported as red line. Bold parts of CoP and CoM traces highlight displacement during platform movement.

2.4 Electromyographic data acquisition and processing

Muscles activity was assessed through surface electromyography technique (sEMG) and myoelectric signals were recorded bilaterally from tibialis anterior (TA), gastrocnemius medialis (GAS), rectus femoris (FR), vastus lateralis (VL), biceps femoris (BCF) and erector spinae longus (ERSL). TA and GAS were chosen for their role in the ankle joint control and thus in the foot dorsi/plantar flexion. RF, VL and BCF were chosen for their role in knee and hip joint control: RF is a knee extensor and hip flexor, while VL is a pure knee flexor and BCF is a knee flexor and hip extensor; ERSL was chosen for its trunk extensor function (Fig. 12). Single differential sEMG probes were placed on the muscles belly, following the guidelines reported by Freriks *et al.* (2000). EMG

signals, acquired with a sampling rate of 1 kHz, have been then band-pass filtered, with a linear-phase FIR filter between 20 and 450 Hz, in order to remove low frequency movement artifacts and avoid loss of information from the signal full bandwidth (De Luca *et al.*, 2010). Myoelectric signals acquired for each muscle have been then processed in order to assess the muscular response to balance perturbations.

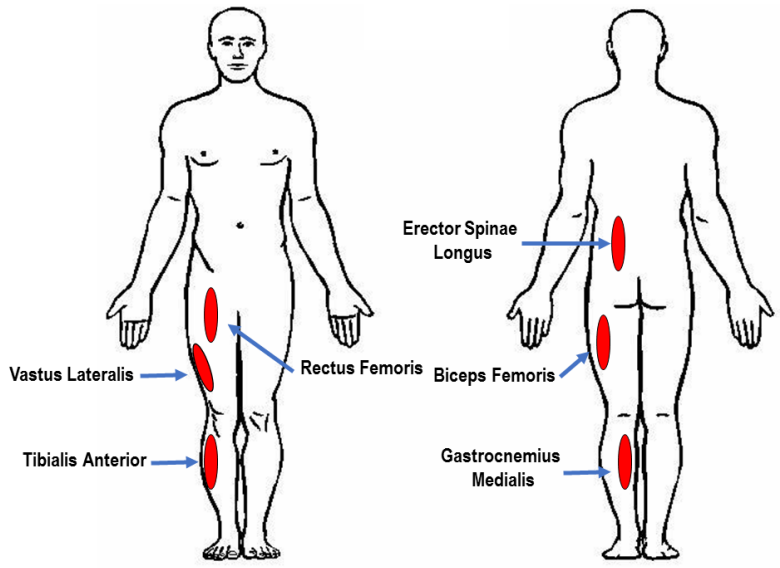

Figure 12. Graphical illustration of considered muscles location.

Electromyography was the first technique used by early researchers to characterize patterns of muscular response to support surface perturbation (Nashner, 1976; Horak and Nashner, 1986; Diener *et al.*, 1988) and the latency of muscles responses, defined as the time interval between the platform onset and the beginning of the muscle burst, represents yet one of the most used parameters to describe and quantify the perturbation response and balance recovery (Schieppati *et al.*, 1995; Henry *et al.*, 2001; de Lima Pardini *et al.*, 2012; Tsai *et al.*, 2014; Cheng *et al.*, 2014; Schmid and Sozzi, 2016). Thus, in this study muscular latencies have been assessed for each acquired muscle and the arise of muscle response was quantified as follows: firstly, the sEMG signal was rectified and the root mean square value (RMSV) was computed through an averaging window of 25 ms. Then, the mean value of the sEMG signal was computed among a RMSV epoch where only noise in present, i.e. with no muscular activity; this epoch was chosen as 1 s before the perturbation onset. Eventually, the first

muscular burst was identified whether the sEMG signal overtook an amplitude value equal to the mean value of signal computed earlier plus two standard deviations and maintained this value for at least 25 ms (de Lima Pardini *et al.*, 2012; Murnaghan and Robinovitch, 2013, Fig. 13).

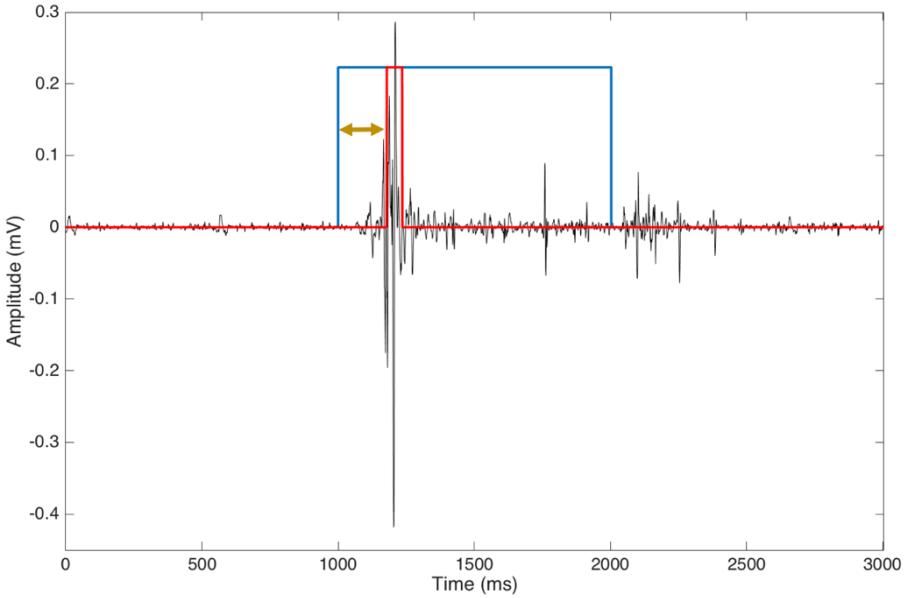

Figure 13. Muscular latency has been computed as the time interval between platform movement onset (blue line) and muscular burst (red square wave).

Chapter References

Alexandrov A.V., Frolov A.A., Horak F.B., Carlson-Kuhta P., Park S., "Feedback equilibrium control during human standing", *Biological Cybernetics*, 2005.

Cappozzo A., Catani F., Della Croce U., Leardini A., "Position and orientation in space of bones during movement: anatomical frame definition and determination", *Clinical Biomechanics*, 1995.

Cheng K.B., "Does knee motion contribute to feet-in-place balance recovery?", *Journal of Biomechanics*, 2016.

De Lima Pardini A.C., Papegaaij S., Cohen R.G., Teixeira L.A., Smith B.A., Horak F.B., "The interaction of postural and voluntary strategies for stability in Parkinson's disease", *Journal of Neurophysiology*, 2012.

De Luca C.J., Gilmore L.D., Kuznetsov M., Roy S.H., "Filtering the surface EMG signal: Movement artifact and baseline noise contamination", *Journal of Biomechanics*, 2010.

Diener H.C., Horak F.B., Nashner L.M., "Influence of Stimulus Parameters on Human Postural Responses", *Journal of Neurophysiology*, 1988.

Freriks B., Hermens H.J., Disselhorst-Klug C., Rau G., "Development of recommendations for sEMG sensors and sensor placement procedures", *Journal of Electromyography and Kinesiology*, 2000.

Grood E.S., Suntay W.J., "A Joint Coordinate System for the Clinical Description of Three-Dimensional Motions: Application to the Knee", *Journal of Biomechanical Engineering*, 1983.

Henry S.M., Fung J., Horak F.B., "Effect of Stance Width on Multidirectional Postural Responses", *Journal of Neurophysiology*, 2001.

Horak F.B., Nashner L.M., "Central programming of postural movements: adaptation to altered support-surface configurations", *Journal of Neurophysiology*, 1986.

Leach J.M., Mancini M., Peterka R.J., Hayes T.L., Horak F.B., "Validating and Calibrating the Nintendo Wii Balance Board to Derive Reliable Center of Pressure Measures", *Sensors*, 2014.

Leardini A., Sawacha Z., Paolini G., Ingrosso S., Nativo R., Benedetti M.G., "A new anatomically based protocol for gait analysis in children", *Gait and Posture*, 2007.

Murnaghan C.D., Robinovitch, "The effects of initial movement dynamics on human responses to postural perturbations", *Human Movement Science*, 2013.

Nashner L.M., "Adapting Reflexes Controlling the Human Posture", *Experimental Brain Research*, 1976.

Nonnekes J., Scotti A., Oude Nijhuis L.B., Smulders K., Queralt A., Geurts A.C.H., Bloem B.R., Weerdesteyn V., "Are postural responses to backward and forward perturbations processed by different neural circuits?", *Neuroscience*, 2013.

Quant S., Maki B.E., McIlroy W.E., "The association between later cortical potentials and later phases of postural reactions evoked by perturbations to upright stance", *Neuroscience Letters*, 2005.

Runge C.F., Shupert C.L., Horak F.B., Zajac F.E., "Ankle hip postural strategies defined by joint torques", *Gait and Posture*, 1999.

Schieppati M., Nardone A., Siliotto R., Grasso M., "Early and late stretch responses of human foot muscles induced by perturbation of stance", *Experimental Brain Research*, 1995.

Schmid M., Sozzi S., "Temporal features of postural adaptation strategy to prolonged and repeatable balance perturbation", *Neuroscience Letters*, 2016.

Tsai Y.C., Hsieh L.F., Yang S., "Age-related changes in posture response under a continuous and unexpected perturbation", *Journal of Biomechanics*, 2014.

Winter D.A., Patla A.E., Price F., Ishac M., Gielo-Perczak K., "Stiffness Control of Balance in Quiet Standing", *Journal of Neurophysiology*, 1998.

Winter D.A., Patla A.E., Rietdyk S., Ishac M.G., "Ankle Muscle Stiffness in the Control of Balance During Quiet Standing", *Journal of Neurophysiology*, 2001.

Chapter 3

Evaluation of alternative devices for dynamic measurements

The impossibility to use a classic, 6 components, laboratory force platform (FP) for the assessment of ground reaction forces (GRF) during posturography trials, leaded to consider the use of several alternative devices. In recent years the Wii Balance Board (WBB, Nintendo, Kyoto, Japan) has attracted growing attention as a portable, inexpensive and widely available instrument for balance assessment. The WBB was initially designed as a game controller, however due to its characteristics similar to those of laboratory FP and consequently the possibility to measure some of the ground GRF components, its use in the characterization of standing balance has been well evaluated (Clark *et al.* 2010; Huurnink *et al.* 2013; Park and Lee 2014; Bartlett *et al.* 2014). On the other hand, poor information is available about the use of the WBB in dynamic tasks (Abujaber *et al.* 2015) and its reliability in motor tasks with a fast changing in force distribution and CoP displacement has not been yet established. Consequently, the choice of the WBB for the measurement of the vertical component of the GRF and the CoP displacement during perturbed balance trials has been subordinated to its validity evaluation in such kind of tasks. Therefore, data extracted from the WBB measurement have been compared with those computed from laboratory FP during a variety of dynamic balance tests. All the evaluations were performed on signals acquired simultaneously through the two devices and because the FP is considered the gold standard for GRF measurement, all the WBB measurements and parameters were compared to those extracted from the FP.

3.1 Wii Balance Board characteristics

The Wii Balance Board is composed by a rigid platform with four uni-axial vertical force transducers, located in the feet at the board corners. Transducers are load cells with a strain gauge that converts applied force into a voltage that is digitized and transmitted wirelessly (Bluetooth) to laptop computer. Data retrieving from WBB to computer was performed through the Wiimote Physics, a freely available software developed to connect Nintendo devices to computers (http://wiimotephysics.codeplex.com/).

The reference frame of the WBB is located at the center of the plate (Fig. 1), the dimensions of the usable surface are 433 mm for the X axis (medio-lateral direction, ML) and 238 mm for the Y axis (antero-posterior direction, AP) and thus the total usable surface of the WBB has an area of approximately 0.1 m².

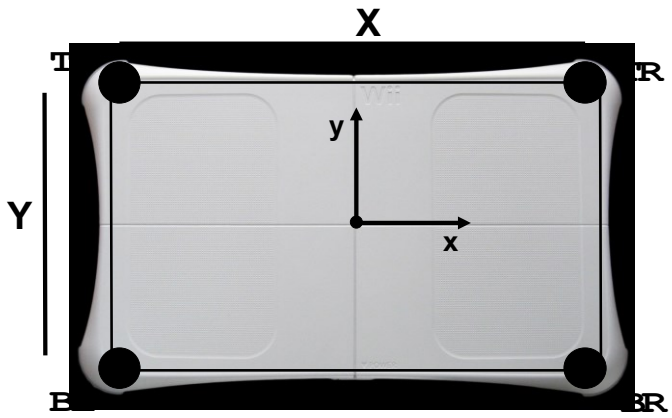

Figure 1. Wii Balance Board measures. The four transducers located on the four corners are usually indicated as Top and Bottom Left (TL and BL) transducers and Top and Bottom Right (TR and BR) transducers. The WBB reference frame is located at the center of the plate and the antero-posterior and medio-lateral directions are labeled as Y and X respectively.

Each transducer is able to measure only the vertical component of the GRF (F_z) and thus the CoP displacement is computed according to:

$$CoP_x = \frac{X}{2}\frac{F_{TR} + F_{BR} - F_{TL} - F_{BL}}{F_{TR} + F_{TR} + F_{BL} + F_{BR}} \qquad CoP_y = \frac{Y}{2}\frac{F_{TR} + F_{TL} - F_{BR} - F_{BL}}{F_{TR} + F_{TR} + F_{BL} + F_{BR}} \qquad (1)$$

where F_{TL}, F_{TR}, F_{BR} and F_{BL} are the vertical forces measured by each transducer and X and Y represent the distance (mm) between each transducer assuming that each transducer is positioned at the center of ech foot-peg and CoP_X and CoP_Y represent the CoP displacement (mm) in the medio-lateral and antero-posterior directions. A substantial drawback of the WBB is given by its sampling rate, low and variable during data acquisition, thus affected by time jitter; this feature leaded to the need of specific raw signal processing in order to obtain two synchronized signals from the WBB and the FP. The WBB has a maximum force limit of 1471 N.

3.2 Methods

Sixteen young subjects volunteered for the WBB reliability evaluation. All of them were undergraduate students, with no physical or neurological pathologies that could potentially affect the motor tasks execution. The laboratory FP provides the gold standard measure of balance and thus the WBB behavior has been compared to that of the FP. The WBB was placed upon a FP (Bertec 4060H) which measured 60×40 cm and was mounted flush with the laboratory floor. Due the characteristics of the postural response in dynamic posturography tests, two non-static tasks were chosen for the evaluation of the WBB reliability: the squat (SQ) and the functional reach (FR) tests. Those tests are widely used in clinical and research contexts (Dionisio *et al.* 2008; Gray *et al.* 2012; Kim *et al.*2014; Chen *et al.* 2015; Huang and Brown, 2015) and each subject performed a total of three consecutive FR tasks and three consecutive SQ tasks. Subjects performed both motor tasks barefoot, with feet apart on the WBB placed upon the FP. Due the subjects position the AP and ML directions are defined by the Y- and X-axis of the WBB respectively (Fig. 1). Signals acquisition started with the subject in standing position and ended when the subject had completed the task and is returned to the upright position. Moreover, in addition to the aforementioned tasks, also an eyes-open and eyes-closed standing balance tasks were performed. Since the validity and reliability of the WBB during double-leg stance has been established (Clark *et al.* 2010; Huurnink *et al.* 2013; Park and Lee, 2014)

and considering that the main aim was to evaluate the WBB for motor tasks with a fast CoP displacement and high force changing, in the following are reported the results relative to SQ and FR tests.

Sampling rate of laboratory FP was 500 Hz, whereas the WBB actual output rate has been shown to be variable (about 98 Hz): time interval between samples of WBB data was inconsistent (time jitter) and this value changed during data recording, leading to a temporal delay of the signal acquired through the WBB respect to that acquired through the laboratory FP (Fig. 2). Moreover, the delay is not steady but increases in time and thus the more the acquisition lasted, the higher was the delay (Fig. 3). In particular, the mean value of the time delay increase, considered as the linear regression coefficient between FP samples and the CoP_{FP} – CoP_{WBB} time difference and computed among all the 128 motor trials, resulted 0.012±0.002 samples/samples. In order to overcome this drawback, a first resampling at 98 Hz was performed on the WBB acquired raw signals, followed by a second resampling at 500 Hz, aimed to achieve two synchronized signals (Fig. 4). Then, both WBB and FP signals were low-pass filtered through a second order, Butterworth digital filter, with a cut-off frequency of 40 Hz, according to Abujaber *et al.* (2015), which tested the validity of WBB in a dynamic task (sit-to-stand).

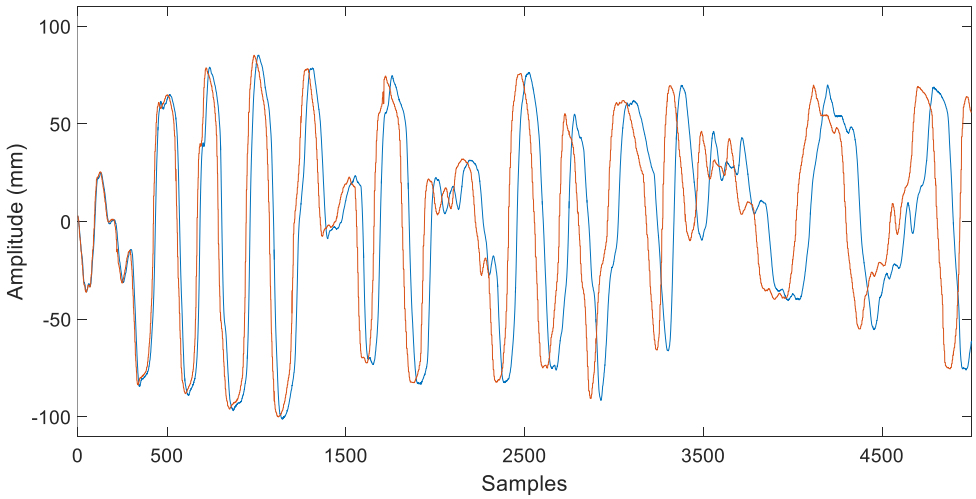

Figure 2. Two representative signals (Antero-posterior CoP displacement) acquired through FP (blu line) and WBB (red line). As the time increases the WBB signal presents an increasing delay with respect to the FP signal.

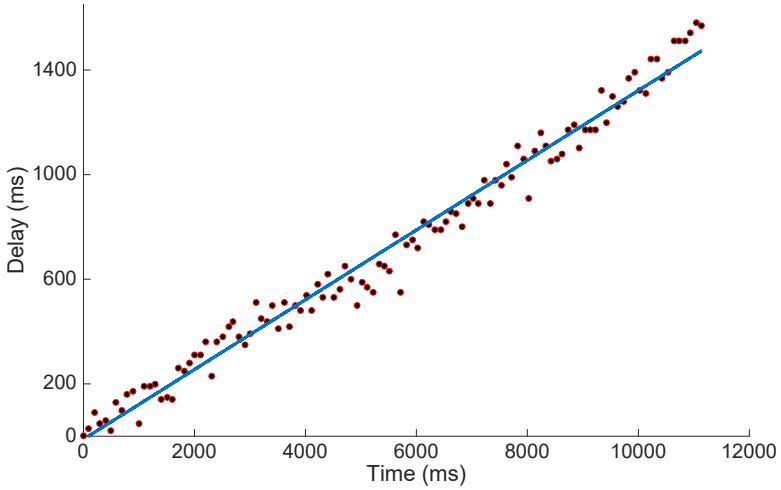

Figure 3. Graphical representation of the time delay between FP signal and WBB signal in a representative case. Each circle represents the delay value (y-axis) computed at the correspondent time value (x-axis). The value of the delay increase is computed as the linear regression coefficient. In this particular case it resulted 0.013 samples/samples.

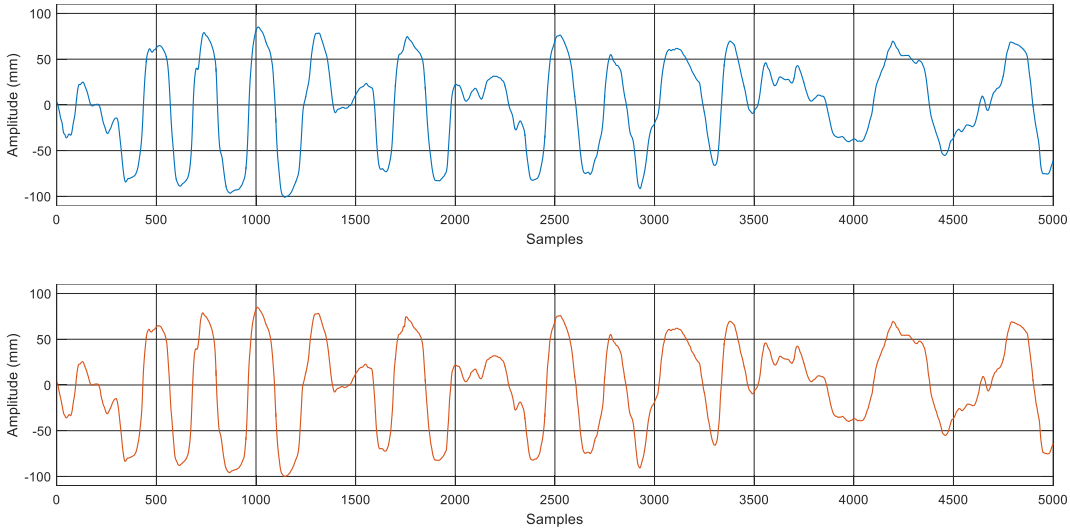

Figure 4. FP (top panel) and WBB (bottom panel) antero-posterior CoP displacement after the resampling and filtering. The time delay of the WBB signal has been fixed, obtaining two synchronized signals.

The two synchronized signals obtained after the aforementioned processing maintain a certain degree of amplitude gap, where the WBB underestimates or overestimates the reference FP signal in a a-priori non-definable way in both AP and ML directions. The average values of this amplitude gap between the two signals, computed among all the trials, resulted 2.1±3.2 mm and 3.4±2.9 mm for the AP and ML directions respectively, in line with those reported by Leach *et al.* (2014). This not-removable amplitude gap leaded to wonder if not only the CoP displacement but also the parameters

usually computed for the characterization of balance and postural steadiness (Prieto *et al.* 1996) are in agreement between the two measurement devices. Although these parameters are usually employed for postural steadiness evaluations, they were used for the WBB evaluation in order to have a set of indexes accounting for CoP displacement and velocity, thus related to parameters computed in perturbed posturography trials where CoP and CoM have been evaluated (De Lima Pardini *et al.* 2012; Tsai *et al.* 2013) Therefore AP and ML components of CoP_{WBB} were computed according to (1) and for each postural task the CoP-related measures described in the following have been considered and then the WBB performance was quantified by comparing the aforementioned measures with those extracted from the FP. Despite in the experimental protocol designed for the evaluation of balance the choice of a pure AP perturbation leads to a CoP displacement mainly in that direction, the CoP-related parameters have been computed for both AP and ML direction, in order to better examine the WBB characteristics; the CoP measure error has been defined as the percent difference between FP- and WBB-based measures. The error was computed for each CoP measure, considering the measure derived from the CoP_{FP} as the truth value:

$$CoP_{error} = \frac{FP_{measure} - WBB_{measure}}{FP_{measure}} \times 100 \qquad (2)$$

The average error among all subjects and trials has been then computed separately for each parameter and for both the considered dynamic tasks, the SQ and FR. Moreover, the correlation coefficient between any couple of FP and WBB measures has been also computed and the average value among all the trials is reported. Eventually, a graphical representation of the agreement between the two measurement devices has been performed through the Bland-Altman plots (Bland and Altman, 1986).

The measures extracted from the AP and ML CoP of FP and WBB are listed below:

- **Mean Distance**: Average distance from the mean CoP.

- **Mean Distance AP**: Mean absolute value of the AP time series and is the average AP distance from the mean CoP.
- **Mean Distance ML**: Mean absolute value of the ML time series and is the average ML distance from the mean CoP.
- **RMS Distance**: Root mean square value of the distance from the mean CoP.
- **RMS Distance AP**: Standard deviation of the AP time series.
- **RMS Distance ML**: Standard deviation of the ML time series.
- **Range**: Maximum distance between two points belonging to the CoP trajectory.
- **Range AP**: Difference between the maximum and the minimum value of the AP CoP trajectory.
- **Range ML**: Difference between the maximum and the minimum value of the ML CoP trajectory.
- **Mean velocity**: Average velocity of the CoP.
- **Mean velocity AP**: Average velocity of the CoP in the AP direction.
- **Mean velocity ML**: Average velocity of the CoP in the ML direction.
- **AREA – CC**: Area of a circle with a radius equal to the one-sided 95% confidence limit of the RD time series.
- **AREA – CE**: Area of the 95% bivariate confidence ellipse.
- **Sway area**: Area enclosed by the CoP path per unit of time.
- **Mean frequency**: Rotational frequency of the CoP if it had traveled the total excursion around a circle with a radius of the mean distance.
- **Mean frequency AP**: Frequency of a sinusoidal oscillation with an average value of the mean distance-AP and a total path length of total excursions-AP.
- **Mean frequency ML**: Frequency of a sinusoidal oscillation with an average value of the mean distance-ML and a total path length of total excursions-ML.
- **Fractal dimension CE**: Measure of the degree to which an ellipse fills the CoP trajectory.

- **Fractal dimension CC**: Measure of the degree to which a circle fills the CoP trajectory.
- **Fractal dimension PD**: Measure of the degree to which a circle with a radius equal to the range fills the CoP trajectory.
- **Power AP**: Integrated area of the power spectrum.
- **Power ML**: Integrated area of the ML CoP power spectrum.
- **Power RD**: Integrated area of the RD time series power spectrum.
- **Centroidal frequency AP**: Frequency at which the spectral mass is concentrated for the AP CoP.
- **Centroidal frequency ML**: Frequency at which the spectral mass is concentrated for the ML CoP.
- **Centroidal frequency RD**: Frequency at which the spectral mass is concentrated for the RD.
- **Frequency dispersion AP**: A measure of the variability in the frequency content of the AP CoP power spectral density.
- **Frequency dispersion ML**: A measure of the variability in the frequency content of the ML CoP power spectral density.
- **Frequency dispersion RD**: A measure of the variability in the frequency content of the RD power spectral density.
- **Total excursion (TOTEX)**: Total length of the CoP path.
- **Total excursion AP (TOTEXAP)**: Total length of the CoP path in the AP direction.
- **Total excursion ML (TOTEXML)**: Total length of the CoP path in the ML direction.

3.3 Results and Discussion

For each motor task a total of 48 trials have been considered. Representative CoP displacement for FR and SQ motor task are reported in figure 5 and 6.

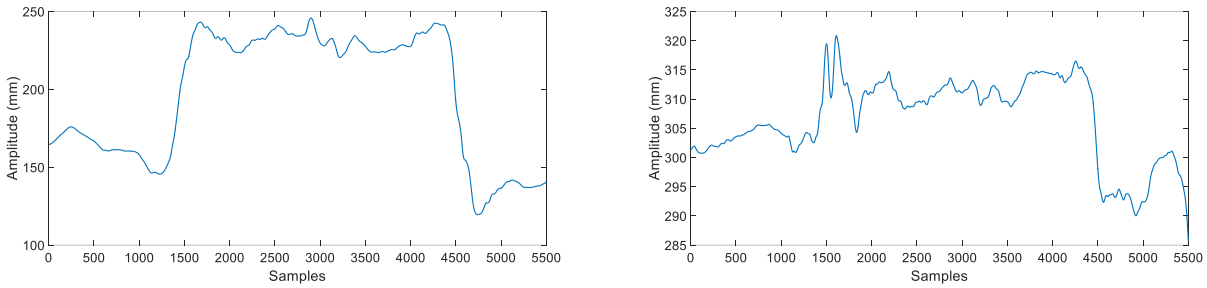

Figure 5. Representative CoP displacement in AP (left panel) and ML (right panel) directions during a FR motor task.

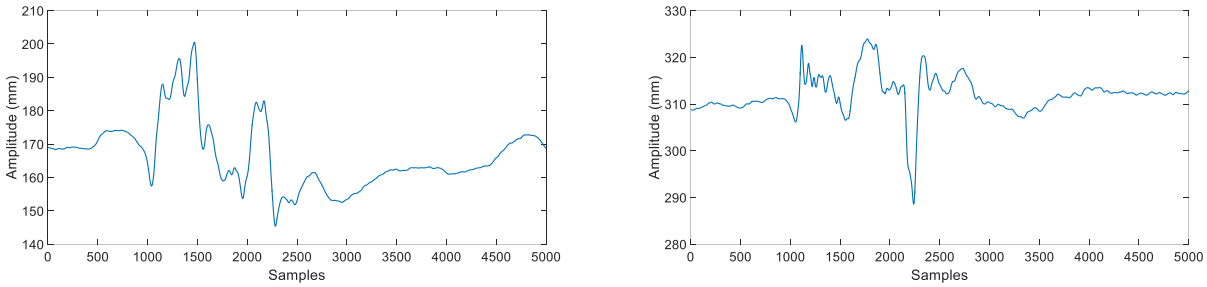

Figure 6. Representative CoP displacement in AP (left panel) and ML (right panel) directions during a SQ motor task.

The moderate range of ML displacement confirms the assumption that in the selected motor tasks the main interested CoP component is the AP one, as happens in dynamic balance tasks with a pure translational perturbation. Values of the mean percentage errors for each parameter between FP and WBB and relative to FR motor task are reported in Table 1. For each parameter, the error value remains under the 5%, apart from that relative to sway area, which reaches 5.3%. This aspect highlights a good correspondence between measures extracted from CoP components calculated from GRF signals acquired through the two devices during FR motor task, for both spatial and velocity measures. The agreement between the two devices is confirmed also considering the correlation coefficient between each couple of the same parameter values. The average correlation coefficients for each parameter are reported in Table 2, underlining also in this case a close

correspondence between the measures obtained through the two devices: in any case the correlation coefficient is higher than 0.95. When comparing measures obtained by two or more different devices or techniques the correlation coefficient, even if high, could not mean that the two methods agree: an high correlation coefficient indicates the strength of a relation between two measures, not necessarily the agreement between them (Bland and Altman, 1986). In order to give a further index about the agreement between the two measurement systems, the slope of the linear regression line has been computed for any series of measure: a perfect agreement is given only if the points reported in Figure 5 lie along the line of equality. The values of the slope, reported in Table 3, has been computed for each parameter, considering the FP and WBB data distributions.

	Functional Reach	
Parameters	**Mean value (%)**	**SD**
Mean distance	0,92	0,83
Mean distance AP	0,95	0,84
Mean distance ML	1,71	0,96
RMS distance	1,02	0,86
RMS distance AP	1,06	0,93
RMS distance ML	1,92	1,83
Range	1,84	1,75
Range AP	2,05	2,22
Range ML	2,41	1,56
Mean velocity	3,16	2,17
Mean velocity AP	3,04	2,03
Mean velocity ML	4,13	3,12
Area - CC	2,19	1,78
Area - CE	2,03	1,67
Sway area	5,30	2,18
Mean frequency	2,39	2,20
Mean frequency AP	2,26	1,49
Mean frequency ML	4,14	3,26
Fractal dimension CE	0,30	0,29
Fractal dimension CC	0,31	0,28
Fractal dimension PD	0,32	0,31
Power AP	2,30	1,99
Power ML	3,73	2,69
Power RD	2,13	1,76
Centroidal frequency AP	1,02	0,75
Centroidal frequency ML	2,32	3,41
Centroidal frequency RD	1,02	0,83
Frequency dispersion AP	1,43	1,07
Frequency dispersion ML	1,80	2,92
Frequency dispersion RD	1,49	1,40
Total excursion (TOTEX)	3,16	2,17
Total excursion AP (TOTEXAP)	3,04	2,03
Total excursion ML (TOTEXML)	3,91	2,81

Table 1. Average values of the percentage error between the FP and WBB measures, computed for each considered parameter during the FR motor task. On the right column, the relative standard deviation is reported.

	Functional Reach	
Parameters	**CC**	**P value**
Mean distance	0,99	1,00E-62
Mean distance AP	0,99	5,51E-61
Mean distance ML	0,99	1,68E-65
RMS distance	0,99	1,27E-59
RMS distance AP	0,99	6,74E-55
RMS distance ML	0,99	5,23E-64
Range	0,99	4,63E-42
Range AP	0,98	1,32E-34
Range ML	0,99	1,74E-49
Mean velocity	0,99	3,26E-46
Mean velocity AP	0,99	1,31E-50
Mean velocity ML	0,99	2,17E-38
Area Cerchio	0,99	4,63E-54
Area Ellisse	0,99	4,75E-60
Sway area	0,99	6,99E-43
Mean frequency	0,99	1,93E-54
Mean frequency AP	0,99	2,20E-59
Mean frequency ML	0,99	1,06E-39
Fractal dimension CE	0,98	5,01E-37
Fractal dimension CC	0,98	4,51E-38
Fractal dimension PD	0,98	2,66E-33
Power AP	0,99	2,24E-48
Power ML	0,99	2,77E-79
Power RD	0,99	1,99E-53
Centroidal frequency AP	0,99	2,21E-67
Centroidal frequency ML	0,99	6,08E-44
Centroidal frequency RD	0,99	1,08E-65
Frequency dispersion AP	0,99	3,10E-44
Frequency dispersion ML	0,95	7,50E-24
Frequency dispersion RD	0,99	1,63E-38
Total excursion (TOTEX)	0,98	2,33E-34
Total excursion AP (TOTEXAP)	0,98	3,77E-37
Total excursion ML (TOTEXML)	0,97	2,43E-31

Table 2. Correlation coefficients between the two measures of FP and WBB of each parameter for the FR motor task. On the right column, the relative *p* value is also reported.

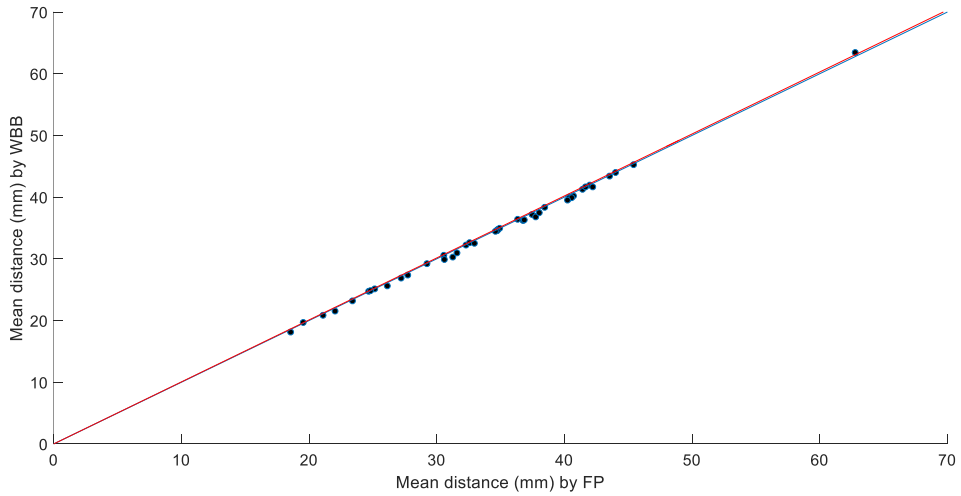

Figure 5. Representative scatter plot illustrating the relationship between parameter (mean distance) computed using the FP and WBB in the FR motor task. Line of equality (blue color) and linear fitting line (red color) are also reported.

	Functional Reach
Parameters	**Slope**
Mean distance	1,004
Mean distance AP	1,008
Mean distance ML	0,987
RMS distance	1,008
RMS distance AP	1,01
RMS distance ML	0,984
Range	0,997
Range AP	1,038
Range ML	0,963
Mean velocity	0,938
Mean velocity AP	0,934
Mean velocity ML	0,963
Area Cerchio	1,023
Area Ellisse	1,011
Sway area	1,023
Mean frequency	0,94
Mean frequency AP	0,949
Mean frequency ML	0,95
Fractal dimension CE	0,953
Fractal dimension CC	0,946
Fractal dimension PD	0,964
Power AP	1,01
Power ML	0,965
Power RD	1,018
Centroidal frequency AP	0,986
Centroidal frequency ML	0,907
Centroidal frequency RD	0,987
Frequency dispersion AP	0,995
Frequency dispersion ML	1,004
Frequency dispersion RD	0,991
Total excursion (TOTEX)	0,968
Total excursion AP (TOTEXAP)	0,951
Total excursion ML (TOTEXML)	1,001

Table 3. Slope of the linear fitting line between parameters values computed from FP CoP and WBB CoP. A perfect agreement between the two measures is present if the slope is equal to 1.

Values reported in Table 3 show a high degree of agreement between parameter values computed by FP and WBB data, with linear fitting line slopes close to 1 for all the considered measures.

The same kind of information has been evaluated for the SQ motor task. Also in this case the percentage error computed considering the FP measure as the true measure not overtakes 6% (sway area) and presents low values for distance, velocity and frequency parameters (Table 4), as in the case of FR motor task. The correlation coefficients, reported in Table 5, confirm a high correlation between parameters extracted from FP and WBB CoP, with values in any case not lower than 0.90. Eventually, as in the case of the former motor task and for the same reasons, also for the SQ motor task the slope of the linear fitting line (Fig. 6) has been evaluated for each parameter couple; as

reported in Table 6 these values are close to the unit, highlighting once more a good correspondence between CoP-related measures extracted from FP and WBB GRF signals.

	Squat	
Parameters	**Mean value (%)**	**SD**
Mean distance	1,87	1,45
Mean distance AP	2,22	1,82
Mean distance ML	1,52	1,33
RMS distance	2,24	1,72
RMS distance AP	2,55	2,05
RMS distance ML	1,79	1,42
Range	4,17	3,26
Range AP	4,59	3,44
Range ML	3,05	2,23
Mean velocity	5,18	2,94
Mean velocity AP	5,61	3,17
Mean velocity ML	3,18	2,28
Area - CC	5,00	3,68
Area - CE	4,51	3,40
Sway area	6,00	4,12
Mean frequency	3,95	4,01
Mean frequency AP	4,98	3,04
Mean frequency ML	2,24	1,61
Fractal dimension CE	0,55	0,75
Fractal dimension CC	0,59	0,76
Fractal dimension PD	0,38	0,44
Power AP	5,09	3,80
Power ML	4,02	3,09
Power RD	4,42	3,25
Centroidal frequency AP	3,56	2,60
Centroidal frequency ML	1,89	1,50
Centroidal frequency RD	3,40	2,29
Frequency dispersion AP	1,74	1,99
Frequency dispersion ML	0,63	0,54
Frequency dispersion RD	1,39	1,79
Total excursion (TOTEX)	5,18	2,94
Total excursion AP (TOTEXAP)	5,75	3,25
Total excursion ML (TOTEXML)	3,18	2,28

Table 4. Average values of the percentage error between the FP and WBB measures, computed for each considered parameter during the SQ motor task. On the right column, the relative standard deviation is reported.

	Squat	
Parameters	**CC**	**P value**
Mean distance	0,98	8,85E-38
Mean distance AP	0,98	5,51E-36
Mean distance ML	0,99	1,53E-59
RMS distance	0,98	7,97E-32
RMS distance AP	0,97	1,01E-30
RMS distance ML	0,99	6,11E-61
Range	0,98	8,47E-32
Range AP	0,97	1,42E-30
Range ML	0,99	1,02E-55
Mean velocity	0,99	2,15E-43
Mean velocity AP	0,99	2,58E-38
Mean velocity ML	0,99	2,99E-44
Area - CC	0,95	1,01E-24
Area - CE	0,96	5,83E-27
Sway area	0,99	2,93E-39
Mean frequency	0,99	3,03E-38
Mean frequency AP	0,98	4,64E-38
Mean frequency ML	0,99	1,06E-44
Fractal dimension CE	0,98	5,83E-33
Fractal dimension CC	0,98	7,84E-33
Fractal dimension PD	0,97	2,61E-30
Power AP	0,95	2,13E-24
Power ML	0,99	1,26E-59
Power RD	0,96	1,48E-26
Centroidal frequency AP	0,98	3,34E-34
Centroidal frequency ML	0,99	1,56E-52
Centroidal frequency RD	0,99	1,24E-39
Frequency dispersion AP	0,96	1,28E-26
Frequency dispersion ML	0,99	1,54E-51
Frequency dispersion RD	0,96	1,94E-25
Total excursion (TOTEX)	0,98	7,84E-38
Total excursion AP (TOTEXAP)	0,98	2,57E-35
Total excursion ML (TOTEXML)	0,99	3,17E-39

Table 5. Correlation coefficients between the two measures of FP and WBB of each parameter for the SQ motor task. On the right column, the relative *p* value is also reported.

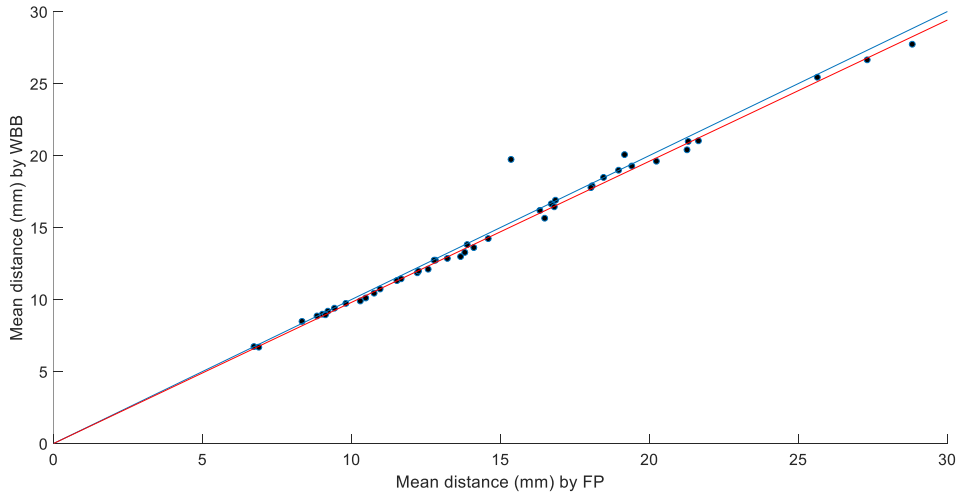

Figure 6. Representative scatter plot illustrating the relationship between parameter (mean distance) computed using the FP and WBB in the SQ motor task. Line of equality (blue color) and linear fitting line (red color) are also reported.

	Squat
Parameters	Slope
Mean distance	0,98
Mean distance AP	0,988
Mean distance ML	0,986
RMS distance	1,004
RMS distance AP	1,018
RMS distance ML	0,976
Range	0,989
Range AP	1,01
Range ML	0,96
Mean velocity	0,867
Mean velocity AP	0,858
Mean velocity ML	0,907
Area - CC	1,011
Area - CE	0,984
Sway area	0,878
Mean frequency	0,953
Mean frequency AP	0,94
Mean frequency ML	0,983
Fractal dimension CE	1,032
Fractal dimension CC	1,017
Fractal dimension PD	0,997
Power AP	1,007
Power ML	0,945
Power RD	0,989
Centroidal frequency AP	0,964
Centroidal frequency ML	0,964
Centroidal frequency RD	0,942
Frequency dispersion AP	1,014
Frequency dispersion ML	0,977
Frequency dispersion RD	1,016
Total excursion (TOTEX)	0,926
Total excursion AP (TOTEXAP)	0,914
Total excursion ML (TOTEXML)	0,951

Table 6. Slope of the linear fitting line between parameters values computed from FP CoP and WBB CoP. A perfect agreement between the two measures is present if the slope is equal to 1.

A further way to compare the goodness of agreement between two measurement methods or techniques is that proposed by Bland and Altman (1986), where the average values of the two measures obtained by the two different methods, considered as an estimate of the unknown true value, are examined with respect to the mean difference between the two measures. This graphical representation allows to evaluate the existence of any systematic difference between the measurements and in the present case Bland-Altman plots have been evaluated for each considered CoP-related parameter, for both FR and SQ motor task. The Bland-Altman plots of four parameters are reported (Fig. 7 and 8), chosen as representative of distance parameters, velocity parameters and frequency parameters, in order to give a representative view for each the different kind of parameter.

The same behavior is shown by all the parameters and thus not all the 35 Bland-Altman plots are reported for either motor task.

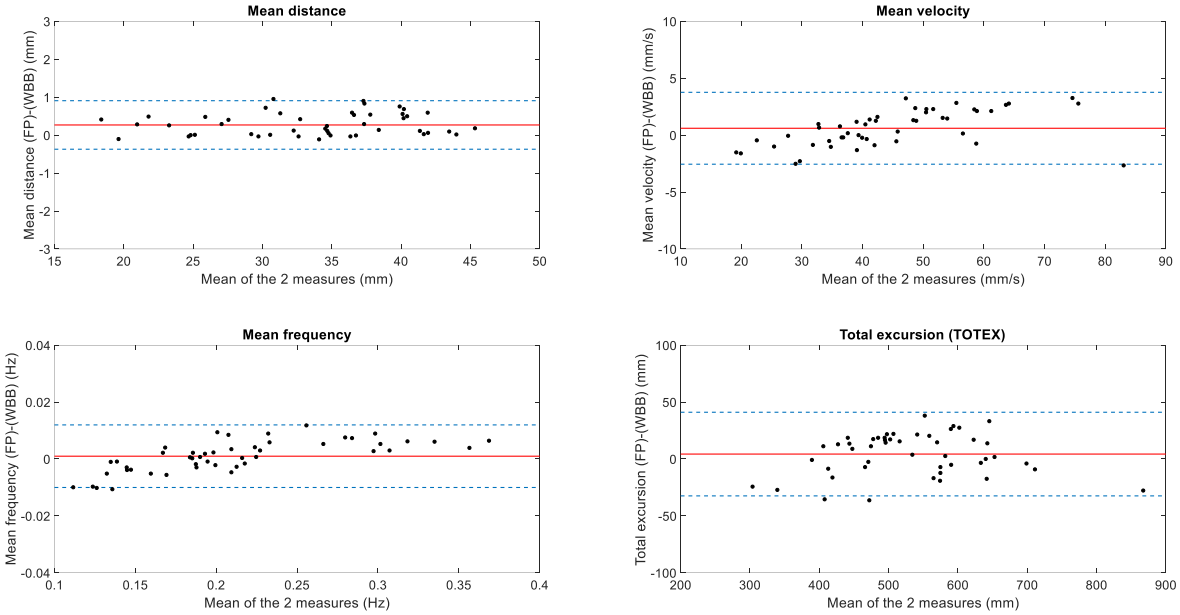

Figure 7. Bland-Altman plots of four parameters computed for FR motor task. Horizontal red line represents the mean value of the difference between FP and WBB measures, whereas the horizontal, dashed blue lines define the confidence interval (±1.96·SD).

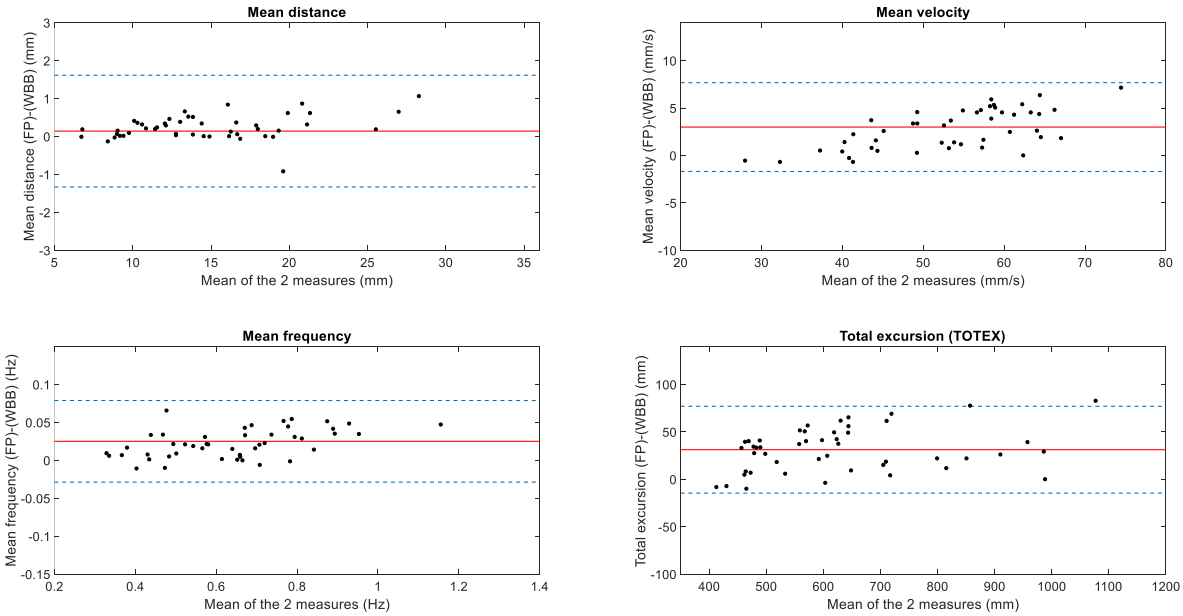

Figure 8. Bland-Altman plots of four parameters computed for SQ motor task. Horizontal red line represents the mean value of the difference between FP and WBB measures, whereas the horizontal, dashed blue lines define the confidence interval (±1.96·SD).

In both FR and SQ motor task and for all the considered parameters, data distributions lie close to the mean difference between the two platforms and in any case are bound in the confidence area defined by the mean difference value ±1.96·SD. As indicated previously this random spread error characterizes all the 35 considered parameters, pointing out the absence of a proportional bias and thus the two devices seem to agree equally through the measurement range. (Bland and Altman, 1986).

The evaluation performed in this part of the work, about whether the use of a commercial and low cost device for the measurement of the GRF during dynamic motor tasks is acceptable, indicated that the WBB and its related measures have a good agreement with those computed using a laboratory grade FP. Results for both the motor task performed by the subjects show the same trend: the mean percentage error of the WBB measures (Table 1 and 4) respect to the FP ones for all the considered parameters presents values under the 6.0% for both motor tasks, with the exception of sway area (6.0% for SQ motor task). The correlation coefficients between every two measures (Table 2 and 5) are much higher than 0.90 and the slope of the linear fitting line between each couple of measure has its higher difference respect to the unit in the case of the SQ mean velocity AP (0.142); for all the other parameters and for both motor task the difference remains bounded by this value. The concurrence of these aspects show a high degree of agreement between the measures obtained through the two different devices, in terms of the WBB deviation respect to the FP reference and for all kind of parameters (distance, velocity and frequency related parameters). The eventual evaluation of the Bland-Altman plots (Fig. 7 and 8) confirms a good correspondence between the WBB and FP measures, with no systematic difference between the measurements for all the 35 considered CoP parameters. These outcomes seem in agreement with those reported by Abujaber *et al.* (2015), that evaluated WBB reliability in a dynamic motor task (sit-to-stand).

The results of the WBB evaluation show an overall good agreement with the FP, that supports the possibility to use the WBB in order to measure GRF in motor task with a faster and larger CoP displacements respect to those obtained in standing balance tasks. The WBB presents several

limitations as a low sample rate, an inconsistent sampling interval, the impossibility to measure the AP and ML force components and a limited maximum load. Although these aspects restrict the use of this device for a complete replacement of classical FP, however the WBB appeared sufficiently accurate for quantifying CoP trajectory and the related parameters in dynamic motor tasks where the main CoP displacement is in the AP direction and thus its use for the type of experimental setup employed in the present study appears suitable.

Chapter References

Abujaber S., Gillispie G., Marmon A., Zeni Jr. J., "Validity of the Nintendo Wii Balance Board to assess weight bearing asymmetry during sit-to-stand and return-to-sit task", *Gait and Posture*, 2015.

Bartlett H.L., Ting L.H., Bingham J.T., "Accuracy of force and center of pressure measures of the Wii Balance Board", *Gait and Posture*, 2014.

Bland J.M., Altman D.G., "Statistical methods for assessing agreement between two methods of clinical measurement", *The Lancet*, 1986.

Chen H.L., Yeh C.F., Howe T.H., "Postural control during standing reach in children with Down syndrome", *Research in Developmental Disabilities*, 2015.

Clark R.A., Bryant A.L., Pua Y., McCrory P., Bennell K., Hunt M., "Validity and reliability of the Nintendo Wii Balance Board for assessment of standing balance", *Gait and Posture*, 2010.

De Lima Pardini A.C., Papegaaij S., Cohen R.G., Teixeira L.A., Smith B.A., Horak F.B., "The interaction of postural and voluntary strategies for stability in Parkinson's disease", *Journal of Neurophysiology*, 2012.

Dionisio V.C., Almeida G.L., Duarte M., Hirata R.P., "Kinematic, kinetic and EMG patterns during downward squatting", *Journal of Electromyography and Kinesiology*, 2008.

Gray V.L., Ivanova T.D., Garland S.J., "Control of fast squatting movements after stroke", *Clinical Neurophysiology*, 2012.

Kim J.W., Kwon Y., Ho Y., Jeon H.M., Bang M.J., Jun J.H., Eom G.M., Park B.K., Cho Y.B., "Age–gender differences in the postural sway during squat and stand-up movement", *Bio-Medical Materials and Engineering*, 2014.

Huang M.H., Brown S.H., "Effects of task context during standing reach on postural control in young and older adults: A pilot study", *Gait and Posture*, 2015.

Huurnink A., Fransz D.P., Kingma I., van Dieen J.H., "Comparison of a laboratory grade force platform with a Nintendo Wii Balance Board on measurement of postural control in single-leg stance balance tasks", *Journal of Biomechanics*, 2013.

Leach J.M., Mancini M., Peterka R.J., Hayes T.L., Horak F.B., "Validating and Calibrating the Nintendo Wii Balance Board to Derive Reliable Center of Pressure Measures", *Sensors*, 2014.

Park D.S., Lee G., "Validity and reliability of balance assessment software using the Nintendo Wii balance board: usability and validation", *Journal of Neuroengineering and Rehabilitation*, 2014.

Prieto T.E., Myklebust J.B., Hoffman R.G., Lovett E.G., Myklebust B.M., "Measures of Postural Steadiness: Differences Between Healthy Young and Elderly Adults", *IEEE Transaction on Biomedical Engineering*, 1996.

Tsai Y.C., Hsieh L.F., Yang S., "Age-related changes in posture response under a continuous and unexpected perturbation", *Journal of Biomechanics*, 2014.

Chapter 4
Results

In this chapter are reported the results of kinematic, dynamic and electromyography evaluation performed on each type of posturgraphy trial. For each test condition (fixed velocity, increasing velocity, sensory deprivation) the computed parameters regarding CoP and CoM that showed a clear, repeatable and significant trend are reported in this section, split on the basis of perturbation direction (backward and forward).

4.1 Fixed velocity

The AP component of both CoP and CoM showed, in all trials and for all subjects, a characteristic displacement with two peaks, corresponding to the maximum anterior displacement after the perturbation onset and the maximum posterior displacement reached during the counterbalance period (Fig. 1). Due to this repeatability, hereafter the maximum and minimum peaks will be indicated as the first peak and the second peak respectively. The entire CoP and CoM displacement, from 1 s before the perturbation onset and 3 s after the perturbation offset, has been divided in four temporal periods (Fig. 1) and each of the CoP-CoM-related parameters refer to one of this periods.

The CoP temporal parameters, i.e. the first peak time (FPT) and the inter-peaks time (IPT), results showed a quasi-static value of the FPT throughout the trials (Fig. 2), with the exception of the first one that presented a value of 372±85 ms, whereas in the remaining trails the higher value was 352±76 ms (4^{th} trial). On the contrary the IPT (Fig. 2) had a slightly decreasing value from the second trial (467±104 ms to 448±131 ms), with a significant higher value in the first one (571±169 ms). For what concerns the amplitude and spatial parameters the first and second peak amplitude (FPA and

SPA) showed a clear decrease of the SPA and values never beyond 0.50 (Fig. 2). This trend is confirmed also by the first and second peak space (FPS and SPS, fig. 3). Eventually also the inter-peaks space had a decreasing trend throughout the trials, whereas the movement displacement (MD) presented similar values from the first to the last trial (0.49 to 0.52, fig. 3).

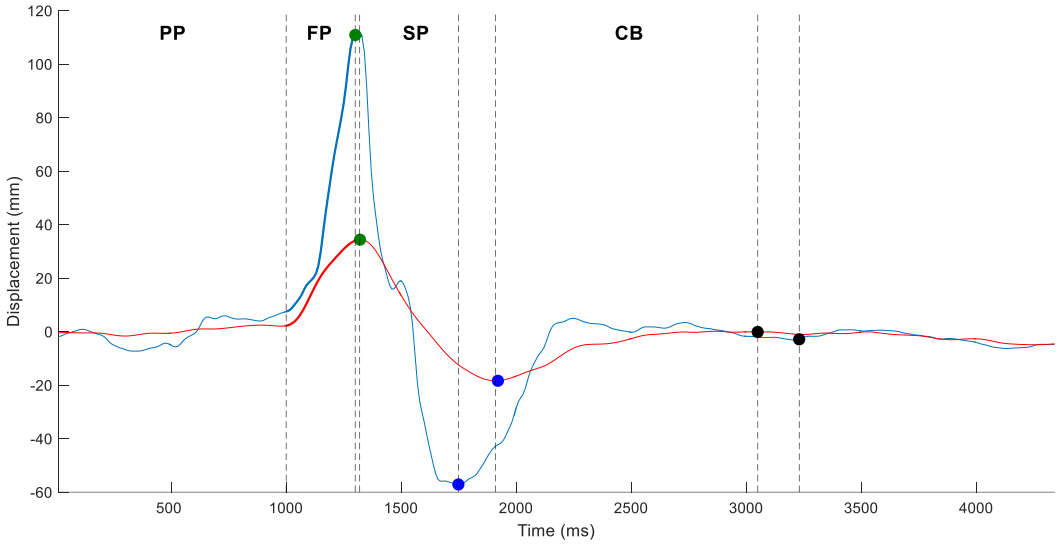

Figure 1. Representative AP CoP (blue line) and CoM (red line) displacement in a fixed velocity backward trial. Green dots points out the maximum displacement (first) peak, whereas the blue and black dots indicate the minimum displacement (second) peak and the steady state reaching point. Pre-perturbation (PP), first peak (FP), second peak (SP) and the counterbalance (CB) time periods are also reported, divided by vertical dashed lines. Positive values of displacement indicate anterior direction whereas negative ones stand for posterior direction.

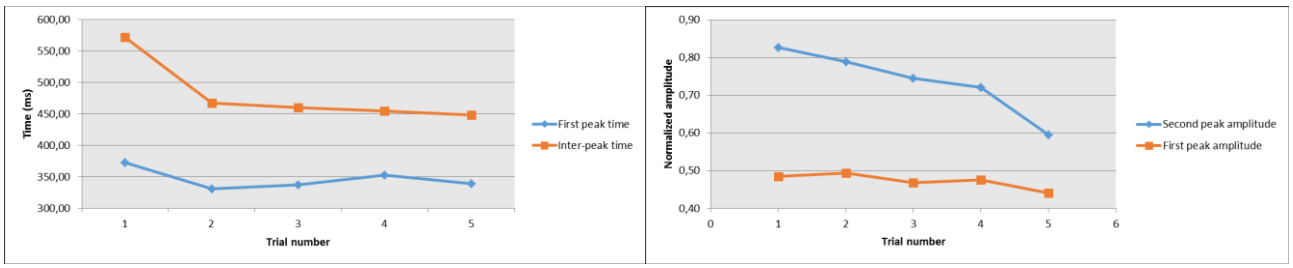

Figure 2. CoP first peak time and inter-peaks time values throughout the trials (left panel) and first and second peak amplitude (right panel).

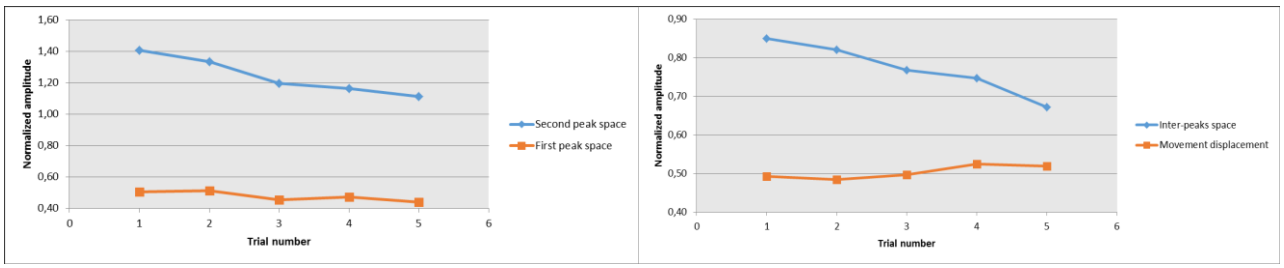

Figure 3. CoP first and second peak space (left panel) and inter-peaks space and movement displacement (right panel).

For what concerns the CoM, the IPT showed a trend similar to that of CoP, with an higher first value (1015±527 ms) and then a decreasing linear tendency (Fig. 4). Also for the FPA and SPA the CoM evolution was similar to the CoP, with a higher FPA first value (0.29) and the others with similar values (0.18 to 0.17) and a decreasing SPA (from 0.36 to 0.21, fig. 4). The FPS, SPS and IPS (Fig. 5) presented limited variations throughout the trials (FPS, from 0.22 to 0.18) and a decreasing tendency (SPS and IPS) that mirrors that of the CoP (Fig. 3).

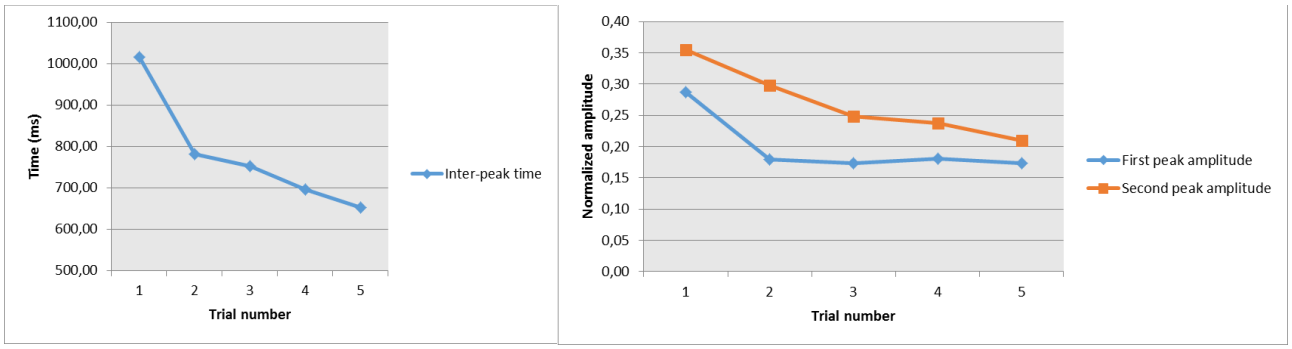

Figure 4. CoM inter-peaks time (left panel) and first and second peak amplitude.

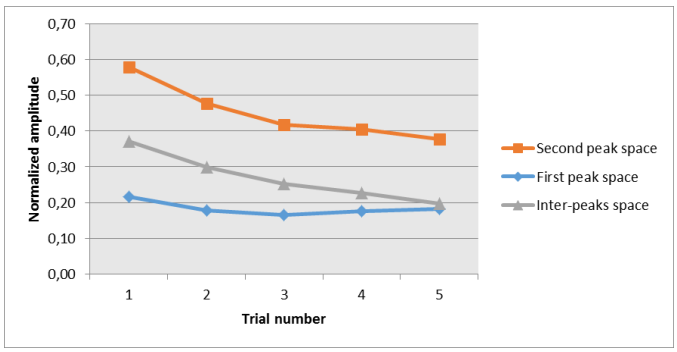

Figure 5. CoM first, second and inter-peaks space

The CoP-CoM curve (Fig. 6) for the fixed velocity backward test presented a significantly higher CoP/CoM inter-peaks amplitude (CCIPA) in the first trial (104±98 mm) and from the second a linear decreasing tendency, from 65±18 mm to 49±15 mm (Fig. 7), whereas the area under the curve, computed during the perturbation period (Fig. 6) and the positive portion of this area both showed increasing values throughout the trials (Fig. 7). Consistently the negative portion of the area showed a decreasing trend (Fig. 7) The CoP/CoM inter-peaks time (CCIPT) though did not present a

significant trend from the first to the last trial: CoP and CoM reach the first peak not always in the same order, with the CoP that anticipates the CoM or vice versa in a non-systematic or repeatable way throughout the trials.

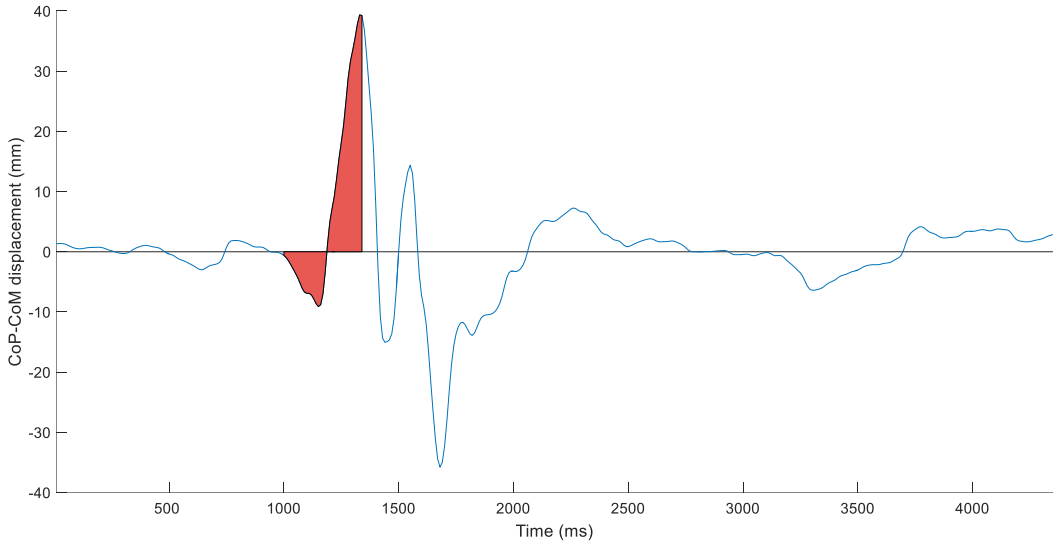

Figure 6. Representative CoP-CoM curve. Also in this case the curve is considered from 1 s before perturbation onset to 3 s after perturbation offset. Area under the curve during the platform movement is highlighted by red color. Positive values of displacement indicate anterior direction whereas negative ones stand for posterior direction.

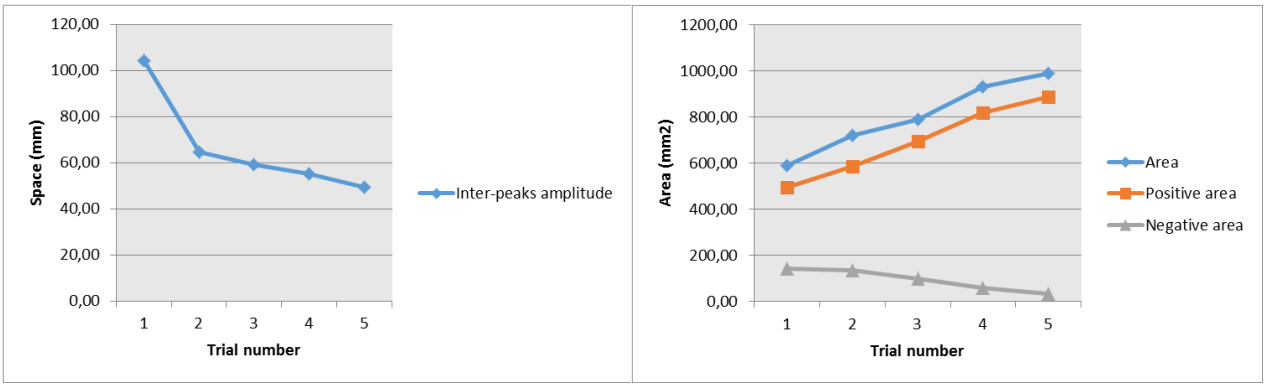

Figure 7. Inter-peaks amplitude between CoP and CoM (left panel) and area under the CoP-CoM curve during the perturbation (right panel) with its positive and negative components.

Eventually, also the temporal interval during which both CoP and CoM reached a steady state after the perturbation offset (steady-state time, SST), defined as reported in Methods section, has been considered (Fig. 8). CoM SST was greater respect to the CoP one in all the five trials, with a limited range of variation, from a minimum of 153±46 ms (2nd trial) to a maximum of 159±30 ms (5th

trial). CoP SST however showed a tidy decreasing trend from the first to the last trial (Fig. 8), from 154±31 ms to 140±13 ms.

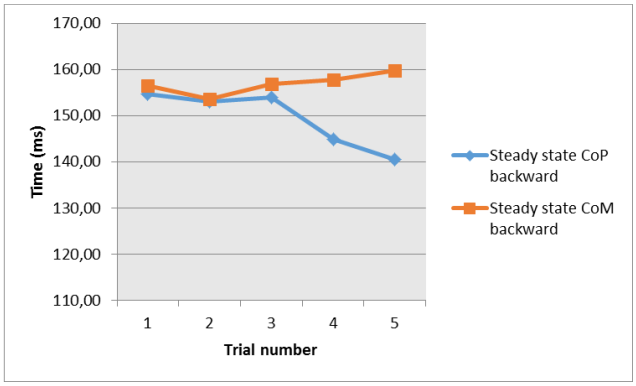

Figure 8. Steady-state reaching time for CoP and CoM in backward perturbation test.

Angular range of variation for backward trials, computed during perturbation time, appeared significantly higher in the first trial for all the considered joints, whereas they lay on similar values during the remaining trials (Fig. 9). For the inter-joint coordination, an ellipse embracing the 95% of the values of the angle-angle plot (Fig. 10) for ankle, knee and hip has been computed (see Methods section). The ellipse area value, axes length and the axes ratio appeared not useful to a clear estimate of which joint, and consequently which balance strategy, played the major role in maintaining balance after the perturbation onset. However, the fitted ellipse slope computed for the ankle-knee, ankle-hip and knee-hip couples appeared to indicate well the preponderance of one joint respect to the considered other one. Thus, based on the ellipse slope, postural strategies have been defined in each trial as percentage of total subject (Fig. 10).

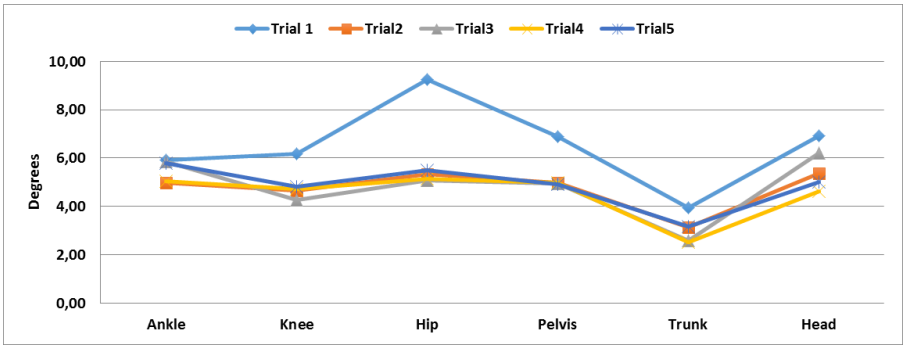

Figure 9. Angular range variation for all the considered joints.

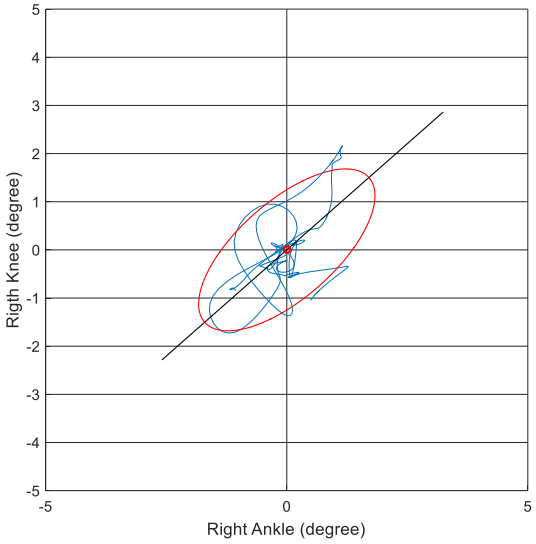

Figure 10. Representative calculation of the ankle joint angle versus knee joint angle (blue line). Superimposed are represented the 95% fitted ellipse (red line) and the line identifying the relative slope (black line).

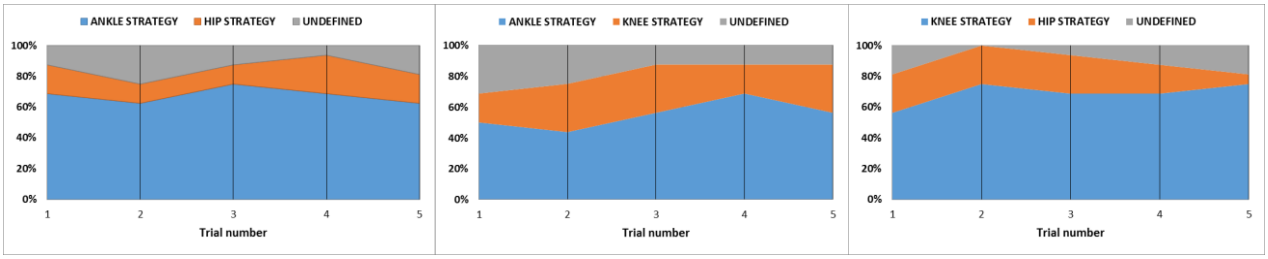

Figure 11. Evaluation of ankle versus hip (left panel), ankle versus knee (central panel) and knee versus hip (right panel). Columns heights represent the percentage of total subjects where a joint strategy has been detected. Grey columns indicate the number of subject where none of the two strategies has been clearly recognized.

The ankle-strategy was the most recurrent among both hip and knee; however, knee-strategy seems to be more recurrent than the hip-strategy respect to ankle (Fig. 11 left and central panel) and also directly compared to the hip (Fig. 11 right panel).

Forward perturbation trials appeared harder to be characterized by means of dynamic related parameters. CoP and CoM waveform displacements were characterized by the same double peak behavior observed in backward trials. Obviously first and second peak resulted in reverse directions respect of the backward trials, with the first peak in posterior direction and the second peak in anterior direction (Fig. 12).

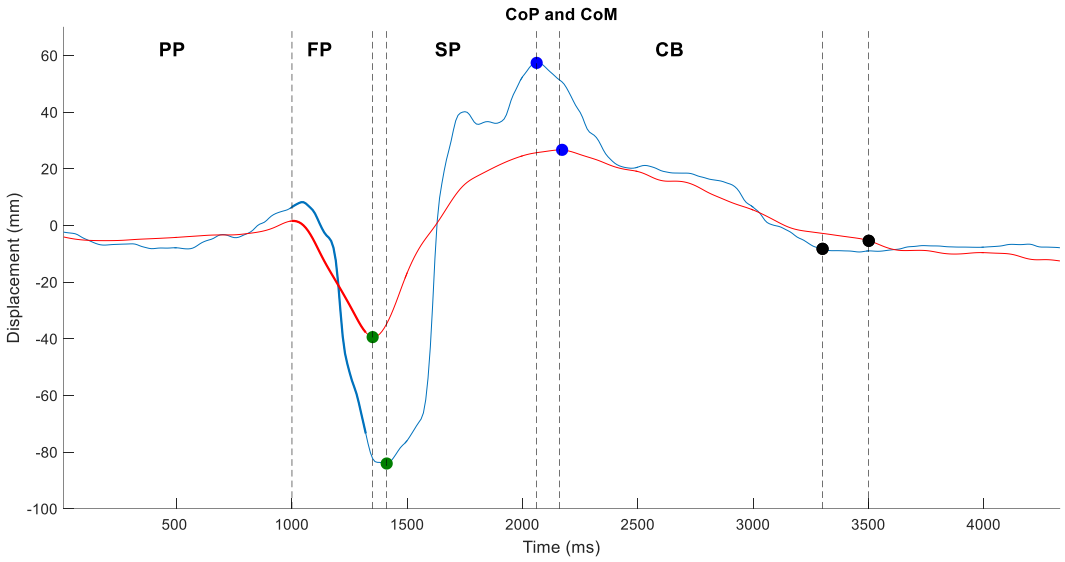

Figure 12. Representative AP CoP (blue line) and CoM (red line) displacement in a fixed velocity forward trial. Green dot points out the maximum displacement (first) peak, whereas the blue and black dots indicate the minimum displacement (second) peak and the steady state reaching point. Pre-perturbation (PP), first peak (FP), second peak (SP) and the counterbalance (CB) time periods are also reported, divided by vertical dashed lines. Positive values of displacement indicate posterior direction whereas negative ones stand for anterior direction.

CoP presented a slightly decreasing trend for the FPT and a substantially constant trend, except for the higher first value, for the IPT (Fig. 13). The FPA presented a quasi-static a value throughout the trials, from 0.36 to 0.42 and the same trend is followed by the SPA, from 0.71 to 0.67 (Fig. 13). Moreover, both the SPS and IPS showed a high value during the first trial and then values significantly lower than the first and bounded in a 0.05 interval (Fig. 14).

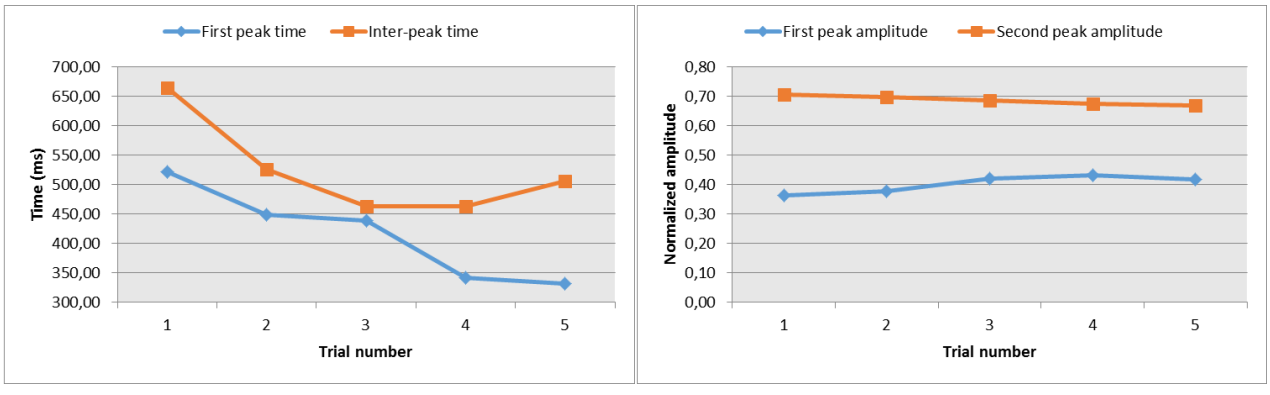

Figure 13. Time (left panel) and amplitude of the first and second peak of CoP.

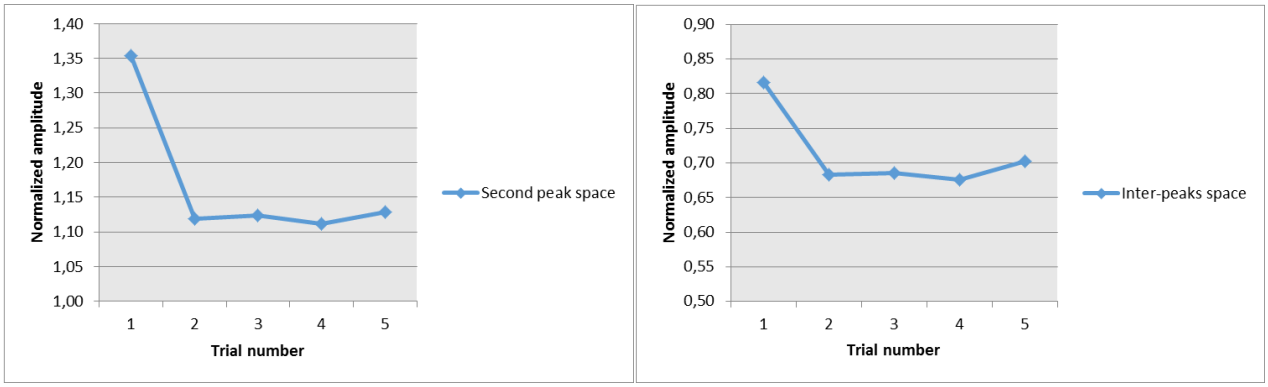

Figure 14. CoP second peak space (left panel) and inter-peak space (right panel).

For what concerns CoM, it presented a decreasing FPT and IPT throughout the trials (Fig. 15) and a decreasing SPA and IPS, whereas the FPA remained unchanged from the first to the last trial, bounded from 0.15 to 0.17 (Fig. 16).

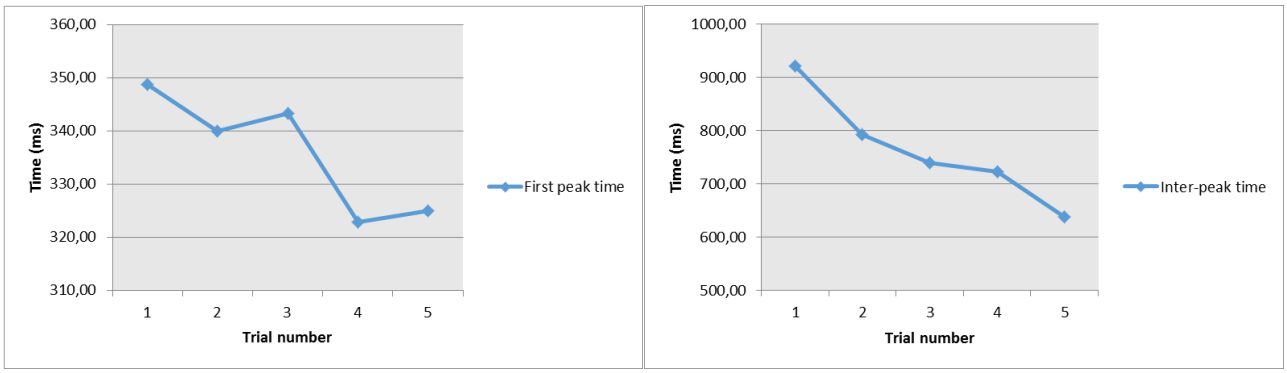

Figure 15. CoM first peak time (left panel) and inter-peak time (right panel).

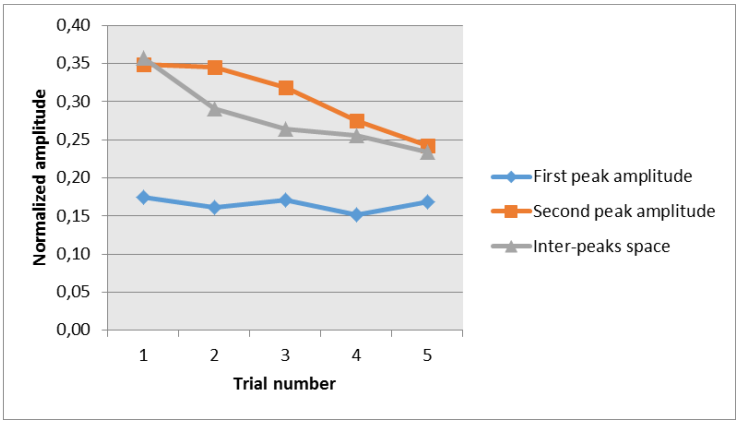

Figure 16. CoM first and second peak amplitude and inter-peaks space.

The CoP-CoM curve presented in forward perturbation test a clear increasing trend for the IPA, moving from an initial value of 36.6±9 mm to a final value of 54.0±22 mm (Fig. 17), thus showing an opposite behavior respect to the backward perturbation test. A different trend respect to the backward configuration is recognizable also regarding the area under the CoP-CoM curve computed during the platform movement appeared, that not presented a clear evolution throughout the forward perturbation trials (Fig. 17).

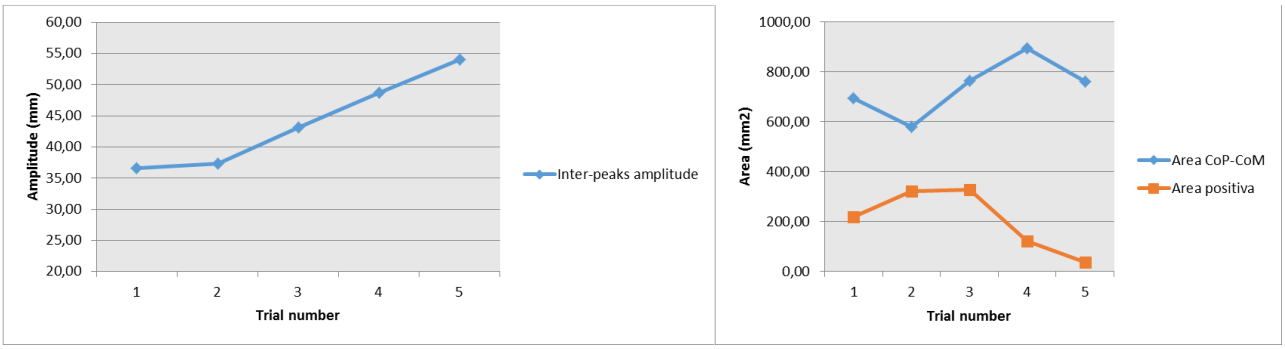

Figure 17. Inter-peaks amplitude between CoP and CoM (left panel) and area and its positive part of the Cop-CoM curve.

In forward condition, the SST for both CoP and CoM showed a decreasing trend throughout the trials, in partial contrast with what has been observed in backward configuration, but with higher values for the CoM SST respect to those of CoP (Fig. 18), in agreement with the backward behavior (Fig. 8).

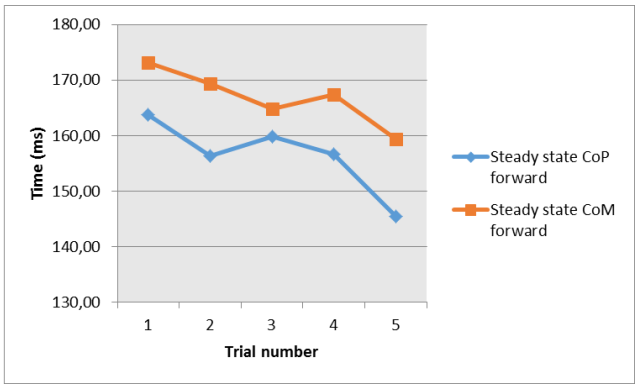

Figure 18. Steady-state reaching time for CoP and CoM in backward perturbation test.

Angular range variations for forward trials, computed during perturbation time, showed higher values for ankle and knee joints during the first trial, whereas the other joints presented angular range variations comparable in all the five trials (Fig. 19). In order to evaluate the inter-joint coordination an ellipse embracing the 95% of the values of the angle-angle plot has been computed for ankle, knee and hip joint, as in the case of backward perturbation. The ellipse area value, axes length and the axes ratio appeared also in the forward configuration not useful to estimate clearly which joint, and consequently which balance strategy, played the major role in maintaining balance after the perturbation onset. Thus, the fitted ellipse slope computed for the ankle-knee, ankle-hip and knee-hip couples has been considered in order to obtain an indication of the preponderance of one joint respect to the considered other one. Thus, based on the ellipse slope, postural strategies have been defined in each trial as percentage of total subject (Fig. 20).

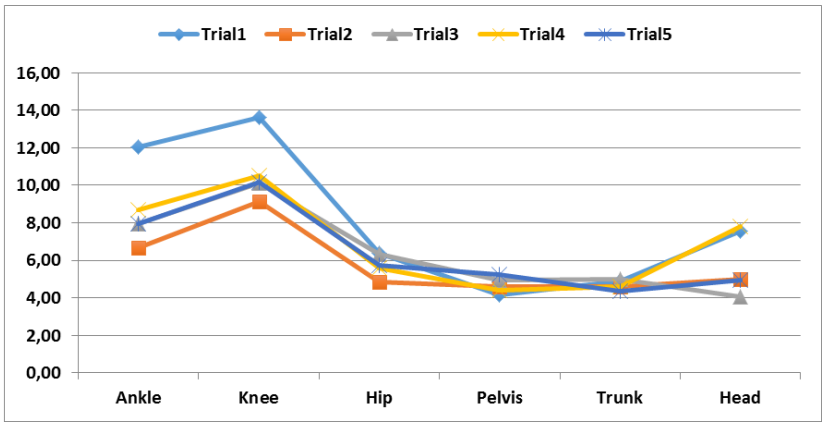

Figure 19. Angular range variation for all the considered joints.

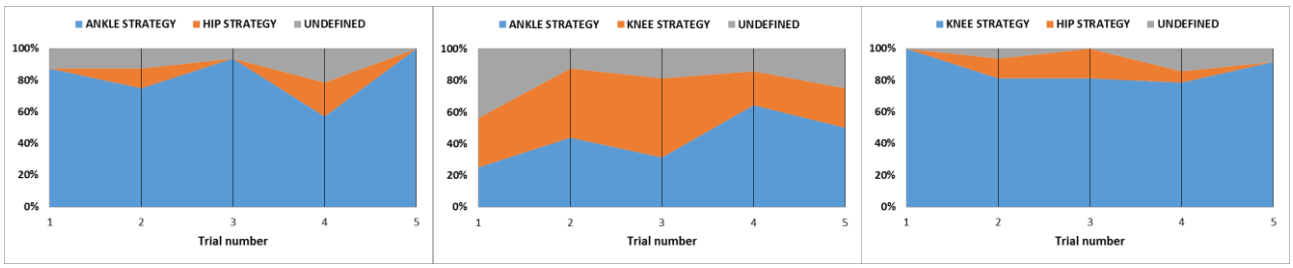

Figure 20. Evaluation of ankle versus hip (left panel), ankle versus knee (central panel) and knee versus hip (right panel). Columns heights represent the percentage of total subjects where a joint strategy has been detected. Grey columns indicate the number of subject where none of the two strategies has been clearly recognized.

Ankle strategy appeared the most employed respect to the hip strategy (Fig. 20, left panel) in all the considered trials. However, knee strategy in the forward case seemed to have an equal weight respect to the ankle one (Fig. 20, central panel) and moreover knee strategy showed a strong prevalence in terms of subjects who employed it if compared to the hip strategy (Fig. 20, right panel).

A direct comparison between backward and forward trial blocks has been performed for CoM initial and ending position (Fig. 21), temporal interval between perturbation onset and CoP-CoM overtaking (Fig. 22) and the steady state reaching time for both CoP and CoM.

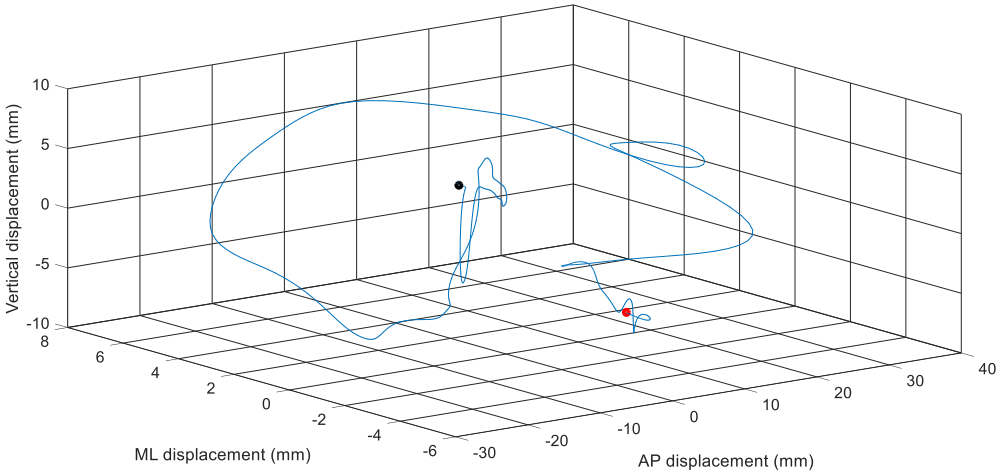

Figure 21. Representative CoM movement during backward trial. Positive values stand for anterior displacement, whereas negative indicate posterior displacement. Blue dot represents CoM position at perturbation onset, red dot represents CoM position when steady state has been reached.

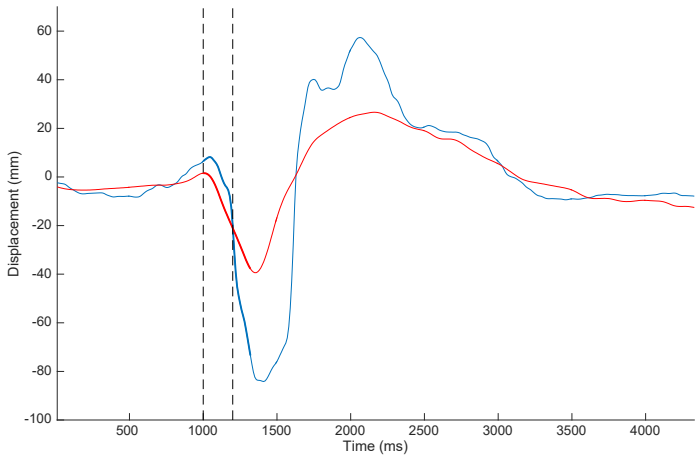

Figure 22. Representation of temporal interval between the perturbation onset (first dashed line) and CoP overtaking of CoM (second dashed line). Blue line represents CoP AP displacement, whereas red line represents CoM AP displacement.

The CoM distance between initial and final position appeared lower in forward trial block respect to the backward (Fig. 23, left panel), even though they showed close values throughout the trials: backward CoM varied from a minimum of 17.5±5.1 mm to 21.0±9.5 mm, whereas the forward CoM was bounded between 13.4±3.2 mm and 19.1±8.7 mm. The time of the CoP-CoM overtake showed a strong relation with the perturbation direction, with values in forward configuration significantly higher than those observed during backward perturbations (Fig. 23, right panel).

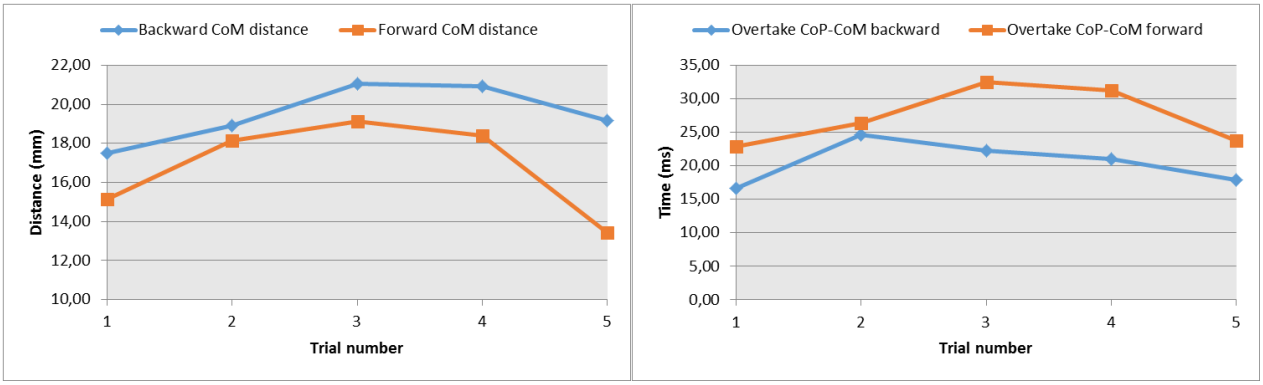

Figure 23. CoM distance between initial and final position (left panel) and time interval between perturbation onset and CoP overtaking of CoM (right panel).

The steady state achievement for CoP resulted higher in all the trials in forward configuration respect to the backward (Fig. 24, left panel) and with a clear decreasing trend throughout the trials in both backward and forward configurations. Considering the CoM it showed lower values of the steady state time in backward trials respect to the forward ones, without a clear increasing or decreasing trend (Fig. 24, right panel).

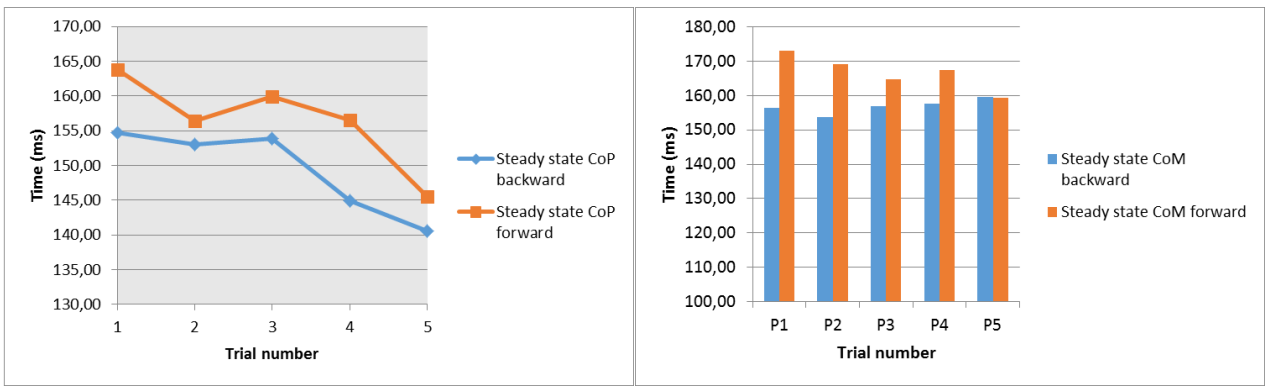

Figure 24. Steady state time for CoP (left panel) and CoM (right panel) in backward and forward configuration.

Comparing the angular joints range between backward and forward tests, for all the trials the ankle and knee resulted significantly higher in forward trials respect to the backward ones (Fig. 25), whereas the hip range of angular variation showed a higher value for the first trial in backward configuration and similar values between backward and forward for the remaining trials.

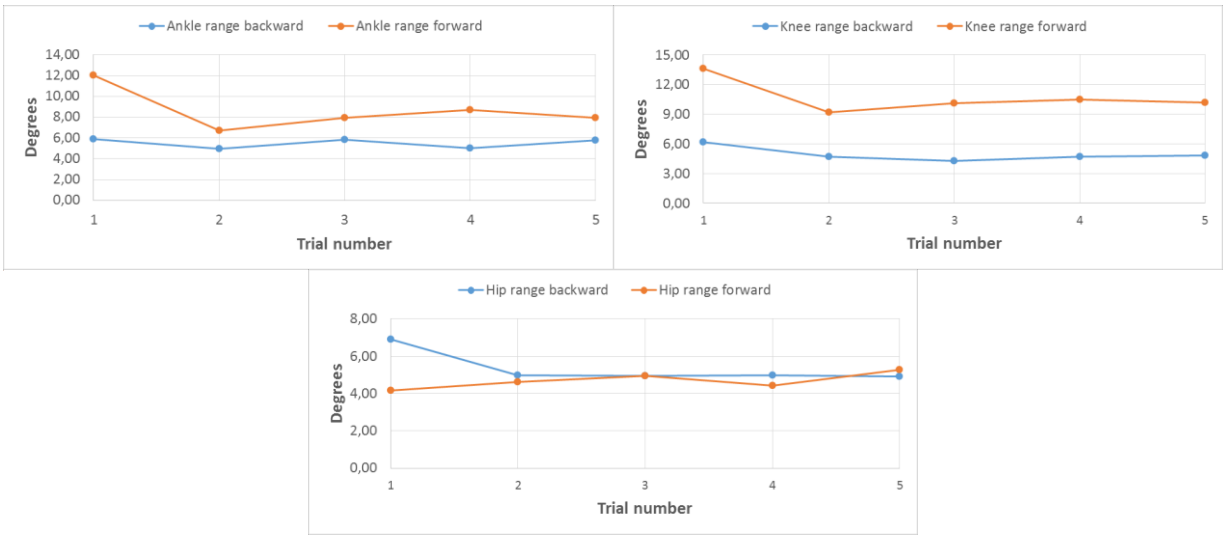

Figure 25. Angular range of variation for ankle (top left panel), knee (top right panel) and hip (bottom panel) in backward and forward trials block.

Activity of the acquired muscles (Tibialis Anterior, TA, Gastrocnemius Medialis, GAS, Vastus Medialis, VM, Rectus Femoris, FR, Biceps Femoris, BCF, Erector Spinae, ERSL) has been quantified in terms of temporal latency between perturbation onset and muscular activation onset (Fig. 26). Due to the high degree of variability in terms of muscular activation and deactivation during the entire posturography trial, only the onset latency has been quantified, because muscular deactivation resulted not always within the perturbation period and moreover myoelectric activity can last for the entire acquisition period (Fig. 26, right panel).

For what concerns backward perturbations, GAS showed a significantly lower latency throughout the trials, followed by the TA. Conversely, the ERSL presented the higher latency in all the considered trials (Fig. 27, left panel). Thigh muscles had similar latency values between them and respect to the trial series. Considering the muscles activation sequence, for backward trials the GAS shorter latency was confirmed and moreover appeared a clear bottom-up activation sequence, where

the first muscular bursts are those of ankle muscles (TA and GAS), thigh muscles seemed to have a similar activation timing higher than ankle muscles but lower respect to the ERSL, which was the last activating muscle. (Fig. 27, left and right panel).

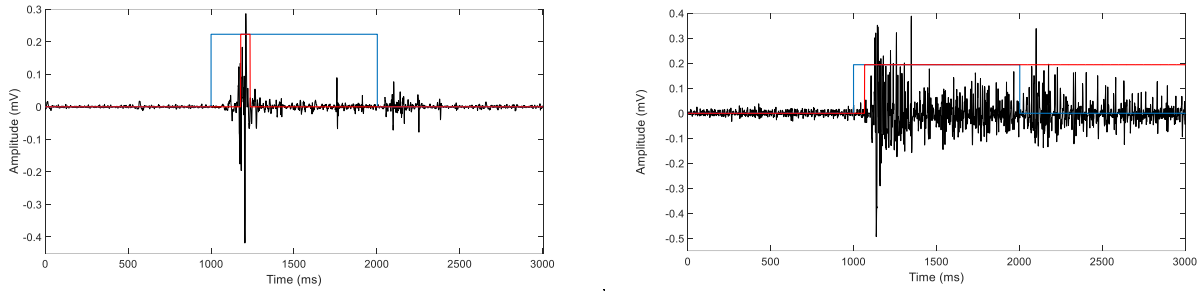

Figure 26. Representative muscular activity during a perturbed posturography trial of ERSL (left panel) and RF (right panel). Temporal latency has been quantified as the time interval between the perturbation onset (red line) and the muscular activation onset (blue line).

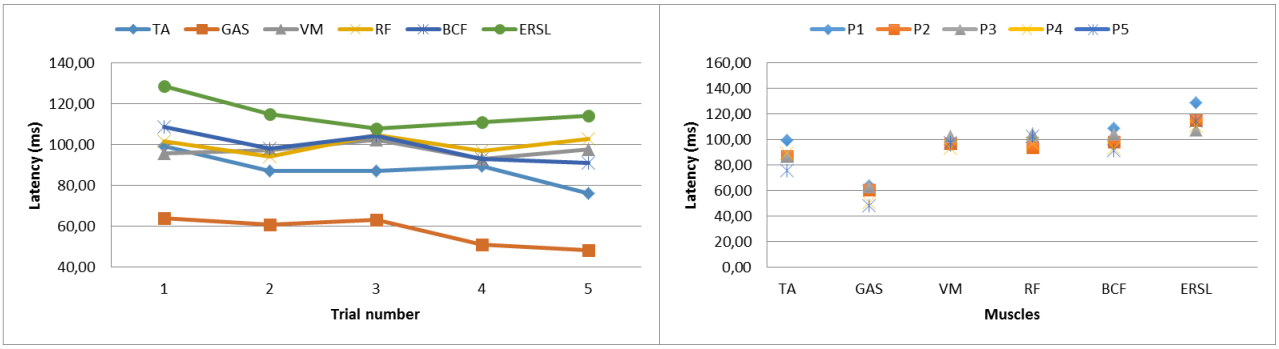

Figure 27. Muscular latencies throughout the backward trials (left panel) and temporal latencies for each muscle in all the five trials (right panel).

In the forward trial block TA and GAS showed the lower and higher latencies in all the five trials, whereas thigh muscles and ERSL had similar latency values (Fig. 28, left panel). The muscles activation sequence confirmed the TA/GAS opposite behavior, not showing a clear activation sequence for the other muscles (Fig. 28, right panel), as reported earlier for backward trial block (Fig. 27). Eventually, the direct comparison of all muscles latencies between backward and forward configuration highlighted an opposite temporal behavior of TA and GAS (Fig. 29) and lower time latencies in forward configuration for all the other muscles (Fig. 30 and 31).

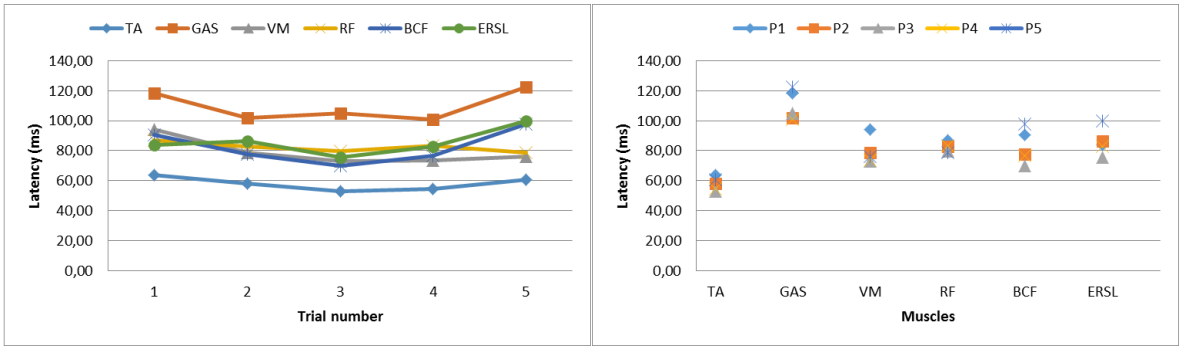

Figure 28. Muscular latencies throughout the forward trials (left panel) and temporal latencies for each muscle in all the five trials (right panel).

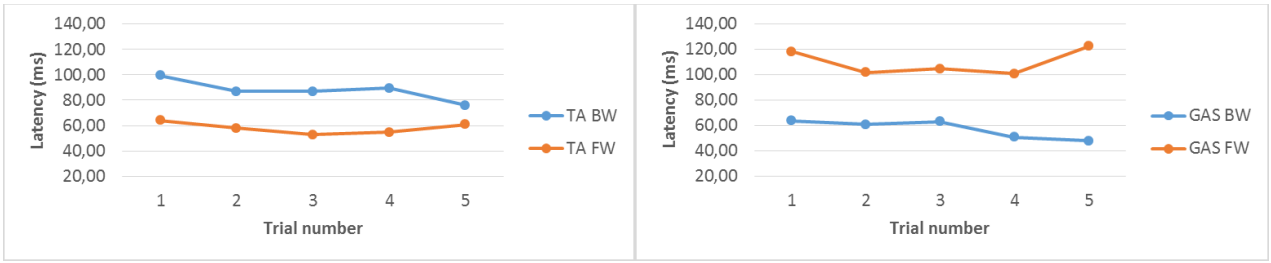

Figure 29. Direct comparison between backward and forward trial blocks of TA (left panel) and GAS (right panel) latencies.

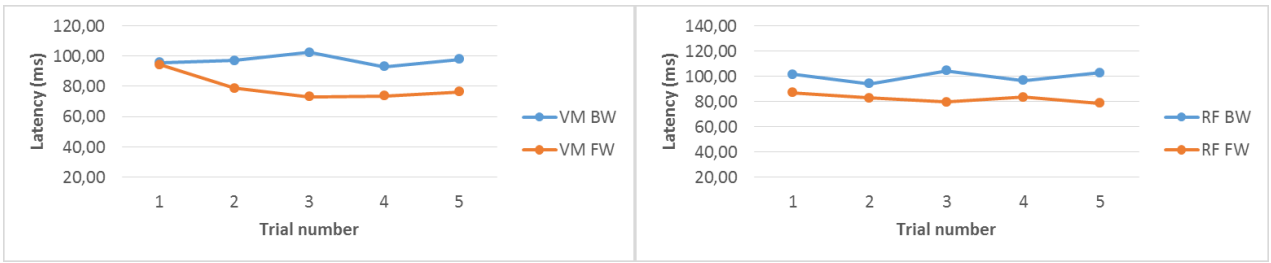

Figure 30. Direct comparison between backward and forward trial blocks of VM (left panel) and RF (right panel) latencies.

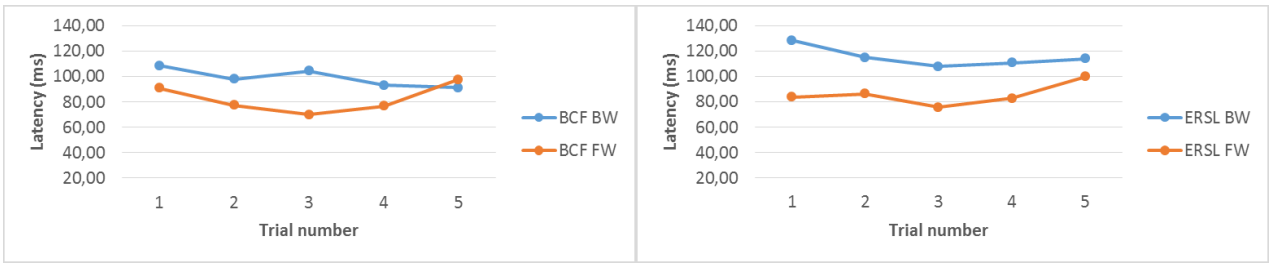

Figure 31. Direct comparison between backward and forward trial blocks of BCF (left panel) and ERSL (right panel) latencies.

4.2 Increasing velocity

In the trial block where the perturbation velocity has been progressively increased, from a minimum of 15 cm/s (1st trial) to a maximum of 35 cm/s (5th trial), the same parameters reported for the fixed velocity trial block have been computed, from dynamic, kinematic and electromyographic signals. However, in particular for dynamic data, the characterization of a regular and repeatable shape for the CoP AP displacement resulted more difficult respect to the fixed velocity trial block. In many cases, with the increase of velocity, the AP response of CoP seemed to lose the characteristic double peak shape (Fig. 32) and thus some parameters reported in the previous section showed a lack of significance. In this section this type of parameter will be omitted. Furthermore, due to the elevated velocity of the last trial not all the subjects performed or correctly completed the task at 35 cm/s and thus data extracted from the last trial in many cases could be of hard interpretation.

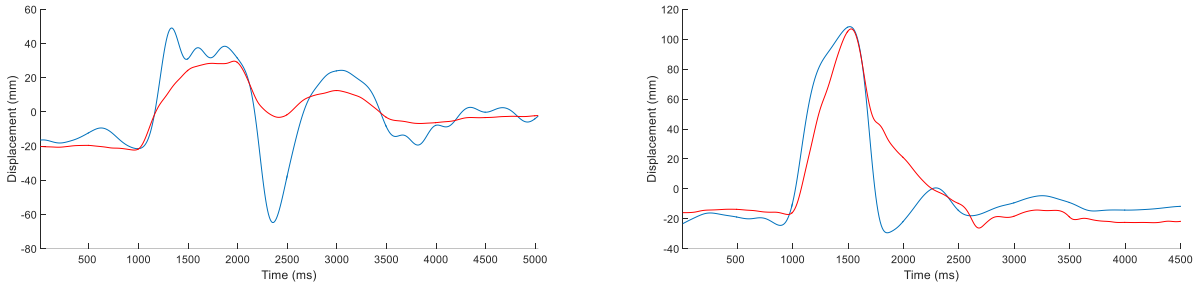

Figure 32. Representative CoP displacement in the first (left panel) and in the last (right panel) trial. The double peak shape in the first trial disappears in the last trial, where only the first peak is recognizable.

In the backward increasing velocity trials, CoP showed an increasing FPT from the first to the last trial (Fig. 33, left panel), whereas the IPT had a less clear evolution throughout the trials, with the two last higher values probably due to the absence of the second peak in the last trial (Fig. 33, left panel). The first peak presented also an increasing amplitude, from 0.43 to 0.61 of normalized value and conversely the second peak had an amplitude value bounded from 0.72 to 0.81 of normalized value (Fig. 33 right panel). Center of mass appeared on the contrary to have a clearer trend from a time and space point of view, as happened for fixed velocity trials. The FPT showed a decreasing

trend throughout the trials, from an initial value of 717±209 ms to 476±42 ms (Fig. 34, left panel), whereas the IPT showed a clear and significant increasing trend (Fig. 34 right panel).

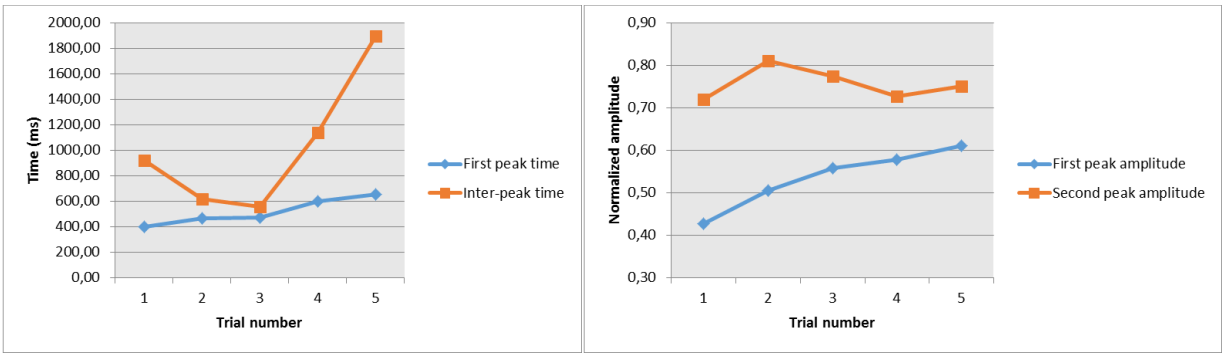

Figure 33. CoP first peak time and inter-peak time (left panel) and first peak amplitude and second peak amplitude (right panel). Trial from 15 cm/s to 35 cm/s are indicated as trial 1 to trial 5.

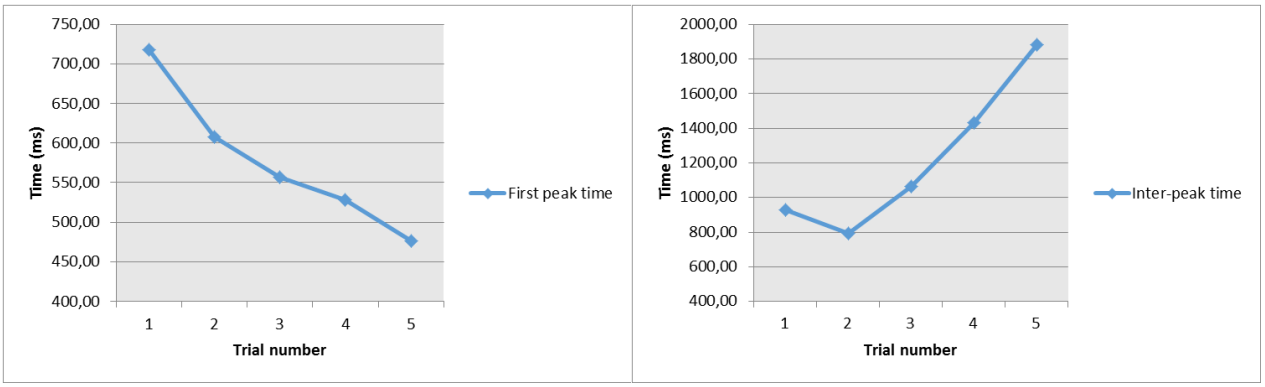

Figure 34. CoM first peak time (left panel) and inter-peak time (right panel). Trial from 15 cm/s to 35 cm/s are indicated as trial 1 to trial 5.

Conversely all the spatial parameters exhibited increasing trend throughout the trials, for both the first and the second peak (Fig. 35 and 36).

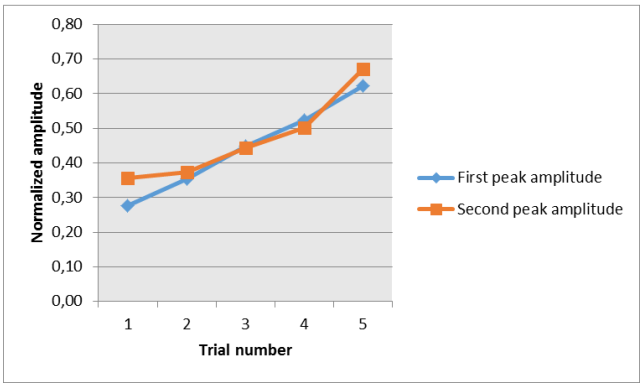

Figure 35. CoM first and second peak normalized amplitude. Trial from 15 cm/s to 35 cm/s are indicated as trial 1 to trial 5.

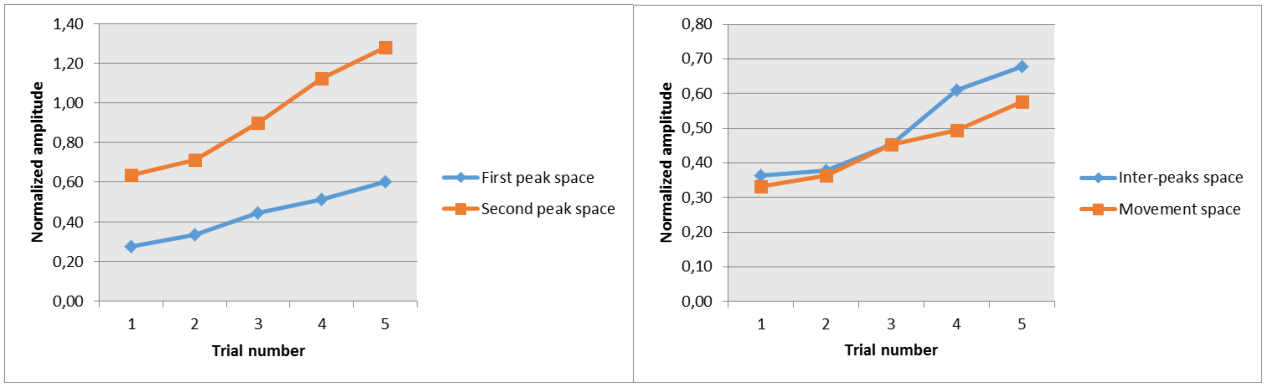

Figure 36. CoM first and second peak space (left panel) and inter-peaks and movement space (right panel). Trial from 15 cm/s to 35 cm/s are indicated as trial 1 to trial 5.

For what concerns the relation between CoP and CoM, the IPA appeared to decrease for increasing velocities (Fig. 37, left panel) and the same behavior was exhibited by both the CoP-CoM area and its positive section during the perturbation (Fig. 37, right panel). It is noteworthy that the total area and positive area from different initial values (1665±421 mm² and 1430±307 mm²) reached during the last trial approximatively the same value (817±266 mm² and 793±282 mm²).

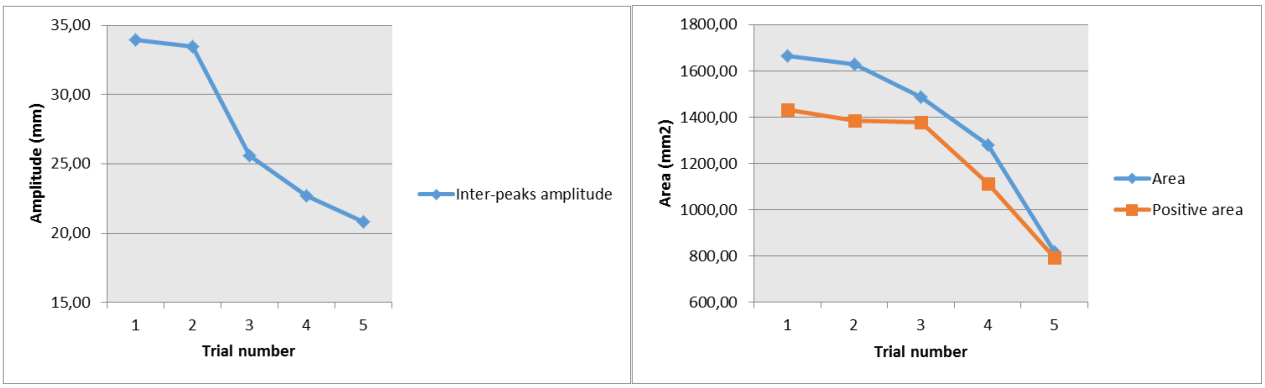

Figure 37. Inter-peaks amplitude between CoP and CoM (left panel) and area and its positive portion of CoP-CoM curve (right panel). Trial from 15 cm/s to 35 cm/s are indicated as trial 1 to trial 5.

Eventually, the evaluation of SST in backward conditions showed an increasing development throughout the trials for both CoP and CoM (Fig. 38), with comparable values in each trial (maximum difference resulted 9 ms in the third trial at 25 cm/s).

Angular range of variation for all the considered joints appeared significantly higher in the trial with the maximum velocity, particularly for ankle, knee. hip and head (Fig. 39) and with low values in first trial.

Notably, the ankle, knee and hip range value in the last trial resulted 13.5±8.2°, 17.3±0.4° and 16.6±5.0° respectively whereas the maximum values reached in the remaining trials were 6.9±2.8°, 14.0±7.2° and 16.0±5°. Balance strategies have been quantified the same way as fixed velocity and in backward condition turned out an equal presence of ankle and hip strategy throughout the trials (Fig. 40, left panel) and a predominant employment of ankle respect to the knee (Fig. 40, central panel). Eventually, the knee seemed to be more used than the hip, when directly compared (Fig. 40, right panel).

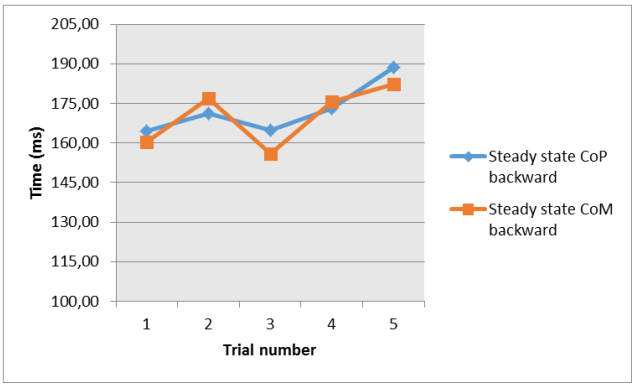

Figure 38. Steady-state reaching time for CoP and CoM in backward perturbation test. Trial from 15 cm/s to 35 cm/s are indicated as trial 1 to trial 5.

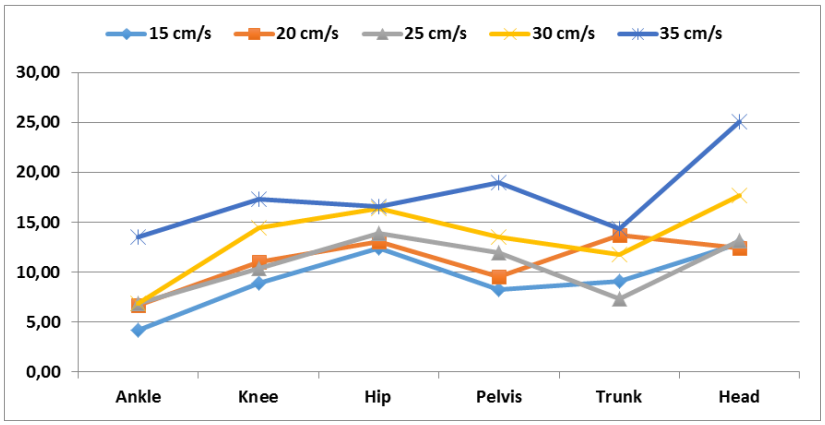

Figure 39. Angular range variation for all the considered joints.

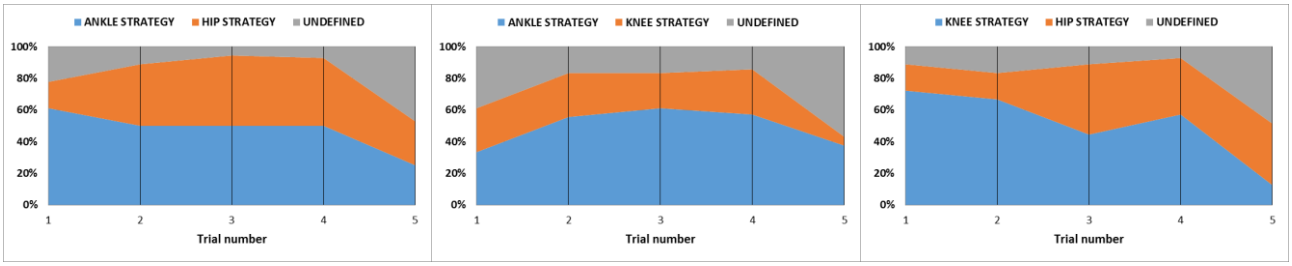

Figure 40. Evaluation of ankle versus hip (left panel), ankle versus knee (central panel) and knee versus hip (right panel). Columns heights represent the percentage of total subjects where a joint strategy has been detected. Grey columns indicate the number of subject where none of the two strategies has been clearly recognized. Trial from 15 cm/s to 35 cm/s are indicated as trial 1 to trial 5.

In the forward perturbation trials, CoP FPA showed slightly increasing values from the first to the last trial, whereas SPA had a significantly greater values during the first three trials respect to those of the last two trials, with higher velocities (30 and 35 cm/s, Fig. 41, left panel). Moreover, CoP displacement during perturbation was characterized by a decreasing trend up to the 4th trial and by a similar value in the 5th (Fig. 41, right panel). On the other hand, CoM FPA and SPA appeared to have an opposite development, with an increasing FPA and a decreasing SPA throughout the trials (Fig. 42, left panel); accordingly, the CoM displacement during platform movement resulted much higher in the final trial respect to the first one, with a linear increasing trend (Fig. 42, right panel).

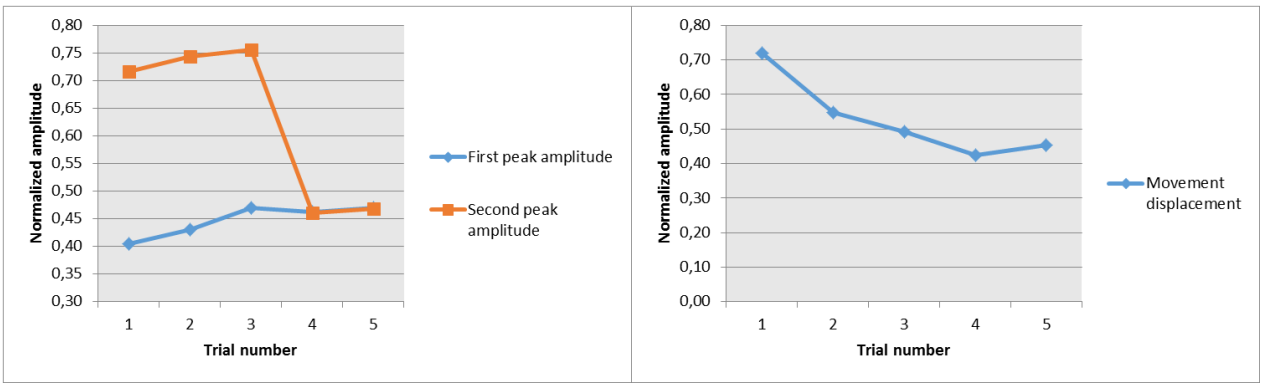

Figure 41. CoP first and second peak normalized amplitude (left panel) and normalized CoP displacement during platform movement (right panel). Trial from 15 cm/s to 35 cm/s are indicated as trial 1 to trial 5.

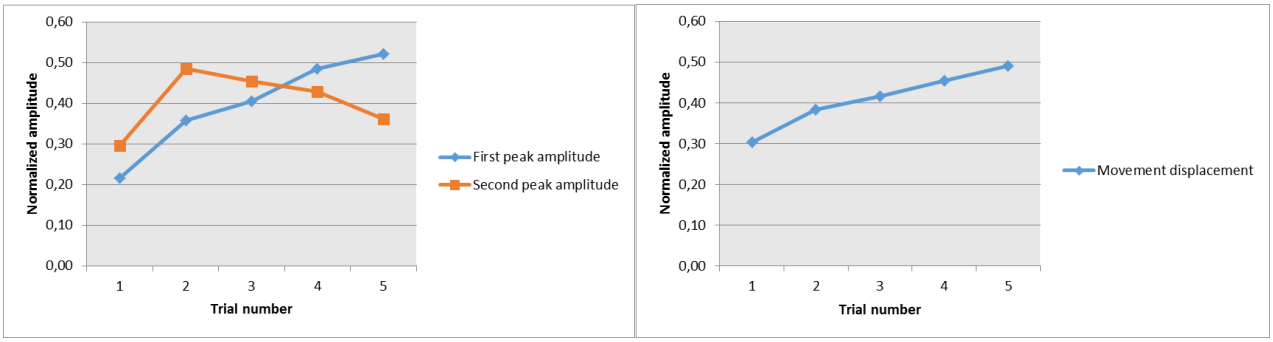

Figure 42. CoM first and second peak normalized amplitude (left panel) and normalized CoM displacement during platform movement (right panel). Trial from 15 cm/s to 35 cm/s are indicated as trial 1 to trial 5.

Relation between the CoP and CoM first peak in terms of amplitude pointed out a clear decreasing trend from the first to the last trials (from 38.9±18.4 mm to 6.4±2.6 mm), with similar values for the 4th and 5th trial (6.4±2.6 mm and 5.9±1.3 mm respectively, Fig. 43, left panel).

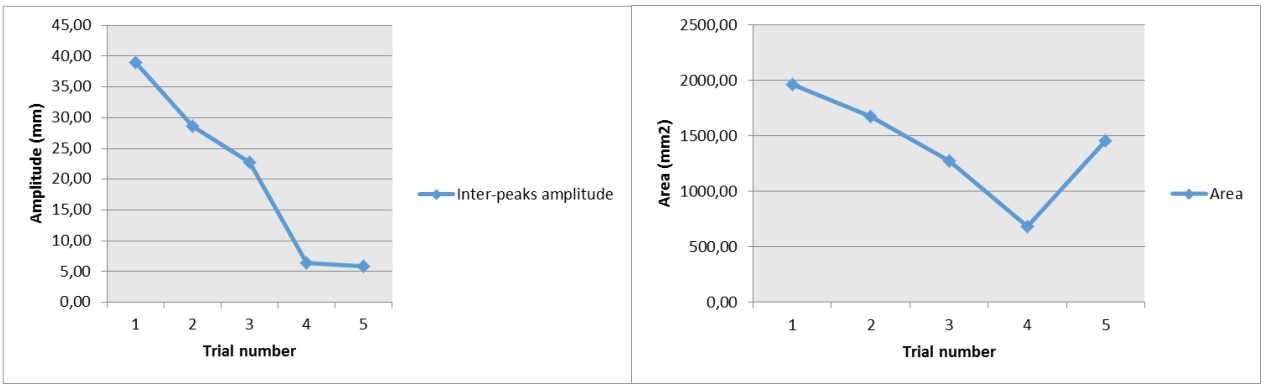

Figure 43. CoP-CoM inter-peaks amplitude (left panel) and area under the CoP-CoM curve, computed during platform movement (right panel). Trial from 15 cm/s to 35 cm/s are indicated as trial 1 to trial 5.

Furthermore, also the area under the CoP-CoM curve, computed during the platform movement, showed a decreasing development throughout the increasing velocity trials (Fig. 43, right panel). It is worth noticing that the high area value observed in the last trial could be ascribed to the low number of subjects that performed the forward trial at 35 cm/s, yielding to a poor data amount for this particular velocity configuration.

Angular joints variations showed an increasing trend for ankle joint from the first to the last trial (7.8±3.7° and 17.7±9.8° respectively) and a decreasing trend for the head movement, whereas the other considered joints varied in a similar range throughout the trials (Fig. 44).

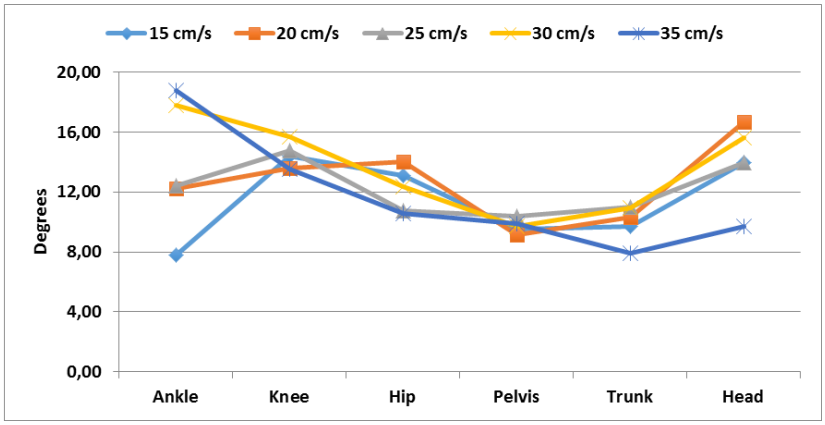

Figure 44. Angular range variation for all the considered joints.

The more recruited postural balance strategy seemed to be both the ankle and knee strategy, that had a strong predominance respect to the hip one and in particular, during the last, most challenging trial, none of the subjects employed the hip strategy (Fig. 45, left and right panel). When directly compared, ankle and knee strategies resulted definitely in the same percentage of subject during the central trials (2nd and 3rd), whereas in the first one appeared an ankle predominance and conversely in the fourth only knee-strategy has been assessed (Fig. 45, central panel). It is noteworthy that in an elevated percentage of subject not the ankle nor the knee strategy have been clearly recognized, underlining a lack of prevalence of one of them when directly compared (Fig. 45, central panel).

A direct comparison between backward and forward trial blocks was performed following what has been reported for fixed velocity trials (see previous section). The CoM distance between initial and final position resulted in all cases significantly lower in backward configuration, with higher values in the first trial respect to the others in both cases (Fig. 46, left panel). The temporal distance between the perturbation onset and the CoP overtaking of CoM showed a slightly decreasing development in backward configuration, from an initial value of 54.1±37.2 ms to a final one of 38.5±0.7 ms (Fig. 46, right panel). Conversely, in forward trials this temporal parameter resulted bounded in a slot of less than 10 ms (Fig. 46, right panel).

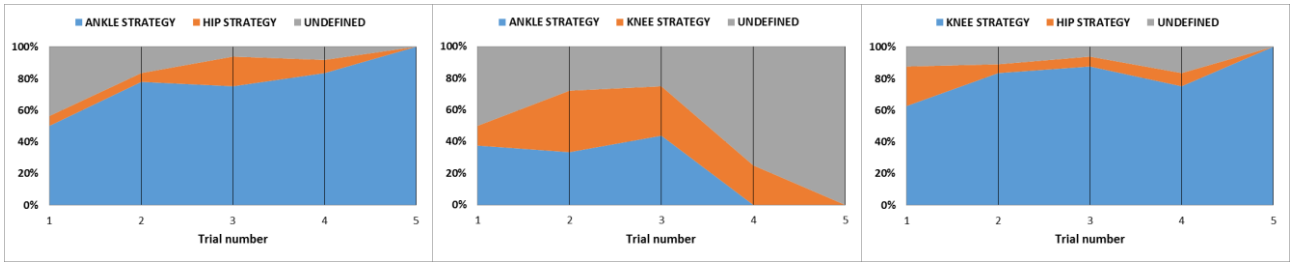

Figure 45. Evaluation of ankle versus hip (left panel), ankle versus knee (central panel) and knee versus hip (right panel). Columns heights represent the percentage of total subjects where a joint strategy has been detected. Grey columns indicate the number of subject where none of the two strategies has been clearly recognized. Trial from 15 cm/s to 35 cm/s are indicated as trial 1 to trial 5.

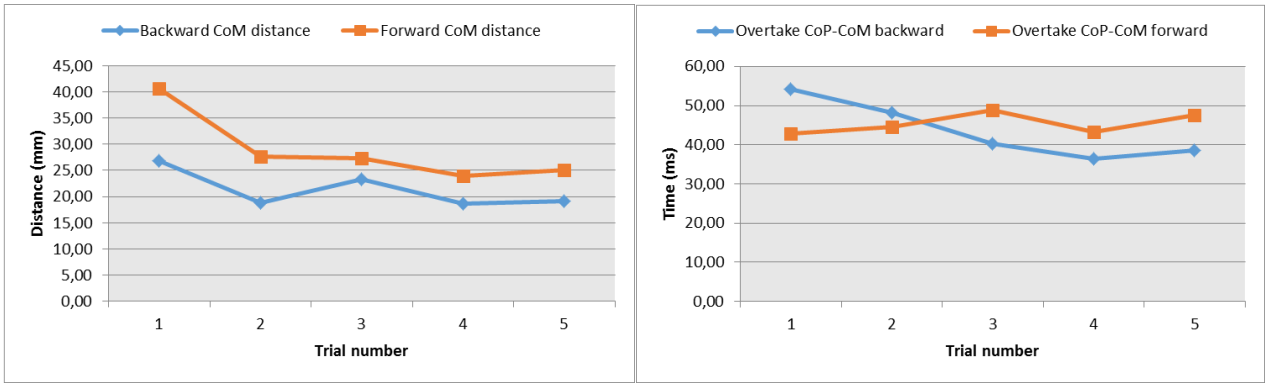

Figure 46. CoM distance between initial and final position (left panel) and time interval between perturbation onset and CoP overtaking of CoM (right panel). Trial from 15 cm/s to 35 cm/s are indicated as trial 1 to trial 5.

The steady state achievement (SST) of CoP resulted delayed in backward condition respect to the forward (Fig. 47, left panel), both showing a slightly increasing trend. For what concerns the CoM, in backward configuration the steady state time showed a non-straight development throughout the trials, with values remaining in a band of 15 ms (Fig. 47, right panel). In forward trial block, SST had a clearer decreasing trend, except for the last value: this discrepancy could be probably due to the poor data amount for trial at maximum velocity, leading to inconsistent outcomes in this case.

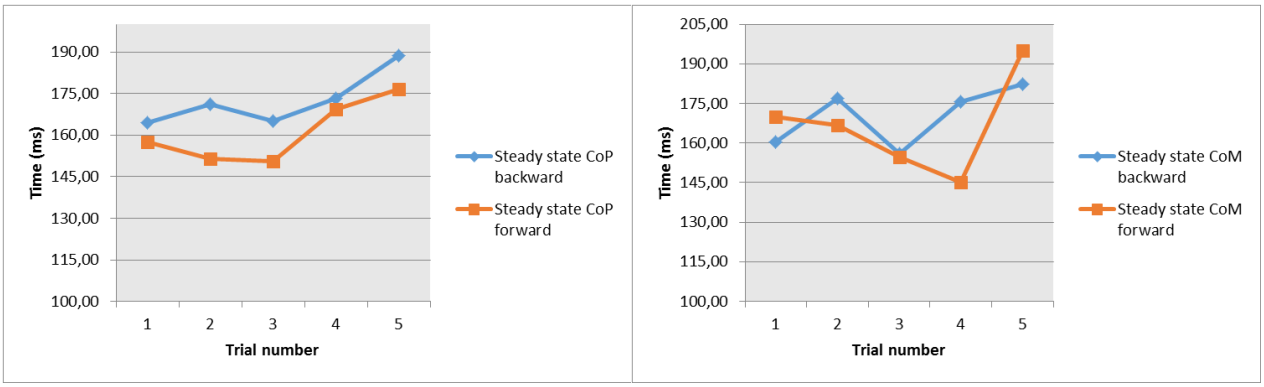

Figure 47. Steady state time for CoP (left panel) and CoM (right panel) in backward and forward configuration. Trial from 15 cm/s to 35 cm/s are indicated as trial 1 to trial 5.

Angular joints values of ankle and knee resulted significantly higher in forward configuration (Fig. 48, top panels), whereas hip presented quite constant values until the last trial (Fig. 48, bottom panel), similar to those of backward configuration; in the last trial, the hip range of variation increased, reaching 18.9±12.7°, while the maximum value in the remaining trials was 13.5±1.7°.

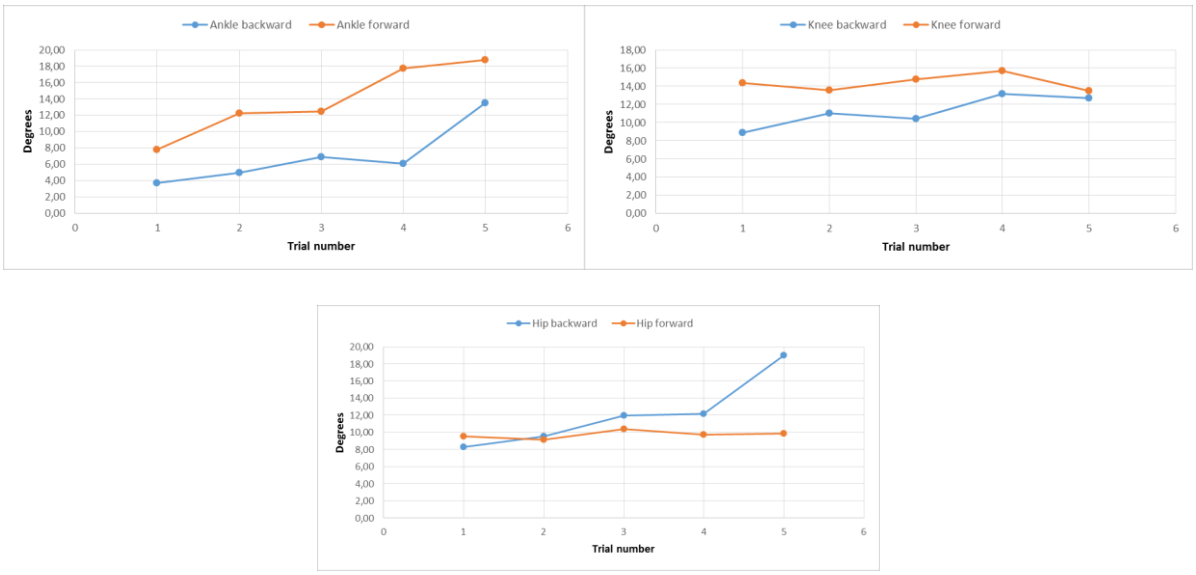

Figure 48. Angular range of variation for ankle (top left panel), knee (top right panel) and hip (bottom panel) in backward and forward trials block. Trial from 15 cm/s to 35 cm/s are indicated as trial 1 to trial 5.

Myoelectric activity of the acquired muscles has been assessed as for fixed velocity configuration, through the computation of temporal latency between perturbation start and muscular response onset. In backward trials block GAS showed the lower temporal latency for all the velocity configurations (Fig. 49, left panel). TA and BCF activated after the GAS, with latency similar

values throughout the trials; the higher latency values belonged to ERSL, which was the last to activate. The muscles activation sequence (Fig. 49, right panel) confirmed this behavior, with the GAS that activated first, then TA and BCF with the same latency, RF and VM after them and eventually the ERSL. For what concerns the forward configuration, TA showed the lower latency for all the trials (Fig. 50, left panel) and the ERSL, as seen previously, confirmed its higher latency values. Muscular activation sequence (Fig. 50, right panel) highlighted an activation sequence starting with TA, ending with ERSL and following the TA-GAS-VM-RF-BCF-ERSL path.

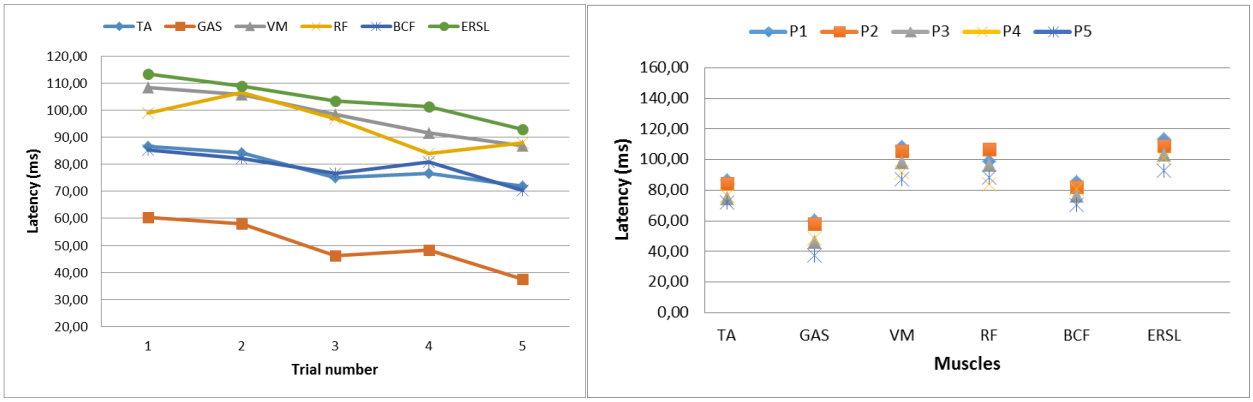

Figure 49. Muscular latencies throughout the backward trials (left panel) and temporal latencies for each muscle in all the five trials (right panel). Trial from 15 cm/s to 35 cm/s are indicated as trial 1 to trial 5.

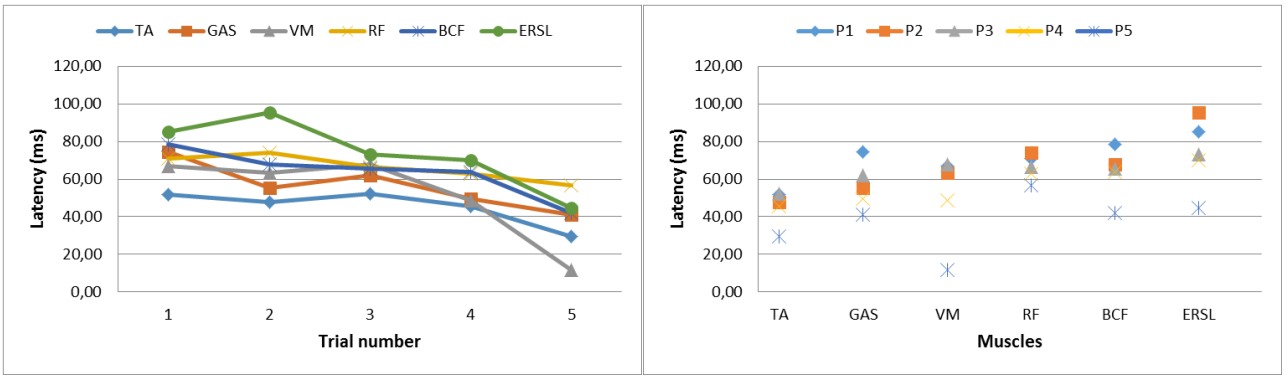

Figure 50. Muscular latencies throughout the forward trials (left panel) and temporal latencies for each muscle in all the five trials (right panel). Trial from 15 cm/s to 35 cm/s are indicated as trial 1 to trial 5.

Direct comparison between backward and forward latencies for all the considered muscles (Fig. 51, 52 and 53), confirmed the higher latency values of the backward trial block, as reported in the previous section for the fixed velocity trials. This characteristic behavior was infringed only by the

GAS muscle, showing lower or at least equal latency values in backward configuration (Fig. 51, right panel).

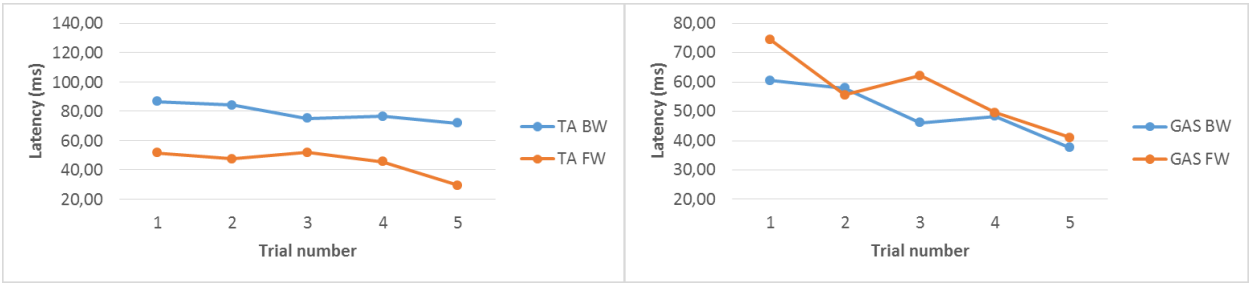

Figure 51. Direct comparison between backward and forward trial blocks of TA (left panel) and GAS (right panel) latencies. Trial from 15 cm/s to 35 cm/s are indicated as trial 1 to trial 5.

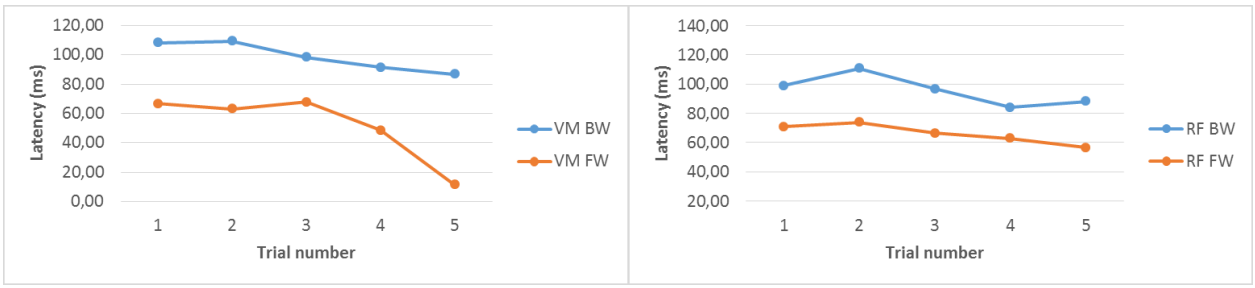

Figure 52. Direct comparison between backward and forward trial blocks of VM (left panel) and RF (right panel) latencies. Trial from 15 cm/s to 35 cm/s are indicated as trial 1 to trial 5.

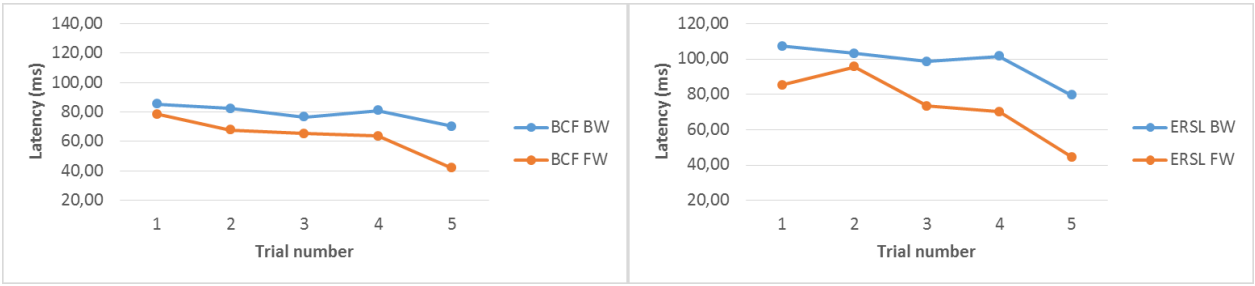

Figure 53. Direct comparison between backward and forward trial blocks of BCF (left panel) and ERSL (right panel) latencies. Trial from 15 cm/s to 35 cm/s are indicated as trial 1 to trial 5.

4.3 Sensory deprivation

In sensory deprivation trials a direct comparison between parameters obtained in eyes open (EO) and eyes closed (EC) has been performed, in order to directly evaluate whether the sensory deprivation had measurable effects on the balance maintenance characteristics. The CoP FPT and the IPT presented similar values between EO and EC trials, (Fig. 54, left panel), matching with the amplitude CoP parameters, which not showed significant differences between the two test conditions (Fig. 54, right panel).

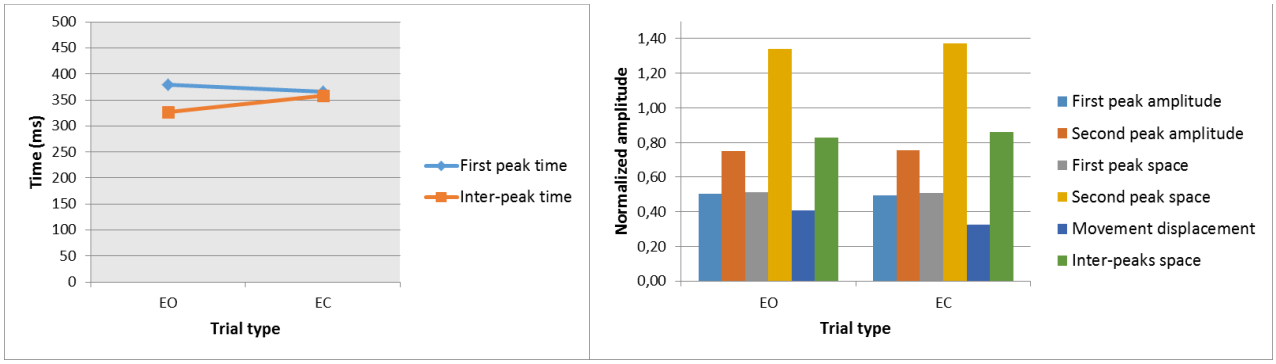

Figure 54. CoP first and inter-peak time (left panel) in eyes open and eyes closed trial. In the right panel the amplitude CoP parameters values are reported.

For what concerns the CoM, the FPT presented similar values in EO and EC trials (291±82 ms and 271±21 ms respectively, Fig. 55, left panel), whereas the IPT showed a lower value in EC trial. As for the CoP, also in this case all the spatial parameters exhibited small differences between the two trial type (Fig. 55, right panel).

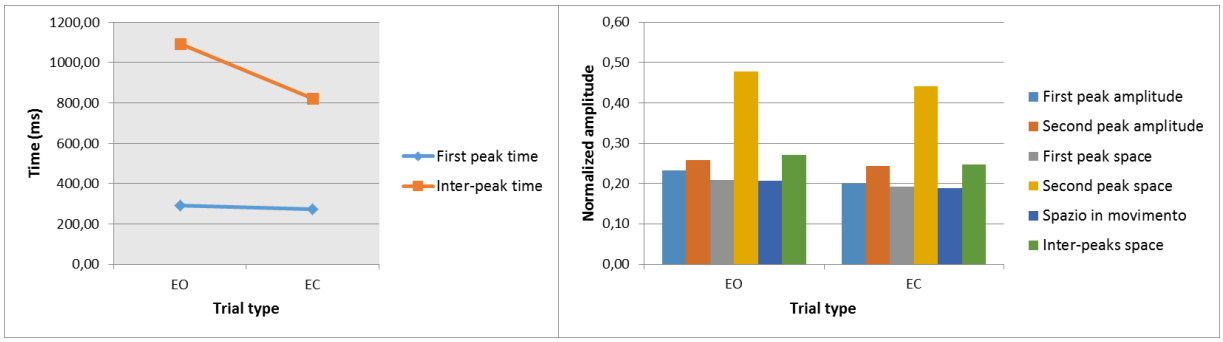

Figure 55. CoM first and inter-peak time (left panel) in eyes open and eyes closed trial. In the right panel the amplitude CoM parameters values are reported.

The amplitude difference between the CoP and CoM first peaks showed similar valuee in EO and EC trials (58.4±8.9 mm versus 60.5±11.9 mm, Fig. 56, left panel) and the same behavior was observed for the area under the CoP-CoM curve, computed during the platform movement (Fig. 56, right panel).

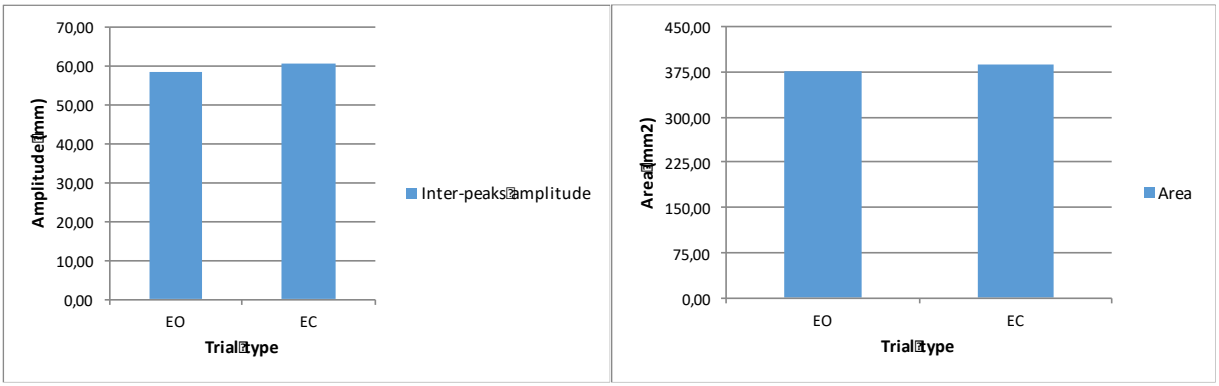

Figure 56. Inter-peaks amplitude between CoP and CoM first peaks (left panel) and area under the CoP-CoM curve computed during platform movement (right panel).

The steady-state resulted achieved by the CoP with the same temporal delay in EO and EC trials, whereas CoM showed a higher delay in EC trial type (169±27 ms versus 182±24 ms, Fig. 57).

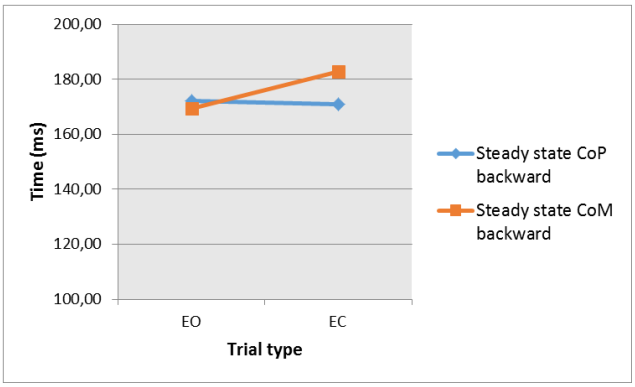

Figure 57. Steady state time for CoP and CoM in both EO and EC trial type.

For EO and EC backward trials, angular range highlighted limited higher values in EC condition for all the considered joint, except for the trunk (Fig. 58); however, the differences in all the cases not overtook 2 degrees, thus not leading to significant gaps.

For forward trials, the CoP FPT lied on the same values in EO and EC condition (Fig. 59, left panel) but the IPT showed a lower value in EC condition, in contrast with what has been observed in backward trials.

Spatial parameters however not showed significant differences between the two sensorial conditions (Fig. 59, right panel). A temporal behavior matching with that observed in backward configuration was showed by the CoM, with a constant FPT and a decreasing IPT from EO to EC trial type (Fig. 60, left panel).

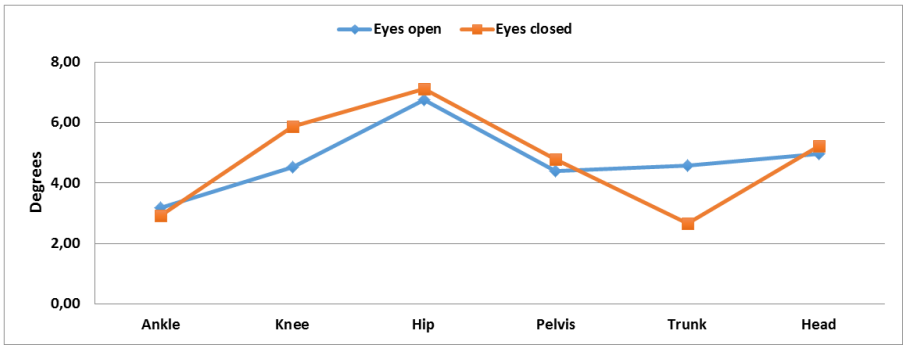

Figure 58. Angular range variations in both EO and EC condition for backward perturbation.

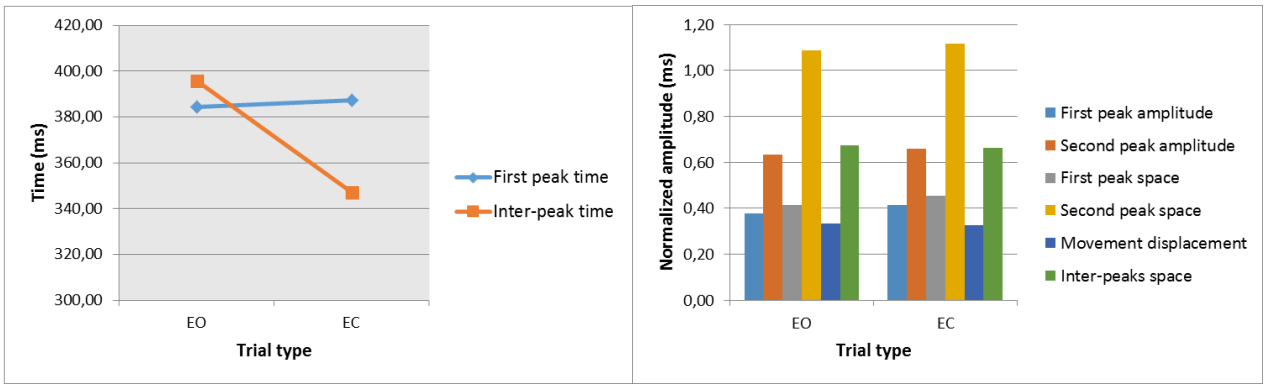

Figure 59. CoP first and inter-peak time (left panel) in eyes open and eyes closed trial. In the right panel the amplitude CoP parameters values are reported.

As for the CoP, also in this case spatial parameters exhibited similar values in EO and EC condition (Fig. 60, right panel). The amplitude difference between the CoP and CoM first peaks and the area under the CoP-CoM curve followed both what has been observed in backward trial blocks, with similar values of the IPA and of the area in EC condition (Fig. 61).

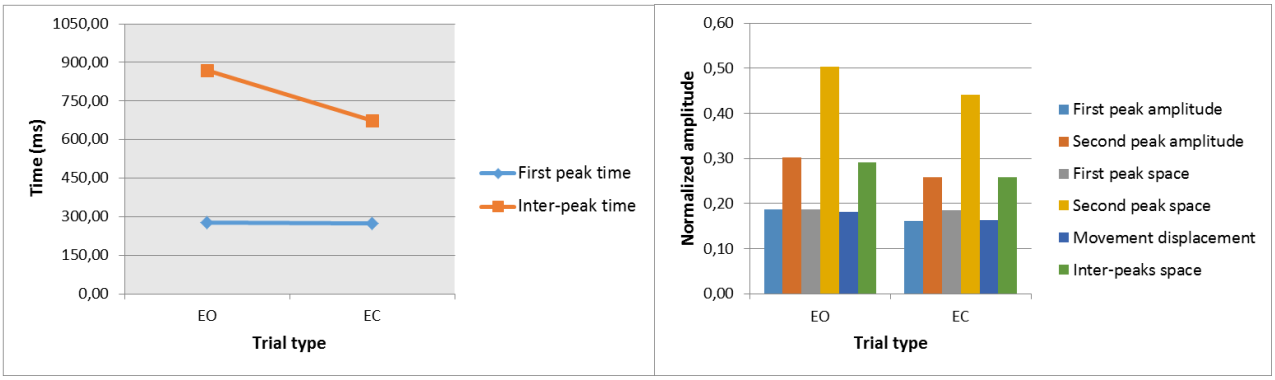

Figure 60. CoM first and inter-peak time (left panel) in eyes open and eyes closed trial. In the right panel the amplitude CoM parameters values are reported.

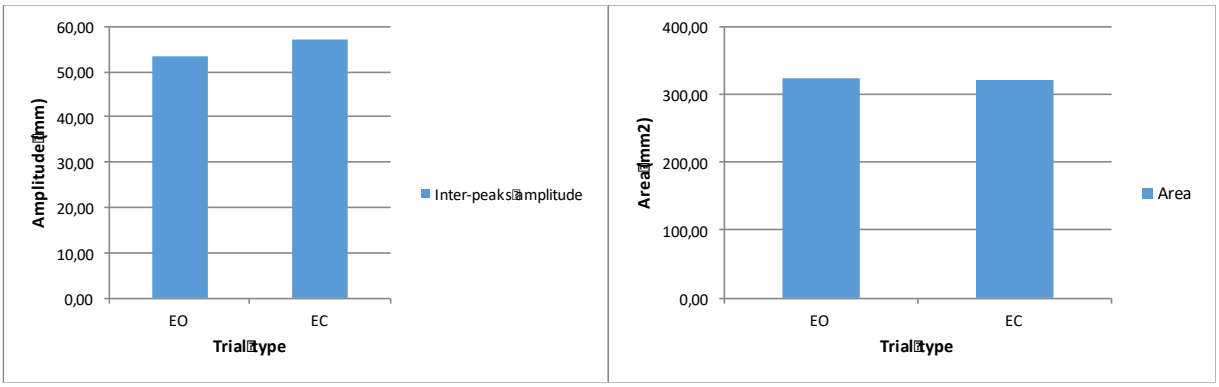

Figure 61. Inter-peaks amplitude between CoP and CoM first peaks (left panel) and area under the CoP-CoM curve computed during platform movement (right panel).

The steady-state resulted achieved by the CoP and CoM with the same temporal delay in EO and EC trials (139±29 ms versus 140±36 ms for the CoP and 149±22 ms versus 155±34 ms for the CoM, Fig. 62).

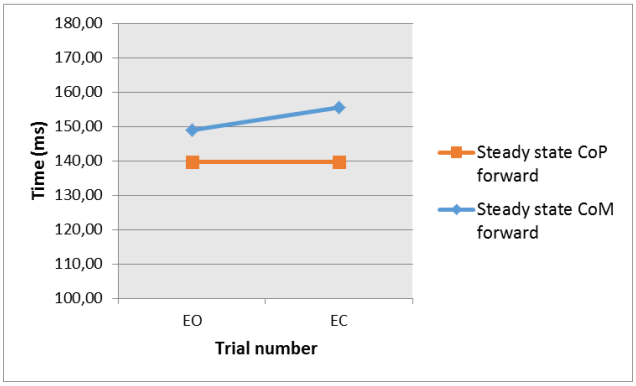

Figure 62. Steady state time for CoP and CoM in both EO and EC trial type.

Angular range variations in forward perturbation trials exhibited small differences between EO and EC condition (Fig. 63), where the maximum gap resulted for the knee joint, with an angular range of 9.1±2.3° and 6.7±0.8° for EO and EC condition respectively.

The direct comparison between backward and forward configurations highlighted concordant trend for the CoM distance between the initial and final position (Fig. 64, left panel), the CoP overtaking of CoM after the perturbation onset (Fig. 64, right panel) and the steady state achievement time of CoP (Fig. 65, left panel). Nevertheless, CoM steady state achievement showed a quite constant value in the forward configuration and a higher value in backward EC condition respect to the EO (Fig. 65, right panel).

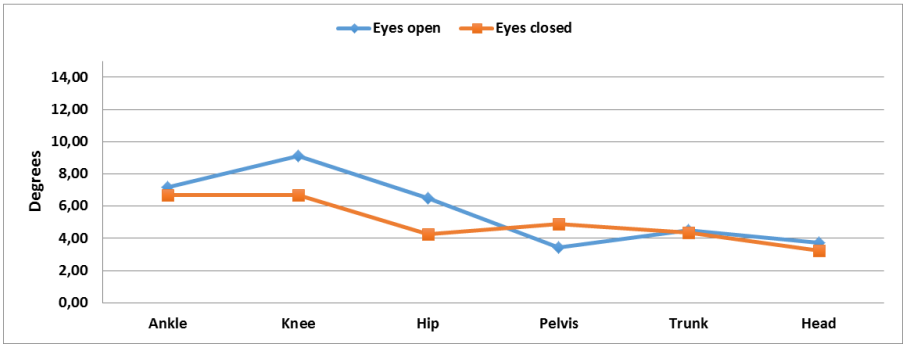

Figure 63. Angular range variations in both EO and EC condition for forward perturbation.

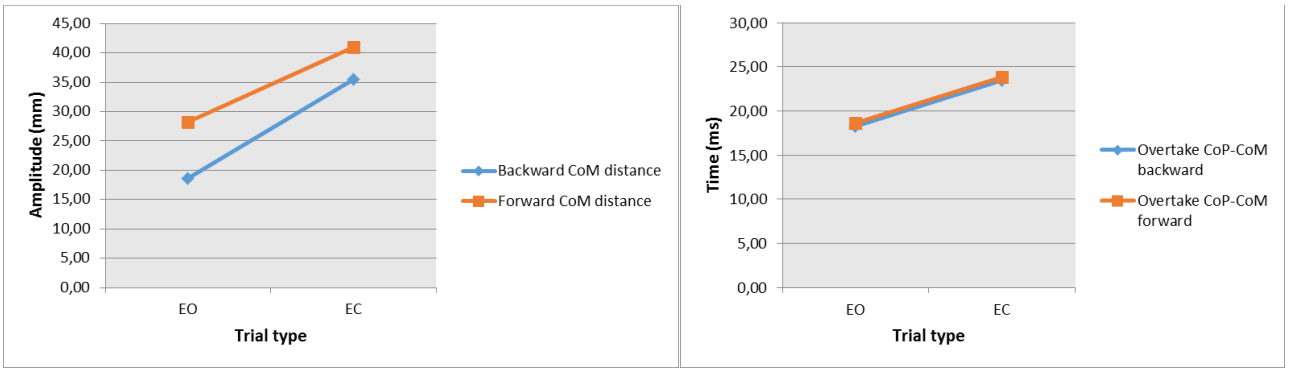

Figure 64. CoM distance between initial and final position (left panel) and time interval between perturbation onset and CoP overtaking of CoM (right panel).

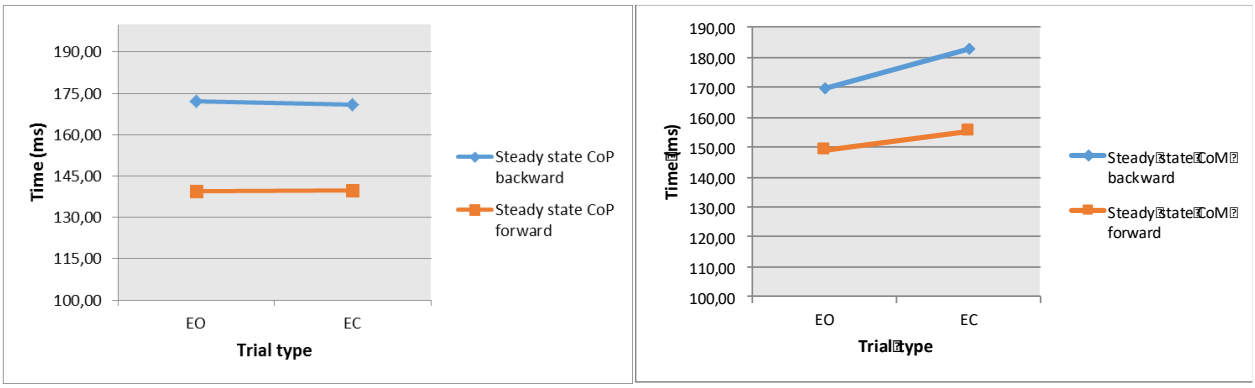

Figure 65. Steady state time for CoP (left panel) and CoM (right panel) in backward and forward configuration.

Balance strategies have been compared between backward and forward perturbation in EC condition. The joints inter-comparison (Fig. 66) displayed a substantially equal employment of the ankle, hip and knee joint during backward perturbation, an increase of the ankle strategy during the forward perturbation respect to the hip and an increase of the knee joint employment in forward perturbation, when directly compared with both the ankle and the hip (Fig. 66).

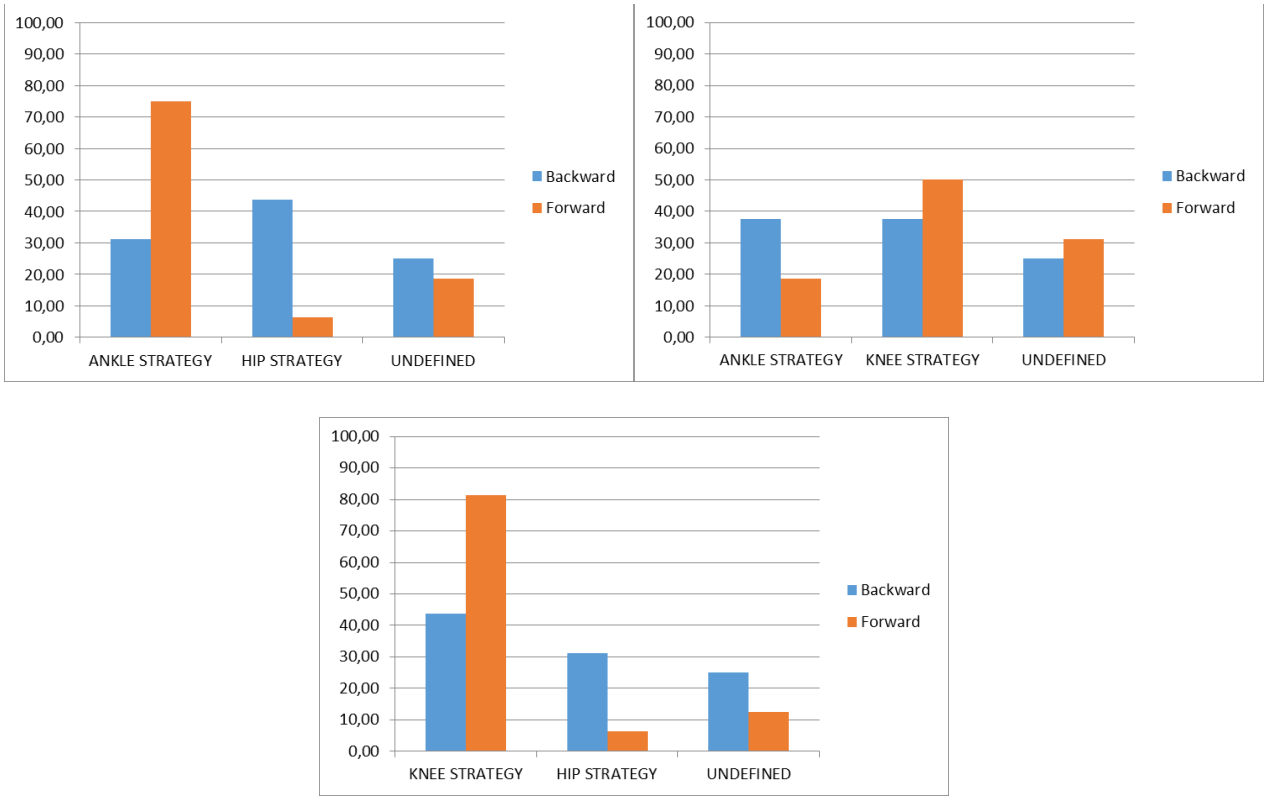

Figure 66. Direct comparison of the ankle, knee and hip joint employment in backward and forward EC configuration. Columns heights represent the percentage of total subjects where a joint strategy has been detected.

Myoelectric activity has been assessed, as indicated previously for fixed and increasing velocity configurations, as the temporal latency between the perturbation onset and the arise of muscular response. In backward trials, no significant differences have been observed between EO and EC muscles latencies (Fig. 67, left panel), with the GAS showing the lower latency in both the sensorial condition, followed by the simultaneous activation of TA and BCF. The muscular activation sequence (Fig. 67, right panel) underlined this trend, highlighting the already observed muscles recruitment that moves from bottom the upper muscles.

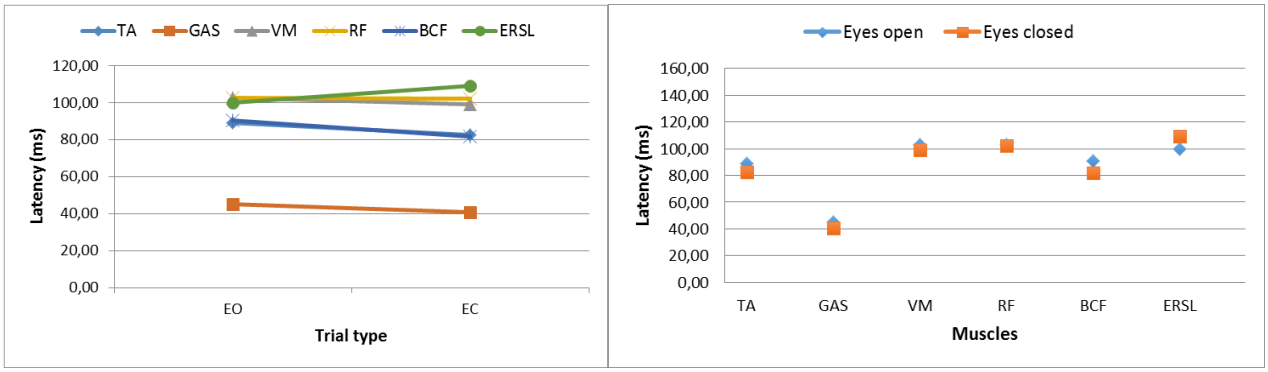

Figure 67. Muscular latencies in EO and EC backward trials (left panel) and temporal latencies for each muscle in EO and EC trials (right panel).

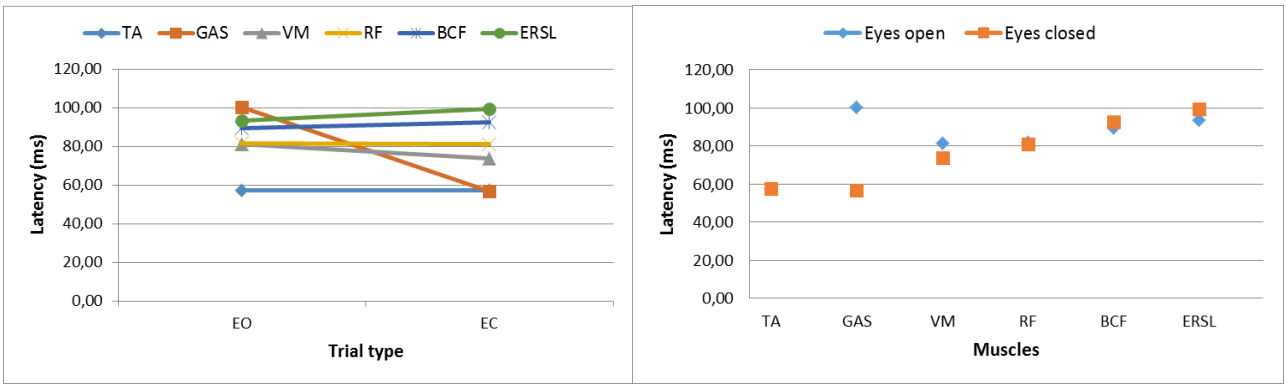

Figure 68. Muscular latencies in EO and EC forward trials (left panel) and temporal latencies for each muscle in EO and EC trials (right panel).

In forward perturbation trials, no significant differences have been observed between EO and EC conditions in muscles latencies, except for the GAS, which exhibited a strong latency decrease in EC condition (Fig. 68, left panel), moving from being the last activating muscle to a latency value similar to that of TA.The muscular activation sequence confirmed, a part from the GAS in EC conditions, the

muscular activation sequence, already observed in forward fixed and increasing velocity trials, that follows the TA-GAS-VM-FR-BCF-ERSL path (Fig. 68, right panel).

Chapter 5
Discussion

In this study an evaluation of balance responses to external postural perturbations has been performed. Many types of balance perturbations have been employed in order to observe and gain insights in specific neurological and mechanical features of balance control; although also other types of perturbation have been used (Santos *et al.*, 2010), the first and most common perturbation is represented by base of support movement (Nashner, 1977; Corbeil *et al.*, 2013). In this kind of configuration, subjects underwent sudden (Murnaghan and Robinovitch, 2013) or continuous (Schieppati *et al.*, 2002) balance perturbation, in either single (Nonnekes *et al.*, 2013) or multiple (Dimitrova *et al.*, 2004) directions. Sudden perturbations are in general similar to those a subject, either pathological or non-pathological, can experience in everyday life (Commissaris *et al.*, 2002) and thus in this study perturbations with a limited temporal duration (maximus duration 430 ms) have been employed. The type of platform movement represents another central issue in dynamic posturography, where the two most used perturbations are tilt (Schieppati *et al.*, 1995; Hebert and Corboy, 2013; Perucca *et al.*, 2014) and translation (Horak *et al.*, 1989; Runge *et al.*, 1999; Nonnekes *et al.*, 2013) of the base of support. In this study, horizontal translation of platform (one degree of freedom) has been chosen as the unique type of perturbation, in order to obtain data that can be compared not only within the same kind of trial blocks but also between different kind of perturbation tests, i.e. fixed velocity, increasing velocity and sensorial deprivation (see Methods section).

Direction of platform translation is a further central characteristic in dynamic posturography studies. Although multiple direction translations represent a frequently used type of test (Henry *et al.*, 1998; Henry *et al.*, 2001; Dimitrova *et al.*, 2004), in many studies, from the earlier to the most recent ones, the AP direction of perturbation resulted the most used (Horak and Nashner, 1986;

Diener *et al.*, 1988; Horak *et al.*, 1989; Alexander *et al.*, 1992; Runge *et al.*, 1999; Nonnekes *et al.*, 2013) and thus in this study a horizontal backward and forward translation has been employed in all the trial blocks. This choice is supported also by the fact that the single or double inverted pendulum is still the most common used biomechanical model for the characterization of both standing and perturbed balance (Winter *et al.*, 2001; Davidson *et al.*, 2011; Ersal *et al.*, 2014; Li *et al.*, 2012). This aspect leads to consider mainly the sagittal plane for kinematics response and the AP direction for CoP and CoM displacement during balance or balance recovery and supports the choice of a perturbation direction eliciting the latter type of biomechanical response during perturbation withstand. Eventually, in the literature there is no consensus in the choice to perform forward direction perturbations, which are often avoided or included in order to discourage preplanning of anticipatory postural responses (Quant *et al.*, 2005). In this study forward platform translations were added to the backward ones with the purpose of performing a as wide as possible balance recovery characterization and to carry out a direct comparison between balance responses in backward and forward perturbation conditions.

5.1 Fixed velocity

In fixed velocity trials, each subject underwent to five consecutive platform translations in backward direction and five consecutive platform translations in forward direction. Velocity and displacement of perturbations (15 cm/s, 5 cm) were chosen according with Diener *et al.* (1988) and Hansen *et al.* (1988) and to obtain a quasi-impulsive stimulus, with a perturbation duration equal to 330 ms. To limit the influence of acceleration and deceleration, the maximum obtainable value (3 m/s^2) was chosen, allowing the reaching of the desired platform speed in 50 ms.

The analysis of AP CoP displacement showed in all trials a characteristic and repeatable shape with two main peaks (Fig. 1), the first one occurred in the opposite direction respect to the platform movement, underlining an initial loss of balance due to the body inertia, while the second peak was

in the same perturbation direction and regarded the return to the initial upright position. It is worth noticing that the second peak maximum amplitude overtakes the initial, mean value of the CoP position in the unperturbed, upright position. Thus, the translation of the base of support seems to elicit a double balance challenging configurations, the first linked directly to the stimulus and the second due to the voluntary counterbalancing, seldom observed in previous studies. This repeatable behavior allows the characterization of CoP from a temporal and spatial point of view. All of these observations also apply to the CoM AP displacement, which is controlled by the CoP and thus shows lower displacement values for both peaks (Fig. 2 and 4). The decreasing trend from the first to the final trial of the second peak amplitude and space (Fig. 2, 3, 4 and 5) for CoP and CoM and the constant amplitude value of the first peak for CoP and CoM seem to highlights a habituation rate throughout the trial, leading to a more robust control of the voluntary, counterbalancing mechanisms. This enhanced control seems to be more oriented to the amplitude rather than the speed of movement, considering that the decreasing amplitude value of the second peak of CoP and CoM is joined to decreasing time in which this second peak is reached (more evident for the CoM, Fig. 4). A further evidence of an enhanced control of the counterbalance phase seems to be given by the time in which CoP achieves the steady state, that decreases from the first to the final trial (Fig. 8). The relationship between CoP and CoM AP trajectories during the platform movement can provide a measure of the postural stability also in dynamic tasks (de Lima Pardini *et al.*, 2012) and thus the increase of the area under the CoP-CoM curve and its positive part throughout the trials (Fig. 7) and the simultaneous decrease of its negative part highlights an increase in the postural stability from the first to the last trial, suggesting the presence of an habituation rate in backward trial with constant velocity (Nanhoe-Mahabier *et al.*, 2012). The neuromuscular control system appeared thus able to reduce the counterbalance magnitude movement of both CoP and CoM and to enhance the postural stability according to the trials sequence. Dynamic posturography studies yet reported the so-called “first trial effect” (Visser *et al.*, 2010; Nanhoe-Mahabier *et al.*, 2012), characterized by larger balance responses to the first disturbance compared to the subsequent

responses to identical balance perturbations (Bloem *et al.*, 1998; Allum *et al.*, 2011). Evidences of this feature can be observed in CoP and CoM inter-peaks time (Fig. 2 and 4), in CoM first peak amplitude (Fig. 4) and in the inter-peaks amplitude between CoP and CoM (Fig. 7), which present much higher values in first trial compared to the ensuing ones. A first trial effect can be observed also evaluating the angular ranges of all the considered joints, which show greater values or at least equal (ankle joint) in response to the very first perturbation (Fig. 9), in according with what has been reported by Allum *et al.* (2011). Instead, the first trial effect seems to be absent in muscular responses (Fig. 27), where at most a limited habituation rate is observable, with a slightly decreasing latency values for all muscles except for RF and VM. The absence of an EMG-identifiable first trial effect follows what has been reported by Oude Nijhuis *et al.* (2009), where this type of biomechanical feature was observed in EMG signal amplitude rather than in the onset of muscles bursts.

Electromyography data confirmed the activation sequence already observed in previous studies (Horak and Nashner, 1986; Diener *et al.*, 1988; Schieppati *et al.*, 1995): in order to counteract the forward body lean induced by backward perturbations and the resultant ankle dorsi-flexion, the GAS activates first, followed by TA (Fig. 27). Quadriceps muscles and BCF activate with the same latencies in each trial after TA onset and ERSL activity arise last, showing an activation sequence, from the ankle, to thigh and trunk muscles that matches with what has been indicated by Horak and Nashner (1986). The early activations of GAS and TA highlight the dominant role of the ankle joint in withstanding backward perturbations, whereas thigh muscles and ERSL seem to be connected to the recovery of the initial upright position. Moreover, the short latency of TA respect to both thigh muscles and ERSL could point out its role in a balance correcting response, aiming at controlling and limiting the posterior body sway due to the GAS earlier activation (Carpenter *et al.*, 2004).

The central role of the ankle joint in controlling balance seems to be confirmed also by the recurrence of postural strategies (Fig. 11), where a pure ankle strategy appeared in a higher number of subjects respect to the hip and knee strategy. The ankle and hip strategies are considered as the two coordinative patterns employed by neuromuscular system to maintain upright stance in response to

balance perturbations (Horak and Nashner, 1986; Diener *et al.*, 1989; Runge *et al.*, 1999; Perucca *et al.*, 2014). Ankle strategy arises during standing balance (Gage *et al.*, 2004) and small perturbations (low amplitude and/or velocity), restoring the equilibrium by moving the body around the ankle joint, whereas the hip strategy appears with larger perturbations and the body motion is focused around the hip joint (Horak and Nashner, 1986). Thus, the predominance of the ankle strategy and the limited recurrence of the hip strategy in this type of trial, with limited and constant amplitude and velocity, are in agreement with their accepted role. Moreover, the prevalence of the ankle strategy is also strengthened by the muscle activation sequence (Fig. 27), which exhibits the distal-to-proximal pattern described for the ankle strategy, while in a hip strategy focused response this pattern resulted inverted, with reduced time latency of trunk and hip muscles (Horak and Nashner, 1986; Diener *et al.*, 1988). Nevertheless, the hip strategy has been observed in a non-negligible percentage of total subjects (minimum value 12.5%, Fig. 11) in all the five trials; the hip strategy produces a slow CoM displacement to counterbalance body after a challenging perturbation (Horak and Nashner, 1986; Diener *et al.*, 1988) and thus the high value of hip joint angular range and of the CoM inter-peaks time in response to the first perturbation (Fig. 9 and 4) seem to suggest the presence of this balance strategy during the first trial, highlighting its more challenging characteristics for maintaining upright stance and the presence of the aforementioned "first trial effect", which could lead to the employment of balance strategies usually observable in large perturbation tests (Horak and Nashner, 1986; Runge *et al.*, 1999; Creath *et al.*, 2005). Beside the ankle and hip strategies, in recent years also a balance strategy involving the knee has been proposed to better explain upright posture maintenance in both standing and perturbed conditions (Hsu *et al.*, 2007; Runge *et al.*, 1999; Alexandrov *et al.*, 2005). Although there is still no complete agreement on the presence and relevance of this type of strategy, knee motions have been observed in response to support surface movement (Runge *et al.*, 1999; Creath *et al.*, 2005) and the usage of a knee strategy has been reported in response to large perturbations and when a rapid balance restoration is needed (Alexandrov *et al.*, 2001; Di Giulio *et al.*, 2013). In agreement with these observations, the presence of

a knee strategy in a significant percentage of subjects has been observed, respect to both ankle and hip (Fig. 11). However, knee joint angular range appears similar to those of ankle and hip throughout the trials (Fig. 9) and BCF muscle does not show a reduced latency respect to the other thigh muscles, with no evidences of an anticipated knee flexion and thus its relevance could be overestimated and the presence of a knee strategy should be considered carefully. Considering the first trial, unlike the hip there are no evidences of a knee central role, with an angular range and BCF muscle latency similar to the other joints and muscles (Fig. 9 and 27).

In forward platform movement trials, CoP and CoM show the already observed double peak shape (Fig. 12). First peak for both of them presents constant amplitude values throughout the trials and decreasing reaching time (Fig. 13, 15 and 16), in contrast with what was observed in backward trials. In this configuration the first peak is the most critical, because forward perturbations elicit backward body sway and thus CoP has reduced stability margin respect to forward body sway (approximately from the malleolus to the calcaneus and from the malleolus to the front edge of the foot respectively). CoP first peak reaches in all the five trials an amplitude, normalized to the foot length, which not overtook 0.43 and the normalized average distance, among all the subjects, between lateral malleolus and calcaneus resulted 0.45±0.07; thus, CoP reaches the margin of stability in all the forward perturbation trials, highlighting the more challenging characteristics of this type of stimulus. CoM second peak shows decreasing values for the inter-peaks time and peak amplitude, underlining, as in backward case, a control pattern focused on the counterbalance phase. The decrease of the CoM first and inter-peaks time (Fig. 15) could indicate also the development of an earlier balance recovery, connected to the habituation rate observed also in backward perturbation trials and highlighted also by the linear decrease in the steady state achievement of both CoP and CoM (Fig. 18) and in agreement with Chen *et al.* (2014). On the other hand, a "first trial effect" is barely recognizable from CoP and CoM displacements, whereas higher angular range of ankle and knee joints were observable in the very first trial respect to the following (Fig. 19), pointing out a larger angular displacement for the lower limb. It is noteworthy that the hip joint exhibited however

similar angular range values in all the considered trials, while ankle and knee had the greater angular variations irrespective of the number of trial (Fig. 19). This aspect mirrors in the almost equal recurrence of the ankle and knee strategies and in their higher recurrence when compared with the hip strategy (Fig. 20), matching with a knee-joint role in controlling upright stance when a rapid balance restoration is required (Alexandrov *et al.*, 2001; Cheng, 2016). A limited hip strategy can be recognized also in the absence of a proximal-to-distal muscles activation sequence, which characterizes this type of balance recovery strategy (Horak and Nashner, 1986; Diener *et al.*, 1988).

Muscles activity revealed the expected lower latency of TA, which activates first in order to counterbalance the foot plantar-flexion induced by the posterior body sway (Horak and Nashner, 1986; Diener *et al.*, 1988; Schieppati *et al.*, 1995) and a GAS activity with the higher latency among all considered muscles (Fig. 28). This aspect seems to confirm the central role of the ankle joint in upright posture control and the more challenging perturbation of a forward movement of the base of support: the last activation of GAS, even after thigh and ERSL muscles, could reflect the need to firstly counterbalance upright stance through TA and also thigh muscles activity, avoiding an early plantar-flexion which could enhance rather than limit the posterior body sway induced by the selected perturbation. Moreover, due to its function of knee flexor, the temporally isolated GAS activity could play a role in the clear knee strategy previously reported.

A direct comparison between backward and forward trial blocks underlines the more challenging nature of the platform forward movement and thus of a posterior-induced body sway. After the stimulus onset, the CoP overtaking of CoM occurs earlier in backward perturbations respect to the forward ones (Fig. 23) and the same behavior is observable also for the steady state time of CoP and CoM (Fig. 24): despite a decrease which suggests an improvement in control strategy and an early balance recovery, the steady state time remains in any case greater in forward trials respect to the backward ones (Fig. 24). Forward perturbations evoked faster muscular activations respect to backward platform movement (Fig. 30 and 31), matching with Chen *et al.* (2014) and underlining the need for a faster response to withstand this type of perturbation. Latency

pattern of TA and GAS (Fig. 29) seem to be related with their ankle control and thus follow the typical pattern already reported independently from the perturbation direction; this aspect highlights the central role of the ankle in controlling upright stance, with muscular activation which follow a mechanical rather than a temporal pattern. Eventually, the larger angular ranges of ankle and knee agree with the enhanced role of these joints during forward stimuli (Chen *et al.*, 2014), confirming the need not only for a faster but also for a larger response to counteract body posterior sway.

5.2 Increasing velocity

In increasing velocity trials, each subject underwent to five consecutive platform translations in backward direction and five consecutive platform translations in forward direction. Also in this case, velocity sequence (15, 20, 25, 30 and 35 cm/s) were chosen according with Diener *et al.* (1988); displacement of perturbations (15 cm) was chosen to maximize velocity effects. In order to limit the influence of acceleration and deceleration, the maximum obtainable value (3 m/s^2) was chosen, allowing the achievement of the desired speed in the shortest possible time. In general, increasing velocity trials appeared hardest to characterize from a dynamic point of view, especially for the frequent, but not ubiquitous, disappearing of the counterbalancing second peak, which biases in particular the temporal parameters of both CoP and CoM.

As expected, increasing velocities of perturbation leaded to a greater postural sway, highlighted by the increase of both first and second peak amplitude parameters of CoP and CoM (Fig. 33, 35 and 36). However, CoP second peak amplitude shows constant values throughout the trials, suggesting, as in fixed velocity configuration, a limiting effect on sway in counterbalance phase. As velocity increases, a more challenging control of CoM by the CoP is recognizable also in the decrease of the distance between CoP and CoM first peaks and in the decrease of the area under the CoP-CoM curve (Fig. 37), which reflects a reduction in the postural stability during the balance perturbation phase

(Winter *et al.*, 1998; de Lima Pardini *et al.*, 2012). A further aspect which highlights a more difficult upright stance control is the steady state time, which shows greater values in according with the velocity increase (Fig. 38)

The expected increase in the amplitude response for larger stimuli, i.e. higher velocities, is observable also in joint angular ranges (Fig. 39), which resulted higher in the last, most challenging trial, for each considered joint. It is worth noticing that the joint angular ranges increasing follows the velocity increase sequence, with the lower value in correspondence of the first trial, the second lower value in correspondence of the second trial and so on until the last trial, confirming that the more the perturbation is large, the higher the angular changes (Chen *et al.*, 2014). The comparison of postural strategies (Fig. 40) suggests an enhanced role of the hip strategy respect to the fixed velocity trials, which presents an occurrence comparable with that of the ankle and knee, especially in trials with higher velocity, while in the first trial hip strategy occurrence is in line with values observed in fixed velocity trials (Fig. 11). The role of the hip strategy for balance recovery seems to be confirmed also by hip joint range of variation (Fig. 39), which is greater in all the trials respect to the ankle and knee joints. These findings match with what has been reported about the presence of a hip strategy with larger perturbations or in general when the subject undergoes to more challenging balance conditions, e.g. reduced length of support surface (Horak and Nashner, 1986; Alexandrov *et al.*, 2001; Park *et al.*, 2004; Creath *et al.*, 2005). On the other hand, the knee joint seems to maintain a non-negligible weight as balance strategy, considering its recurrence when directly compared with the hip strategy (Fig. 40) and the latency of BCF muscle (Fig. 49). BCF shows activation with low latency values, similar to those of TA, suggesting an early control of the knee joint, as observed also in fixed velocity configuration. The other considered muscles show activation sequences which match with the classical distal-to-proximal sequence, already observed in fixed velocity trials. Thus, increases in perturbation velocity seem to have no effects on the muscular activation sequence and only a slightly decrease in latencies is observable for all muscles, according to the velocity increase.

Also in forward perturbation trials, the control of CoM displacement appears focused on the counterbalance phase: the second peak presents a decreasing amplitude value throughout the trials, whereas the first peak amplitude increases from the first to the last trial (Fig. 42). A more challenging control of body sway is recognizable also in the lower values of the distance between CoP and CoM first peaks and the area under the CoP-CoM curve (Fig. 43), which indicates, as reported earlier, a decrease in postural stability in correspondence of high velocities. Angular ranges of variation appear with similar value throughout the trials and without a clear amplitude sequence, as observed conversely in backward perturbation trials. Only the ankle joint shows increasing ranges of variation which follow the increase of perturbation velocity (Fig. 44), suggesting a central role of the ankle joint, confirmed by the high recurrence of the ankle strategy respect to the hip strategy (Fig. 45). Knee joint appears with a limited weight respect to the ankle, however in a high percentage of subjects was not possible to define ankle or knee strategy as the dominant one (Fig. 45), suggesting the employment of a mixed strategy which has been yet reported (Creath *et al.*, 2005). The limited role of a hip balance strategy seems to be suggested not only by the direct comparison with the ankle and knee strategies but also considering the muscular activation sequence (Fig. 50), which not present the proximal-to-distal pattern of activation observed when this type of strategy is clearly employed (Horak and Nashner, 1986; Diener *et al.*, 1988). Muscles activation latencies exhibit, as expected, an early activation of TA to withstand the ankle plantar-flexion due to the posterior body sway. It is worth noticing that from the second to the last trial GAS and TA latencies are very similar (maximum gap 10 ms), while in the first one GAS shows a retarded activation, as observed in forward fixed velocity trials. This aspect matches with what has been reported by Hughes *et al.* (1995) about ankle joint stabilization through co-contraction of TA and GAS in forward platform movement trials, suggesting an adaptive muscular behavior in response to changing trial conditions. Moreover, in each trial muscles latencies present close values, with a limited range of variation, suggesting the need for a more rapid response in this more challenging test condition. This aspect is confirmed by the comparison between latencies in backward and forward test (Fig. 51, 52 and 53), where lower

muscular latencies have been assessed for thigh and ERSL muscles forward perturbation trial blocks. Ankle muscles show instead their distinctive activation pattern, with GAS lower latency in backward perturbation tests and TA lower latency in forward perturbation tests, confirming one more time the central role played by the ankle joint in counteracting body sway caused by sudden movements of the base of support. The need for larger and faster responses when facing more challenging perturbations could be viewed in the latencies decrease for all the considered muscles from the first to the last trial in both experimental directions (Fig. 51 – 53). The need for faster responses is highlighted also by the higher angular range variations in forward perturbation trials for ankle and knee joints (Fig. 48) which show also an increasing trend for increasing velocity trials. Larger magnitudes of response appear also to lead to a more difficult recovery of the previous upright stance, as showed by larger CoM distance between initial and final position for forward perturbations (Fig. 46) and by increasing time of steady state achievement for both CoP and CoM, accordingly to the velocity increase (Fig. 47).

5.3 Sensory deprivation

In sensory deprivation trials, each subject underwent to two consecutive trials with platform translations in backward direction and two consecutive trials with platform translations in forward direction; before the second trial, subjects were asked to maintain their eyes closed for the entire trial duration. In this case, perturbation velocity and displacement (20 cm/s, 5 cm) were chosen to provide a stimulus able to elicit considerable postural responses (Diener *et al.*, 1988) through a sudden platform movement. To limit the influence of acceleration and deceleration, the maximum obtainable value (3 m/s^2) was chosen, allowing the achievement of the desired speed in the shortest possible time.

In backward test, CoP related parameters do not show significant differences between EO and EC conditions, for neither time nor amplitude parameters (Fig. 54). Center of mass exhibits a

significant reduction of the inter-peaks time in EC condition (1094.3±533.0 ms versus 822.8±292.8 ms, Fig. 55), suggesting, as observed previously, a control focused in the counterbalancing peak in the most challenging configuration (EC); however, considering also the high value of standard deviations, this observation is not supported by the other temporal or amplitude parameters, which show very close values between EO and EC conditions (Fig. 55). The same behavior is exhibited by the distance between the CoP and CoM first peak and by the area under the CoP-CoM curve, both of which have similar values in EO and EC test conditions (Fig. 56). The more challenging nature of EC test condition could be recognizable in the higher steady state achievement time of CoM in EC condition respect to EO (182±24 ms versus 169±27 ms, Fig. 57).

Angular ranges of variations are very close between EO and EC conditions (Fig. 58), with a higher value for the hip which suggests a large use of the hip strategy, supported by its high recurrence when compared with both ankle and knee strategies in backward configuration (Fig. 66). Muscular activity presents the expected early GAS activation, followed by the close activations of TA and BCF (Fig. 67), highlighting also in this case a role of the knee joint supported by the occurrence of the knee strategy observed in EC backward trials (Fig. 66). No significant differences have been recognized in muscular latencies between EO and EC conditions, in no backward nor forward perturbation test. However, in forward configuration GAS latency presents a strong reduction from EO to EC condition (Fig. 68), leading to a simultaneous activation with TA muscle. This result matches with Hughes *et al.* (1995), which reported a co-contraction of TA and GAS in response to forward perturbations and is in line with what has been observed in forward increasing velocity trials, thus supporting the hypothesis of the need for a more rapid response in more challenging configurations (forward platform movement with closed eyes represent one of the most challenging test type). This characteristic seems to be supported also by the lower values in EC condition of the inter-peaks time for CoP and CoM in forward perturbation trials (Fig. 59 and 60), although not joined to any significant variation in the others temporal parameters (Fig. 59 – 61), amplitude parameters (Fig. 59 – 61) or steady state achievement time (Fig. 62).

A direct comparison between backward and forward test type confirms the rapid response in counterbalancing the body sway induced by forward perturbations (Chen *et al.*, 2014), with lower values for the steady state achievement of CoP and CoM. Eventually, the presence of a clear knee strategy in EC forward trials (Fig. 66) is in line with what has been observed also in fixed and increasing velocity trials, suggesting the presence of a balance recovery response pattern which lies principally on the characteristics of the perturbation and not modified by the chosen test protocol. The quite poor differences observed between EO and EC conditions agree with a visual feedback independent CoP adaptation in different dynamic task conditions (Buchanan and Horak, 1999); however, visual information appeared to have a strong influence on CoM movement, also in particularly challenging configurations (Dietz *et al.*, 1993; Buchanan and Horak, 1999). This discrepancy could be partially connected to the type of perturbation employed in this study, which could be not able to elicit balance responses where vision feedback plays a central role. Indeed, in this study a sudden translational perturbation was employed, whereas the exploitation of visual information on upright stance maintenance was observed mainly through sinusoidal base of support translations at different frequencies (Dietz *et al.*, 1993; Berger *et al.*, 1995; Buchanan and Horak, 1999; Schieppati *et al.*, 2002). The main role of visual information is the control and stabilization of the head, trunk and CoM in space and this role is enhanced as the frequency of translation increases (Buchanan and Horak, 1999; Schieppati *et al.*, 2002). Due to this stabilizing role of vision in withstanding long-lasting balance perturbations, vision appears as a long term adaptive mechanism which may not be elicited through sudden and brief movements as the ones employed in this study. Maximum trial duration was 1 s in this study, while in the reported studies, periodic platform displacement lasts for a minimum of 12 s to a maximum of 60 s and thus perturbation type chosen in this study appears more suitable to extract information about the lower part of the body and their coordinative patterns, which depend more on proprioceptive rather than visual information (Buchanan and Horak, 1999).

Chapter References

Alexander N.B., Shepard N., Gu M.J., Schultz A., "Postural Control in Young and Elderly Adults When Stance Is Perturbed: Kinematics", *Journal of Gerontology*, 1992.

Alexandrov A.V., Frolov A.A., Massion J., "Biomechanical analysis of movement strategies in human forward trunk bending. II. Experimental study", *Biological Cybernetics*, 2001.

Alexandrov A.V., Frolov A.A., Horak F.B., Carlson-Kuhta P., Park S., "Feedback equilibrium control during human standing", *Biological Cybernetics*, 2005.

Allum J.H.J., Tang K.S., Carpenter M.G., Oude Nijhuis L.B., Bloem B.R., "Review of first trial responses in balance control: Influence of vestibular loss and Parkinson's disease", *Human Movement Science*, 2011.

Berger W., Tripple M., Assainte C., Zijlstra W., Dietz V., "Devel- opmental aspects of equilibrium control during stance: a kinematic and EMG study", *Gait and Posture*, 1995.

Bloem B.R., van Vugt J.P., Beckley D.J., Remler M.P., Roos R.A., "Habituation of lower leg stretch responses in Parkinson's disease", *Electroencephalography and clinical Neurophysiology*, 1998.

Buchanan J.J, Horak F.B., "Emergence of Postural Patterns as a Function of Vision and Translation Frequency", *Journal of Neurophysiology*, 1999.

Carpenter M.G., Allum J.H.J., Honegger F., Adkin A.L., Bloem B.R., "Postural abnormalities to multidirectional stance perturbations in Parkinson's disease", *Journal of Neurology, Neurosurgery and Psychiatry*, 2004.

Chen C.L., Lou S.Z., Wu H.W., Wu S.K., Yeung K.T., Su F.C., "Effects of the type and direction of support surface perturbation on postural responses", *Journal of Neuroengineering and Rehabilitation*, 2014.

Cheng K.B., "Does knee motion contribute to feet-in-place balance recovery?", *Journal of Biomechanics*, 2016.

Commissaris D.A., Nieuwenhuijzen P.H., Overeem S., de Vos A., Duysens J.E., Bloem B.R., "Dynamic posturography using a new movable multidirectional platform driven by gravity", *Journal of Neuroscience Methods*, 2002.

Corbeil P., Bloem B.R., van Meel M., Maki B.E., "Arm reactions evoked by the initial exposure to a small balance perturbation: A pilot study", *Gait and Posture*, 2013.

Creath R., Kiemel T., Horak F., Peterka R., Jeka J., "A unified view of quiet and perturbed stance: simultaneous co-existing excitable modes", *Neuroscience Letters*, 2005.

Davidson B.S., Madigan M.L., Southward S.C., Nussbaum M.A., "Neural Control of Posture During Small Magnitude Perturbations: Effects of Aging and Localized Muscle Fatigue", *IEEE Transactions on Biomedical Engineering*, 2011.

De Lima Pardini A.C., Papegaaij S., Cohen R.G., Teixeira L.A., Smith B.A., Horak F.B., "The interaction of postural and voluntary strategies for stability in Parkinson's disease", *Journal of Neurophysiology*, 2012.

Diener H.C., Horak F.B., Nashner L.M., "Influence of Stimulus Parameters on Human Postural Responses", *Journal of Neurophysiology*, 1988.

Dietz V., Trippel M., Ibrahim I.K., Berger W., "Human stance on a sinusoidally translating platform: balance control by feedforward and feed- back mechanisms", *Experimental Brain Research*, 1993.

Dimitrova D., Horak F.B., Nutt JG., "Postural Muscle Responses to Multidirectional Translations in Patients with Parkinson's Disease", *Journal of Neurophysiology*, 2004.

Di Giulio I., Baltzopoulos V., Maganaris C.N., Loram I.D., "Human standing: does the control strategy preprogram a rigid knee?", *Journal of Applied Physiology*, 2013.

Ersal T., McCrory J.L., Sienko K.H., "Theoretical and experimental indicators of falls during pregnancy as assessed by postural perturbations", *Gait and Posture*, 2014.

Gage W.H., Winter D.A., Frank J.S., Adkin A.L., "Kinematic and kinetic validity of the inverted pendulum model in quiet standing", *Gait and Posture*, 2004.

Hansen P.D., Woollacott M.H., Debu B., "Postural responses to changing task conditions", *Experimental Brain Research*, 1988.

Hebert J.R., Corboy J.R., "The association between multiple sclerosis-related fatigue and balance as a function of central sensory integration", *Gait and Posture*, 2013.

Henry S.M., Funf J., Horak F.B., "EMG Responses to Maintain Stance During Multidirectional Surface Translations", *Journal of Neurophysiology*, 1998.

Henry S.M., Fung J., Horak F.B., "Effect of Stance Width on Multidirectional Postural Responses", *Journal of Neurophysiology*, 2001.

Horak F.B., Diener H.C., Nashner L.M., "Influence of Central Set on Human Postural Responses", *Journal of Neurophysiology*, 1989.

Horak F.B., Nashner L.M., "Central programming of postural movements: adaptation to altered support-surface configurations", *Journal of Neurophysiology*, 1986.

Hsu W.L., Scholz, J.P., Schoner G., Jeka J.J., Kiemel T., "Control and Estimation of Posture During Quiet Stance Depends on Multijoint Coordination", *Journal of Neurophysiology*, 2007.

Hughes M.A., Schenkman M.L., Chandler J.M., Studenski S.A., "Postural responses to platform perturbation: kinematics and electromyography", *Clinical Biomechanics*, 1995.

Li Y., Levine W.S., Loeb G.E., "A Two-Joint Human Posture Control Model With Realistic Neural Delays", *IEEE Transactions on Neural Systems and Rehabilitation Engineering*, 2012.

Murnaghan C.D., Robinovitch S.N., "The effects of initial movement dynamics on human responses to postural perturbations", *Human Movement Science*, 2013.

Nanhoe-Mahabier W., Allum J.H.J., Overeem S., Borm G.F., Oude Nijhuis L.B., Bloem B.R., "First Trial Reactions and Habituation Rates over Successive Balance Perturbations in Parkinson's Disease", *Neuroscience*, 2012.

Nashner L.M., "Fixed Patterns of Rapid Postural Responses among Leg Muscles during Stance", *Experimental Brain Research*, 1977.

Nonnekes J., Scotti A., Oude Nijhuis L.B., Smulders K., Queralt A., Geurts A.C.H., Bloem B.R., Weerdesteyn V., "Are postural responses to backward and forward perturbations processed by different neural circuits?", *Neuroscience*, 2013.

Oude Nijhuis L.B, Allum J.H.J., Borm G.F., Honegger F., Overeem S., Bloem B.R., "Directional Sensitivity of "First Trial" Reactions in Human Balance Control", *Journal of Neurophysiology*, 2009.

Park S., Horak F.B., Kuo A.D., "Postural feedback responses scale with biomechanical constraints in human standing", *Experimental Brain Research*, 2004.

Perucca L., Caronni A., Vidmar G., Tesio L., "Electromyographic latency of postural evoked responses from the leg muscles during EquiTest Computerised Dynamic Posturography: Reference data on healthy subjects", *Journal of Electromyography and Kinesiology*, 2014.

Quant S., Maki B.E., McIlroy W.E., "The association between later cortical potentials and later phases of postural reactions evoked by perturbations to upright stance", *Neuroscience Letters*, 2005.

Runge C.F., Shupert C.L., Horak F.B., Zajac F.E., "Ankle hip postural strategies defined by joint torques", *Gait and Posture*, 1999.

Santos M.J., Kanekar N., Aruin A.S., "The role of anticipatory postural adjustments in compensatory control of posture: 1. Electromyographic analysis", *Journal of Electromyography and Kinesiology*, 2010.

Schieppati M, Nardone A., Siliotto R., Grasso M., "Early and late stretch responses of human foot muscles induced by perturbation of stance", *Experimental Brain Research*, 1995.

Schieppati M., Giordano A., Nardone A., "Variability in a dynamic postural task attests ample flexibility in balance control mechanisms", *Experimental Brain Research*, 2002.

Visser J.E., Oude Nijhuis L.B., Janssen L., Bastiaanse C.M., Form G.F., Duysens J., Bloem B.R., "Dynamic Posturography in Parkinson's Disease: Diagnostic Utility and the "First Trial Effect"", *Neuroscience*, 2010.

Winter D.A., Patla A.E., Prince F., Ishac M., Gielo-Perczak C., "Stiffness Control of Balance in Quiet Standing", *Journal of Neurophysiology*, 1998.

Winter D.A., Patla A.E., Rietdyk S., Ishac M.G., "Ankle Muscle Stiffness in the Control of Balance During Quiet Standing", *Journal of Neurophysiology*, 2001.

Chapter 6
Conclusions

In this study, upright stance was perturbed with three different types of movement, varying on the basis of both magnitude of perturbation and subject sensorial condition. The characterization of CoP and CoM displacement, seldom performed in this kind of balance studies, showed a typical double peak waveform, more pronounced in CoP, which allowed to divide AP CoP and CoM displacement in temporal epochs based on the imbalance and counterbalance phases. A "first trial effect" and a habituation rate were confirmed on the basis of CoP and CoM related parameters, with evidences of a motor control oriented, as expected, in counterbalance period, i.e. during the second peak, in order to regain the upright stance. In the most challenging test conditions, i.e. high velocities and/or forward movement of the base of support, balance restoring is achieved through larger and faster responses, supporting the hypothesis about the existence of response patterns tailored to the characteristics of the perturbation, the most important of which appeared the platform movement direction. Indeed, forward movement of the base of support results in posterior body sway and the distance from the ankle to the boundary of the foot support area (heel) is smaller respect to an anterior leaning, where the CoP can move up to the anterior part of the foot. Thus, depending on the platform movement direction, muscular response appeared not only more rapid for all the considered muscles (forward platform movement), but also with a different activation sequence, which leads to a different biomechanical response. Angular ranges of variation resulted in general larger not only in forward compared to backward perturbations, but also considering the increase in velocity of the platform movement, supporting also in this case what has been reported in other studies about an increased magnitude of the response to withstand larger perturbations. The attempt to assess the role of the ankle, knee and hip joint in maintenance upright stance e regain balance highlighted the central role of the ankle joint in rapidly counteracting the

perturbation; this role as the first response to the imbalance, was supported also by muscular latencies and the sequence of activation, which started in any case from one of the two ankle muscles. Furthermore, among the ankle, knee and hip strategies, the knee strategy appeared to have a non-negligible role respect to the others, confirming what has been reported about a significant knee role in withstanding large and in general particularly challenging perturbations requiring rapid balance restoration. However, rather than the presence of a single balance strategy, outcomes seem to suggest the co-existence of these strategies, in which one of them can predominate depending on the characteristic of balance perturbation.

Relatively less information has been extracted from sensory deprivation tests, where the visual feedback was withdrawn. The difficulty in characterizing balance responses in EC condition and the apparent absence of meaningful differences with the EO condition may be due to the chosen test configuration, with a sudden balance perturbation instead of a sinusoidal translation of the base of support, which would have elicited the long-term response joined to the visual information feedback, adapting the balance response to the periodic base of support movement. Beyond this aspect, some limitations are present in this study, such as the limited number of volunteers, the choice to limit the perturbation variables to the velocity and displacement of perturbation, not involving other types of perturbations, such as reducing the size of the base of support or decreasing proprioceptive feedback and the choice to avoid, as much as possible, the effect of the acceleration. However, the acceleration of the base of support represents a further source of balance perturbation and the same role is played by the deceleration phase, which could interfere with the responses triggered by the previous phase.

This study represents a first attempt to characterize the upright stance perturbation considering the effect of a trial series of equal perturbation and a trial series with increasing velocity, avoiding the effect of the acceleration. This characterization has been performed considering also CoP and CoM displacement, which are seldom considered in studies regarding balance perturbation, attempting to describe them in terms of imbalance and counterbalance periods. Moreover, also a

direct comparison between backward and forward perturbation have been performed, in order to gain further insight on the different response mechanisms elicited by these two opposite stimuli. Future developments could involve the enlargement of the tested population, the characterization of the responses also in terms of joint torques, with the perspective of extract information through the measure of the antero-posterior ground reaction force component.

Chapter 7
Balance Response Modeling

Throughout the years, many attempts have been made in order to modeling upright posture, in both static and dynamic configurations (Winter *et al.*, 1998; Li *et al.*, 2012). The first and most used model is the single inverted pendulum (Winter *et al.*, 1998; Winter *et al.*, 2001), where balance control is achieved shifting body around the pivot point represented by the ankle joint. In perturbed configurations however the presence of at least two postural strategies to recover balance, i.e. the ankle strategy and hip strategy, leaded to a model with more degrees of freedom, such as the double inverted pendulum (Li *et al.*, 2012; Engelhart *et al.*, 2015). In the latter type of models, balance is maintained or regained controlling body sway through the movement of both the ankle and the hip joint (Horak and Nashner, 1986). The choice of one or other of the models depends on what kind of balance task is considered: when perturbation of upright stance is absent or has a small magnitude, the single inverted pendulum models well balance maintenance. On the contrary, with large balance perturbations, the double inverted pendulum explains better the upright stance recovery (Li *et al.*, 2012; Ersal *et al.*, 2014).

In this work, a first attempt at modeling the perturbed upright stance has been made using a single inverted pendulum, thus suitable when the base of support movement has a limited velocity and/or displacement, with a classical proportional-derivative-integrative (PID) control scheme. Then, in order to consider also the other type of perturbations employed in this study, also a double inverted pendulum model has been developed, using a control scheme seldom employed in this kind of applications.

7.1 Single Inverted Pendulum

Single inverted pendulum with proportional-derivative or PID controller has been yet employed in modeling upright stance (Peterka, 2000; Maurer and Peterka, 2005; Masani *et al.*, 2006). In Figure 1 there is the schematic representation of the used model, in which $a_a(t)$ represent platform acceleration, $\theta(t)$ the sway angle and $T_a(t)$ the control torque exerted about the ankle joint.

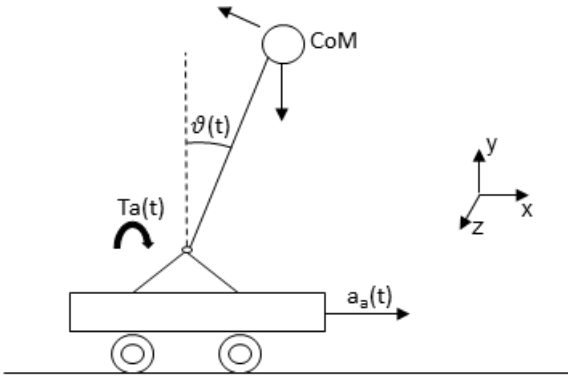

Figure 1. Model of the single inverted pendulum

CoM acceleration is expressed as:

$$\overrightarrow{a_B} = \overrightarrow{a_g} + \overrightarrow{a_a} + \dot{\vec{\omega}} \times \vec{r}_{aB} + \vec{\omega} \times (\vec{\omega} \times \vec{r}_{aB}) \qquad (1)$$

where a_g represents the gravitational component of CoM acceleration, ω the CoM angular velocity and r_{aB} the CoM distance from the ankle joint. Thus, the equation (1) can expressed as:

$$\begin{bmatrix} \ddot{x}_{COM} \\ \ddot{y}_{COM} \\ 0 \end{bmatrix} = \begin{bmatrix} 0 \\ -g \\ 0 \end{bmatrix} + \begin{bmatrix} \ddot{x}_a \\ 0 \\ 0 \end{bmatrix} + \begin{bmatrix} 0 \\ 0 \\ \ddot{\vartheta} \end{bmatrix} \times \begin{bmatrix} h_B \cdot \sin\vartheta \\ h_B \cdot \cos\vartheta \\ 0 \end{bmatrix} + \begin{bmatrix} 0 \\ 0 \\ \dot{\vartheta} \end{bmatrix} \times \left(\begin{bmatrix} 0 \\ 0 \\ \dot{\vartheta} \end{bmatrix} \times \begin{bmatrix} h_B \cdot \sin\vartheta \\ h_B \cdot \cos\vartheta \\ 0 \end{bmatrix} \right) = \begin{bmatrix} \ddot{x}_a \\ -g \\ 0 \end{bmatrix} + \begin{bmatrix} -\ddot{\vartheta} \cdot h_B \cdot \cos\vartheta \\ \ddot{\vartheta} \cdot h_B \cdot \sin\vartheta \\ 0 \end{bmatrix} -$$

$$\dot{\vartheta}^2 \cdot \begin{bmatrix} h_B \cdot \sin\vartheta \\ h_B \cdot \cos\vartheta \\ 0 \end{bmatrix} \qquad (2)$$

where h_B is the vertical distance of the CoM respect to the ankle joint and $\ddot{x}_a$ is the acceleration provided by the platform. The CoM undergoes a force equal to:

$$\vec{F}_i = -m_B \cdot \vec{a}_B \qquad (3)$$

and a torque equal to:

$$\vec{M}_i = \vec{r}_{aB} \times \vec{F}_i \qquad (4)$$

thus, equation (3) can be expressed as:

$$\vec{M}_i = \begin{bmatrix} h_B \cdot sin\,\vartheta \\ h_B \cdot cos\,\vartheta \\ 0 \end{bmatrix} \times m_B \cdot \begin{bmatrix} -(\ddot{x}_a - \ddot{\vartheta} \cdot h_B \cdot cos\,\vartheta - \dot{\vartheta}^2 \cdot h_B \cdot sin\,\vartheta) \\ -\left(-g + \ddot{\vartheta} \cdot h_B \cdot sin\,\vartheta - \dot{\vartheta}^2 \cdot h_B \cdot cos\,\vartheta\right) \\ 0 \end{bmatrix} =$$

$$\begin{bmatrix} 0 \\ 0 \\ -m_B h_B\, sin\,\vartheta\left(-g + \ddot{\vartheta} h_B\, sin\,\vartheta - \dot{\vartheta}^2 h_B\, cos\,\vartheta\right) + m_B h_B\, cos\,\vartheta(\ddot{x}_a - \ddot{\vartheta} h_B\, cos\,\vartheta - \dot{\vartheta}^2 h_B\, sin\,\vartheta) \end{bmatrix} \qquad (4)$$

Considering small perturbations which lead to small variations of the sway angle (Davidson *et al.*, 2011; Ersal *et al.*, 2014), equation (4) can be linearized for $\vartheta \approx 0$ and thus, since $\sin\vartheta = \vartheta + o(\vartheta^3)$ and $cos\,\vartheta = 1 + o(\vartheta^2)$, equation (4) can be expressed as:

$$\vec{M}_i \approx \begin{bmatrix} 0 \\ 0 \\ m_B h_B \vartheta g + m_B h_B \ddot{x}_a - m_B h_B^2 \ddot{\vartheta}\, cos\,\vartheta \end{bmatrix} \qquad (5)$$

The mechanical equilibrium at the ankle joint is expressed by:

$$M_i - T_a(t) - K\vartheta - B\dot{\vartheta} = J_B\ddot{\vartheta} \qquad (6)$$

where K and B are the passive ankle stiffness and passive ankle damping respectively, which yield a momentum proportional to body sway and its velocity. J_B is the momentum of inertia of the body segment around the ankle joint z axis. The negative sign of $T_a(t)$, $K\vartheta$ and $B\dot{\vartheta}$ indicates their opposition to the system dynamics. Substituting (5) in (6), the dynamic equation of the system in linear, first order form is:

$$m_B h_B \ddot{x}_a + m_B g h_B \vartheta - T_a(t) - K\vartheta - B\dot{\vartheta} = 2J_B\ddot{\vartheta} \qquad (7)$$

The initial conditions for the system expressed by (7) have been chosen as:

$$\begin{cases} \vartheta(0^+) = 0 \\ \dot{\vartheta}(0^+) = 0 \end{cases}$$

and $\ddot{x}_a$ will be indicated in the following as $u(t)$.

In the Laplace representation, (7) can be expressed as follows:

$$\vartheta(s) = \frac{m_B h_B u(s)}{(2J_B s^2 + Bs + K - m_B g h_B)} - \frac{T_a(s)}{(2J_B s^2 + Bs + K - m_B g h_B)} \qquad (8)$$

The dynamic control of the model has been developed through a proportional, derivative and integrative, time-delayed control system, with a reference body sway angle set to zero which represents the desired equilibrium point at the ankle joint (Fig. 2).

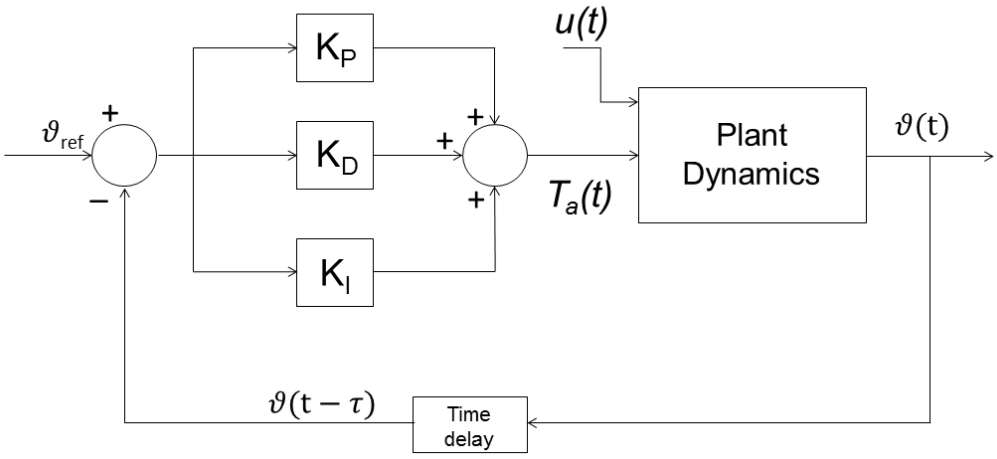

Figure 2. Schematic of the dynamic model that includes the plant and the PID controller.

The control torque $T_a(s)$ is given by:

$$T_a(s) = e^{-s\tau_d}\vartheta(s)(K_P + sK_D + \frac{K_I}{s}) \qquad (9)$$

The term $e^{-s\tau_d}$ represents the time delay due to neural transmission and substituting (9) in (8) the transfer function of the system is obtained as follows:

$$\frac{\vartheta(s)}{u(s)} = \frac{m_B h_B}{(2J_B s^2 + Bs + K - m_B g h_B) + e^{-s\tau_d}(K_P + sK_D + \frac{K_I}{s})} \qquad (10)$$

The term $e^{-s\tau_d}$ introduces a nonlinearity in the system and following what has been reported by Qu and Nussbaum (2009) this term is linearized as:

$$e^{-s\tau_d} = 1 - s\tau_d + \frac{s^2\tau_d^2}{2} + o(s^3) \qquad (11)$$

thus leading to the following formulation of the closed loop transfer function:

$$\frac{\vartheta(s)}{u(s)} = \frac{m_B h_B}{(2J_B s^2 + Bs + K - m_B g h_B) + (\frac{s^2 \tau_d^2}{2} - s\tau_d + 1)(K_P + sK_D + \frac{K_I}{s})} \qquad (12)$$

The optimization of the PID parameters K_P, K_D and K_I has been performed following the approach reported by Peterka (2000), through the minimization of the difference between the measured AP CoP displacement and the simulated AP CoP displacement. Thus, the error function is given by:

$$e(K_P, K_D, K_I) = \sum_{sample=1}^{n} ((COP_{mis(n)} - COP_{sim(n)})\text{^}2 \qquad (13)$$

In order to obtain the CoP AP displacement from the model output, a single inverted pendulum in unperturbed conditions was considered (Fig. 3):

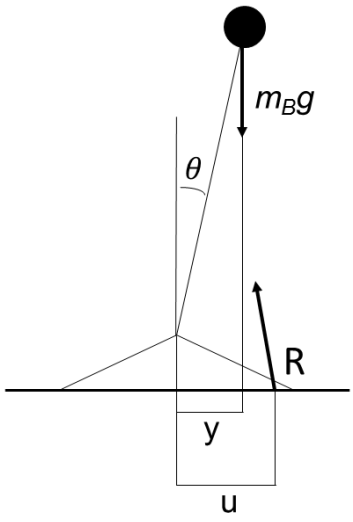

Figure 3. Scheme of the classic, unperturbed inverted pendulum. CoM position is indicated by y, while CoP position is denoted by u. R is the ground reaction force.

The linearized system equation of the inverted pendulum is given by:

$$J_p \ddot{\vartheta} = m_B g h_B \vartheta + \tau_{ANKLE} \qquad (14)$$

where J_p is the moment of inertia of the body, m_B is the body mass, h_B is the distance of the CoM from the ankle, ϑ is the sway angle and τ_{ANKLE} is the total ankle torque. The ankle torque have to satisfy an equilibrium equation for the foot:

$$\tau_{ANKLE} + R_v u = 0 \qquad (15)$$

where R_v is the vertical component of the ground reaction force and u is the CoP position. Considering that in quiet standing $R_v \approx m_B g$, and $J_p = m_B h_B^2$, CoP position can be obtained as:

$$J_p \ddot{\vartheta} = m_B g h_B \vartheta - m_B g u \;\Rightarrow COP(\vartheta, t) = h_B \left(\frac{\ddot{\vartheta}}{g} h_B + \vartheta\right) \qquad (16)$$

and in the Laplace domain:

$$\frac{COP(s)}{\vartheta(s)} = s^2 \frac{h_B^2}{g} + h_B \qquad (17)$$

Thus, the final transfer function is represented by:

$$\frac{COP(s)}{u(s)} = \frac{m_B h_B \left(s^2 \frac{h_B^2}{g} + h_B\right)}{(2J_B s^2 + Bs + K - m_B g h_B) + \left(\frac{s^2 \tau_d^2}{2} - s\tau_d + 1\right)\left(K_P + sK_D + \frac{K_I}{s}\right)} \qquad (18)$$

Parameters values of the PID controller have been obtained through an optimization procedure: to this aim, the Nelder-Mead search was used (Maurer and Peterka, 2005). Nelder-Mead algorithm is a local nonlinear search and thus the initial parameters value is crucial in order to maximize the likelihood of global optimal values. To this aim, optimization began with values for parameters of the controller, similar to those proposed by Davidson *et al.* (2011) and Peterka (2000). Neural delay value was set equal to 0.171 s (Davidson *et al.*, 2011). Values of the model parameters were J_B = 76.6 kg·m², h_B = 1.2 m, K = 10.2 N·m/deg, B = 3 N·m·s/deg. The platform acceleration was the perturbative input of the system and was modeled as reported in Fig. 4. The choice of this waveform lied on the consideration that only the acceleration phase provides the system perturbation, since only in this period, together with the deceleration phase, the pendulum undergoes to a force; on the constant velocity phase no forces are applied to the system. Simulations began at the time of perturbation onset and lasted for 3.5 s and were performed considering trials with a perturbation velocity of 15 cm/s and an acceleration of 3 m/s². The acceleration waveform (Fig. 4) leads to a quasi-impulsive perturbation which not strictly follows the test characteristics, i.e. the phase with constant velocity is

absent. However, since a force in applied to the system only when the acceleration is different from zero, the chosen system input can simulate the real test conditions in a first approximation. A total of 20 simulations where performed, on data belonging to a single subject from fixed velocity trials.

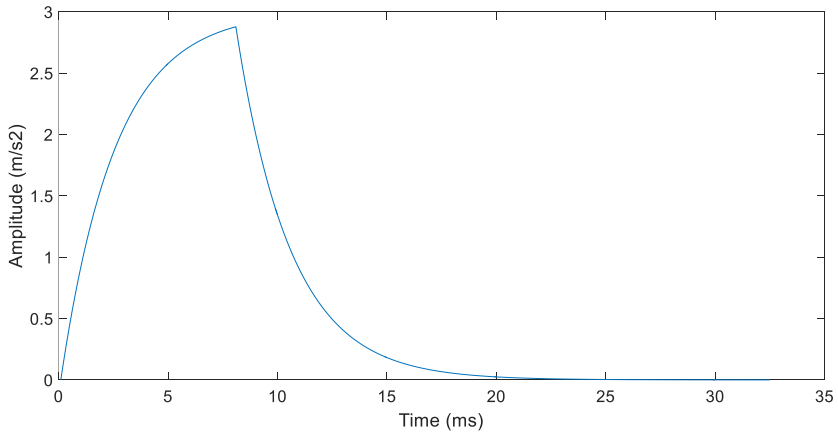

Figure 4. Platform acceleration.

A good correspondence was found between model output and measured CoP (Fig. 5) and the mean fit value (R^2) resulted 0.70±0.11. Despite the limited value of the fit goodness, the simulated CoP presented comparable amplitude values of displacement with the measured CoP and furthermore showed the typical double peak shape which characterize this type of balance tests.

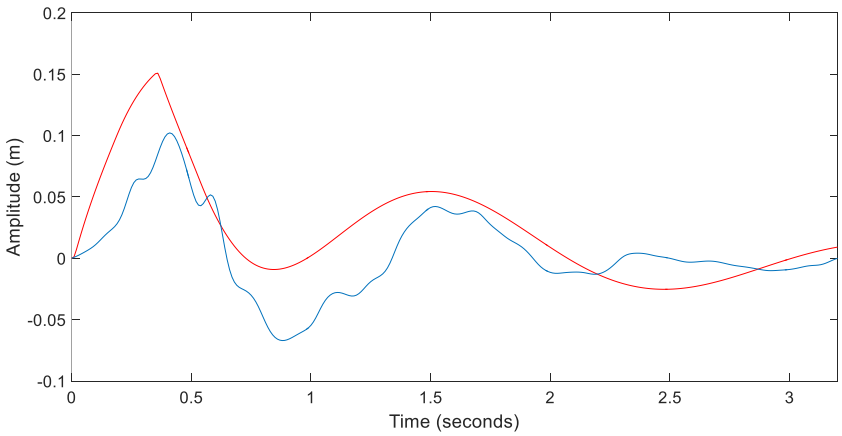

Figure 5. Representative results of a simulation. Measured AP CoP displacement (blue line) and simulated AP CoP displacement (red line). Simulated CoP follows well the double peaks shape of the measured CoP.

However, optimized PID parameters exhibited higher values respect to those reported by Peterka (2000) and Davidson *et al.* (2011). For instance, in the reported simulation (Fig. 5), K_P, K_D and K_I were

1624.3 N·m/deg, 479.5 N·m·s/deg and 0.56 N·m/s·deg respectively. This discrepancy could be explained with the different type of test performed in those studies, i.e. absence of perturbations in Peterka (2000) and perturbation administered through a ballistic pendulum with stimuli applied to the upper trunk (Davidson *et al.*, 2011). In the latter case, perturbations had a small or moderate magnitudes (10 N·s and 7 N·s).and moreover perturbations have been reduced by body inertia. In the inverted pendulum model, on the contrary, the input is an acceleration, which is multiplied by the $m_B h_B$ term.

The good but not high correspondence between simulated and measured CoP displacement obtained with this kind of model matches with what has been reported about the unsuitableness of a single-segmented model for this kind of applications (Ersal *et al.*, 2008; Ersal *et al.*, 2014). Furthermore, the well-known importance of the hip joint for balance recovering after base of support perturbations, leaded to an attempt to model upright balance through a double inverted pendulum (Li, *et al.*, 2012; Ersal *et al.*, 2014; Engelhart *et al.*, 2015).

7.2 Double Inverted Pendulum

To model the perturbed upright stance taking into consideration also the hip joint, a double-link inverted pendulum with lumped masses was used (Fig. 6).

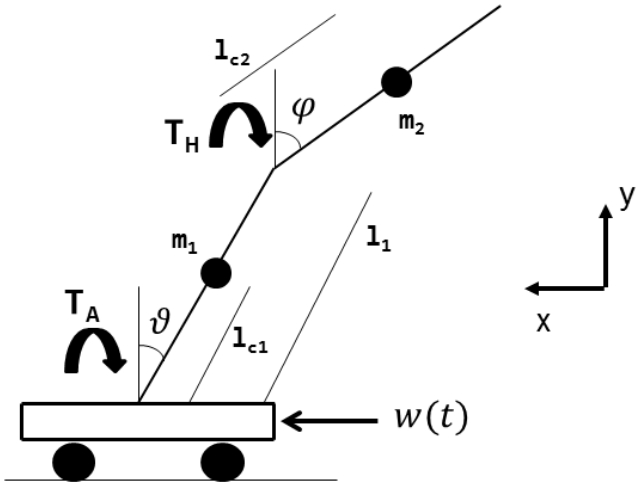

Figure 6. Scheme of the double-link inverted pendulum. Lumped masses of the lower limb and the upper part of the body are indicated as m_1 and m_2. Length of the lower limb is indicated as l_1, while l_{c1} and l_{c2} stand for the center of mass heights. Force applied to the platform is indicated as w(t). T_A and T_H are active torques at the ankle and hip joint respectively.

Dynamic model of the double inverted pendulum has been assessed through the lagrangian approach. Generalized variables have been defined as follows:

$$q_0 = \begin{vmatrix} x \\ 0 \end{vmatrix} \qquad q_1 = \begin{vmatrix} x - l_{c1}\sin\vartheta \\ l_{c1}\cos\vartheta \end{vmatrix} \qquad q_2 = \begin{vmatrix} x - l_1\sin\vartheta - l_{c2}\sin\varphi \\ l_1\cos\vartheta + l_{c1}\cos\varphi \end{vmatrix}$$

where q_0 defines the ankle position, q_1 is the position of the lower limb center of mass and q_2 is the position of the center of mass of the upper body. Lagrangian approach defines the difference between the kinetic and potential energy:

$$L(\dot{q}, q, t) = K(\dot{q}, q, t) - P(q, t)$$

Kinetic and potential energy are obtained as follows:

$$K = \frac{1}{2}[m_0\|\dot{q}_0(t)\|^2 + m_1\|\dot{q}_1(t)\|^2 + m_2\|\dot{q}_2(t)\|^2]$$

$$P = m_1 g q_1 + m_2 g q_2$$

where m_0 is the platform mass.

Dynamic equations are defined in the lagrangian approach as:

$$F = \frac{d}{dt}\left\{\frac{\partial L}{\partial \dot{q}_0}\right\} - \frac{\partial L}{\partial q_0}$$

$$T_A = \frac{d}{dt}\left\{\frac{\partial L}{\partial \dot{q}_1}\right\} - \frac{\partial L}{\partial q_1}$$

$$T_H = \frac{d}{dt}\left\{\frac{\partial L}{\partial \dot{q}_2}\right\} - \frac{\partial L}{\partial q_2}$$

Also in this case the system has been linearized considering small perturbations and thus limited variations of ϑ and φ (Ersal *et al.*, 2014). The system equations, linearized around the upright equilibrium are given by:

$$\begin{vmatrix} (m_1 l_{c1}^2 + m_2 l_1^2) & m_2 l_1 l_{c2} \\ m_2 l_1 l_{c2} & m_2 l_{c2}^2 \end{vmatrix} \begin{vmatrix} \ddot{\vartheta} \\ \ddot{\varphi} \end{vmatrix} = \begin{vmatrix} g(m_1 l_{c1} + m_2 l_1) & 0 \\ 0 & g m_2 l_{c2} \end{vmatrix} \begin{vmatrix} \vartheta \\ \varphi \end{vmatrix} + \begin{vmatrix} 1 & -1 \\ 0 & 1 \end{vmatrix} \begin{vmatrix} T_A \\ T_H \end{vmatrix} + \begin{vmatrix} (m_1 l_{c1} + m_2 l_1) \\ m_2 l_{c2} \end{vmatrix} d$$

where d is the acceleration applied by the platform to the pendulum. Representing the system in a compact form, the following equation in obtained:

$$C_a \ddot{\gamma} = D\gamma + NT + Pd$$

The system has been expressed in the state space form:

$$\begin{cases} \dot{x} = Ax + B_1 u + B_2 d \\ y = Cx \end{cases}$$

where

$$\begin{vmatrix} \dot{\vartheta} \\ \vartheta \\ \dot{\varphi} \\ \varphi \end{vmatrix} = x \qquad A = C_a^{-1} D \qquad B_1 = C_a^{-1} \qquad B_2 = C_a^{-1} P \qquad C = \begin{vmatrix} 0100 \\ 0001 \end{vmatrix} \qquad u = \begin{vmatrix} T_A - T_H \\ T_H \end{vmatrix}$$

The platform acceleration can be considered as a disturbance of the system (w(t)) and the goal of the control problem is to obtain a null error between the output (controlled variable) and the reference. In this case the reference is represented by the value of ankle and hip angles in unperturbed upright stance condition. A system with a disturbance on the plant (Fig. 7) and a reference which must be

tracked by the output can be represented considering the disturbance and the reference as a whole disturbance acting on the plant (Fig. 8):

$$\widehat{w}(t) = \begin{vmatrix} w(t) \\ y_d(t) \end{vmatrix}$$

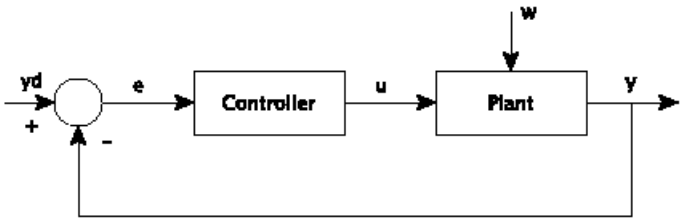

Figure 7. Control system structure. The disturbance is indicated as w, while the reference is y_d.

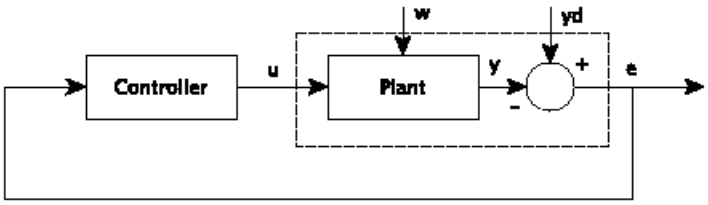

Figure 8. Equivalent structure of the control system.

Through this kind of representation, only the response to the disturbance $\widehat{w}(t)$ is considered. If the original plant (Fig. 7) was represented by:

$$\begin{cases} \dot{x} = Ax + Bu + Pw \\ y = Cx + Qw \end{cases}$$

the system in the dashed box in Fig. 8 is given by:

$$\begin{cases} \dot{x} = Ax + Bu + Pw \\ e = -Cx - Qw + y_d \end{cases}$$

and thus:

$$\begin{cases} \dot{x} = Ax + Bu + \hat{P}\widehat{w} \\ e = \hat{C}x + \hat{Q}\widehat{w} \end{cases} \quad \hat{P} = |P \quad 0| \quad \hat{C} = -C \quad \hat{Q} = |-Q \quad 0|$$

In this context, $\widehat{w}$ is a polynomial signal which enclosed both the original disturbance and the reference, generated by a system described by the following linear differential equation:

$$\dot{\hat{w}} = S\hat{w}$$

The solutions of the latter equation corresponds to the functions describing both disturbance and references of the system represented in Fig. 8. In this context, the controller is due by:

$$u = Kx + L\hat{w}$$

where K is the classical feedback matrix, based on the desired characteristic polynomial and L is obtainable resolving:

$$\begin{cases} \Pi S = (A + BK)\Pi + \left(\hat{P} + BL\right) \\ 0 = \hat{C}\Pi + \hat{Q} \end{cases}$$

thus the final system is that reported in Fig. 9.

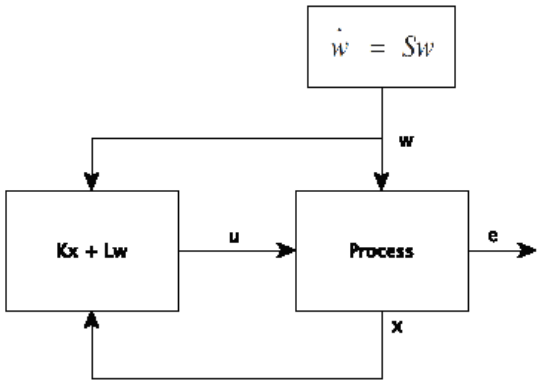

Figure 9. Equivalent control system.

For the model simulation, typical value for masses and body lengths have been chosen according to Suzuki *et al.* (2012). The employed approach entails that the disturbance belongs to a known class of signal, such as polynomial, sinusoidal, exponential and so on. Thus, a disturbance which mimics that acceleration used for the single inverted pendulum is inapplicable in this case; in order to verify the model and control strategy, the disturbance, i.e. the acceleration waveform, has been modeled as a ramp, which simulate thus a continuous accelerated movement of the base of support. In this case, the internal model of the disturbance $\hat{w}$ resulted:

$$\hat{w} = \begin{vmatrix} \alpha t \\ \alpha \\ \vartheta \\ \varphi \end{vmatrix} \qquad \dot{\hat{w}} = \begin{vmatrix} \alpha \\ 0 \\ 0 \\ 0 \end{vmatrix} \qquad S = \begin{vmatrix} 0 & 1 & 0 & 0 \\ 0 & 0 & 0 & 0 \\ 0 & 0 & 0 & 0 \\ 0 & 0 & 0 & 0 \end{vmatrix}$$

The reference for both ankle and hip angles was set on 5°. Results of the simulations for ramp slope set equal to 1 and 10^{-4} are reported in Fig. 10.

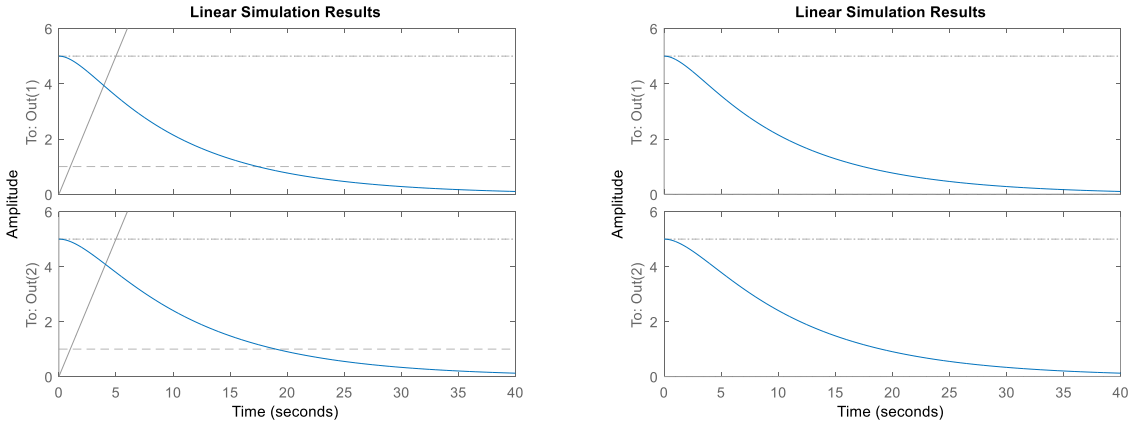

Figure 10. Error between reference value and system output for a ramp with slope equal to 1 (left panel) and with a slope equal to 10^{-4} (right panel). Error waveform is reported in blue color.

In both cases the error between the reference angles value and the system output decreases to zero, thus rejecting the disturbance effect on the controlled variable and satisfying the requirements.

The employment of this control procedure seems to cancel the effect of the disturbance on the double-link pendulum system, allowing its control and confirming its reliability in the upright stance balance recovery simulation. The error between the desired response and the system output has a slow decrease to zero, however this feature may depend on the choice of the eigenvalues of the A+BK matrix and thus could be set in the phase of the controller definition. However, several drawbacks are still present, questioning the applicability of this approach in this context. The strict limits for the modeling of the disturbance and reference signals is the major one, hampering the use of this control approach when, as in the presented case, the real disturbance waveform is not a polynomial, sinusoidal or exponential signal. What has been presented is the initial part of an attempt to adapt the internal model approach to the control of a double inverted pendulum, which models the upright stance recovery and maintenance in perturbed configurations. The next step will be the testing of the pendulum model and the control approach in providing outputs which present a good correspondence with the measures, i.e. the CoP displacement principally.

Chapter References

Engelhart D., Schouten A.C., Aarts R.G., van der Kooij H., "Assessment of Multi-Joint Coordination and Adaptation in Standing Balance: A Novel Device and System Identification Technique", *IEEE Transactions on Neural Systems and Rehabilitation Engineering*, 2015.

Ersal T., Fathy H.K., Louca L.S., Rideout D.G., Stein J.L., "A Review of Proper Modeling Techniques", *Journal of Dynamic Systems Measurement and Control*, 2008.

Ersal T., McCrory J.L., Sienko K.H., "Theoretical and experimental indicators of falls during pregnancy as assessed by postural perturbations", *Gait and Posture*, 2014.

Horak F.B., Nashner L.M., "Central programming of postural movements: adaptation to altered support-surface configurations", *Journal of Neurophysiology*, 1986.

Li Y., Levine W.S., Loeb G.E., "A Two-Joint Human Posture Control Model With Realistic Neural Delays", *IEEE Transactions on Neural Systems and Rehabilitation Engineering*, 2012.

Masani K., Vette A.H., Popovic M.R., "Controlling balance during quiet standing: Proportional and derivative controller generates preceding motor command to body sway position observed in experiments", *Gait and Posture*, 2006.

Maurer C., Peterka R.J., "A New Interpretation of Spontaneous Sway Measures Based on a Simple Model of Human Postural Control", *Journal of Neurophysiology*, 2005.

Peterka R.J., "Postural control model interpretation of stabilogram diffusion analysis", *Biological Cybernetics*, 2000.

Suzuki Y., Nomura T., Casadio M., Morasso P., "Intermittent control with ankle, hip, and mixed strategies during quiet standing: A theoretical proposal based on a double inverted pendulum model", *Journal of Theoretical Biology*, 2012.

Winter D.A., Patla A.E., Prince F., Ishac M., Gielo-Perczak C., "Stiffness Control of Balance in Quiet Standing", *Journal of Neurophysiology*, 1998.

Winter D.A., Patla A.E., Rietdyk S., Ishac M.G., "Ankle Muscle Stiffness in the Control of Balance During Quiet Standing", *Journal of Neurophysiology*, 2001.

Part 2

Motor Control in Walking Task

Chapter 1
Introduction

Gait analysis is defined as the systematic study of human locomotion aided by instrumentation for measuring body mechanics and muscles activity. A central role in controlling walking mechanics is played by lower limb muscles, of both thigh and shank (Perry, 1992; Winter and Yack, 1987; Sutherland, 2001). In order to obtain a whole evaluation of the physiological gait characteristics, the muscles usually selected for the analysis are Tibialis Anterior and Gastrocnemius Lateralis or Medialis for the shank and Rectus Femoris, Vastus Lateralis or Medialis and Biceps Femoris for the thigh. In particular, ankle joint appears to be fundamental in determining gait patterns: ankle plantar-flexor muscles control the forward rotation of the tibia over the talus during stance phase, provide joints stability, and conserve energy by minimizing vertical oscillation of the whole-body center of mass (Sutherland, 2001). Ankle dorsi-flexor muscles prevent slapping of the foot on the ground during the initial stance, favor the forefoot to clear the ground in initial swing and lock the ankle joint for the initial contact (Perry, 1992).

Surface electromyography (sEMG) represents a central part of the gait analysis, providing the assessment of the activation patterns of muscles involved in gait (Perry, 1992; Sutherland, 2001; Winter and Yack, 1987) and supporting the objective description of muscular function during walking. The sEMG signals can show a wide inter-person variability and they can also differ for the same motion even within the same person, reflecting the variability in muscles activity during walking. Thus, sEMG seems to be useful to deepen this the natural variability, related with the myoelectric activity during gait (Agostini *et al.*, 2010; Di Nardo *et al.*, 2013).

Concerning the control of lower body mechanics in walking task, two aspects appear to deserve a specific attention: gender-based differences in muscles activity of both thigh and shank muscles and the assessment of co-contraction behavior of antagonist muscles controlling the ankle joint, i.e.

tibialis anterior and gastrocnemius (lateralis and/or medialis). Gender-specific morphology of pelvis and thigh have been yet reported (Horton and Hall, 1989; Hurd *et al.*, 2004,). These biomechanical differences indicate that gender could be a factor influencing movement patterns during gait. Moreover, compared with males, females show a higher cadence and have a shorter stride length (Oberg *et al.*, 1993; Richard *et al.*, 1995) and during walking they present an increased sagittal-plane hip flexion and a decreased knee flexion in preparation for weight bearing, together with changes in knee-flexion moment and power absorption during pre-swing (Kerrigan *et al.*, 1998). Excursions in frontal and transverse planes were lower at the hip and knee for males compared to females (Hurd *et al.*, 2004) and clear gender differences were observed even in hip kinematics across a variety of walking speeds and surface inclinations (Chumanov *et al.*, 2008). Furthermore, Nakagawa *et al.* (2012) reported a female increased hip adduction and knee abduction during the downward and upward phases of the gait task.

Given these differences in joint kinematics, it is likely that gender differences in underlying muscle activities are also present. However, only few studies reported the influence of gender on walking, provided by analyzing myoelectric signals recorded from the lower limb muscles (Chiu and Wang, 2007; Chumanov *et al.*, 2008; Chung and Wang, 2010). Through the sEMG signals from biceps femoris, rectus femoris, gastrocnemius and tibialis anterior, Chiu and Wang (2007) showed that females produce significantly higher muscle activity only in tibialis anterior during walking, while tibialis anterior activity increases at higher walking speed (Chung and Wang, 2010). Thus, the study of tibialis anterior and its antagonist muscle for ankle plantar/dorsiflexion, the gastrocnemius, could be relevant for analyzing possible gender-related differences during walking. However, many of the reported kinematics/kinetics differences between males and females during walking (Chumanov *et al.*, 2008; Hurd *et al.*, 2004; Kerrigan *et al.*, 1998; Nakagawa *et al*, 2012) concern the role of proximal leg joints. Moreover, different studies (Arendt *et al.*, 1999) documented a higher risk of anterior cruciate ligament injury in females, compared to male, suggesting a different workload of muscles crossing knee. Accordingly, also proximal muscles may provide significant insights concerning the

gender-related differences in muscle activity. Moreover, it was observed that also advancing age modifies the timing of onset/offset activation of lower limb muscles and the duration of the activity of agonist and antagonist muscles (Hortobagyi *et al.*, 2009; Tirosh *et al.*, 2005). This suggests the suitability of developing electromyographic databases, separated for young and old subjects.

For what concerns co-contraction activity of lower limb muscles during walking, generally speaking the muscle co-contraction is defined as a simultaneous contraction of agonist and antagonist muscles crossing a joint (Olney, 1985). Its purpose is to enhance the ligament maintenance of joint stability, providing resistance to rotation at a joint and equalizing pressure distribution at the articular surface (Baratta *et al.*, 1988). The development of torque by a single, unopposed agonist muscle group about a joint creates an uneven pressure distribution over the articular surfaces. Co-activation of an antagonist muscle group would, therefore, aid in the distribution of forces at the articular surface and simultaneously increase joint stability by increasing the degree of bone-to-bone fit of the articular ends. Moreover, it is well-recognized that muscle co-contraction has an important role in movement regulation during motor learning activities, enhancing joint stability (Darainy and Ostry, 2008). Thus, muscle co-contraction should be a crucial factor to consider during motor rehabilitation (Den Otter *et al.*, 2006). The assessment of muscle co-contraction during dynamic tasks, such as walking, requires the analysis of the relative variations in agonist and antagonist contraction over time. This complex relationship between the activity of agonist and antagonist muscles that underlies muscle co-contraction is generally explored by means of surface electromyography (sEMG) (da Fonseca *et al.*, 2004).

The importance played by these two aspects, i.e. gender-based differences in walking mechanics and the central role of ankle muscles co-contraction in controlling gait dynamic, suggested thus the evaluation of the gender-related differences in the myoelectric activity of lower limb muscles during walking at self-selected speed and cadence, in terms of activation patterns of each muscle and of its occurrence frequency. sEMG signal acquired from Tibialis Anterior (TA), Gastrocnemius Lateralis (GL), Rectus Femoris (RF), Biceps Femoris (BF) and Vastus Lateralis (VL) have been considered, in

order to perform an analysis on the whole lower limb. Moreover, due the previously reported importance of the ankle muscles co-contraction activity during walking, also the assessment of the co-contractions of tibialis anterior and gastrocnemius in healthy adults during gait at self-selected speed and cadence has been performed, evaluating the relative variations in agonist and antagonist contraction for ankle plantar/dorsiflexion over time. This goal was pursued by performing a statistical analysis of surface EMG signal from a large number (hundreds) of strides per subject. The method chosen to quantify muscular co-contractions is the assessment of the period of overlap between activation intervals of the antagonist muscles (Den Otter *et al.*, 2006; Dietz *et al.*, 1981; Prosser *et al.*, 2010).

Eventually, it was reported (Franz and Kram, 2013; Hortobagyi and Devita, 2006; Peterson and Martin, 2010) that, in healthy adults, co-contractions during walking could be affected by age and velocity, showing a greater amount of co-activations for shank muscles in the elderly. The dependency of antagonist muscles activity on these factors leads to wonder whether also the gender could play a role in the co-contraction behavior of shank muscles. Also the differences between males and females detected in muscular activity during gait (Chiu and Wang, 2007) support the hypothesis of a possible influence of gender on muscle co-contraction. Chiu and Wang (2007), indeed, documented both a significantly greater myoelectric activity in tibialis anterior and a significantly greater ankle joint range of motion for females during gait.

Thus, in the presented work, an evaluation of the gender-based differences in myoelectric activity of lower-limb muscles (TA, GL, RF, VL and BF) was firstly performed, followed by an analysis aimed to assess co-contraction activity of ankle muscles (TA and GL) during walking. Eventually these two aspects have been joined together in order to compare co-activation patterns of TA and GL in males and females during walking task.

Chapter References

Agostini V., Nascimbeni A., Gaffuri A., Imazio P., Benedetti M.G., Knaflitz M., "Normative EMG activation patterns of school-age children during gait", *Gait and Posture*, 2010.

Arendt E.A., Agel J., Dick R., "Anterior cruciate ligament injury patterns among collegiate men and women", *Journal of Athletic Training*, 1999.

Baratta R., Solomonow M., Zhou B.H., Letson D., Chuinard R., D'Ambrosia R., "Muscular coactivation. The role of the antagonist musculature in maintaining knee stability", *The American Journal of Sports Medicine*, 1988.

Chiu M.C., Wang M.J., "The effect of gait speed and gender on perceived exertion, muscle activity, joint motion of lower extremity, ground reaction force and heart rate during normal walking", *Gait and Posture*, 2007.

Chumanov E.S., Wall-Scheffler C., Heiderscheit B.C., "Gender differences in walking and running on level and inclined surfaces", *Clinical Biomechanics*, 2008.

Chung M.J., Wang M.J., "The change of gait parameters during walking at different percentage of preferred walking speed for healthy adults aged 20–60 years", *Gait and Posture*, 2010.

da Fonseca S., Silva P.L., Ocarino J.M., Guimaràes R.B., Oliveira M.T., Lage C.A., "Analyses of dynamic co-contraction level in individuals with anterior cruciate ligament injury", *Journal of Electromyography and Kinesiology*, 2004.

Darainy M., Ostry D.J., "Muscle cocontraction following dynamics learning", *Experimental Brain* Research, 2008.

Den Otter A.R., Geurts A.C., Mulder T., Duysens J., "Gait recovery is not associated with changes in the temporal patterning of muscle activity during treadmill walking in patients with post-stroke hemiparesis", *Clinical Neurophysiology*, 2006.

Di Nardo F., Ghetti G., Fioretti S., "Assessment of the activation modalities of gastrocnemius lateralis and tibialis anterior during gait: A statistical analysis", *Journal of Electromyography and Kinesiology*, 2013.

Franz J.R., Kram R., "How does age affect leg muscle activity/coactivity during uphill and downhill walking?", *Gait and Posture*, 2013.

Hortobagyi T., Solnik S., Gruber A., Rider P., Steinweg K., Helseth J., De Vita P., "Interaction between age and gait velocity in the amplitude and timing of antagonist muscle coactivation", *Gait and Posture*, 2009.

Hortobagyi T., Devita P., "Mechanisms responsible for the age-associated increase in coactivation of antagonist muscles", *Exercise and Sport Sciences Reviews*, 2006.

Horton M.G., Hall T.L., "Quadriceps femoris muscle angle: normal values and relationships with gender and selected skeletal measures", *Physical Therapy*, 1989.

Hurd W.J., Chmielewski T.L., Axe M.J., Davis I., Snyder-Mackler L., "Differences in normal and perturbed walking kinematics between male and female athletes", *Clinical Biomechanics*, 2004.

Kerrigan D.C., Todd M.K., Della Croce U., "Gender differences in joint biomechanics during walking: normative study in young adults", *American Journal of Physical Medicine and Rehabilitation*, 1998.

Nakagawa T.H., Moriya É.T., Maciel C.D., Serrão A.F., "Frontal plane biomechanics in males and females with and without patellofemoral pain", *Medicine and Science in Sports and Exercise*, 2012.

Oberg T., Karsznia A., Oberg K., "Basic gait parameters: reference data for normal subjects, 10-79 years of age", *Journal of Rehabilitation Research and Development*, 1993.

Olney S.J., Quantitative evaluation of cocontraction of knee and ankle muscles in normal walking. Biomechanics, international series on biomechanics, 1985.

Perry J., "Gait Analysis – Normal and Pathological Function", *USA, Slack Inc.*, 1992.

Peterson D.S., Martin P.E., "Effects of age and walking speed on coactivation and cost of walking in healthy adults", *Gait and Posture*, 2010.

Prosser L.A., Lee S.C., VanSant A.F., Barbe M.F., Lauer R.T., "Trunk and hip muscle activation patterns are different during walking in young children with and without cerebral palsy", *Physical Therapy*, 2010.

Richard R., Weber J., Mejjad O., Polin D., Dujardin F., Pasquis P., Le Loët X., "Spatiotemporal gait parameters measured using the Bessou gait analyzer in 79 healthy subjects. Influence of age, stature, and gender", *Revue du rhumatisme*, 1995.

Sutherland D.H., "The evolution of clinical gait analysis part 1: kinesiological EMG", *Gait and Posture*, 2001.

Tirosh O., Sparrow W.A., "Age and walking speed effects on muscle recruitment in gait termination", *Gait and Posture*, 2005.

Winter D.A., Yack H.J., "EMG profiles during normal human walking: stride to stride and inter-subject variability", *Electroencephalography and Clinical Neurophysiology*, 1987.

Chapter 2
Methods

For the evaluation of gender-related differences in muscles activity during walking, twenty-two healthy adults were recruited, whereas for the co-contraction assessment twenty-four subjects volunteered and eventually for the evaluation of gender on the co-contraction activity of ankle muscles data from thirty subjects were analyzed. In gender-based studies two aged-matched groups were considered; for more details see (Di Nardo *et al.*, 2015a; Di Nardo *et al.*, 2015b; Mengarelli *et al.*, 2017). Subjects were excluded if they reported pathologies and/or pain of lower limb joints, neurological disorders, prior orthopedic surgery, BMI≥25 or abnormal gait. The participants were adult, healthy and volunteers. Before the experiment, procedures and purposes of the study were explained and questions pertaining to the study were answered.

2.1 Signal acquisition

sEMG signal was acquired (sampling rate: 2 kHz, resolution: 12 bit) by a multichannel recording system, Step32 (Version PCI-32 ch2.0.1. DV), Medical Technology, Italy. The employed sampling rate ensures, according to the Nyquist criterion, the detection of the full spectrum of the sEMG signal, that spans up to 500 Hz. Each lower limb was instrumented with an electro-goniometer, three foot-switches and two sEMG probes. The electro-goniometer (accuracy: 0.5 deg) was placed on the lateral side of the limb, to measure knee joint angle in the sagittal plane. The foot-switches (surface: 1.21 cm2, activation force: 3 N), were pasted beneath the heel, the first and the fifth metatarsal heads of the foot. Single differential sEMG probes with fixed geometry were placed on the muscle belly to detect the sEMG signals (Ag/Ag-Cl disk; electrode diameter: 0.4 cm; inter-electrode distance: 0.8 cm;

gain: 1000; high-pass filter: 10 Hz; input impedance: 1.5 GΩ; CMRR: 126 dB; input referred noise: ≤ 1μVrms). sEMG signals were further amplified and low-pass filtered (linear-phase FIR filter, cut-off frequency: 450 Hz) by Step32. Skin was shaved, cleansed with abrasive paste and wet with a soaked cloth. Probes were placed over GL and TA following the SENIAM recommendations (Freriks *et al.*, 2000) for electrodes location with respect to tendons, motor points and fiber orientation. Each volunteer walked barefoot at preferred speed for about 5 minutes, following an eight-shaped path.

2.2 Signal processing

Footswitch signals were debounced, converted to four levels corresponding to Heel Strike (H), Flat Foot Contact (F), Push-off (P) and Swing (S) and processed to identify the different gait cycles (GC) (Agostini *et al.*, 2014). Electro-goniometer signals were filtered with a low-pass FIR filter (cut-off frequency: 15 Hz, 100 taps). Knee angles, along with sequence and duration of gait phases derived by basographic signal, were used by a multivariate statistical filter to identify and discard cycles with a proper sequence of gait phases (H-F-P-S) but with an anomalous timing. Thus, strides relative to acceleration, deceleration or reversing were discarded. The multivariate statistical filter compares knee angles and gait phases duration from every stride of walking. In addition, the multivariate statistical filter is used to determine if knee angles and/or gait-phases duration in a single stride are significantly different (Hotelling t-test, α=0.05) from their mean value computed over each single subject, the corresponding stride is discarded (Agostini *et al.*, 2014). Thus, only strides corresponding to straight walking were considered in the present study.

Electromyographic signals were processed by a high-pass, linear-phase FIR filter (100 taps, cut-off frequency: 20 Hz), in order to avoid phase distortion effects. The cut-off frequencies of the resulting band-pass filtering (20 – 450 Hz) were chosen in order to remove movement artifact noise and avoid loss of information from the sEMG signal full bandwidth. Moreover, the electromyographic signals were processed by a double-threshold statistical detector, to identify

muscle activation intervals (Bonato *et al.*, 1998). The double-threshold algorithm first selects two threshold values, ζ and ro and then considers m successive samples. The probability that at least r_o samples out of m cross ζ, is given by:

$$P_{r_0}(r \geq r_0; m) = \sum_{k=r_0}^{m} \binom{m}{k} P^k (1-P)^{m-k} \qquad (1)$$

where P is the probability that a single sample crosses the threshold (Bonato *et al.*, 1998). Whether at least ro out of m consecutive samples are above the ζ value, the presence of muscle activation is acknowledged. The probability that noise samples are recognized as signal is defined by:

$$P_{fa} = \sum_{k=r_0}^{m} \binom{m}{k} P_\zeta^k \left(1-P_\zeta\right)^{m-k} \qquad (2)$$

where P_ζ is the probability that a specific noise sample is above the fixed threshold (Bonato *et al.*, 1998) and depends on the noise variance σ_n^2:

$$P_\zeta = e^{-\zeta/2\sigma_n^2} \qquad (3)$$

A main improvement of a double threshold statistical detector is that, for a given P_{fa} and m value, it provides a higher detection probability P_d respect to a single threshold detector (Bonato *et al.*, 1998):

$$P_d = \sum_{k=r_0}^{m} \binom{m}{k} P_{dk}^k (1-P_{dk})^{m-k} \qquad (4)$$

P_{dk} is the probability that the kth sample surpasses the threshold (Bonato *et al.*, 1998) and it is related to both σ_n^2 and the SNR, according to:

$$P_{dk} = e^{-\zeta/2\sigma_n^2(1+10^{SNR/10})} \quad (5)$$

The value of the first threshold (ζ) is related to the background noise level, while ro is based upon the SNR. Background noise level and SNR are estimated, following the approach reported by Agostini and Knaflitz (2012). The mean noise power P_{noise} and the mean signal power P_{signal} are computed averaging the histogram bins of an auxiliary time series, obtained considering the sEMG signal as a Gaussian process (Agostini and Knaflitz, 2012).

$$P = \frac{\sum bins_i \cdot Freq_i}{\sum Freq_i} \quad (6)$$

Depending on which local maximum of the bimodal distribution histogram is considered, P represents the calculated power of noise or signal (Agostini and Knaflitz, 2012). The root mean square value of the background noise is computed as follows:

$$e_{noise} = \sqrt{P_{noise}} \quad (7)$$

whereas the SNR is estimated as

$$SNR = 10 \cdot \log_{10} \frac{P_{signal} - P_{noise}}{P_{noise}} \quad (8).$$

Footswitch and goniometric signal processing, sEMG-signal filtering, identification of muscle activation intervals and statistical gait analysis in each single subject were off-line performed by Step32 system. Muscular co-activations (including the occurrence frequencies) were assessed as the overlapping periods among activation intervals of the considered muscles in the same strides (Den Otter *et al.*, 2006). A muscular activity shorter than 30 ms does not yield an active control on a joint

motion during gait (Bonato *et al.*, 1998), thus overlapping periods with a time length lower than 30 ms were discarded.

2.3 Statistical gait analysis

The statistical gait analysis (Agostini *et al.*, 2010) describes human walking considering the spatial-temporal and sEMG parameters over hundreds of consecutive strides, belonging to the same walking trial. Statistical gait analysis relies on the cycle-dependency of muscle-activation during gait. Thus, sEMG parameters should be averaged considering each single activation modality by itself, i.e. only over onset/offset instants of cycles including the same number of activations. An activation modality is defined as the number of times a single muscle activates during a single gait cycle (GC), i.e. the n-activation modality consists of n active intervals for the considered muscle during a single GC. To get the mean activation intervals for each activation modality, the muscle activations relative to every GC were identified, obtaining their onset/offset instants in temporal space (Staude *et al.*, 2001). Then muscle activations were grouped according with the number of active intervals, i.e. relative to their activation modality. Eventually, the onset/offset time instants of each activation modality were averaged separately over the two populations. Averaged onset/offset percentage time instants were normalized with respect to GC, providing mean activation intervals in percentage of GC. The statistical gait analysis allowed quantifying ankle-muscle co-contractions not only in terms of the onset-offset muscular activation, but also in terms of the occurrence frequency. Occurrence frequency is defined as the frequency each muscle activation occurs with, quantified by the number of strides in which the muscle is recruited with that specific activation modality.

2.4 Statistics

All data are reported as mean ± standard deviation (SD). Shapiro-Wilk test was used to evaluate the normality of each data distribution x_i, according to the value of the parameter W:

$$W = \frac{\left(\sum_{i=1}^{n} w_i x_{(i)}\right)^2}{\left(\sum_{i=1}^{n} x_i - \mu\right)^2} \quad (9)$$

where μ is the sample mean. Comparisons between data distributions were performed with two-tailed, non-paired Student's t-test (10) between normally distributed samples and with Mann-Whitney U-test (11) between non-normally distributed samples.

$$t = \frac{\mu_1 - \mu_2}{\sqrt{\frac{s_1^2(n_1-1)+s_2^2(n_2-1)}{n_1+n_2-2}}} \quad (10)$$

$$U = n_1 n_2 + \frac{n_2(n_2+1)}{2} - \sum_{i=n_1+1}^{n_2} R_i \quad (11)$$

In (10) and (11) n_1 and n_2 are the sample size of the two data distributions. In (10), μ_1 and μ_2 are the distributions mean, s_1^2 and s_2^2 are the distributions variances, whereas in (11) R_i is the rank of the sample size. The analysis of variance (ANOVA) was used to compare the different activation modalities within each gender group for normally distributed samples x_i, according to:

$$F = \frac{\sum_{i=1}^{p} n(x_i - \mu)^2}{\sum_{i=1}^{p} (n-1)s_i^2} \cdot \frac{N-p}{p-1} \quad (12)$$

where μ is the distribution mean, p is the total number of distributions, n is the number of samples in a distribution, s_i^2 is the distribution variance and N is the total number of samples among all the distributions. Kruskal-Wallis test was used for non-normally distributed samples, following (13):

$$H = \frac{12}{N(N+1)} \sum_{i=1}^{p} \frac{R_i^2}{n_i} - 3(N+1) \qquad (13)$$

where R_i is the rank sum of each data distribution. ANOVA and Kruskal-Wallis tests were followed by multiple comparison test, according to the Tukey's procedure, where the null hypothesis is rejected if:

$$|t| = \frac{|\mu_i - \mu_j|}{\sqrt{MSE\left(\frac{1}{n_i} + \frac{1}{n_j}\right)}} > \frac{1}{\sqrt{2}} q_{\alpha,k,N-k} \qquad (14)$$

In (14), MSE is the mean of the distributions variances and $q_{\alpha,k,N-k}$is the upper $100 \cdot (1-\alpha)th$ percentile of the range distribution with $N-k$ degree of freedom; k is the number of distributions and N is the total number of samples. The analysis of covariance (ANCOVA) was performed to remove the bias of the anthropometric variables on the computed data. Consequently, the mean values of the computed parameters were adjusted for the BMI, in each group. Significance was set at 5%. To determine the power of an observed effect based on the sample size and parameter estimates derived from the data set, the statistical power analysis was performed.

Chapter References

Agostini V., Balestra G., Knaflitz M., "Segmentation and Classification of Gait Cycles", *IEEE Transactions on Neural Systems and Rehabilitation Engineering*, 2014.

Agostini V., Knaflitz M., "An algorithm for the estimation of the signal-to-noise ratio in surface myoelectric signals generated during cyclic movements", *IEEE Transactions on Biomedical Engineering*, 2012.

Agostini V., Nascimbeni A., Gaffuri A., Imazio P., Benedetti M.G., Knaflitz M., "Normative EMG activation patterns of school-age children during gait", *Gait and Posture*, 2010.

Bonato P., D'Alessio T., Knaflitz M., "A statistical method for the measurement of muscle activation intervals from surface myoelectric signal during gait", *IEEE Transactions on Biomedical Engineering*, 1998.

Den Otter A.R., Geurts A.C., Mulder T., Duysens J., "Gait recovery is not associated with changes in the temporal patterning of muscle activity during treadmill walking in patients with post-stroke hemiparesis", *Clinical Neurophysiology*, 2006.

Di Nardo F., Mengarelli A., Maranesi E., Burattini L., Fioretti S., "Assessment of the ankle muscle co-contraction during normal gait: A surface electromyography study", *Journal of Electromyography and Kinesiology*, 2015a.

Di Nardo F., Mengarelli A., Maranesi E., Burattini L., Fioretti S., "Gender differences in the myoelectric activity of lower limb muscles in young healthy subjects during walking", *Biomedical Signal Processing and Control*, 2015b.

Freriks B., Hermens H.J., Disselhorst-Klug C., Rau G., "Development of recommendations for sEMG sensors and sensor placement procedures", *Journal of Electromyography and Kinesiology*, 2000.

Mengarelli A., Maranesi E., Burattini L., Fioretti S., Di Nardo F., "Co-contraction activity of ankle muscles during walking: A gender comparison", *Biomedical Signal Processing and Control*, 2017.

Staude G., Flachenecker C., Daumer M., Wolf W., "Onset detection in surface electromyographic signals: A systematic comparison of methods", *EURASIP Journal on Advances in Signal Processing*, 2001.

Chapter 3
Results

3.1 Gender differences in lower limb muscles activity

All the recruited subjects were heel strikers and only gait cycles with the proper sequence of gait phases (H-F-P-S) were considered. Statistical gait analysis of the myoelectric signal showed that muscles show a different number of activation intervals in different strides of the same walking. Variability of sEMG signals across subjects were represented in Fig. 1.

No significant differences were observed in onset/offset instants of activation between M-group and F-group, for all the detected modalities of GL activation (Table 1).

Gastrocnemius lateralis	First activation (% gait cycle)		Second activation (% gait cycle)		Third activation (% gait cycle)	
	ON	OFF	ON	OFF	ON	OFF
F-group ($n = 11$)						
1-activation mod	11.0 ± 6.1	47.3 ± 2.4				
2-activation mod	5.6 ± 3.5	36.7 ± 6.9	70.2 ± 10.8	82.9 ± 8.9		
3-activation mod	1.9 ± 1.3	18.9 ± 8.2	30.3 ± 8.7	53.5 ± 5.2	87.8 ± 3.4	95.9 ± 3.0
M-group ($n = 11$)						
1-activation mod	10.6 ± 7.7	47.2 ± 2.5				
2-activation mod	7.0 ± 5.0	35.5 ± 6.2	66.9 ± 11.8	79.1 ± 8.8		
3-activation mod	3.4 ± 2.8	22.2 ± 11.6	35.1 ± 13.6	56.2 ± 7.9	87.3 ± 7.3	93.0 ± 6.0

Table 1. Activation intervals of gastrocnemius lateralis in its main modalities of activation, expressed as the timing, in the percentage of gait cycle, of signal onset and offset. Values are expressed for female and male population as mean ± standard deviation (SD). No significant differences between F and M groups were detected in all variables.

A significant earlier TA onset instant (Table 2) was detected in M-group during swing and pre-swing phases, for second and third activations in 3-activation modality and for third and fourth activations in 4-activation modality of TA. On the other hand, significant earlier onset instants were detected in F-group during push-off phase in 3- and 4-activation modality for RF (Table 3), and during swing phase in 2- and 3-activation modality for BF (Table 4). Moreover, the F-group showed an earliest

offset time instant (Table 5) during the early stance in the VL 4-activation modality. No further significant differences were observed in onset/offset instants of activation between groups (Tables 1-5).

Tibialis anterior	First activation (% gait cycle)		Second activation (% gait cycle)		Third activation (% gait cycle)		Fourth activation (% gait cycle)	
	ON	OFF	ON	OFF	ON	OFF	ON	OFF
F-group ($n = 11$)								
2-activation mod	0.3 ± 0.3	13.3 ± 9.8	55.2 ± 4.6	99.8 ± 0.2				
3-activation mod	1.2 ± 1.1	7.9 ± 3.7	47.3 ± 9.8**	63.9 ± 9.9	78.4 ± 8.4**	100 ± 0		
4-activation mod	0.3 ± 0.3	5.4 ± 2.4	29.2 ± 9.8	38.3 ± 10.0	56.5 ± 8.1**	71.7 ± 8.5	82.0 ± 8.0*	100 ± 0
M-group ($n = 11$)								
2-activation mod	0.2 ± 0.2	12.1 ± 6.3	56.0 ± 6.1	100 ± 0				
3-activation mod	0.0 ± 0.0	6.5 ± 3.6	37.0 ± 9.4**	53.3 ± 13.6	67.4 ± 8.6**	100 ± 0		
4-activation mod	0.0 ± 0.0	5.0 ± 2.2	24.5 ± 9.3	32.6 ± 11.3	48.2 ± 10.9**	64.1 ± 14.1	74.3 ± 11.1*	100 ± 0

Table 2. Activation intervals of tibialis anterior in its main modalities of activation, expressed as the timing, in the percentage of gait cycle, of signal onset and offset. Values are expressed for female and male population as mean ± standard deviation (SD). ** $p < 0.01$ and * $p < 0.05$ between correspondent value in F-group and M-group.

Rectus femoris	First activation (% gait cycle)		Second activation (% gait cycle)		Third activation (% gait cycle)		Fourth activation (% gait cycle)	
	ON	OFF	ON	OFF	ON	OFF	ON	OFF
F-group ($n = 11$)								
2-activation mod	0.3 ± 0.3	28.4 ± 15.6	76.9 ± 12.4	99.9 ± 0.1				
3-activation mod	0.2 ± 0.2	17.1 ± 5.5	43.7 ± 5.8*	56.7 ± 6.2	83.7 ± 3.0	99.8 ± 0.2		
4-activation mod	0.0 ± 0.0	13.3 ± 2.7	29.2 ± 4.2**	37.7 ± 4.0	51.2 ± 4.7**	61.7 ± 6.0	84.8 ± 3.2	100 ± 0
M-group ($n = 11$)								
2-activation mod	0.2 ± 0.2	24.4 ± 15.7	82.0 ± 9.0	99.9 ± 0.1				
3-activation mod	0.1 ± 0.1	15.7 ± 4.4	48.1 ± 4.3*	57.9 ± 5.4	85.7 ± 3.1	99.9 ± 0.1		
4-activation mod	0.0 ± 0.0	14.8 ± 3.4	34.1 ± 4.4**	40.2 ± 4.7	56.0 ± 5.1**	64.3 ± 5.3	85.8 ± 3.4	100 ± 0

Table 3. Activation intervals of rectus femoris in its main modalities of activation, expressed as the timing, in the percentage of gait cycle, of signal onset and offset. Values are expressed for female and male population as mean ± standard deviation (SD). ** $p < 0.01$ and * $p < 0.05$ between correspondent value in F-group and M-group.

Biceps femoris	First activation (% gait cycle)		Second activation (% gait cycle)		Third activation (% gait cycle)		Fourth activation (% gait cycle)	
	ON	OFF	ON	OFF	ON	OFF	ON	OFF
F-group ($n = 11$)								
2-activation mod	0.5 ± 0.5	17.0 ± 11.5	73.7 ± 5.5*	99.5 ± 0.5				
3-activation mod	0.3 ± 0.3	8.9 ± 2.8	38.5 ± 9.3	50.3 ± 7.4	76.2 ± 4.0**	99.7 ± 0.3		
4-activation mod	0.0 ± 0.0	7.3 ± 2.3	26.6 ± 7.4	35.9 ± 7.0	53.3 ± 9.0	62.6 ± 10.5	78.7 ± 6.8	100 ± 0
M-group ($n = 11$)								
2-activation mod	0.6 ± 0.6	14.8 ± 7.4	77.2 ± 3.3*	99.6 ± 0.4				
3-activation mod	0.2 ± 0.2	9.7 ± 3.8	43.8 ± 12.5	54.8 ± 12.1	80.8 ± 4.7**	99.8 ± 0.2		
4-activation mod	0.0 ± 0.0	8.6 ± 3.1	27.3 ± 7.1	35.3 ± 8.1	55.4 ± 7.8	64.0 ± 8.3	81.5 ± 3.9	100 ± 0

Table 4. Activation intervals of biceps femoris in its main modalities of activation, expressed as the timing, in the percentage of gait cycle, of signal onset and offset. Values are expressed for female and male population as mean ± standard deviation (SD). ** $p < 0.01$ and * $p < 0.05$ between correspondent value in F-group and M-group.

Vastus lateralis	First activation (% gait cycle)		Second activation (% gait cycle)		Third activation (% gait cycle)		Fourth activation (% gait cycle)	
	ON	OFF	ON	OFF	ON	OFF	ON	OFF
F-group ($n = 11$)								
2-activation mod	0.1 ± 0.1	21.8 ± 12.0	81.3 ± 3.0	99.9 ± 0.1				
3-activation mod	0.0 ± 0.2	16.2 ± 6.3	34.3 ± 5.7	42.5 ± 6.1	81.5 ± 4.0	100 ± 0		
4-activation mod	0.0 ± 0.0	13.7 ± 3.0**	23.8 ± 3.8	30.5 ± 4.7	44.0 ± 7.4	52.0 ± 7.8	81.7 ± 4.4	100 ± 0
M-group ($n = 11$)								
2-activation mod	0.1 ± 0.1	22.0 ± 11.7	80.6 ± 3.9	100 ± 0				
3-activation mod	0.0 ± 0.0	17.9 ± 5.8	34.7 ± 9.3	40.8 ± 10.1	80.6 ± 3.8	100 ± 0		
4-activation mod	0.0 ± 0.0	17.2 ± 4.6**	26.5 ± 7.1	31.9 ± 7.1	45.8 ± 8.4	51.1 ± 8.5	80.1 ± 3.7	100 ± 0

Table 5. Activation intervals of vastus lateralis in its main modalities of activation, expressed as the timing, in the percentage of gait cycle, of signal onset and offset. Values are expressed for female and male population as mean ± standard deviation (SD). ** $p < 0.01$ between correspondent value in F-group and M-group.

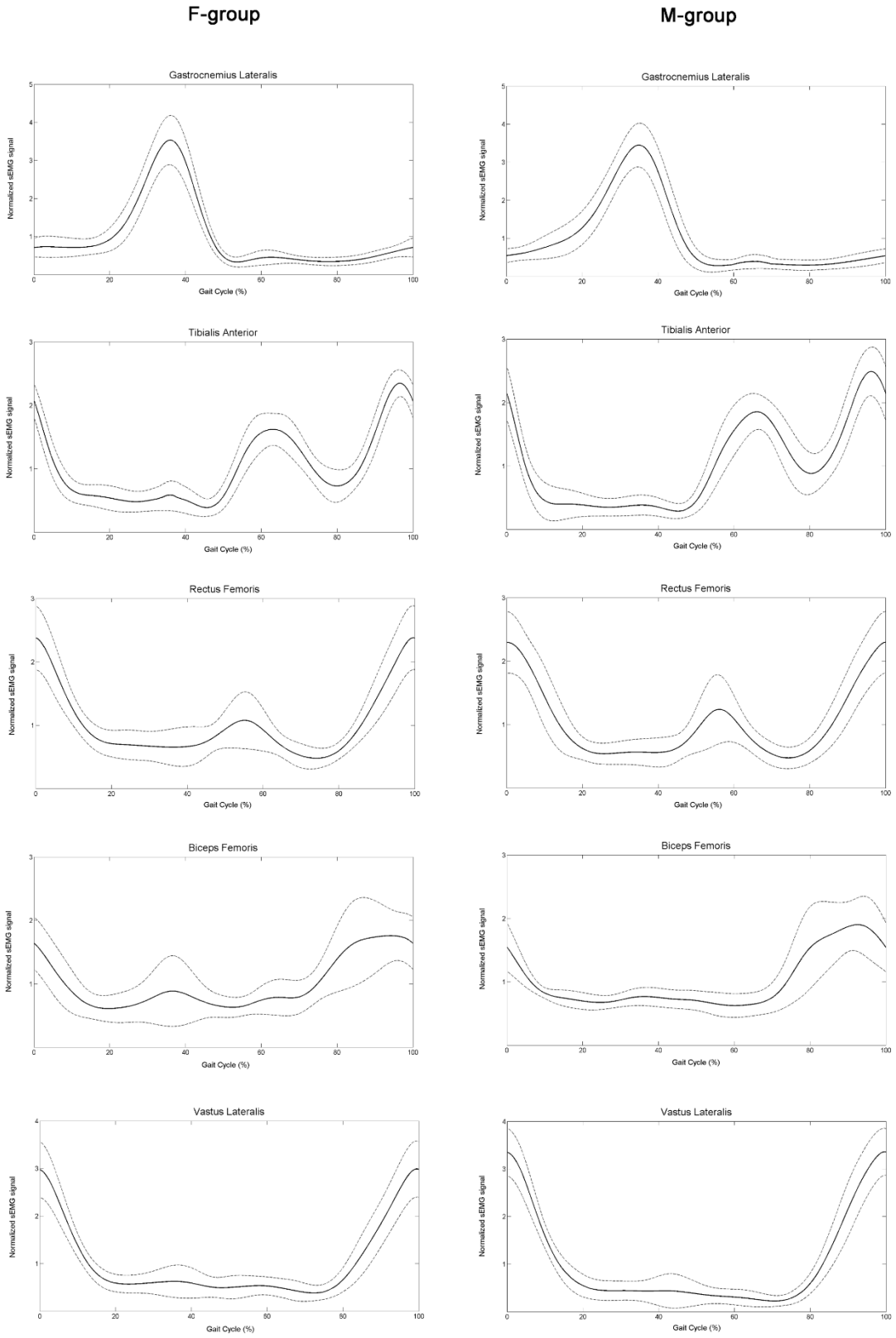

Figure 1. sEMG patterning averaged across female (left panel) and male (right panel) subjects (+SD), for all muscles. Only for this figure, sEMG signals were rectified, low pass filtered (5 Hz), and normalized in amplitude by mean value, for representative reasons.

M-group and F-group were compared also in terms of the frequency each modality of muscle activation occurs with, quantified by the number of strides (%), over total subjects, where the muscle is recruited with the specific activation modality (Figures 2-6). The most recurrent activation modality for each muscle is represented in Fig. 7, for F-group (shaded bars) and M-group (white bars).

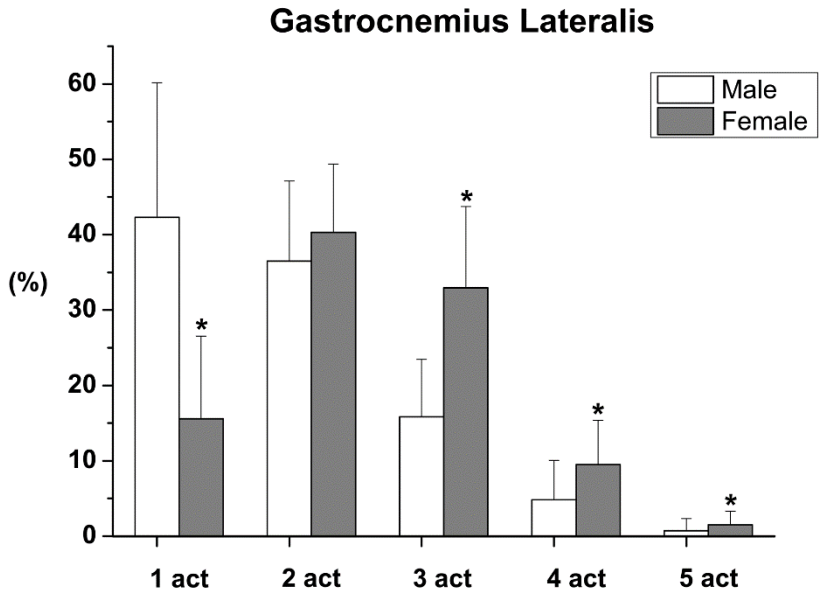

Figure 2. Gastrocnemius Lateralis: mean (+SD) percentage frequency of each of the five different activation modalities, detected during walking in F-group (shaded bars) and in M-group (open bars). * significantly different between groups.

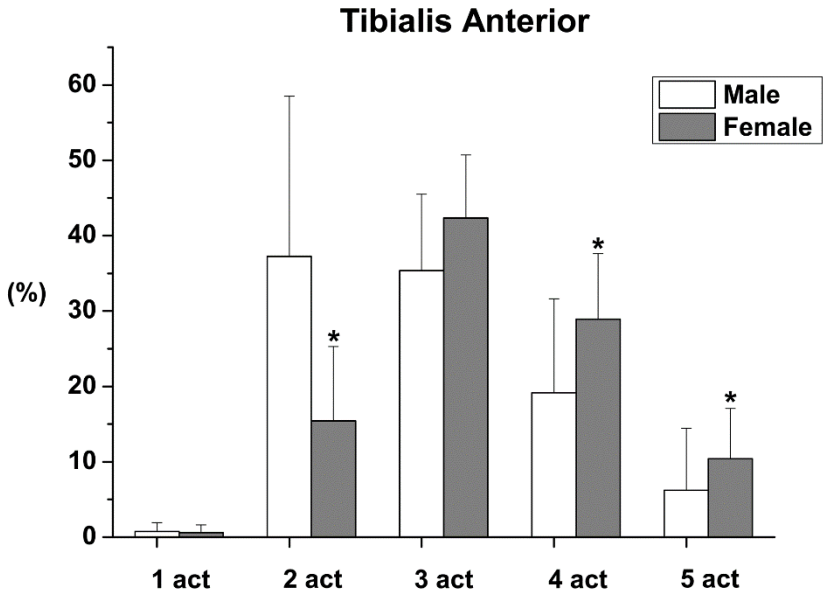

Figure 3. Tibialis Anterior: mean (+SD) percentage frequency of each of the five different activation modalities, detected during walking in F-group (shaded bars) and in M-group (open bars). * significantly different between groups.

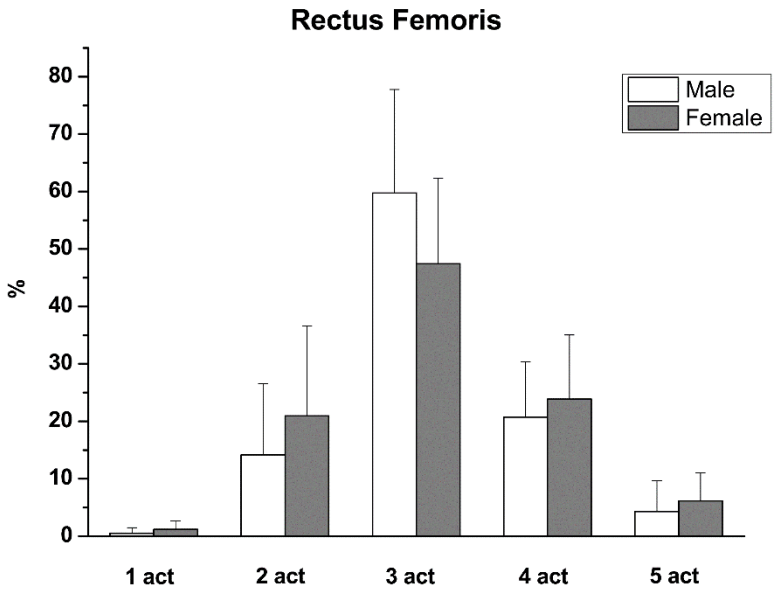

Figure 4. Rectus Femoris: mean (+SD) percentage frequency of each of the five different activation modalities, detected during walking in F-group (shaded bars) and in M-group (open bars). * significantly different between groups.

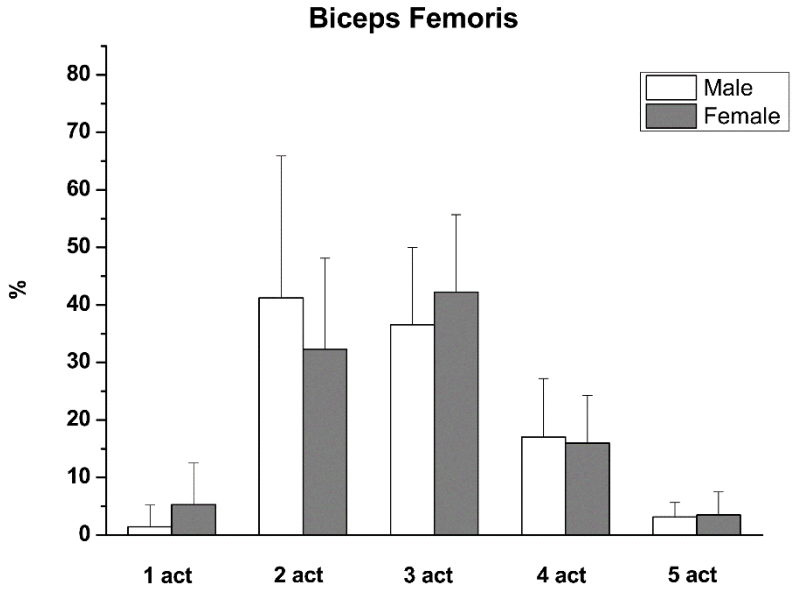

Figure 5. Bicpes Femoris: mean (+SD) percentage frequency of each of the five different activation modalities, detected during walking in F-group (shaded bars) and in M-group (open bars). * significantly different between groups.

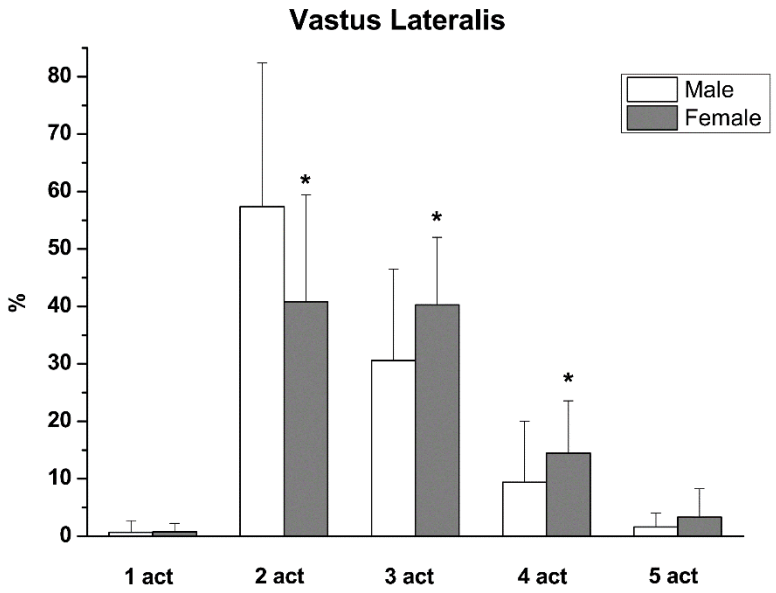

Figure 6. Vastus Lateralis: mean (+SD) percentage frequency of each of the five different activation modalities, detected during walking in F-group (shaded bars) and in M-group (open bars). * significantly different between groups.

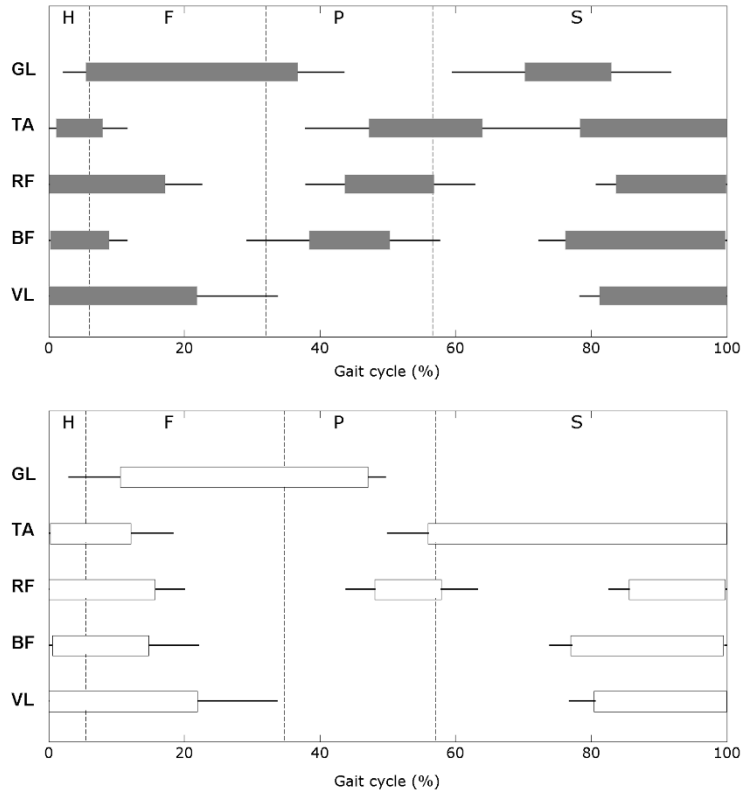

Figure 7. Mean (+SD) muscle activation intervals vs. percentage of gait cycle in F-group (shaded bars, upper panel) and M-group (open bars, lower panel), for Gastrocnemius Lateralis (GL), Tibialis Anterior (TA), Rectus Femoris (RF), Biceps Femoris (BF) and Vastus Lateralis (VL), in their most recurrent activation modality. H, F, P and S phases are delimited by dashed vertical lines.

Concerning GL (Figures 2 and 7), the most recurrent activation modality for F-group is observed in 39.9±9.0% of strides and consists of two activations (2-activation modality); for M-group is observed in 42.3±17.8% of strides and consists of one activation (1-activation modality). In M-group, 1- and 2-activation modalities are more recurrent ($p<0.001$) than 3-activation modality, while in F-group, 2- and 3-activation modalities are more recurrent ($p<0.001$) than 1-activation modality. Compared with F-group, M-group presented, on average, a higher ($p<0.001$) occurrence frequency in 1-activation modality and a lower occurrence frequency in 3-activation modality ($p<0.001$), 4-activation modality ($p<0.005$) and 5-activation modality ($p<0.05$). GL activation interval detected in swing is more recurrent ($p<0.001$) in F-group (84.3±10.8% of strides) than in M-group (57.9±17.8%).

Concerning TA (Figures 3 and 7), the most recurrent activation modality for F-group is observed in 42.2±8.2% of strides and consists of three activations (3-activation modality); for M-group is observed in 37.2±21.2% of stride and consists of two activations (2-activation modality). In M-group, 2- and 3-activation modalities are more recurrent ($p<0.001$) than 4-activation modality, while in F-group, 3- and 4-activation modalities are more recurrent ($p<0.001$) than 2-activation modality. Compared with F-group, M-group showed a higher ($p<0.001$) occurrence frequency in 2-activation modality and a lower occurrence frequency in 4-activation modality ($p<0.01$) and 5-activation modality ($p<0.005$). TA activation interval detected in stance between 20% and 40% of GC is more recurrent ($p<0.005$) in F-group (44.0±15.4% of total strides) than in M-group (21.4±11.9%).

For the RF (Figures 4 and 7), the most recurrent activation modality results 3-activation modality for both F and M groups, observed in 47.4±14.9% and 59.8±18.0% of strides, respectively. In both groups, 3-activation modality is more recurrent ($p<0.001$) than 2- and 4-activation modalities. No significant differences in occurrence frequencies were detected between the two groups, for all activation modalities.

For the BF (Figures 5 and 7), the most recurrent activation modality results 2-activation modality for M-group (41.2±24.7%) and 3-activation modality (42.2±13.5%) for F-group. In M-group, 2- and 3-activation modalities are more recurrent ($p<0.001$) than 4-activation modality, while in F-group, 3-activation modality is more recurrent ($p<0.005$) than 2- and 4-activation modalities. No significant differences in occurrence frequencies were detected between the two groups, for all activation modalities.

Concerning VL (Figures 6 and 7), the most recurrent activation modality for M-group, observed in 57.3±25.0% of strides, results 2-activation modality. In F-group, the most recurrent are 2- (40.8±18.6%) and 3-activation modalities (40.3±11.8%); no significant difference in occurrence frequency was detected between these two activation modalities. In M-group, 2-activation modality is more recurrent ($p<0.05$) than 3-activation modality, which, in turn, is more recurrent ($p<0.01$) than 4-activation modality. Furthermore, F-group shows a higher occurrence frequency for 3-

($p<0.05$) and 4-activation modality ($p<0.05$), and a lower occurrence frequency in 2-activation modality ($p<0.05$), compared to M-group. No further significant differences were observed in occurrence frequency between M-group and F-group (Figures 2-6).

3.2 Co-contraction patterns of ankle muscles

In this case for each subject a mean (±SD) of 471±103 strides have been considered and the statistical analysis of the myoelectric signal indicates that muscles show a different number of activation intervals in different strides of the same walk. As example, EMG signals from the TA muscle of a single subject have been depicted in Fig. 8.

In the strides (30.7±19.9% of total strides, mean ± SD) where GL presents a single activity in the whole gait cycle (Fig. 9), the most recurrent modality of activation for TA consists of three activations and this is observed in 40.8±14.2% of these considered strides; in this modality as well as in the 2-activation modality (27.9±22.4% of the considered strides) for TA, no overlapping between TA and GL activation intervals are detected. The TA 4-activation modality (22.2±14.8% of the considered strides), on the other hand, exhibited an activity from 33.4±7.1% to 42.2±9.4% of gait cycle, mean ± SD), which is completely superimposed to the GL activation interval (Fig. 9).

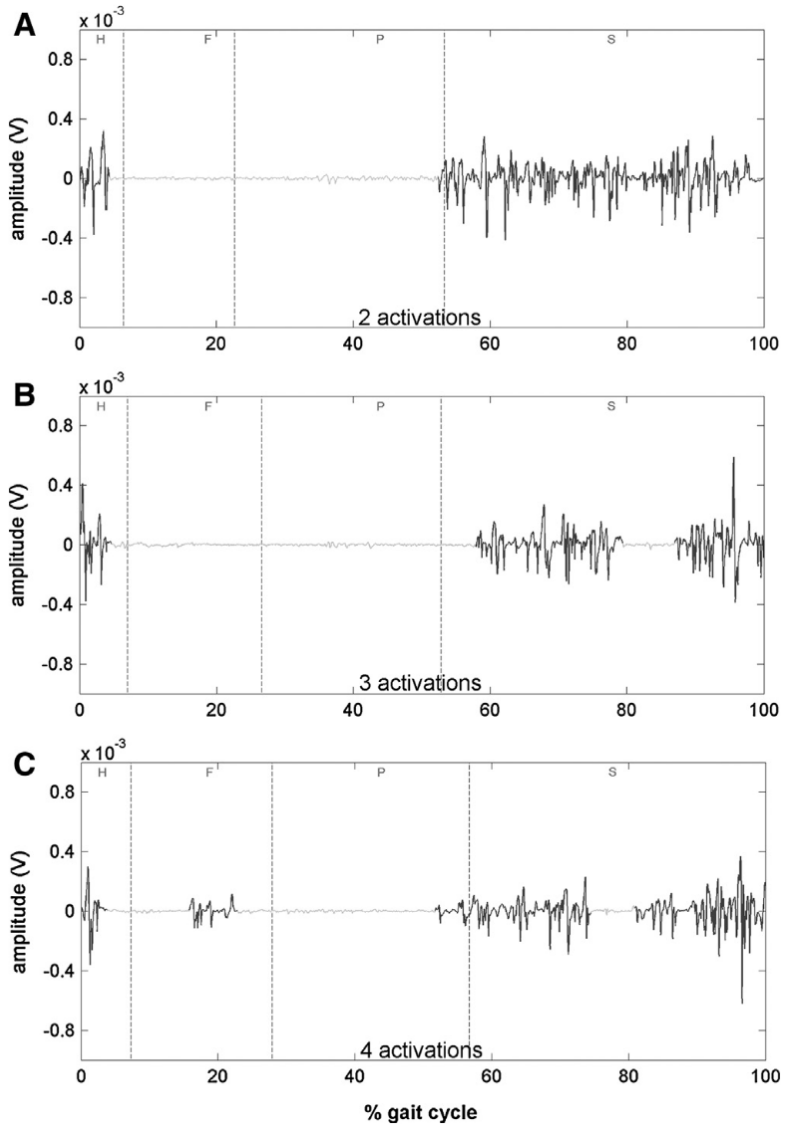

Figure 8. An example of EMG signals of TA muscle showing 2 activations (panel A), 3 activations (panel B) and 4 activations (panel C), respectively. The signals have been extracted from different strides of the same subject, during the same walk. The heel contact, flat foot contact, push off and swing phases are delimited by dashed vertical lines.

In the strides (38.8±9.8% of total strides) characterized by a double activity for GL (Fig. 10), a superimposition between GL and TA activation intervals during the stance (from 31.3±7.0% to 35.7±6.4% of gait cycle) was observed only in the 4-activation modality (24.1±13.7% of these considered strides), but not in 2-activation (25.2±20.3%) and in 3-activation (40.4±11.3%, most recurrent) modalities for TA.

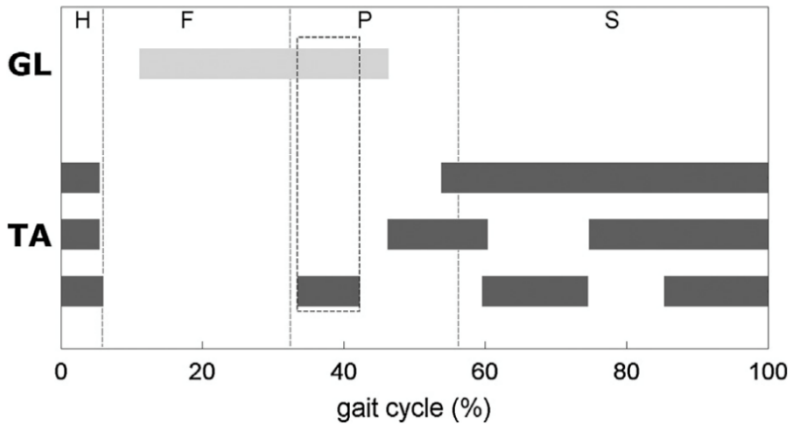

Figure 9. Mean values (+SE) of TA activation intervals (light gray bars) vs. percentage of gait cycle, detected in the strides where GL (dark gray bars) shows the 1-activation modality. TA activation intervals are reported separately for the modalities with 2, 3 and 4 activations. The heel contact, flat foot contact, push off and swing phases are delimited by dashed vertical lines.

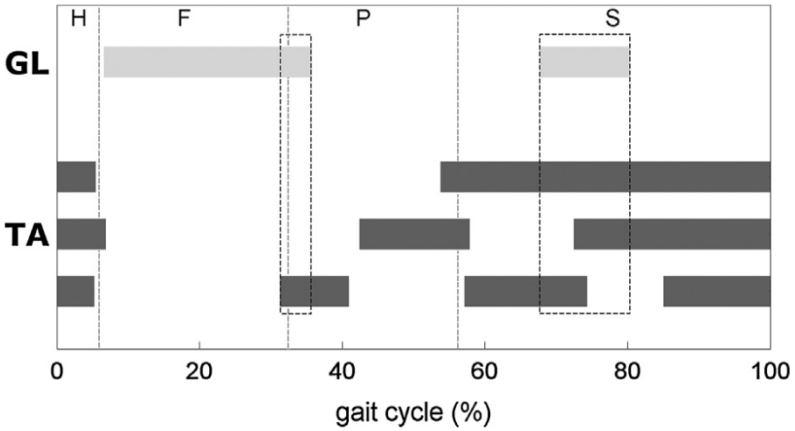

Figure 10. Mean values (+SE) of TA activation intervals (light gray bars) vs. percentage of gait cycle, detected in the strides where GL (dark gray bars) shows the 2-activation modality. TA activation intervals are reported separately for the modalities with 2, 3 and 4 activations. The heel contact, flat foot contact, push off and swing phases are delimited by dashed vertical lines.

During the swing phase, however, a total overlapping between GL and TA activation intervals for the TA 2-activation modality (from 67.7±11.3% to 80.3±8.9% of gait cycle) and a partial superimposition for the 3-activation (from 72.5±10.2% to 80.3±8.9% of gait cycle) and 4-activation (from 67.7±11.3% to 74.3±3.1% of gait cycle) modalities were detected.

In the strides (23.4±12.0% of total strides) where GL presented a triple activity (Fig. 11), a very short superimposition of GL and TA activation intervals were observed in the early stance, for the 2-activation (27.4±21.3% of these considered strides), 3-activation (37.1±12.1%, most recurrent) and 4-activation (24.9±14.9%) modalities of TA.

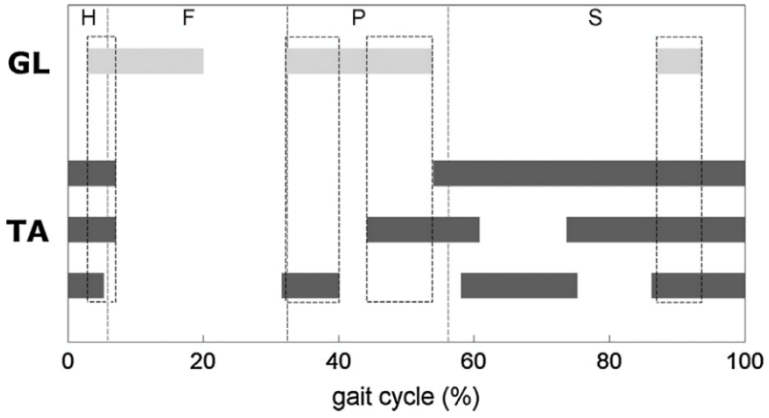

Figure 11 Mean values (+SE) of TA activation intervals (light gray bars) vs. percentage of gait cycle, detected in the strides where GL (dark gray bars) shows the 3-activation modality. TA activation intervals are reported separately for the modalities with 2, 3 and 4 activations. The heel contact, flat foot contact, push off and swing phases are delimited by dashed vertical lines.

A further overlapping between GL and TA activation intervals was detected in stance for TA 3-activation modality (from 44.2±9.7% to 53.9±7.3% of gait cycle) and for the 4-activation modality (from 32.1±11.2% to 40.1±7.6% of gait cycle). During the swing phase, a total superimposition between GL and TA activation intervals (from 87.1±6.6% to 93.7±5.5% of gait cycle) was detected, for the 2-activation (27.4±21.3%), 3-activation (37.1±12.1%, most recurrent) and 4-activation (24.9±14.9%) modalities of TA.

When TA is recruited with the 2-activation modality, the percentage of strides where GL shows a single activation (GL1, white bars in Fig. 12) is comparable to that where GL shows multiple (≥2) activations (GLmul, gray bars in Fig. 12), i.e. 43.1±29.7% vs. 56.9±18.9% (mean ± SD). During the 3-activation modality for TA, GL1 decreases to 30.7±20.3% and, consequently, GLmul increases to

69.3±17.4%. A further decrease for GL1 (25.4±19.4%) and increase for GLmul (74.6±23.4%) is observed during the 4-activation modality for TA (Fig. 12).

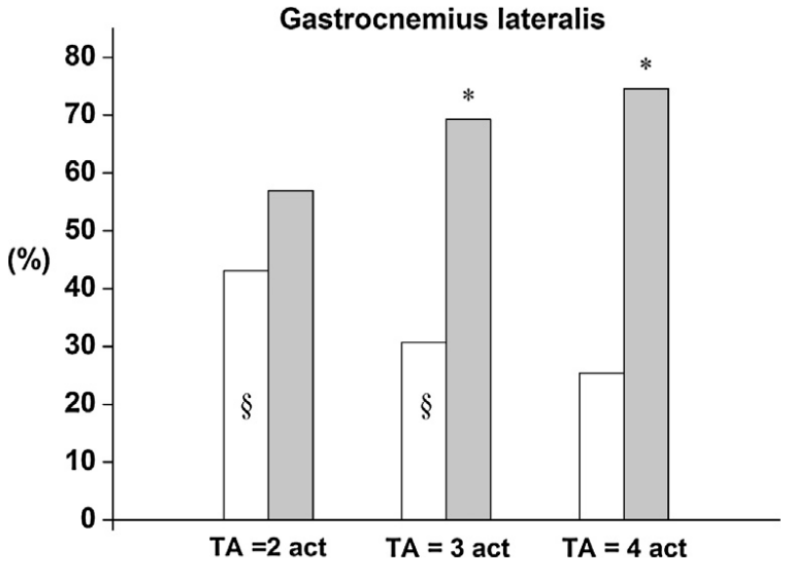

Figure 12. Mean percentage number of strides where GL shows a single activation (GL1 = white bars) vs. mean percentage number of strides where GL shows multiple (≥2) activations (Gmul = gray bars). The percentage values are computed in the strides where TA shows the 2-, 3-, or 4-activation modality, respectively.

3.3 Gender-related differences in ankle muscles co-contraction patterns

Also in this case sEMG-signal analysis showed different number of TA and GL activations in different strides of the same walk, i.e. several different activation modalities were adopted (Figures 13-15). For both groups, TA and GL presented three main modalities, covering about 90% of strides and characterized by different occurrence frequencies. The TA 3-activation modality is defined as the activation modality where TA showed 3 different activation intervals during GC.

The TA 3-activation modality was the most recurrent one, occurring in 39.4±12.4% (M-group) and 43.0±9.0% (F-group) of strides. The difference in mean values between M and F groups was not significant (p=0.199). The TA 2-activation modality is defined as the activation modality where TA

showed 2 different activation intervals during GC and is observed in 33.6±21.8% of strides in the M-group and in 14.3±9.5% of strides in the F-group, respectively. The TA 4-activation modality is defined as the activation modality where TA showed 4 different activation intervals and is observed in 19.5±15.0% of strides in the M-group and in 29.0±8.8% of strides in the F-group, respectively.

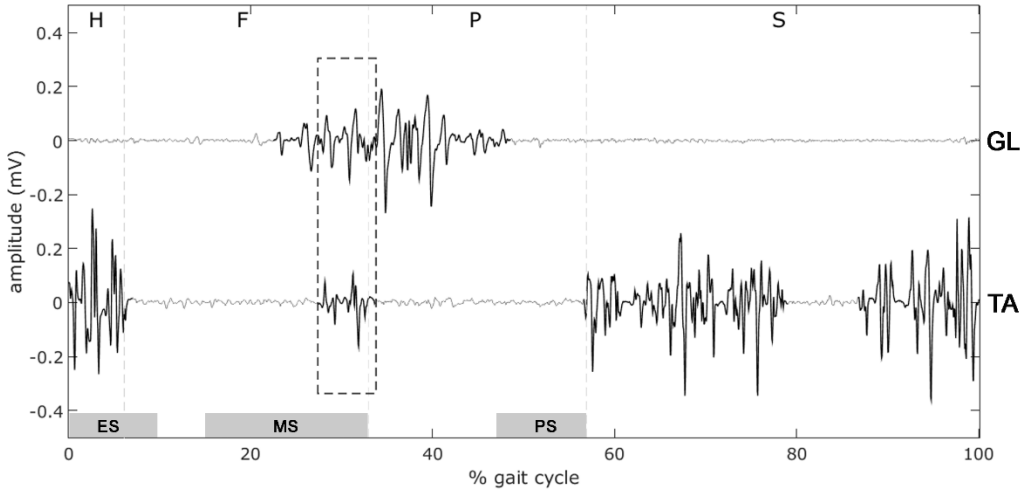

Figure 13. MS co-contraction assessed from raw signals of a representative subject. The activity superimposition is highlighted by the dashed box. H, F, P and S phases are delimited by vertical dashed lines. ES, MS, and PS phases are highlighted in dark grey in the bottom of the figure.

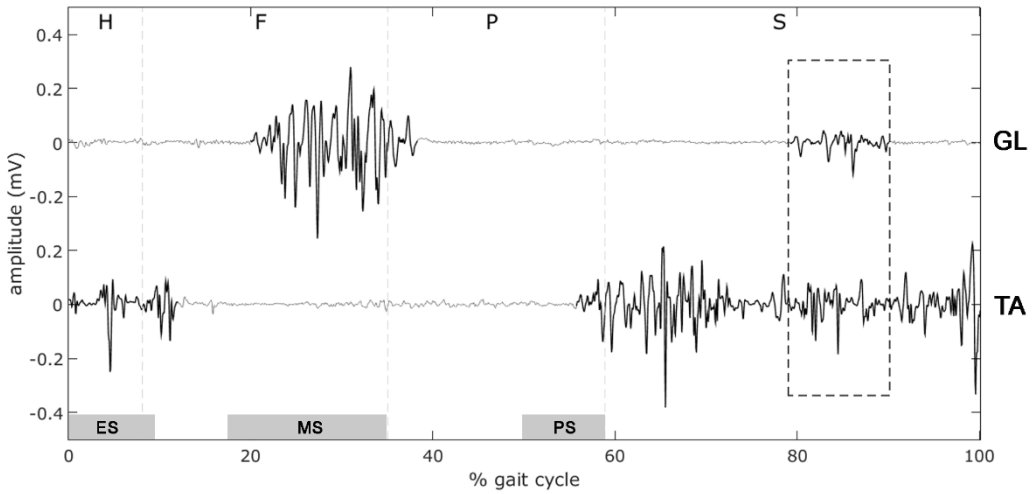

Figure 14. Swing co-contraction (SW), assessed from raw signals of a representative subject. The activity superimposition is highlighted by the dashed box. H, F, P and S phases are delimited by vertical dashed lines. ES, MS, and PS phases are highlighted in dark grey in the bottom of the figure.

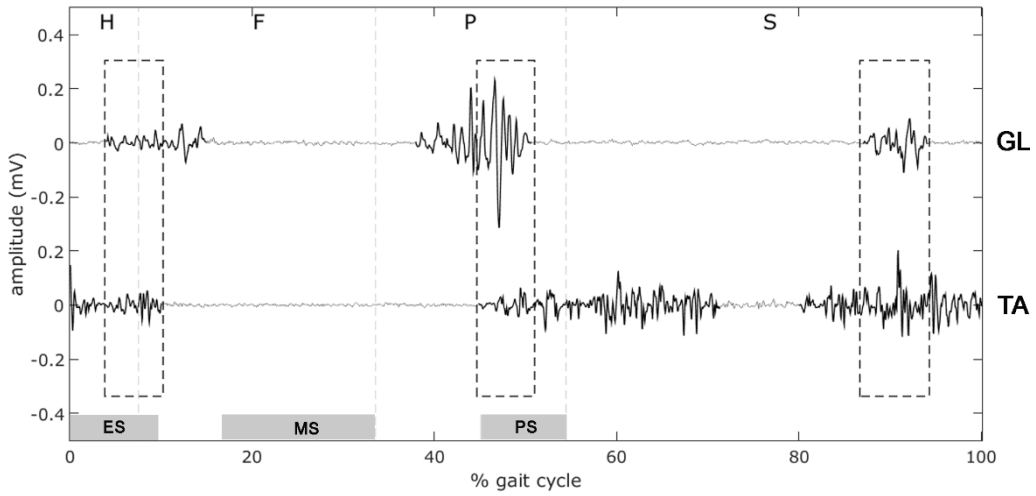

Figure 15. ES, PS and S co-contraction, assessed from raw signals of a representative subject. The superimposition is highlighted by the dashed boxes. H, F, P and S phases are delimited by vertical dashed lines. ES, MS, and PS phases are highlighted in dark grey in the bottom of the figure.

Both differences among groups were significant (p=2.9•10^{-4} and p=0.004). Considering GL, the most recurrent modality was the 1-activation modality in the M-group (43.9±19.2%), followed by the 2- (37.2±10.8%) and 3-activation modality (15.5±9.0%). In the F-group, the 2-activation modality was the most recurrent (39.4±9.8%), while the 1- and 3-activation modality were observed in 19.6±14.0% and 29.6±11.5% of strides. Differences between groups were both significant in the 1-activation (p=1.9•10^{-6}) and 3-activation modalities (p=2.1•10^{-6}), but not in the 2-activation modality (p=0.326).

In both groups, no TA/GL co-contractions (i.e. no overlaps) were detected only in the cycles where TA adopted the 2- and 3-activation modality and simultaneously GL presented the 1-activation modality (Fig. 13). The absence of co-contraction occurred in a higher percentage of strides (p=3.6•10^{-6}) in the M-group (34.0±19.9% of strides) with respect to the F-group (12.5±9.2%).

Four different co-contractions were found in both groups, during the early stance (ES), mid-stance (MS), pre-swing (PS) and swing phase (SW). The ES co-contraction (Fig. 15) was observed in the cycles where GL adopted the 3-activation modality and TA adopted all its most recurrent modalities (2-, 3- and 4-activation modalities). The MS co-contraction (Fig. 13) was detected when GL activated with all its main modalities (1-, 2- and 3-activation modality) and simultaneously TA

showed the 4-activation modality. The PS co-contraction occurred (Fig. 15) when GL and TA adopted simultaneously the 3-activation modality. The co-contraction during the swing (SW, Fig. 14) was observed in the strides where GL showed the 2- and 3-activation modality and TA adopted all its modalities (2-, 3- and 4- activation modality). No significant differences (p>0.05) between groups were detected in time-length or on/off instants of co-contraction intervals (Table 6).

Group	ES		MS		PS		SW	
	Onset	Offset	Onset	Offset	Onset	Offset	Onset	Offset
M-group	4.1 ± 3.6	6.3 ± 4.9	34.3 ± 6.2	43.4 ± 5.8	46.4 ± 15.5	51.4 ± 11.4	80.9 ± 10.9	88.9 ± 8.0
F-group	2.6 ± 2.5	7.7 ± 4.0	32.1 ± 7.1	38.9 ± 7.3	49.7 ± 7.5	53.0 ± 5.7	82.3 ± 9.3	87.7 ± 10.0

Table 6. Mean onset/offset time instants of the four co-contraction intervals for the two populations.

Therefore, the analysis of occurrence frequency of every co-contraction detected in males and females was also considered. The ES co-contraction occurred in 18.9±11.0% of strides for M-group and in 40.7±18.7% for the F-group, with a significant difference (p=1.5•10^{-6}, Fig. 16).

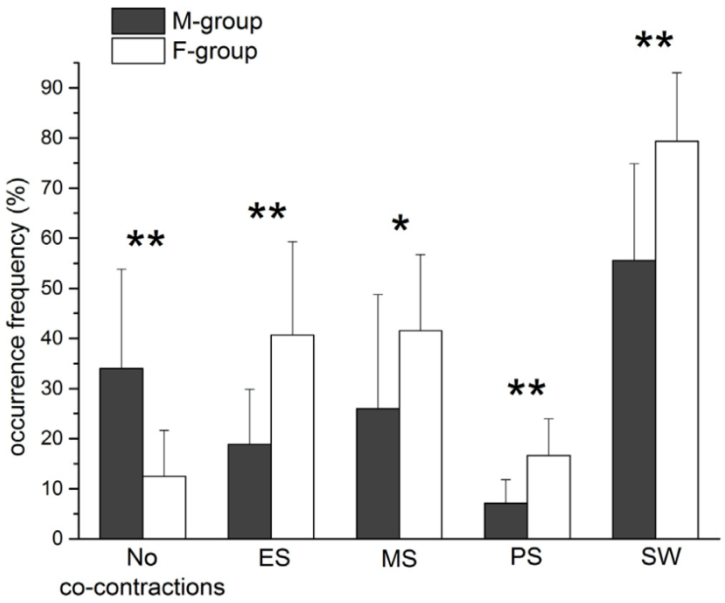

Figure 16. Mean percentage number of strides where each co-contraction period was observed in the M- (dark grey columns) and the F-group (white columns). On the horizontal axis, the absence of co-contractions (i.e. the pure antagonistic behavior) and the four co-contraction intervals are reported: no co-contractions, ES, MS, PS and SW. * p<0.005 and ** p<0.001.

A higher occurrence frequency value in F-group was detected also for the MS (41.5±15.2% vs. 26.0±22.8%, p=0.002), PS (16.6±7.3% vs. 7.1±4.7%, p=2.1•10^{-7}) and SW (79.4±13.7% vs. 55.6±19.3%, p=1.9•10^{-6}) co-contraction pattern (Fig. 16). For a detailed evaluation of the inter-subject and inter-group variability, the occurrence frequency of co-contractions was reported in Table 7 for every subject.

Subject	No co-contractions (%)		ES (%)		MS (%)		PS (%)		SW (%)	
	M-group	F-group	M-group	F-group	M-group	F-group	M-group	F-group	M-group	F-group
#1	54.2	10.3	14.3	26.7	8.5	38.3	4.5	11.6	40.3	82.4
#2	25.9	8.5	26.1	47.6	28.0	37.0	9.4	21.2	65.7	87.7
#3	31.8	5.6	16.7	37.8	17.2	66.2	4.9	16.5	59.5	80.8
#4	14.2	10.2	19.2	48.2	66.0	32.9	6.7	20.2	55.9	83.2
#5	70.9	2.2	3.8	54.1	0.9	44.7	0.6	19.0	24.9	93.7
#6	29.4	11.8	20.0	48.1	25.2	64.3	7.1	10.0	57.2	69.8
#7	35.0	17.8	19.8	33.7	2.2	32.4	6.3	14.9	62.0	76.6
#8	11.0	2.6	27.5	51.9	61.6	57.5	12.4	22.6	76.6	92.1
#9	22.8	31.2	28.4	18.2	17.6	27.5	13.8	7.5	71.5	58.6
#10	9.1	22.8	27.9	20.4	60.2	27.4	7.7	7.9	77.1	66.6
#11	40.1	8.9	22.1	53.1	18.4	39.8	5.7	23.3	54.1	88.5
#12	61.1	16.5	3.0	30.0	10.5	39.3	0.8	15.9	26.5	66.8
#13	26.5	6.7	17.2	66.8	21.2	49.7	9.4	28.1	67.1	90.7
#14	47.8	17.2	15.9	39.5	8.9	16.9	7.6	17.4	47.4	79.7
#15	29.8	14.8	21.1	34.0	43.7	48.9	9.7	13.5	47.7	73.2

Table 7. Occurrence frequencies of the four co-contraction periods and of the pure antagonistic behavior (AN) for each subject. Values are reported as percentage of total strides.

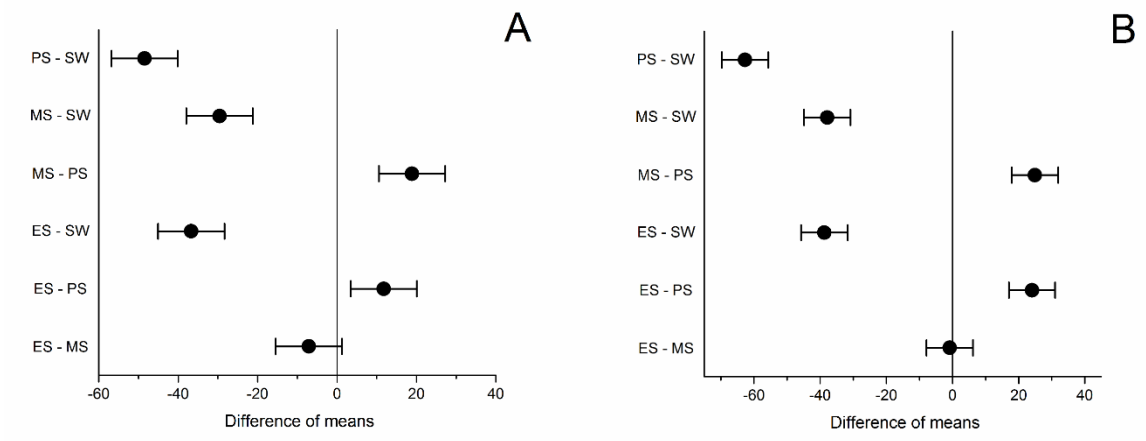

Figure 17. Outcomes of the multiple comparison test (Tukey's post hoc test) performed to compare the occurrence frequency of the different co-contraction intervals, within the M-group (A) and the F-group (B). On the y-axis, the comparison of each co-contraction interval pair is reported, whereas on the x-axis the difference of means between each pair of co-contractions is indicated. If a difference of means with its respective confidence interval does not contain zero, the corresponding means are significantly different. Therefore, the occurrence frequency of PS and SW co-contraction intervals resulted significantly different respect to the others, whereas the occurrence frequency of the ES and MS co-contraction intervals were not significantly different. The feature happened within each gender group.

The occurrence frequencies of the four co-contractions were compared through the analysis of variance (ANOVA and Kruskall-Wallis test, Fig. 17).

PS co-contractions showed a significant lower occurrence frequency respect to the other co-activation, in both M- and F-group. SW co-contractions showed a significant higher occurrence frequency respect to the other co-activation, in both M- and F-group.

The differences detected between groups in all the co-contraction occurrence frequencies were also tested after removing the bias of the anthropometric variables, by adjusting the occurrence frequencies for the BMI (ANCOVA test). The increase of occurrence frequency in female remained statistically significant for ES co-contraction (39.7±6.5% vs. 20.0±5.5%, $p=2.4 \cdot 10^{-6}$), PS co-contraction (16.7±2.9% vs. 7.6±2.5%, $p=1.3 \cdot 10^{-6}$), and SW co-contraction (81.3±8.4% vs. 57.6±7.1%, $p=8.8 \cdot 10^{-6}$), but not for MS co-contraction (38.8±10.6% vs. 27.1±9.0%, $p=0.057$). Moreover, also the difference in the absence of co-contraction remained statistically significant (12.0±8.2% vs. 32.0±7.0%, $p=8.5 \cdot 10^{-5}$).

Chapter 4
Discussion and Conclusions

Gender-related differences in the characteristics of walking tasks are well known (Chiu and Wang, 2007; Chumanov *et al.*, 2008; Chung and Wang, 2010; Hurd *et al.*, 2004; Kerrigan *et al.*, 1998; Nakagawa *et al.*, 2012). However, most of the reported studies are limited by the small number of gait cycles considered for each subject; this may encumber the quantification of the natural variability associated with muscle activity during free walking. To overcome this limitation, in this work a high number of consecutive strides per subject was considered, during an assessment session. In order to manage a large amount of data from a single subject, to extract a large amount of information on the variability of sEMG signal and to summarize mean results in a user-friendly way, considering the information on stride-to-stride variability, thanks to the identification of the different activation modalities, the statistical gait analysis was used.

For what concerns gender differences in muscular patterns of lower limb during walking, the muscle activation intervals followed the typical pattern during walking (Basmajian, 1962, Perry, 1992). According to what reported in previous studies (Agostini *et al.*, 2010; Di Nardo *et al.*, 2013), muscles showed different modalities in number of activations and timing of signal onset/offset, in different strides of the same walking. All muscles, except for GL, are active during the beginning and end of GC. Considering the periodicity of gait, the activation in the beginning of GC is just a continuation of the activation that occurs at the end of the previous GC, in all activation modalities. Thus, following the literature (Perry, 1992), the activation modalities are presented in function of the typical GC, which starts with initial contact and ends with terminal swing. Conforming to this convention, muscle activity during the beginning and end of GC was categorized as two separate activations. This consideration is valid also when the co-contraction assessment was performed.

Analyzing the mean onset/offset instants of activation (Table 1), no differences were observed between F- and M-group in the behavior of gastrocnemius, as reported also by Chung and Wang (2010). Small differences were detected for the other muscles; despite these, sEMG temporal parameters are similar between the two groups, indicating the absence of a relevant gender effect (Tables 1-5). Many studies were proposed for the quantification of gender-related differences, based on sEMG-amplitude parameters (Chiu and Wang, 2007; Chumanov *et al.*, 2008; Chung and Wang, 2010; da Fonseca *et al.*, 2006). Some critical issues were raised about the use of amplitude parameters (peak amplitude, area under curve, mean value) by sEMG for inter-subject comparison, given that their assessment could be affected by the effect of electrode location and volume conductor (Farina *et al.*, 2004; Raez *et al.*, 2006). For this reason, in this work the sEMG signal was studied by analyzing only temporal parameters.

The absence of significant differences in BF and RF occurrence frequencies between M- and F-group (Figures 4 and 5) suggests the absence of relevant gender-related differences in the myoelectric patterns of these muscles. These findings agree with Chiu and Wang (2007) and Chung and Wang (2010). The most relevant differences detected between F- and M-group regard the occurrence frequency of ankle muscles. F-group shows a significantly higher occurrence frequency in the modalities with a higher number of activations and a significantly lower occurrence frequency in the modalities with a lower number of activations for GL and TA, compared to M-group (Figures 2, 3 and 7). Moreover, for the M-group the simplest activation modalities are also the most recurrent ones, while in females the simplest activation modalities occur in a low percentage of strides. Figures 2 and 3 show that in M-group the occurrence frequency decreases gradually with the increase of the complexity in the activation modalities, while in F-group, the occurrence frequency initially increases from 1 to 2 activations for GL and from 2 to 3 activations for TA, and then decreases with the increase of complexity in the activation modalities. These findings indicate that females prefer a more complex muscular activation strategy. The modalities with many activations of GL and TA during walking were associated to the occurrence of uncommon muscular activities in swing for GL

and during mid-stance for TA (Di Nardo *et al.*, 2013). The present findings show that these uncommon activities, detected in every subject of the population, are significantly more recurrent in females than in males for both GL (84.3±10.8% vs. 57.9±17.8% of strides) and TA (44.0±15.4% vs. 21.4±11.9%), strengthening the observation of a propensity of females towards more complex activation modalities of ankle muscles. This finding agrees with the significantly higher ankle joint motion detected in females, compared to age-matched males (Chiu and Wang. 2007). Relevant differences between F- and M-group, similar to those reported for TA and GL, were detected also in sEMG signal of VL (Fig. 6).

Gender differences in lower-limb muscle activity were already reported (Chiu and Wang, 2007; Chumanov *et al.*, 2008; Chung and Wang, 2010). However, this work is a first attempt for quantifying these differences in terms of occurrence frequency, through the high number of consecutive strides considered for each subject, enhancing what has been reported in literature (Chiu and Wang, 2007; Chumanov *et al.*, 2008; Chung and Wang, 2010; Hurd *et al.*, 2004; Kerrigan *et al.*, 1998; Nakagawa *et al.*, 2012). The quantification of the occurrence frequency of every activation modality by means of the statistical gait analysis is what enabled the recognition of a female propensity for a more complex recruitment of TA, GL and VL during walking, compared to males.

The recruitment of TA in stance phase (Table 2) was already linked to the activity of TA as a foot invertor muscle for controlling balance during single support and contralateral limb swing (Di Nardo *et al.*, 2013; Lee and Piazza, 2008). The recruitment of gastrocnemius in swing phase (shaded bars in Fig. 7) was frequently observed, but not clearly explained (Agostini *et al.*, 2010; Perry, 1992). In agreement with Lee and Piazza (2008), recent studies suggest that it was related to a non-sagittal plane activity (Di Nardo *et al.*, 2013). Thus, the results of this study, not sufficient to directly support this hypothesis, suggest the need of further analyses with integrated kinematics, kinetics and sEMG to investigate the link between the female more complex recruitment of ankle muscles and a possible increase of TA and GL activity associated to the non-sagittal ankle motion in females.

The reliability of the present findings depends on the accuracy of the process used for the detection of muscle onset/offset, that, in this study, was performed by means of methodology reported by Bonato *et al.*, (1998) and its reliability was tested by Staude *et al.* (2001), who performed a systematic comparison of methods for the onset detection in sEMG signals evaluating the sensitivity of the method to changes in signal parameters. It was shown that threshold-based signal-power estimation procedures are very sensitive to signal parameters, whereas the algorithm developed by Bonato *et al.* (1998) and other statistically optimized algorithms are more robust. The presence of clear gender-related differences in sEMG activity may give further insights into gait analysis and may be useful for clinical and research studies, in motivating the development of separate biomechanical and electromyographic reference databases for males and females.

For what concerns the evaluation of co-contraction activity of ankle muscles during walking, the muscle activation intervals, detected in each subject at self-selected walking speed, followed also in this case the typical pattern reported for each muscle during gait (Basmajian, 1962; Perry, 1992, Sutherland, 2001). As described above and according to what was reported in previous studies (Agostini *et al.*, 2010; Di Nardo *et al.*, 2013), the statistical analysis highlighted for both GL and TA different modalities in the number of activations and in the timing of signal onset and offset, in different strides of the same walk. In terms of occurrence frequency, since the strides where GL showed 1-, 2- and 3-activation modalities cover the 94.3% of total strides, the analysis was limited to these three modalities of GL activation (Figures 9, 10 and 11).

The main task of GL and TA during gait is to contribute to ankle flexion, as antagonist muscles (Perry, 1992, Sutherland, 2001). Thus, the larger part of myoelectric activity is centered in stance for GL and in swing for TA, with no overlapping between TA and GL activation intervals. The only strides (21.3±8.2% of the total strides) with no overlapping between TA and GL activation intervals are those where simultaneously GL presented a single activity and TA showed the 2- or 3-activation modality, in the whole gait cycle (Fig. 9). Only in these strides, both muscles should be considered performing an antagonist activity for plantar flexion and dorsiflexion of the ankle. In the remaining

78.7±14.4% of total strides, clear superimpositions between GL and TA activation intervals were detected in stance and/or in swing.

In early stance, simultaneous activity of GL and TA has been detected at the transition from initial stance double support to single support (Fig. 9). Previous research suggested that this co-contraction is aimed to increase lower limb stability and to smooth the transition from double to single support (Schmitz *et al.*, 2009; Seyedali *et al.*, 2012). Furthermore, in normal conditions there should be minimal co-contraction due to the dominant patterns of the agonist muscle groups, which in this phase were considered to be the dorsi-flexors. The present work adds that the co-contraction is minimal not only in terms of time length (no more than 7% of gait cycle) but also in terms of frequency, since it occurs only in 29.3±7.3% of total strides.

During mid-stance, a short activity of TA, usually not reported in healthy adults, but observed in children (Agostini *et al.*, 2010; Sutherland *et al.*, 1980a; Sutherland *et al.*, 1980b), was detected in the 4-activation modality of TA (Figures 9, 10, 11). It overlaps the GL activity as ankle plantar flexor in the 32.9±9.3% of total strides. The recruitment of TA in this phase does not occur for the flexion of the ankle but is related to the activity of TA as foot invertor muscle; thus, in this phase, TA and GL do not work with antagonistic task, but in co-contraction for controlling balance during single support and contralateral limb swing. A further interpretation of this unexpected TA activity could lie in the hypothesis of a possible mutual crosstalk between tibialis anterior and peroneus longus (Campanini *et al.*, 2007). However, the presence of this TA activity in each subject and in a limited number of strides (32.9±9.3%) suggests that it is related to the need of fulfilling a specific, less frequent task (as foot inversion) rather than to crosstalk.

In pre-swing, a GL activity overlaps the TA activity as ankle dorsi-flexor in preparation for swing, in 9.4±2.9% of total strides (3-activation modality for both GL and TA, Fig. 11). This GL activation occurs to contribute to the knee flexion or to avoid knee hyperextension (Winter, 1990); thus, this short (9% of the gait cycle occurring between 44-54% of gait cycle) and not frequent co-contraction is due to the fact that TA and GL work on different joints.

During swing, GL showed an uncommon activity, superimposed to the typical activity of TA as ankle dorsi-flexor (Figures 10 and 11). The GL activity during this portion of the gait cycle is seldom acknowledged; however, short activities of GL during mid-swing were reported by Basmjian (1962) and Perry (1992), occurring for the flexion of the ankle and related to the possible activity of GL as a foot invertor muscle during swing. Even though the co-contraction of GL and TA in this phase is quite short (on average 10% of gait cycle), it has been detected in the 68.5±13.4% of total strides and thus it should be considered as a very common condition. Also in this circumstance, GL and TA do not work as antagonists, but act in synergy for the correct positioning of the foot, in preparation for the following heel strike.

It is noteworthy that the only strides with no overlapping between GL and TA activity, i.e. no co-contraction, are those where simpler activation modality for GL (1-activation modality) meets the simpler activation modalities for TA (2- and 3-activation modality; 1-activation modality is not considered since it is not statistically relevant, < 1%). When GL adopts the 2-activation modality, a co-contraction with TA elicited in swing phase (Fig. 10); a further increase in the complexity of GL activation modality (3-activation modality) leads to two further co-contraction intervals in early stance and in pre-swing, respectively (Fig. 11). Same considerations can be made for tibialis: when TA increases to the 4-activation modality a novel co-contraction with GL (not detected in 2- and 3-activation modality) occurs during mid-stance (Figures 9, 10 and 11). These findings indicate that the number and the time-length of the co-contraction intervals between GL and TA increases with the increasing of the complexity of activation modality of GL and/or TA. Moreover, Fig. 12 shows that the increasing of the complexity of TA activity (from 2- to 4-activation modality) entails a decreased number (%) of strides where the 1-activation modality occurs for GL (GL1) and a concomitant increased number (%) of strides where GL acts with multiple (≥2) activations (GLmul). This suggests a direct link between the complexity of the recruitment of the two muscles during gait, i.e. large number of activations for GL implies large number of activations for TA and vice versa.

Briefly summarizing, the statistical analysis showed that GL and TA act as pure antagonists for ankle flexion only in a small percentage of the total strides, where no superimposition between GL and TA activation intervals occurs. The number and the time-length of overlapping intervals are related with the modalities of muscle activations and their increase indicates an increase of complexity in the strategy of recruitment of the two muscles. This increase of complexity over the activity as pure ankle flexors, occurs simultaneously for GL and TA and is finalized to perform further tasks as foot inversion, improvement of the balance during single support, control of ankle stability and knee flexion. The outcome of this work can be useful for focusing the research of possible abnormal muscle co-contraction in the clinical context such as stroke, traumatic brain injury, cerebral palsy or Parkinson´s disease and during motor rehabilitation.

Eventually, considering the influence of gender on co-contraction patterns of TA and GL during gait, in accordance with what has been reported above and in previous studies (Agostini *et al.*, 2010; Di Nardo *et al.*, 2013), TA and GL revealed a high degree of variability in terms of activation modalities adopted during walking and number of strides where each modality occurred. High degree of muscular variability was detected in both populations and the analysis of sEMG signal revealed four different TA/GL superimpositions: at the very beginning of GC (Fig. 15), during mid-stance (Fig. 13), at the end of stance (Fig. 15) and during swing (Fig. 14). The distribution of the co-contractions covered the whole GC in both groups, matching with the presence of co-contraction in stance (Falconer and Winter, 1985; Olney, 1985). Moreover, each co-contraction was observed in every subject, independently from the gender. The absence of significant differences between groups in mean temporal length or onset/offset time instants of the TA/GL co-contractions (Table 6), suggests a similar functional purpose of the co-contractions for males and females.

The acknowledged role of GL and TA during walking is to act as pure antagonists to control the ankle joint in the sagittal plane (i.e. no co-contraction) (Winter, 1990). However, in the present study the strides with no TA/GL co-contraction were rather infrequent and a pure antagonistic behavior is infrequent especially for females, suggesting that women walk without co-contractions in a small

percentage of strides (12.5±9.2%, Fig. 4). The significantly lower percentage of strides with no TA/GL co-contraction in the F-group suggests a greater amount of non-antagonistic activity in females during gait, matching with the higher occurrence frequency in females for all the four co-contraction patterns (Fig. 16).

Along the GC, the first co-contraction was detected in early stance (ES, Fig. 15), where subject moves almost the entire body weight from one leg to the other and a strong stabilization of the ankle joint is needed (Winter, 1990). In the F-group, GL superimposed TA activity in early stance in about twice the strides, with respect to M-group (40.7±18.7% versus 18.9±11.0%, p=1.5·10^{-6}, Fig. 16).

The co-contraction during mid-stance (Fig. 13) was due to the superimposition of an uncommon TA activity with the typical GL activation as ankle plantar-flexor. In mid-stance, the ankle antagonistic pair are recruited in a non-antagonistic way: TA behaves as foot-invertor muscle rather than ankle dorsi-flexor. TA and GL act synergistically on the ankle joint, to control the movement of the tibia over the talus, decelerating the lower-limb forward displacement and stabilizing balance during the contralateral limb swing. F-group showed a 50% increase in the occurrence frequency of MS co-contraction, with respect to M-group (41.5±15.2% vs. 26.0±22.8%, p=0.002). The 50% increase could be explained with the increase of the occurrence frequency of the TA activity in MS detected in females (29.0±8.8% vs. 19.5±15.0%, p=0.004), as previously observed.

The third co-contraction occurred in pre-swing, in the strides where GL and TA adopted the 3-activation modality (Fig. 15). Winter (1990) observed a GL pre-swing activity, probably related to knee flexion to avoid its own hyperextension. Olney (1985) reported a TA/GL co-contraction in pre-swing: the two muscles act on different joints and thus the superimposition between sEMG signals should not be considered as a proper co-contraction. The co-contraction in pre-swing is the less recurrent among the detected ones in both populations and is more frequent in the F-group, with respect to the M-group (16.6±7.3% vs. 7.1±4.7%, p=2.1·10^{-7}, Fig. 16).

The last co-contraction occurred during the swing, in all the strides except for those where GL adopted its simpler modality (1-activation modality, Fig. 13). The co-contraction in swing is due to a

GL activity (Fig. 14 and 15) overlapping the simultaneous TA activation as ankle dorsi-flexor (Fig. 13, 14 and 15) and is likely related to the GL foot-invertor function (Di Nardo *et al.*, 2013), to properly positioning the foot for the next heel strike. The co-contraction in swing is the most recurrent one in both groups, showing a higher occurrence frequency with respect to the others co-contractions. F-group showed a higher occurrence frequency of the co-contraction in swing, compared with M-group, indicating a female increased need of controlling the lifted foot during swing.

Findings on gender effect on co-contractions have been previously observed; however, it was not considered the possibility that the inhomogeneity in anthropometric characteristics detected between groups could bias the results. Significant differences in anthropometric characteristics were detected also in the present study (not reported), but inhomogeneity in height and weight between age-matched groups of females and males should be considered physiological. However, to remove the bias of anthropometric characteristics, analysis of covariance (ANCOVA) was performed, by adjusting the occurrence frequency of the detected co-contractions for the BMI. ANCOVA results confirm the significant increase in F-group of occurrence frequency for every TA/GL co-contraction, except for MS-phase, suggesting that gender alone plays a significant role in motor-control strategies (Figure 17). The detection of a non-significant difference only in MS co-contraction raised the issue if the lack of the statistical significance could be related to number of participants per group. To solve the issue, the statistical power analysis was performed for every difference between M-group and F-group tested in the study. Results showed that the number of participants per group (15) guarantees a power≥0.90 for every occurrence frequency, except for MS co-contraction where the power is 0.71. The lower power value could be recognized as the cause of the non-statistically significance of the tested difference (type II error). Thus, the concomitant results of ANCOVA test and power analysis suggest that the reliability of MS co-contraction should be considered carefully. The uncertain reliability of the assessment of MS-co-contraction occurrence frequency could be acknowledged as a limitation of the study. Besides the occurrence frequency of MS-co-contraction, the suitable number

of volunteers was reached for all the other parameters, supporting the reliability of the present results.

All of these findings concur in indicating an overall higher presence of ankle-muscles co-contraction in females compared to males. The increase of co-contractions in female was detected in terms of occurrence frequency rather than in temporal characteristics. The occurrence frequency is a parameter seldom considered because of the few strides analyzed in classic EMG studies and thus this work can be seen as a first attempt in evaluating a gender-related differences in ankle muscle co-contraction by means of the occurrence frequency and thus direct comparison with other studies, although valuable, are not possible at the moment. Co-contractions occur in order to improve motor control and stability during walking (Olney, 1985, Winter, 1990). Smaller capability to generate joints stiffness and a decreased muscular protection was reported in females (Hurd *et al.*, 2004). Thus, the higher occurrence of co-contractions and the consequent more complex muscular recruitment seem to reflect a female need for a higher level of stabilization of ankle joint and control of lower limb, with respect to males.

Moreover, on average females show a significantly lower height than males that is natural in age-matched groups and likely causes the detected increase in cadence, compared to males. Since females and males walk at the same comfortable speed, a reduced stride length (not measured in this study) in females is also presumable. Gender-related differences in anthropometric and in spatial-temporal parameters match with previous reports (Kerrigan *et al.*, 1998). The no-significant differences detected in walking speed suggest that females adopted a different walking strategy which allows increasing the cadence with respect to males. A different walking strategy in females is also supported by the higher occurrence frequency of co-contractions detected here and by the higher muscle activity detected by previously (Chiu and Wang, 2007). Evidences of no standardization of walking were already reported, even when comparing the same gender individuals (Hollman *et al.*, 2011). The wide variability of sEMG patterns detected in the present study confirms that gait is likely a non-standard function. Despite this, the present findings on the female tendency

for a more complex muscular recruitment during walking suggest the hypothesis that a common sEMG pattern could be identified within subjects of the same gender.

The sEMG-based findings indicated an overall higher presence of ankle-muscles co-contraction in females compared to males. The increase of co-contractions in female was detected in terms of occurrence frequency, rather than in temporal characteristics. More recurring co-contractions in females seem to suggest a female greater need for ankle-joint stabilization during walking. The increased occurrence of the co-contractions contributes to determine a more complex muscular recruitment in females.

In conclusion, the electromyographic characterization of motor control during walking leaded to three main results: the first is the presence of four co-contraction intervals between tibialis and gastrocnemius in a single gait cycle. The second is the assessment of significant differences in myoelectric activation patterns between genders, which point out a more complex muscular recruitment in females respect to males. This higher complexity is mirrored by the higher occurrence frequency of activation modalities which present a high number of active intervals in a single gait cycle, rather than differences in temporal onset/offset of muscular bursts. Considering together these two aspects, significant differences in the occurrence of each co-contraction interval between TA and GL were detected between genders. This leads to a higher recurrence of each co-contraction in females respect to males during walking, thus gender appears as a not negligible factor in the evaluation of muscular co-contraction and the necessity of a gender-based approach in developing co-contraction reference frameworks is highlighted. Ankle-muscles co-contractions were reported for pathological and healthy people irrespective of the gender. Thus, a reference frame for TA/GL co-contractions in women could be a useful tool for discriminating physiological from pathological behavior typical of the female population. In particular, ankle-muscle co-contractions seems to play a role in the higher female rates of ankle sprain and should be likely considering also in evaluating the female increased risk of anterior cruciate ligament injuries. Despite the accuracy of the

methodology and the reliability of the results achieved, further mechanics and kinematics studies are needed to confirm the physiological causes leading to the co-contraction differences among genders.

Chapter References

Agostini V., Nascimbeni A., Gaffuri A., Imazio P., Benedetti M.G., Knaflitz M., "Normative EMG activation patterns of school-age children during gait", *Gait and Posture*, 2010.

Basmajian J.V., "Muscles alive, their functions revealed by electromyography", Williams & Wilkins Company, 1962.

Campanini I., Merlo A., Degola P., Merletti R., Vezzosi G., Farina D., "Effect of electrode location on EMG signal envelope in leg muscles during gait", *Journal of Electromyography and Kinesiology*, 2007.

Chiu M.C., Wang M.J., "The effect of gait speed and gender on perceived exertion, muscle activity, joint motion of lower extremity, ground reaction force and heart rate during normal walking", *Gait and Posture*, 2007.

Chumanov E.S., Wall-Scheffler C., Heiderscheit B.C., "Gender differences in walking and running on level and inclined surfaces", *Clinical Biomechanics*, 2008.

Chung M.J., Wang M.J., "The change of gait parameters during walking at different percentage of preferred walking speed for healthy adults aged 20–60 years", *Gait and Posture*, 2010.

da Fonseca S.T., Vaz D.V., de Aquino C.F., Brício R.S., "Muscular co-contraction during walking and landing from a jump: comparison between genders and influence of activity level", *Journal of Electromyography and Kinesiology*, 2006.

Di Nardo F., Ghetti G., Fioretti S., "Assessment of the activation modalities of gastrocnemius lateralis and tibialis anterior during gait: A statistical analysis", *Journal of Electromyography and Kinesiology*, 2013.

Falconer K., Winter D.A., "Quantitative assessment of co-contraction at the ankle joint in walking", *Electromyography and Clinical Neurophysiology*, 1985.

Farina D., Merletti R., Enoka R.M., "The extraction of neural strategies from the surface EMG", *Journal of Applied Physiology*, 2004.

Hollman J.H., McDade E.M., Petersen R.C., "Normative spatiotemporal gait parameters in older adults", *Gait and Posture*, 2011.

Hurd W.J., Chmielewski T.L., Axe M.J., Davis I., Snyder-Mackler L., "Differences in normal and perturbed walking kinematics between male and female athletes", *Clinical Biomechanics*, 2004.

Kerrigan D.C., Todd M.K., Della Croce U., "Gender differences in joint biomechanics during walking: normative study in young adults", *American Journal of Physical Medicine and Rehabilitation*, 1998.

Lee S.S., Piazza S.J., "Inversion-eversion moment arms of gastrocnemius and tibialis anterior measured in vivo", *Journal of Biomechanics*, 2008.

Nakagawa T.H., Moriya É.T., Maciel C.D., Serrão A.F., "Frontal plane biomechanics in males and females with and without patellofemoral pain", *Medicine and Science in Sports and Exercise*, 2012.

Olney S.J., Quantitative evaluation of cocontraction of knee and ankle muscles in normal walking. Biomechanics, international series on biomechanics, 1985.

Perry J., "Gait Analysis – Normal and Pathological Function", *USA, Slack Inc.*, 1992.

Raez M.B., Hussain M.S., Mohd-Yasin F., "Techniques of EMG signal analysis: detection, processing, classification and applications", *Biological Procedures Online*, 2006.

Schmitz A., Silder A., Heiderscheit B., Mahoney J., Thelen D.G., "Differences in lower-extremity muscular activation during walking between healthy older and young adults", *Journal of Electromyography and Kinesiology*, 2009.

Seyedali M., Czerniecki J.M., Morgenroth D.C., Hahn M.E., "Co-contraction patterns of trans-tibial amputee ankle and knee musculature during gait", *Journal of Neuroengineering and Rehabilitation*, 2012.

Staude G., Flachenecker C., Daumer M., Wolf W., "Onset detection in surface electromyographic signals: A systematic comparison of methods", *EURASIP Journal on Advances in Signal Processing*, 2001.

Sutherland D.H., Cooper L., Daniel D., "The role of the ankle plantar flexors in normal walking", *The Journal of Bone and Joint Surgery*, 1980a.

Sutherland D.H., Olshen R., Cooper L., Woo S.L., "The development of mature gait", *The Journal of Bone and Joint Surgery*, 1980b.

Sutherland D.H., "The evolution of clinical gait analysis part 1: kinesiological EMG", *Gait and Posture*, 2001.

Winter D.A., "Biomechanics and motor control of human movement", New York: Wiley, 1990.